SANDIA REPORT

SAND2015-7963
Unlimited Release
Printed September 2015

Characterization of U.S. Wave Energy Converter (WEC) Test Sites: A Catalogue of Met-Ocean Data

2nd Edition

Ann R. Dallman, Vincent S. Neary

Prepared by
Sandia National Laboratories
Albuquerque, New Mexico 87185 and Livermore, California 94550

Sandia National Laboratories is a multi-program laboratory managed and operated by Sandia Corporation, a wholly owned subsidiary of Lockheed Martin Corporation, for the U.S. Department of Energy's National Nuclear Security Administration under contract DE-AC04-94AL85000.

Sandia National Laboratories

Issued by Sandia National Laboratories, operated for the United States Department of Energy by Sandia Corporation.

Available to DOE and DOE contractors from
U.S. Department of Energy
Office of Scientific and Technical Information
P.O. Box 62
Oak Ridge, TN 37831

Telephone: (865) 576-8401
Facsimile: (865) 576-5728
E-Mail: reports@adonis.osti.gov
Online ordering: http://www.osti.gov/bridge

Available to the public from
U.S. Department of Commerce
National Technical Information Service
5285 Port Royal Rd
Springfield, VA 22161

Telephone: (800) 553-6847
Facsimile: (703) 605-6900
E-Mail: orders@ntis.fedworld.gov
Online ordering: http://www.ntis.gov/help/ordermethods.asp?loc=7-4-0#online

SAND2015-7963
Unlimited Release
Printed September 2015

Characterization of U.S. Wave Energy Converter (WEC) Test Sites: A Catalogue of Met-Ocean Data

2nd Edition

Ann R. Dallman, Vincent S. Neary
Water Power Technologies
Sandia National Laboratories
P.O. Box 5800
Albuquerque, New Mexico 87185-MS1124

Abstract

This report presents met-ocean data and wave energy characteristics at eight U.S. wave energy converter (WEC) test and potential deployment sites. Its purpose is to enable the comparison of wave resource characteristics among sites as well as the selection of test sites that are most suitable for a developer's device and that best meet their testing needs and objectives. It also provides essential inputs for the design of WEC test devices and planning WEC tests, including the planning of deployment, and operations and maintenance. For each site, this report catalogues wave statistics recommended in the International Electrotechnical Commission Technical Specification (IEC 62600-101 TS) on Wave Energy Characterization, as well as the frequency of occurrence of weather windows and extreme sea states, and statistics on wind and ocean currents. It also provides useful information on test site infrastructure and services.

ACKNOWLEDGMENTS

This study was supported by the Department of Energy (DOE), Office of Energy Efficiency and Renewable Energy (EERE), Wind and Water Power Technologies Office (WWPTO). Sandia National Laboratories is a multi-program laboratory managed and operated by Sandia Corporation, a wholly owned subsidiary of Lockheed Martin Corporation, for the U.S. Department of Energy's National Nuclear Security Administration under contract DE-AC04-94AL85000.

The following people provided valuable input to this project:

- The bulk of the methodology for wave resource characterization used in this catalogue came from the now published International Electrotechnical Commission (IEC) Technical Specification (TS) on Wave Energy Resource Assessment and Characterization (IEC TS 62600-101 Ed. 1.0; also described in Folley et al. 2012). Much of this originated from work done at OSU (Lenee-Bluhm et al. 2011, Lenee-Bluhm 2010).
- Luis Vega (HINMREC, University of Hawaii (UH)), who provided information on the Wave Energy Test Site (WETS) and facilitated data analysis of the UH hindcast dataset for this catalogue. Kwok Fai Cheung and Ning Li at the University of Hawaii for providing the analysis of their hindcast dataset.
- Belinda Batten (OSU, NNMREC), who provided information on the North Energy Test Site (NETS) and South Energy Test Site (SETS) offshore of Newport, OR and feedback on the site descriptions.
- Tuba Özkan-Haller, Merrick Haller, and Gabriel García-Medina, (OSU), who provided helpful suggestions and feedback regarding the characterization methodology.
- Gabriel García-Medina (OSU), who provided the Oregon coast hindcast dataset (García-Medina et al. 2014) to Sandia National Laboratories for use in this catalogue.
- Pukha Lenee-Bluhm and Ken Rhinefrank, Columbia Power Technologies, for providing feedback on the methodology and data presented in the catalogue.
- Colin Sheppard, Humboldt State University, who provided information on the potential Humboldt Site and suggestions on the characterization methodology and presentation of data.
- Diana Bull, Water Power Technologies, Sandia National Laboratories, for providing information from previous wave resource assessment efforts near Humboldt Bay.
- Billy Edge and Lindsay Dubbs at the University of North Carolina Coastal Studies Institute for providing information on the Jennette's Pier Wave Energy Test Site and providing data from their hindcast for both the Jennette's Pier and the U.S. Army Corps of Engineers (USACE) Field Research Facility (FRF) sites.
- Michael Forte and Jeffrey Waters at the USACE FRF for providing information on the USACE FRF site.
- Kent Hathaway at the USACE FRF for providing historical measured data near the Jennette's Pier and USACE FRF sites.

- Jim Thomson at the Advanced Physics Laboratory at the University of Washington (APL-UW) for providing information on the Lake Washington site and providing buoy data from APL-UW measurement campaigns in the lake.
- Jonathan Berg, staff member at Sandia National Laboratories, who developed the first version of the MATLAB® script for the inverse form reliability method (IFORM) for generating environmental contours for extreme sea states.
- Aubrey Eckert-Gallup, staff member at Sandia National Laboratories, for estimating the extreme significant wave height for the selected sites that do not work well with IFORM.
- Jenessa Duncombe, summer student intern at Sandia National Laboratories, for gathering and organizing information for some of the site descriptions.
- Alex Campbell, summer student intern at Sandia National Laboratories, for processing some of the surface current and wind data.
- Christopher Simmons, student intern at Sandia National Laboratories, for processing surface current and wind data for the 2nd edition of the catalogue, and migrating the report to LaTeX.

CONTENTS

FIGURES

TABLES

NOMENCLATURE

ADCP	Acoustic Doppler Current Profiler
CDIP	Coastal Data Information Program
CFSR	Climate Forecast System Reanalysis
CFSv2	Climate Forecast System version 2
DOE	Department of Energy
EquiMar	Equitable Testing and Evaluation of Marine Energy Extraction Devices in terms of Performance, Cost and Environmental Impact
EMF	Electromagnetic Fields
ESA	Environmental Site Assessment
FERC	Federal Energy Regulatory Commission
HINMREC	Hawaii National Marine Renewable Energy Center
HNEI	Hawaii National Energy Institute
HSU	Humboldt State University
HWC	Humboldt WaveConnect
IEC	International Electrotechnical Commission
IFORM	Inverse First Order Reliability Method
MCBH	Marine Corps Base Hawaii
NETS	North Energy Test Site
NAVFAC	Naval Facilities Engineering Command
NDBC	National Data Buoy Center
NNMREC	Northwest National Marine Renewable Energy Center
NOAA	National Oceanic and Atmospheric Administration
OSCAR	Ocean Surface Current Analyses - Real time
OSU	Oregon State University
OWC	Oscillating Water Column
PG&E	Pacific Gas & Electric
PMEC	Pacific Marine Energy Center
PPLP	Pilot Project Licensing Process
SETS	South Energy Test Site
SNL	Sandia National Laboratories
TS	Technical Specification

UH	University of Hawaii
UNC CSI	University of North Carolina Coastal Studies Institute
USACE FRF	US Army Corps of Engineers Field Research Facility
VAFB	Vandenberg Air Force Base
WEC	Wave Energy Converter
WETS	Wave Energy Test Site
WET-NZ	Wave Energy Technology - New Zealand

1. INTRODUCTION

1.1. Motivation

The present study was motivated by the lack of a single information source that catalogues, with documented and consistent methodologies, met-ocean data and wave energy characteristics at U.S. wave energy converter (WEC) test sites and potential deployment sites. Such information allows WEC developers to compare wave resource characteristics among test sites as well as select test sites that are most suitable for their device and that best meet their testing needs and objectives. It also serves as an initial data set and framework to support a wave classification system, much like the wind classification system, which has become a standard for wind turbine design.

This catalogue includes wave statistics recommended in the International Electrotechnical Commission Technical Specification on Wave Energy Characterization (IEC TS 62600-101 Ed. 1.0; also described in Folley et al. 2012); but it also provides additional information on wave resource characteristics, including the frequency of occurrence of weather windows and extreme sea states, and statistics on wind and ocean currents. This additional information can assist developers in planning WEC tests, servicing their test devices, and assessing opportunities and risks at the test site.

1.2. Wave Resource Characterization

Wave energy resources are analyzed and presented in various ways throughout the literature. For example, efforts have included analyses of measured buoy data and/or hindcast simulation data; some consider full directional spectra while others only consider bulk parameters; extreme event analyses are often neglected or considered in separate studies. This ambiguity and difficulty in comparing assessments are some of the reasons that the IEC began the process of creating a technical specification (Folley et al. 2012). The IEC Technical Specification (TS) on Wave Energy Characterization is now completed and published (IEC TS 62600-101 Ed. 1.0).

Wave energy resource is defined in the IEC TS as "the amount of energy that is available for extraction from surface gravity waves," (IEC TS 62600-101 Ed. 1.0). The TS includes guidelines for three classes of resource assessment. Class 1, or *reconnaissance*, is the lowest level and produces estimates with high uncertainty. This would be appropriate for large areas as the first assessment in a region. Class 2, or *feasibility*, produces estimates with greater certainty, and is appropriate for refining a reconnaissance assessment before a Class 3 assessment is done. Class 3, or *design*, produces an assessment with the least uncertainty and would be the final and most detailed assessment for small areas. This catalogue provides a Class 3 (*design*) assessment for the eight sites considered. For a detailed resource assessment at a particular site of interest, the energy characterization should be based on the analysis of directional wave spectra produced from a simulated hindcast. Measurements (e.g., from

buoys) can be useful for boundary conditions, and independent measured data should be used to validate the hindcast model.

In a related effort to the IEC TS, EquiMar (Equitable Testing and Evaluation of Marine Energy Extraction Devices in terms of Performance, Cost and Environmental Impact), published wave resource assessment guidance, Deliverable 2.7 (Davey et al. 2010), available at http://www.equimar.org/equimar-project-deliverables.html. According to this protocol, an assessment should provide an estimate of the available energy and the operating and survival characteristics of a site, which can be achieved by using a combination of in-situ measurements and numerical modelling. Similarly to the IEC TS, three stages of resource assessment are addressed, and the one closest to the IEC TS 'design' would be the EquiMar 'Project Development,' which should provide "detailed information on a deployment site including information on spectra and extremes," (Davey et al. 2010). The period of record of data considered should be 10 years, and many cases would use numerical modeling. The EquiMar resource assessment is in general consistent with the IEC TS methodology adopted in this catalogue. The EquiMar project issued a brief catalogue, where several test sites were characterized with the best data available (O'Connor and Holmes 2011).

The IEC TS, and recent papers regarding the U.S. Pacific Northwest coast (Lenee-Bluhm et al. 2011, García-Medina et al. 2014), recommend six parameters to characterize the wave resource at a test site. In addition, they advocate calculating these parameters from simulated hindcast spectral wave data. These six parameters are omnidirectional wave power, significant wave height, energy period, spectral width, direction of maximum directionally resolved wave power, and directionality coefficient. Equations for calculating these statistics are provided in the Methodology section.

The IEC TS recommends that seasonal variation of wave statistics be considered, and monthly plots of the six parameters, along with seasonal cumulative distributions, should be provided. It is also recommends that wave roses and time histories of the six parameters for one representative year be included. Wave roses provide a direct and intuitive means to visualize wave directions for corresponding wave bulk properties, typically omnidirectional wave power and significant wave height.

Although extreme sea states are not addressed in the IEC TS, they provide critical information needed to assess the risks of deploying a WEC at the test site and to design a WEC to survive wave loads associated with extreme sea states of a given return period. For this reason, the 100-year environmental contours are provided, as explained in Section 2.2. Although 100-year recurrence intervals (return periods) are common for marine structures, lower return periods can be used, if acceptable for survivability, when the design service life is less than 100 years (DNV 2005).

Additional wave statistics and met-ocean data, not specified in the IEC TS, but provided in this report, include weather windows as well as wind and ocean current statistics. This information is also valuable to developers for the purpose of assessing risks at the site and planning for testing and servicing of the WEC test device.

1.3. Format of Report

Three high energy wave sites were included in the First Edition of the catalogue, which was released in 2014: (1) the Pacific Marine Energy Center (PMEC) North Energy Test Site (NETS) offshore of Newport, Oregon; (2) Kaneohe Bay Naval Wave Energy Test Site (WETS) offshore of Oahu, HI; and (3) a potential test site offshore of Humboldt Bay (Eureka, CA). Five additional sites are now included in this edition of the catalogue: (4) the Jennette's Pier Wave Energy Converter Test Site in North Carolina; (5) the US Army Corps of Engineers (USACE) Field Research Facility (FRF) offshore of Duck, North Carolina; (6) the PMEC Lake Washington test site; (7) the proposed PMEC South Energy Test Site (SETS) offshore of Newport, Oregon; and (8) the proposed CalWave Central Coast WEC Test Site at Vandenberg Air Force Base (VAFB).

Chapter 2 describes the methodology, including the data presented, analysis procedures, and data sources. Next is a chapter for each site (Chapters 3 - 10) that include descriptions of the site and testing infrastructure, and a discussion of the results of the met-ocean data. The established test sites are presented first, and potential test sites follow. A summary of the study and conclusions are presented in the final chapter (Chapter 11). Additional data is provided in plots and tables in the appendices.

2. METHODOLOGY

2.1. Overview

For this study, the third-generation phase-averaged spectral model SWAN (Simulating Waves Nearshore) was used to generate all wave climate hindcasts, from which wave statistics are calculated. For NETS and SETS, hindcast data was generated by researchers at the Northwest National Marine Renewable Energy Center (NNMREC) (García-Medina et al. 2014). The dataset for WETS was generated by the Hawaii National Marine Renewable Energy Center (HINMREC) (Li & Cheung 2014, Li et al. 2015). The datasets for the Jennette's Pier and USACE FRF sites was generated by the University of North Carolina Coastal Studies Institute (UNC CSI). The dataset for Lake Washington was generated by Coast & Harbor (Coast and Harbor Engineering 2015). The CalWave VAFB data was generated by Humboldt State (see Appendix in Williams et al. 2015). Finally, for the Humboldt site, the dataset was generated by Sandia National Laboratories (Dallman et al. 2014). All hindcast simulations were validated by comparing predicted wave statistics against buoy observations prior to processing data and plots presented in this catalogue. HINMREC analyzed hindcast wave data for WETS, while Sandia National Laboratories (SNL) analyzed hindcast wave data for the rest of the sites.

2.2. Data Presented

The six parameters recommended by Lenee-Bluhm et al. (2011) and specified in the TS are defined below as in Lenee-Bluhm et al. (2011) and García-Medina et al. (2014). Equations for these parameters are repeated below for completeness.

The omnidirectional wave power, J, which indicates the resource available, is the sum of the contributions to energy flux from each of the components of the wave spectrum,

$$J = \sum_i \rho g c_{g,i} S_i \Delta f_i \tag{1}$$

where ρ is the density of sea water, g is the acceleration due to gravity, $c_{g,i}$ is the group velocity, S_i is the variance density, and Δf_i is the frequency bin width at each discrete frequency index i. Significant wave height, H_{m0}, estimated from spectra, is commonly used to describe the sea state and is defined as

$$H_{m0} = 4\sqrt{m_0} \tag{2}$$

where m_0 is the zeroth moment of the variance spectrum. The moments of variance spectrum are

$$m_n = \sum_i f_i^n S_i \Delta f_i. \tag{3}$$

The energy period, T_e, is also widely used to describe the sea state and is more robust than the peak period (due to a high sensitivity to spectral shape). The energy period is calculated

as

$$T_e = \frac{m_{-1}}{m_0}. \tag{4}$$

The spectral width,

$$\epsilon_0 = \sqrt{\frac{m_0 m_{-2}}{m_{-1}^2} - 1}, \tag{5}$$

characterizes the spreading of energy along the wave spectrum. The directionally resolved wave power is the sum of the wave power at each direction θ

$$\begin{gathered} J_\theta = \sum_{i,j} J_{ij} \Delta f_i \Delta\theta_j \cos(\theta - \theta_j)\delta \\ \begin{cases} \delta = 1, & \cos(\theta - \theta_j) \geq 0 \\ \delta = 0, & \cos(\theta - \theta_j) < 0 \end{cases} \end{gathered} \tag{6}$$

where J is the directionally resolved wave power in direction θ. The maximum time averaged wave power propagating in a single direction, J_{θ_J}, is the maximum value of J_θ. The corresponding direction, θ_J, is the direction of maximum directionally resolved wave power and describes the characteristic direction of the sea state. The directionality coefficient, d_θ, is the ratio of maximum directionally resolved wave power to the omnidirectional wave power,

$$d_\theta = \frac{J_{\theta_J}}{J} \tag{7}$$

which is a characteristic measure of directional spreading of wave power (i.e., larger values approaching unity signify narrow directional spread). It is also recommended in the IEC TS that annual and seasonal values be reported.

The average monthly values of the above parameters, along with 5^{th} and 95^{th} percentiles, are presented to capture their variation over a typical year. This information is useful for planning deployments and tests. Optimal deployment windows, for example, are generally in summer months when sea states are less energetic than winter months. For similar reasons, testing of a scaled model WEC is generally more suitable in summer months.

Joint probability distribution (JPD) plots are presented to provide an overall depiction of the wave climate at each site and help inform the design of the WEC test device. These plots also include the mean, 5^{th} and 95^{th} percentiles of wave steepness, defined in this study as the ratio of the significant wave height to length, H_{m0}/γ, where the wavelength is calculated using the Newton-Raphson method to solve the dispersion relation (Holthuijsen 2007) using T_e. Steepness is important because it is related to wave breaking, and it affects wave forces on marine structures such as a WEC (Bitner-Gregersen 2001).

JPD plots, also known as bi-variate scatter plots (Cahill and Lewis 2013), can be used to present the frequency of occurrence of sea states (H_{m0}, T_e pairings) at a site, or the percentage contribution of each sea state to the total annual energy or power density. Wave characterization studies have shown (e.g., Cahill and Lewis 2011, Cahill and Lewis 2013, Lenee-Bluhm et al. 2011) that the sea states that occur most often do not necessarily correspond to those contributing the most to annual energy.

Cumulative distributions of H_{m0} and T_e are shown to describe the percentage of time these parameters are equal to or less than a threshold value. In order to account for duration, weather windows for wave heights equal to or less than threshold values are calculated for multiples of 6-hour periods. Weather windows quantify the number of opportunities in a given season or year to access the site for installation of a test device, or for operations and maintenance, based on their specific device, service vessels, and diving operation constraints.

Following suggestions from the IEC TS, wave roses are generated to visualize the spread and predominant directions of omnidirectional wave power and significant wave height. Rose plots for wind and ocean currents are also generated to examine the spread and predominant direction of wind and ocean currents. From these rose plots, one can also determine the percentage of time that a given statistical parameter (e.g., omnidirectional wave power) is equal or less than a given value at a specified direction sector. The radial thickness of a given bin represents the percentage of the time that the given omnidirectional wave power and direction occurs. Wave, wind, and current directions are defined as degrees clockwise from North. When directions are concentrated around North (0°), plots show positive directions (clockwise from North) and negative directions which are counter-clockwise from North. For example, -45° is equivalent to 315°.

Estimates of extreme sea states (H_{m0}, T_e pairings) are determined from 100-year environmental contours calculated using a modified version of the inverse first order reliability method (IFORM). The IFORM, as described by Winterstein et al. (1993), is standard design practice for generating environmental contours used for estimating extreme sea states of a given recurrence interval or return period (DNV 2014). It provides developers, not only with an estimate of the largest significant wave height, but also extreme sea states at other significant wave heights with energy periods that could compromise the survival of a marine structure or service vessel. The modified IFORM used in this study (Eckert-Gallup et al. 2014, Eckert-Gallup et al. 2015) improves the original fitting method by implementing principal components analysis. MATLAB® scripts to estimate contours using this modified IFORM were created by Sandia National Laboratories and are available on the Water Power website. As currently implemented, neither the IFORM nor the modified IFORM work well for datasets whose variables (H_{m0} and T_e) are bimodally distributed. Such distributions lead to complex dependencies between the variables that cannot be captured by the expression of joint probability used in either method, leading to erroneous representations of extreme sea state contours. This bimodality can be found in the buoy data representing the North Carolina and CalWave Vandenberg sites. For this reason, only the 100 year significant wave height, estimated through the application of extreme value theory, is presented at these sites. This was estimated using two extreme value theory methods for completeness: the generalized extreme value distribution (GEV) and peak over threshold (POT) method. Further details are provided in the chapters for these sites. Lake WA will also be an exception using extreme value theory because the distribution is so narrow due to the waves being short fetched wind waves (see Section 7.4.5).

Estimates of applied wave loads and power response under a diverse range of sea states is required for designing and siting a WEC. Since running simulations for a WEC response to all

frequency spectra occurring at a site would take an unfeasibly long amount of time, it is beneficial to synthesize a fixed number of spectra which can be used to represent each expected sea state (e.g., Lenee-Bluhm 2010). Therefore, representative spectra for the most common sea states at a site (found in the JPD) were calculated by averaging all measured spectra within each sea state. Standard spectra (Bretschneider and JONSWAP) were included for comparison.

The Bretschneider spectrum, which is meant for developing seas, was computed according to the unified form described in Chakrabarti (1987),

$$S(\omega) = \frac{A}{4} H_{m0}^2 \omega_s^4 \omega^{-5} exp\left(-A\left(\frac{\omega}{\omega_s}\right)^{-4}\right), \tag{8}$$

where A = 0.675 is a nondimensional constant and $\omega_s = T_p/1.167$ is the significant frequency. The JONSWAP spectrum (Hasselmann et al. 1973), is an extension of the Pierson-Moskowitz spectrum (for fully developed wind seas) to include fetch-limited wind seas, and therefore describes developing seas. It was computed according the DNV Recommended Practices on Environmental Conditions and Environmental Loads (DNV-RP-C205 2014),

$$S(\omega) = A_\gamma \frac{5}{16} H_{m0}^2 \omega_p^4 \omega^{-5} exp\left(-\frac{5}{4}\left(\frac{\omega}{\omega_s}\right)^{-4}\right) \gamma^{exp\left(-0.5\left(\frac{\omega-\omega_p}{\sigma\omega_p}\right)^2\right)}, \tag{9}$$

where $\omega_p = 2\pi/T_p$ is the angular spectral peak frequency, $A_\gamma = 1 - 0.287\ ln(\gamma)$ is a normalizing factor, $\gamma = 3.3$ is a non-dimensional shape parameter, and is a spectral width parameter where $\sigma = 0.07$ for $\omega \leq \omega_p$ and $\sigma = 0.09$ for $\omega \geq \omega_p$. If the wind speed and fetch were known, the JONSWAP spectrum could be calculated according to the equation in Hasselmann et al. (1973). Use of this equation, however, does not ensure the spectrally estimated H_{m0} would match the input value. Although a better fit could be achieved if a least squares fit was applied to the mean of the measured spectrum, it is assumed that the actual spectral shape would not be known *a priori* and a standard spectrum would be fit to a sea state (H_{m0}, T_e or T_p). Therefore, this comparison shows how well an assumed standard spectrum fits an actual measured spectrum without knowing the shape *a priori*.

As well as wave statistics, monthly averages of wind speed and direction, along with seasonal and annual wind roses are provided for each site. Monthly averages of ocean surface current speed and direction, along with seasonal and annual current roses are provided for each site.

2.3. Data Sources

The majority of the wave climate statistics (e.g., the six parameters of interest described above) were calculated from validated hindcast model simulations, as recommended in the IEC TS. These hindcast datasets are described in the Data Used section for each site.

In general, these phase averaged wave models do not simulate large waves well (for example the hindcast by García-Medina et al. 2014, represents significant wave height only up

to $H_{m0} \approx 8m$), unless specialized input data and versions of models are used for specific storms (e.g., the National Weather Services National Hurricane Center specialized models). Therefore the hindcast models utilized in this catalogue may not be reliable data sources for estimations of extreme events. The location of a buoy at each site does not necessarily coincide with the actual test site, but it is the most reliable data source for this calculation, and is used herein. In addition, results in Feld & Mork (2004) indicate that hindcast model spectra are less peaked than measured buoy data, and therefore representative spectra are also calculated from buoy data. The location and POR of buoys used will be described in each chapter.

Wind data for each site was obtained from 0.5 degree spatial resolution and 6-hour temporal resolution datasets available at the National Centers for Environmental Predictions (NCEP) Climate Forecast System Reanalysis (CFSR) (covering 1979-2010) and CFSv2 (covering 2011-present) (Saha et al. 2010, Saha et al. 2014). Data was selected at a single point or multiple points closest to the site. When multiple points were selected a simple arithmetic average of the data reported at each time step was computed. The wind data available from buoys or onshore meteorological stations greatly varies between sites, so using CFSR allows for a consistent data source between sites. In addition, CFSR data generally has better spatial coverage than buoy data, as well as longer periods of record (POR). The exception to this is the Lake Washington site because CFSR data is not available directly over the lake, and data over nearby land is not a reliable estimate of the local winds. Therefore a met tower on a bridge over the lake is used for that site.

Surface currents near the test sites were obtained from Ocean Surface Current Analyses Real time (OSCAR), part of the National Oceanic and Atmospheric Administration (NOAA). OSCAR calculates near real-time global sea surface currents from NASA satellite data and reports the data publically on their website. Sea surface currents are calculated from (1) sea surface height derived from Satellite altimeter and (2) ocean near-surface wind speed and direction from satellite scatterometers. The result is a global-scale sea surface current speed and direction dataset with a spatial resolution of 1 degree and a temporal resolution of 5 days.

OSCAR current data has been shown to be accurate for time-mean measurements by Johnson et al.(2007). Compared to moored current meters, drifters and shipboard current profilers, OSCAR mean sea surface currents closely match observed data at all latitudes and longitudes. High frequency (HF) radar has a higher resolution and is often a preferred data source for real-time applications and short term analyses, but is unavailable at the Hawaii site and has a much shorter period of record compared to OSCAR. As more systems are setup along the U.S. coast and the POR increases, HF radar will likely become a viable data source for long term characterization. For the purpose of this catalogue, OSCAR data was used because it provides data at each site to maintain consistency, has periods of record of at least 10 years at each site, and has been shown to be accurate for mean current speed and direction. Again, the exception to this is the Lake Washington site, where OSCAR data is unavailable. An estimate of surface currents based on the wind data is provided, and is explained in that chapter.

3. PACIFIC MARINE ENERGY TEST CENTER (PMEC): NORTH ENERGY TEST SITE (NETS)

3.1. Site Description

The Pacific Marine Energy Center (PMEC) is the name of the Northwest National Marine Renewable Energy Centers (NNMREC) marine energy converter testing facilities located in the Pacific Northwest region. NNMREC is a Department of Energy funded entity designed to facilitate development of marine renewable energy technology. Ultimately PMEC will facilitate testing a broad range of technologies being produced by the marine energy industry (NNMREC 2014). The North Energy Test Site (NETS) is an off-grid WEC test site that became operational in the summer of 2012. As shown in Figure 1, it encompasses an area of 1-square nautical mile (roughly 3 square kilometers) within state waters at 44.6899 N, 124.1346 W.

NETS is located near the City of Newport, Oregon and Yaquina Bay. At the test site, the water depth is approximately 45-55 m (25-30 fathoms), the bathymetry is gently sloping, and the sea bed consists of soft sand. Figure 2 shows the bathymetry surrounding promontory Yaquina Head and the test site. The wave climate at the test site varies seasonally, with calmer seas in the summer compared to more energetic seas in the winter. The wave environment at NETS is characterized by an annual average power flux of about 37 kW/m, including a number of events with significant wave heights exceeding 7 m each winter.

NNMREC offers a wide range of technical and testing infrastructure support services for WEC developers, including access to a fully instrumented test buoy and grid connection emulator at NETS. NETS has full scale wave energy resources, and can accommodate devices up to 100 kW connected to the mobile ocean test berth, the Ocean Sentinel, and larger devices if no grid emulation or connection is required.

NNMREC is currently designing a utility-scale, grid-accessible test site, the South Energy Test Site (SETS), which is planned to be operational in 2017.

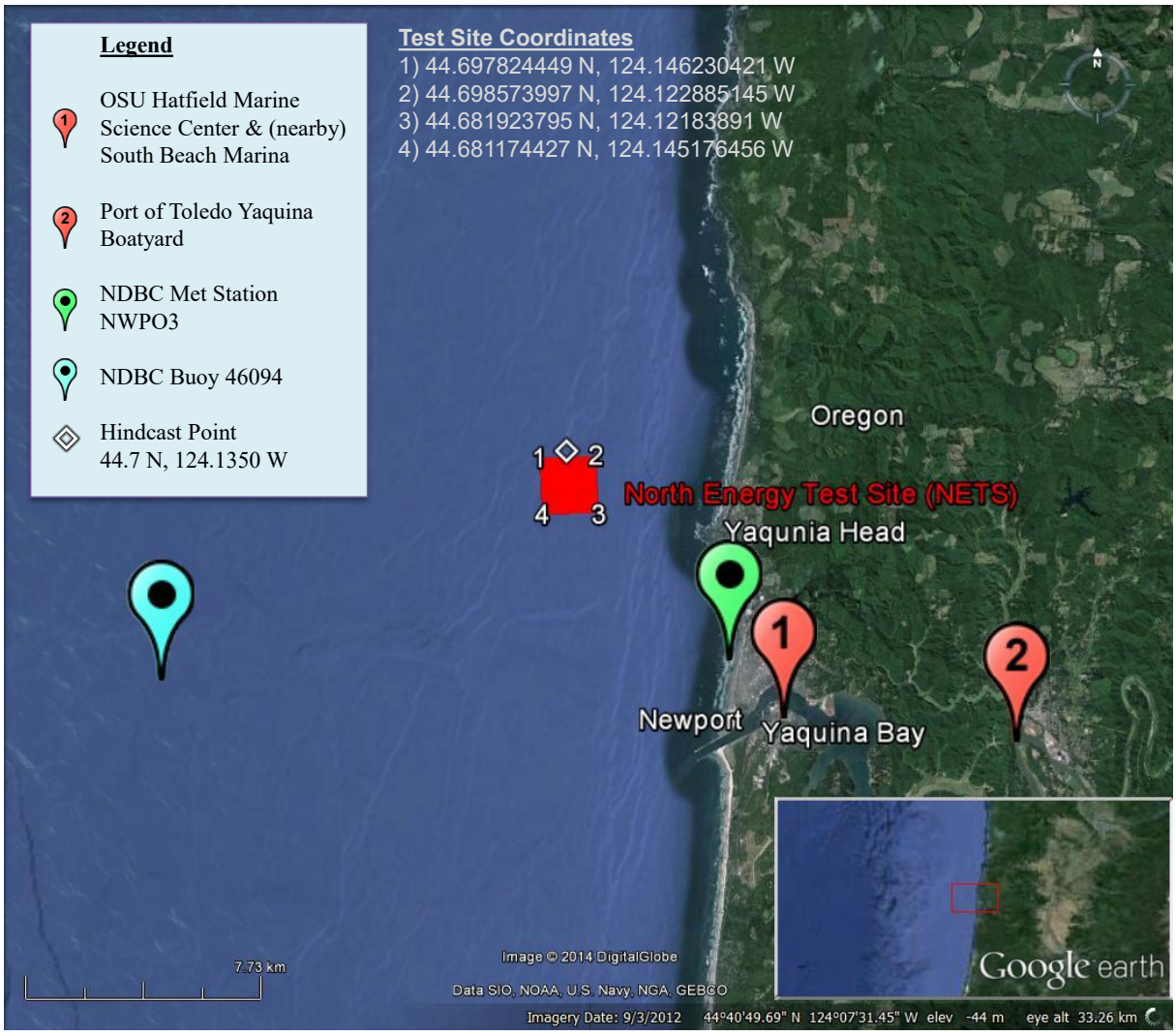

Figure 1: NETS is located in the coastal waters of Oregon near the City of Newport. The test site is 3-5 km off-shore in 45-55 m depth water. One National Data Buoy Center (NDBC) ocean buoy and one NDBC meteorological station are close to the site (see Table 1), as well as Oregon State University's (OSU) test instrumentation buoy (see Section 3.2.7). The South Beach Marina, Port of Toledo Yaquina Boatyard, and OSU Hatfield Marine Science Center offer services valuable for WEC testing. The point of reference for the hindcast simulation is on the north edge of NETS. Image modified from Google Earth (Google Earth 2014).

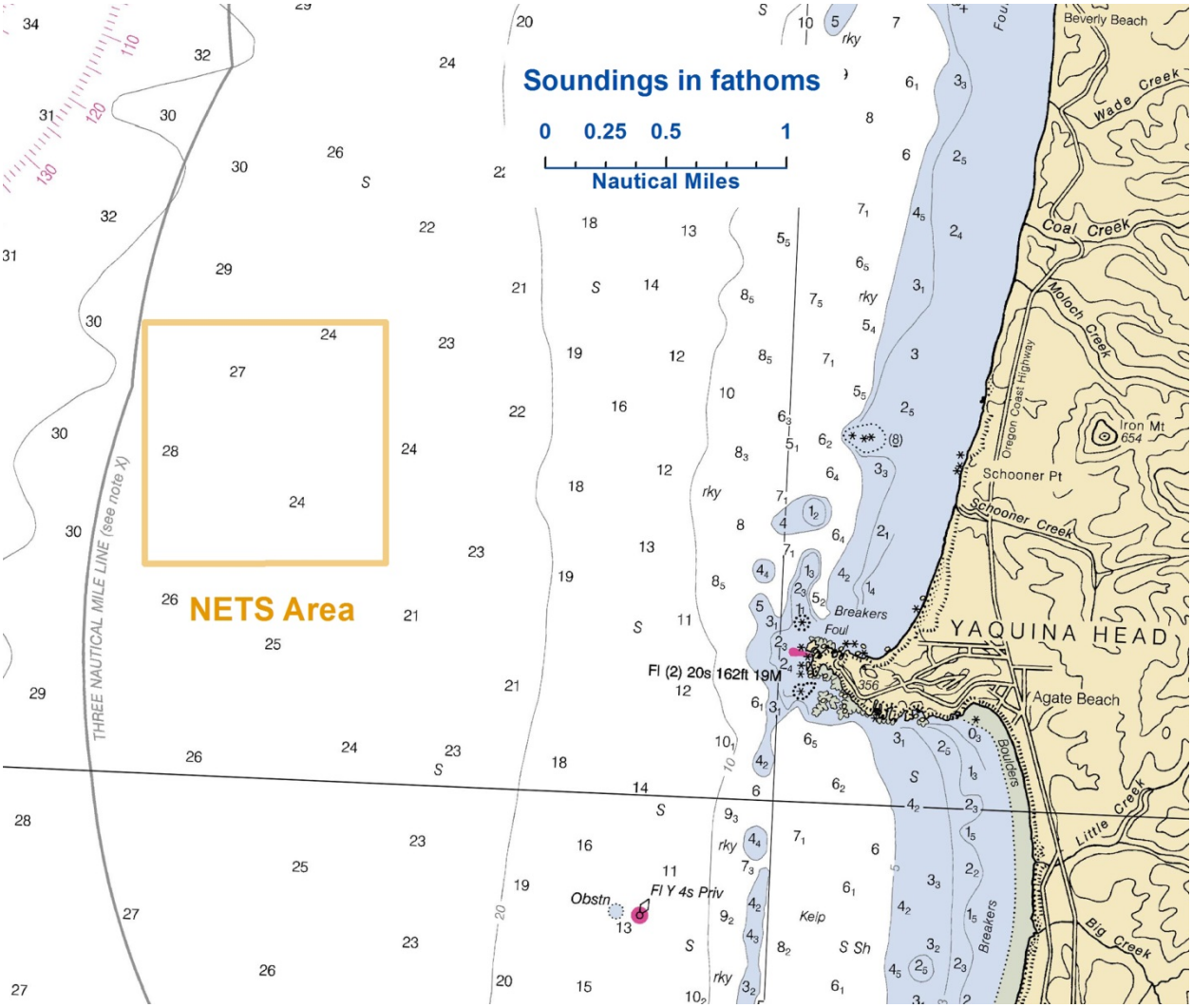

Figure 2: Nautical chart of Yaquina Head and surrounding area shows the gradually sloping bathymetry around NETS. Soundings in fathoms (1 fathom = 1.8288 m). Image modified from nautical chart #18561 (Office of Coast Survey 2011).

3.2. WEC Testing Infrastructure

3.2.1. Mooring Berths

NETS is permitted to test up to two WECs concurrently within the 45-55 m depth site. Mooring systems are not provided and would need to be installed according to the developers design. As an example, a six-point mooring system was used for the WET-NZ during their 2012 test. A layout of their test site mooring is provided in von Jouanne et al. (2013). A three point mooring system is used for OSU's Ocean Sentinel buoy (described in Section 3.2.2) during device deployment in order to hold a tight watch circle along the device and to maintain the connection of the power and communication umbilical with the Ocean Sentinel (NNMREC 2014). During more energetic winter months, the Ocean Sentinel uses a single point mooring system and can be used for environmental testing, but will not be connected

to the device. WEC testing can be done in "stand alone" mode (no electrical connection) during the winter.

3.2.2. Electrical Grid Connection

There is no electrical grid connection at NETS, but the Ocean Sentinel test buoy (Figure 3) was designed as an electrical grid emulator to allow assessment of WEC device performance (von Jouanne et al. 2013). The Ocean Sentinel serves several purposes: (1) it consumes the electrical power generated by the WEC device with an onboard resistor element, (2) it measures the electrical power generated (voltage, current), and (3) it collects year-round met-ocean data, as described in Section 3.2.7.

The Ocean Sentinel can currently accommodate one device with an average power output up to 100 kW during the months May through October (NNMREC 2014). The data collected by the Ocean Sentinel is communicated wirelessly to OSUs Hatfield Maine Science Center, which is located in Yaquina Bay next to the South Beach Marina (Waypoint #1 in Figure 1). This data can be accessed remotely.

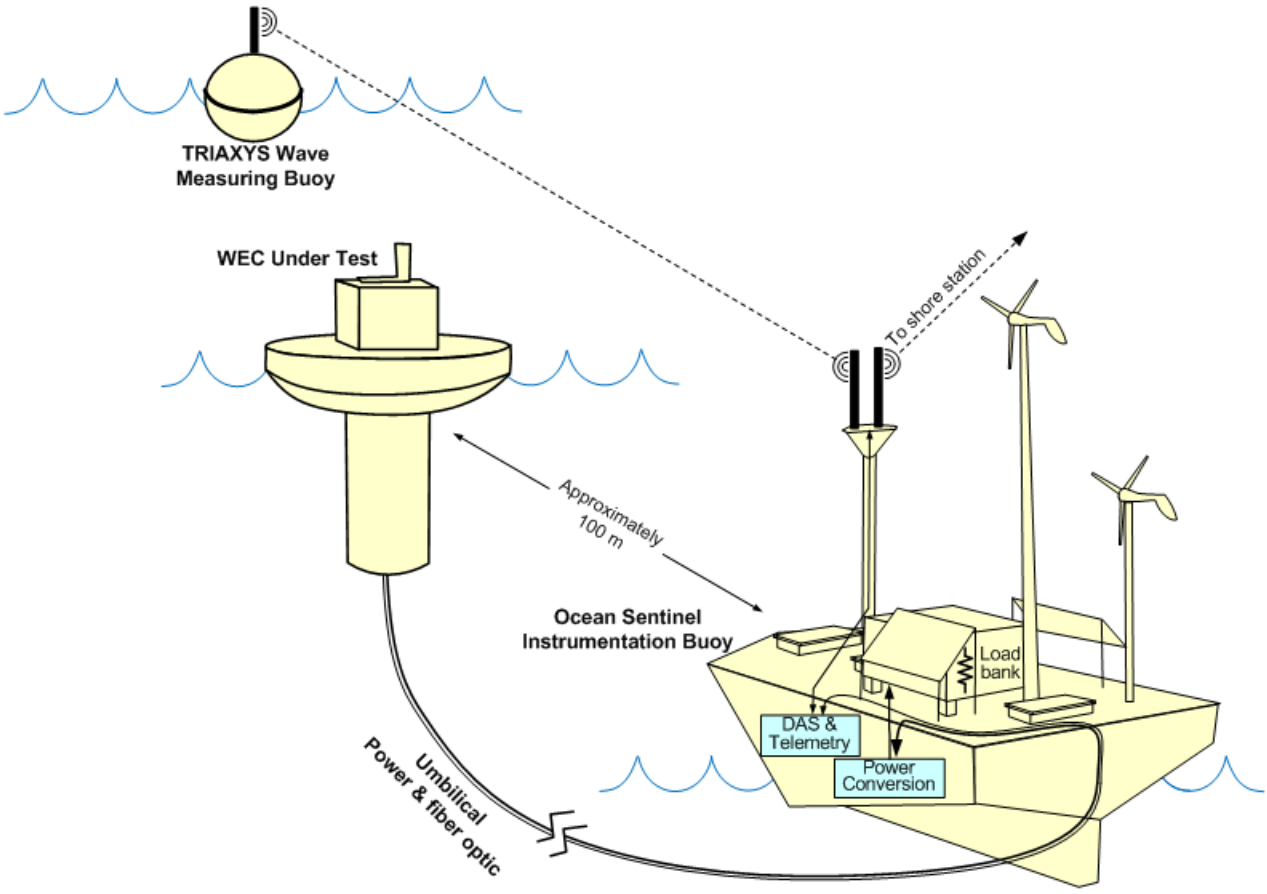

Figure 3: The Ocean Sentinel acts as a grid emulator for WEC devices, as well as records electricity output and monitors surrounding environmental data. The WEC device is connected to the Ocean Sentinel via an umbilical cord.

3.2.3. Facilitating Harbor

NETS is approximately 9 km north/northwest of the entrance to Yaquina Bay, the mouth of the Yaquina River. The South Beach Marina is located near the outlet of Yaquina Bay and offers year-round boat mooring (near Waypoint #1 in Figure 1).

3.2.4. On-Shore Office Space

The fishing and tourist City of Newport, Oregon, where approximately ten thousand people live, is on the north side of Yaquina Bay (U.S. Census Bureau 2012). At this time, developers at NETS are responsible for renting office space in Newport, Oregon or Toledo, Oregon, which is a town up the Yaquina River. Meeting rooms and temporary office space through PMEC are planned to be available in the future following the completion of the South Energy Test Site (SETS) (Batten 2014).

3.2.5. Service Vessel and Engineering Boatyard Access

No dedicated service vessel is available at this time, but following the completion of SETS, more resources may be available through PMEC. Service vessels for hire are likely available in the Newport/Toledo area. The Port of Toledos Yaquina Boatyard (Waypoint #2 in Figure 1) services boats and provides space for self-service. Yaquina Boatyard hauls boats up to 300 tons and has capabilities that include steel fabrication, carpentry, painting, haul-out, and project management (Port of Toledo 2014).

3.2.6. Travel and Communication Infrastructure

Portland International Airport (PDX) is a two and a half hour drive from Newport, Oregon. Eugene Airport is located closer and is a one hour and forty minute drive. Cellular service offers consistent coverage; three Federal Communication Commission (FCC) registered cell phone towers are located in and around Newport, Oregon.

3.2.7. Met-Ocean Monitoring Equipment

The Ocean Sentinel test buoy reports environmental data (waves, currents and winds), and other signals from the installations onboard the WEC test device (NNMREC 2014). As with electrical power data, met-ocean data is communicated wirelessly to OSUs Hatfield Marine Science Center (Waypoint #1 in Figure 1) and is available for remote access.

In addition, there are two National Buoy Data Center (NDBC) buoys that measure and collect ocean data and one NDBC station reporting meteorological data (see Figure 1 for location). Instrument and data specifications for this monitoring equipment are summarized in Table 1. Buoy data is accessible online at the NDBC database. NDBC 46050 (Stonewall Bank) is located 30 km seaward from the test site and provides spectral wave data. NDBC 46094 (NH-10) is slightly closer to the site at only 14 km away and reports standard ocean

wave data (Figure 4(a)). The land based meteorological station is situated directly on the shoreline (Figure 4(b)).

Figure 4: (a) Moored buoy NDBC 46094 located 14 km southwest of the test site, (b) meteorological station NWPO3 on the coastline 8 km southeast of the test site (National Data Buoy Center 2014).

Table 1: Wave monitoring equipment in close proximity to NETS.

Instrument Name (Nickname)	**NDBC Station 46094 (also called NH-10)**	**NDBC Station 46050 (Stonewall Bank)**			**NWPO3**	
Type	Moored buoy	3-meter discus buoy			C-MAN station (MARS payload)	
Measured parameters	-std. met. data -continuous winds -sea surface temp, salinity, density -current measurements	-std. met. data -continuous winds -spectral wave density -spectral wave direction			-std. met. data -continuous winds	
Variables reported, including derived variables (Sampling interval)	*Std Met.:* WDIR WSPD BAR ATMP (10 min sampling period)	*Std Met.:* WDIR WSPD GST WVHT DPD APD PRES ATMP WTMP (1 hr sampling period)	*Contin. Winds:* WDIR WSPD GDR GST GTIME (10 min sampling period)	-Spectral Wave Density -Spectral Wave direction (1 hr sampling period)	*Std Met.:* WD WSPD GST BAR ATMP DEWP (1 hr sampling period)	*Contin. Winds:* WDIR WSPD GDR GST GTIME (10 min sampling period)
Location	directly west of Newport, 14 km southwest from NETS	20 nm (nautical miles, 1 nm = 1.852 km) directly west of Newport, 30 km west of NETS			on the shoreline, near Newport, 8 km southeast of NETS	
Coordinates	44.633 N 124.304 W (44°38'0" N 124°18'13" W)	44.639 N 124.534 W (44°38'20" N 124°32'2" W)			44.613 N 124.067 W (44°36'48" N 124°4'0" W)	
Depth	-depth: 81 m -air temp: 2.5 m above site -anemometer: 3 m above site	-depth: 128 m -air temp: 4 m above water -anemometer: 5 m above water -barometer: sea level -sea temp depth: 0.6 m below water			-site: 9.1 m above sea level -air temp: 6.4 m above site -anemometer: 9.4 m above site -barometer: 11 m above sea level	
Data Start	2/5/2007	-std met: 11/16/1991 -contin winds: 09/07/1997 -spect wave dens: 01/01/1996 -spect wave dir: 03/05/2008			-std met: 1/10/1985 -contin winds: 1/12/1997	
Data End	present; several winters missing data	present			present	
Period of Record	∼8.5 yrs	-std met: ∼24 yrs -contin winds: ∼18 yrs -spect wave dens: ∼20 yrs -spect wave dir: ∼7.5 yrs			-std met: ∼31 yrs -contin winds: ∼19 yrs	
Owner / Contact Person	Oregon Coastal Ocean Observing System/ National Data Buoy Center	National Data Buoy Center			National Data Buoy Center	

3.2.8. Environmental Monitoring

Environmental conditions have been characterized at the site by Oregon State University, NOAA, and NNMREC. The information gathered includes baseline measurements of benthic habitat and organisms, marine mammal populations, electromagnetic fields (EMF), and acoustics (Batten 2013). Developers can contract with NNMREC to monitor environmental effects of WEC deployments during testing. Required environmental monitoring of WEC deployments includes acoustics, electromagnetic fields (EMF), benthic ecosystems, and opportunistic marine mammal observations.

3.2.9. Permitting

The site is fully permitted through the NEPA process, Department of State Lands, the U.S. Coast Guard, and the Army Corp of Engineers (NNMREC 2014). Developers interested in testing WECs at NETS are required to provide plans and present information to show compliance with test center standards and regulatory requirements. Each test requires its own permits for WEC testing in Oregon state waters. The approval process has been streamlined, but it should be noted that completed permit applications and supporting documentation should be submitted at least six months prior to the desired deployment site. More information can be found at NNMRECs website http://nnmrec.oregonstate.edu/permitting-requirements.

3.3. Data used

Researchers at the Northwest National Marine Renewable Energy Center (NNMREC) produced a 7 year hindcast dataset for the area offshore of Oregon (García-Medina et al. 2014) in order to complement the study of temporal and spatial variability in the wave resource over the Pacific Northwest region by Lenee-Bluhm et al.(2011). This dataset was used to calculate statistics of interest for the wave resource characterization at NETS. The hindcast data at the grid point on the north side of NETS was analyzed (see Figure 1). Although a 10 year hindcast would be preferred, García-Medina et al. (2014) showed that the probability density function (PDF) of significant wave height from their hindcast compared to NDBC 46029 buoy data were in agreement up to $\sim$7 m, and, therefore, the hindcast is at least representative of the twenty-seven years of buoy operation, 1985 – 2011.

In addition to the hindcast data set, historical data from buoy NDBC 46050 was used to calculate extreme sea states and representative spectra. Wind data was available from NDBC 46050 and a Coastal-Marine Automated Network (C-MAN) station, NWPO3 located just on-shore. However, to be consistent with the other sites, Climate Forecast System Reanalysis (CFSR) winds were used, as explained in Section 2.3. As with the other sites, current data was downloaded from OSCAR. See Figures 1 and 5 for data locations.

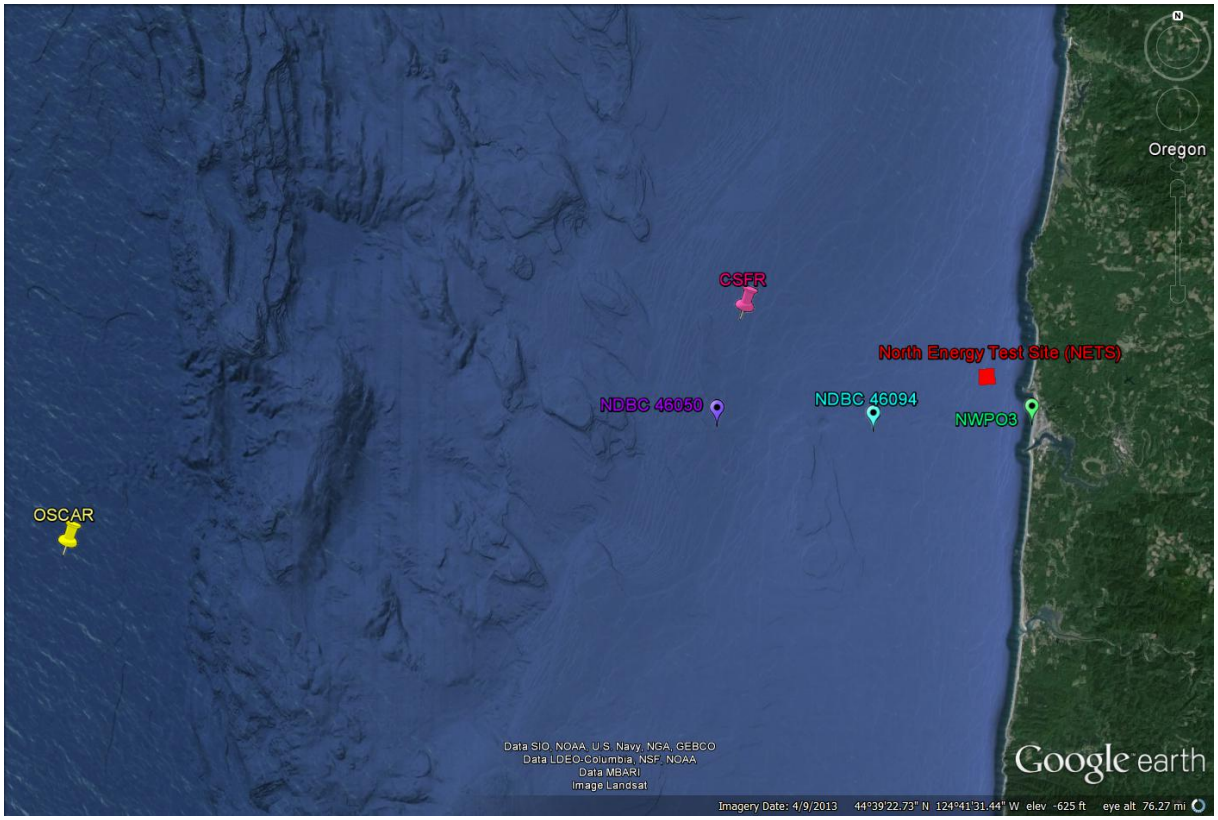

Figure 5: NETS location map showing CSFR wind and OSCAR surface current data points, and NDBC buoy locations (Google Earth 2015).

3.4. Results

The following sections provide information on the joint probability of sea states, the variability of the IEC TS parameters, cumulative distributions, weather windows, extreme sea states, and representative spectra. This is supplemented by wave roses as well as wind and surface current data in Appendix A. The wind and surface current data provide additional information to help developers plan installation and operations & maintenance activities.

3.4.1. Sea States: Frequency of Occurrence and Contribution to Wave Energy

Joint probability distributions of the significant wave height, H_{m0}, and energy period, T_e, are shown in Figure 6. Figure 6 (top) shows the frequency of occurrence of each binned sea state and Figure 6 (bottom) shows the percentage contribution to the total wave energy. Figure 6 (top) indicates that the majority of sea states are within the range 1 m $< H_{m0}$ $<$ 3.5 m and 7 s $< T_e <$ 11 s; but a wide range of sea states are experienced at NETS, including extreme sea states caused by severe storms where H_{m0} exceeded 7.5 m. The site is well suited for testing WECs at various scales, including full-scale WECs, and testing the operation of WECs under normal sea states. Although the occurrence of an extreme sea state for survival testing of a full scale WEC is unlikely during a normal test period, the NETS wave climate offers opportunities for survival testing of scaled model WECs.

As mentioned in the methodology (Section 2.2), previous studies show that sea states with the highest frequencies of occurrence do not necessarily correspond to those with the highest contribution to total wave energy. The total wave energy in an average year is 322,250 kWh/m, which corresponds to an average annual omnidirectional wave power of 36.8 kW/m. The most frequently occurring sea state is within the range 1 m $< H_{m0} <$ 1.5 m and 8 s $< T_e <$ 9 s, while the sea state that contributes most to energy is within the range 3 m $< H_{m0} <$ 3.5 m and 10 s $< T_e <$ 11 s. Several sea states occur at a similar frequency, and sea states within 2 m $< H_{m0} <$ 4.5 m and 9 s $< T_e <$ 11 s contribute a similar amount to energy.

Frequencies of occurrence and contributions to energy of less than 0.01% are considered negligible and are not shown for clarity. For example, the sea state within 0.5 m $< H_{m0}$ $<$ 1 m and 5 s $< T_e <$ 6 s has an occurrence of 0.02%. The contribution to total energy, however, is only 0.001% and, therefore, does not appear in Figure 6 (bottom). Similarly, the sea state within 8.5 m $< H_{m0} <$ 9 m and 12 s $< T_e <$ 13 s has an occurrence of 0.004%, but the contribution to total energy is 0.06%.

Curves showing the mean, 5^{th} and 95^{th} percentiles of wave steepness, H_{m0}/λ, are also shown in Figure 6. The mean wave steepness at NETS is 0.0165 ($\approx 1/61$), and the 95^{th} percentile approaches 1/34.

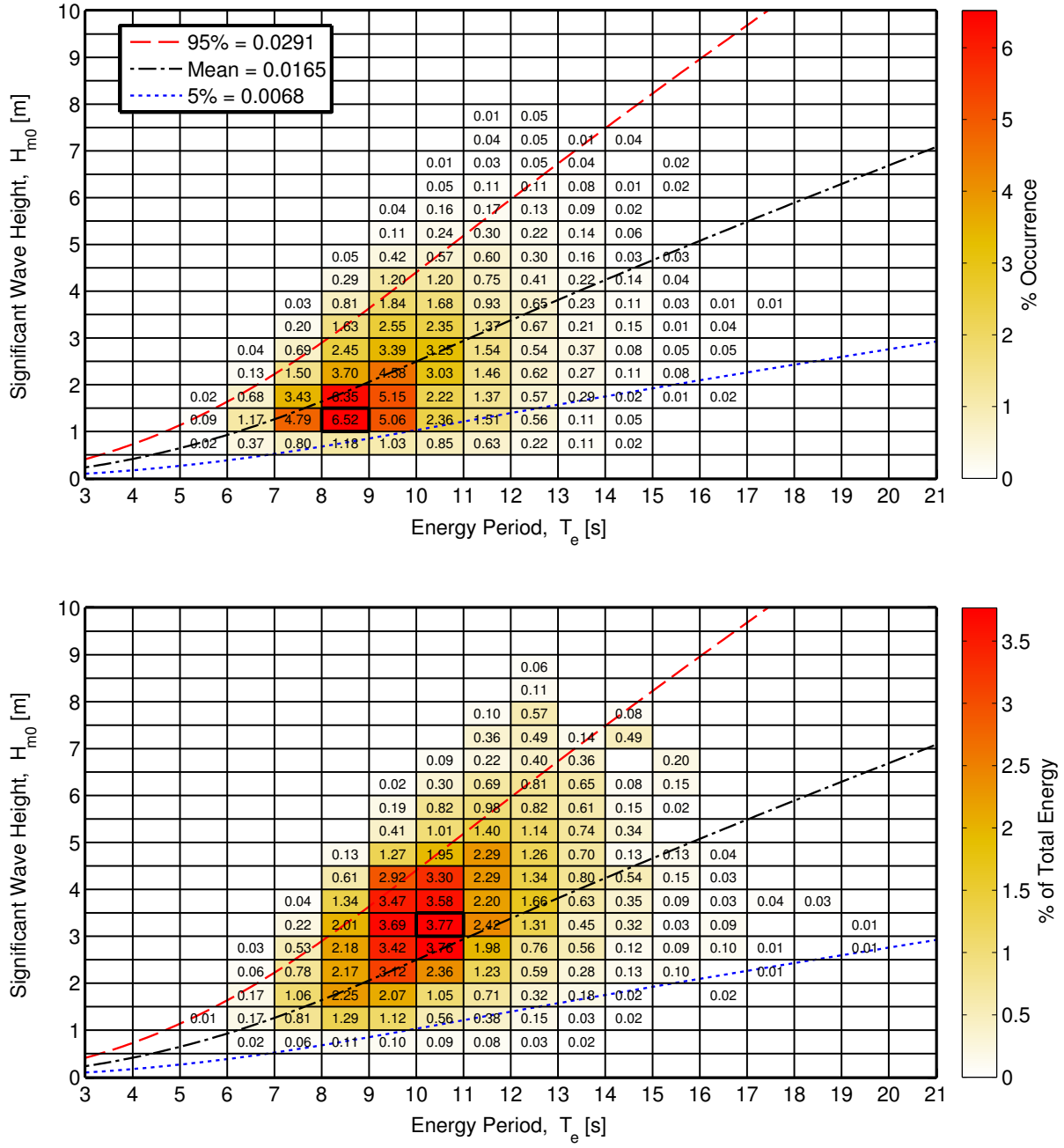

Figure 6: Joint probability distribution of sea states for NETS. The top figure is frequency of occurrence and the bottom figure is percentage of total energy, where total energy in an average year is 322,250 kWh/m.

3.4.2. IEC TS Parameters

The monthly means of the six IEC TS parameters, along with the 5^{th} and 95^{th} percentiles, are shown in Figure 7. The months, March – February, are labeled with the first letter (e.g., March is M). The values in the figure are summarized in Table 9 in Appendix A.

Monthly means of the significant wave height, H_{m0}, and the omnidirectional wave power density, J, show the greatest seasonal variability compared to the other parameters. Values are largest and vary the most during the winter months. The same trend is observed for the monthly mean energy period, T_e, but its variation is less pronounced. These observations are consistent with the relationship between wave power density, significant wave height and energy period, where wave power density, J, is proportional to the energy period, T_e, and the square of the significant wave height, H_{m0}.

Seasonal variations of the remaining parameters, ϵ_0, θ_J, and d_θ, are much less than J, H_{m0}, and T_e, and are barely discernable. Monthly means for spectral width, ϵ_0, remain nearly constant at ~ 0.4. Similarly, monthly means for wave direction, θ_J, remains nearly constant from west at $\sim 275°$, and directionality coefficient, d_θ, remains at ~ 0.9. In summary, the waves at NETS, from the perspective of monthly means, have a fairly consistent spectral width, are predominantly from the west, and exhibit a wave power that has a narrow directional spread.

Wave roses of wave power and significant wave height, presented in Appendix A, Figure 120 and 121, also show the predominant direction of the wave energy at NETS, which is west, with frequent but small shifts to the north and occasional but small shifts to the south. Figure 120 shows two dominant wave direction sectors, west (at 270°) and west/northwest (WNW) at 285°. Along the predominant wave direction, 285°, the omnidirectional wave power density is at or below 35 kW/m about 24% of the time, but greater than 35 kW/m nearly 15% of the time. Along the west direction (270°), wave power density is at or below 35 kW/m about 18% of the time, and greater than 35 kW/m nearly 10% of the time.

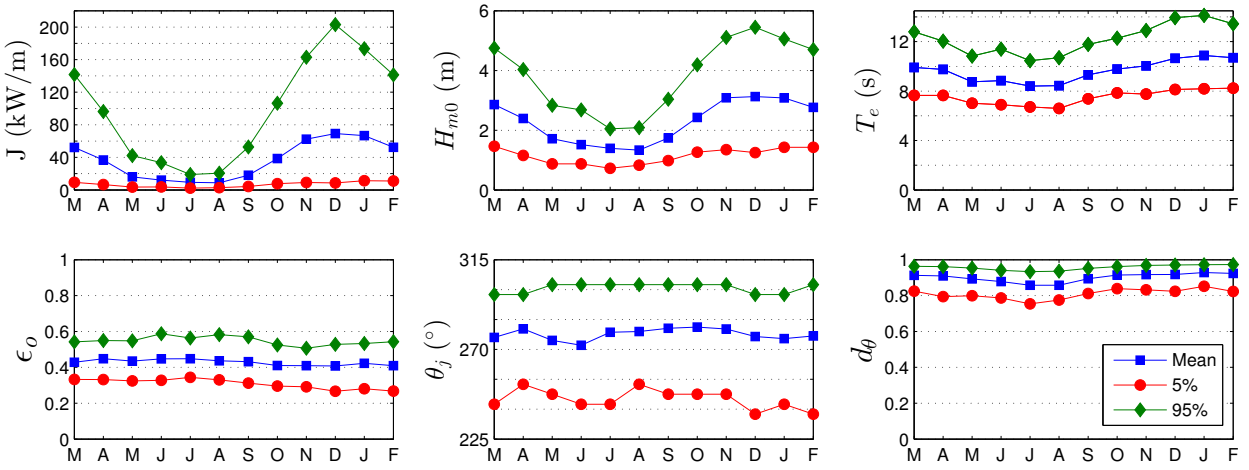

Figure 7: The average, 5^{th} and 95^{th} percentiles of the six parameters at NETS.

Monthly means, however, smear the significant variability of the six IEC parameters over small time intervals as shown in plots of the parameters at 1-hour intervals in Figure 8 for a representative year. While seasonal patterns described for Figure 7 are still evident, these plots show how sea states can vary abruptly at small time scales with sudden changes, e.g., jumps in the wave power as a result of a storm.

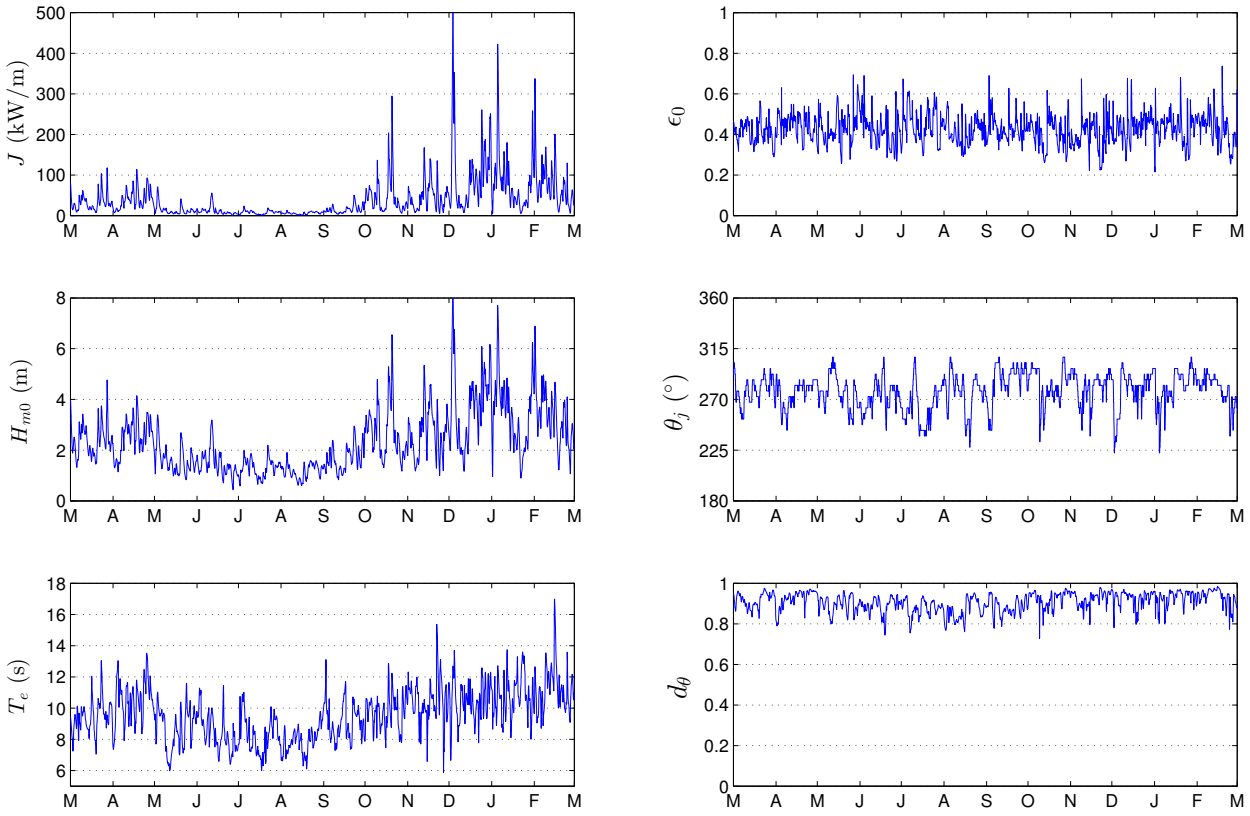

Figure 8: The six parameters of interest over a one-year period, March 2007 – February 2008 at NETS.

3.4.3. Cumulative Distributions

Annual and seasonal cumulative distributions (a.k.a., cumulative frequency distributions) are shown in Figure 9. Note that spring is defined as March – May, summer as June – August, fall as September – November, and winter as December – February. The cumulative distributions are another way to visualize and describe the frequency of occurrence of individual parameters, such as H_{m0} and T_e. A developer could use cumulative distributions to estimate how often they can access the site to install or perform operations and maintenance based on their specific device, service vessels, and diving operation constraints. For example, if significant wave heights need to be less than or equal to 1 m for installation and recovery, according to Figure 9, this condition occurs nearly 6% of the time on average within a given year. If significant wave heights need to be less than or equal to 2 m for emergency maintenance, according to Figure 9, this condition occurs about 49% of time on average within a given year. Cumulative distributions, however, do not account for the duration of a desirable sea state, or weather window, which is needed to plan deployment and servicing of a WEC device at a test site. This limitation is addressed with the construction of weather window plots in the next section.

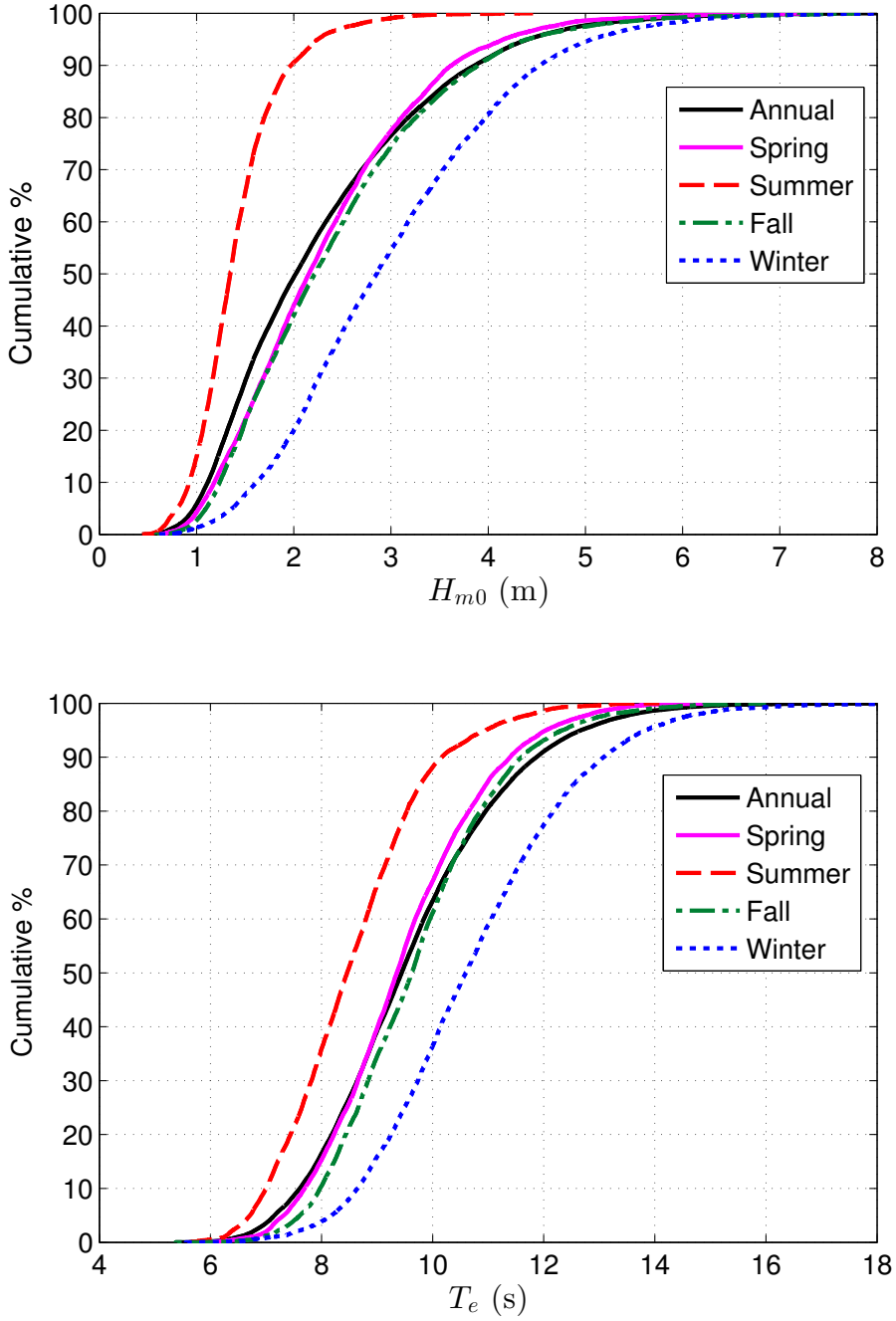

Figure 9: Annual and seasonal cumulative distributions of the significant wave height (top) and energy period (bottom) at NETS.

3.4.4. Weather Windows

Figure 10 shows the number of weather windows at NETS, when significant wave heights are at or below some threshold value for a given duration, for an average winter, spring, summer and fall. In these plots, each occurrence lasts a duration that is some multiple of 6-hours. The minimum weather window is, therefore, 6-hours in duration, and the maximum

is 96-hours (4 days). The significant wave height threshold is the upper bound in each bin and indicates the maximum significant wave height experienced during the weather window. Note that the table is cumulative, so, for example, an occurrence of $H_{m0} \leq 1$ m for at least 30 consecutive hours in the fall is included in the count for 24 consecutive hours as well. In addition, one 12-hour window counts would count as two 6-hour windows. It is clear that there are significantly more occurrences of lower significant wave heights during the summer than winter, which corresponds to increased opportunities for deployment or operations and maintenance.

Weather window plots provide useful information at test sites when planning schedules for deploying and servicing WEC test devices. For example, if significant wave heights need to be less than or equal to 1 m for at least 12 consecutive hours to service a WEC test device at NETS with a given service vessel, there would be, on average, twenty-three weather windows in the summer, but only one in the winter. When wind speed is also considered, Figure 11 shows the average number of weather windows with the additional restriction of wind speed, $U < 15$ mph. The local winds (which are not necessarily driving the waves) are used in these weather windows, and are given in Appendix A.4. That wind data was not available from the hindcast, so data from CFSR was used (see Section 2.3, Appendix A.4). For shorter durations (6- and 12-hour windows), daylight is necessary. Windows with $U < 15$ mph and only during daylight hours are shown in Figure 12. Daylight was estimated as 5am – 10pm Local Standard Time (LST).

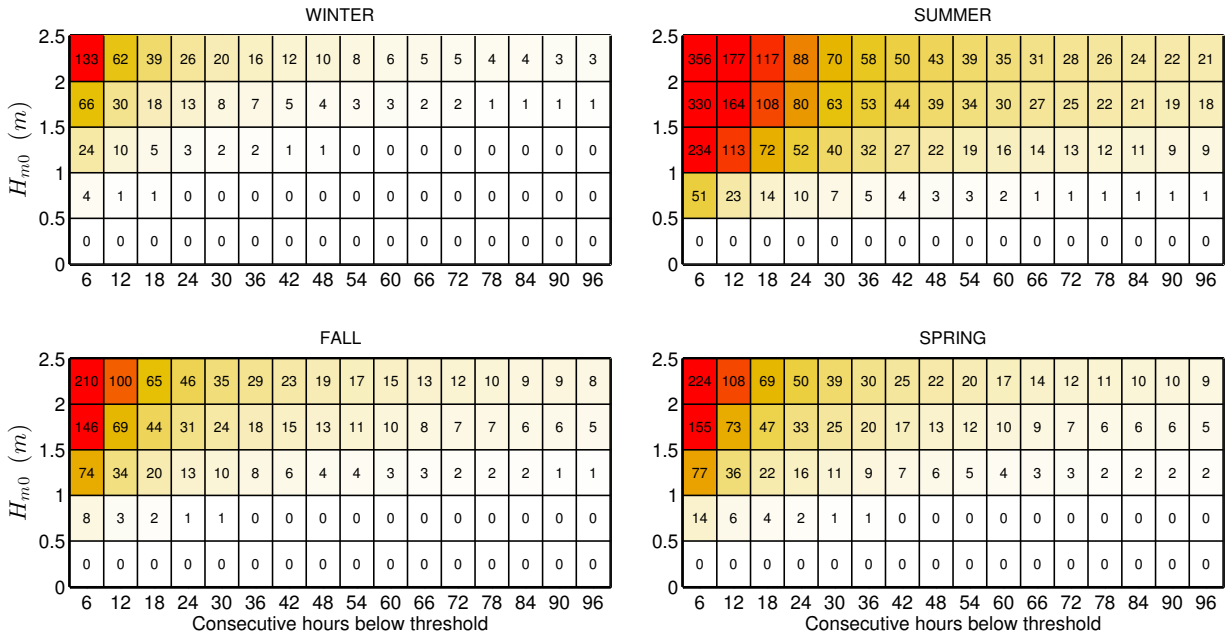

Figure 10: Average cumulative occurrences of wave height thresholds (weather windows) for each season at NETS. Winter is defined as December – February, spring as March – May, summer as June – August, and fall as September – November.

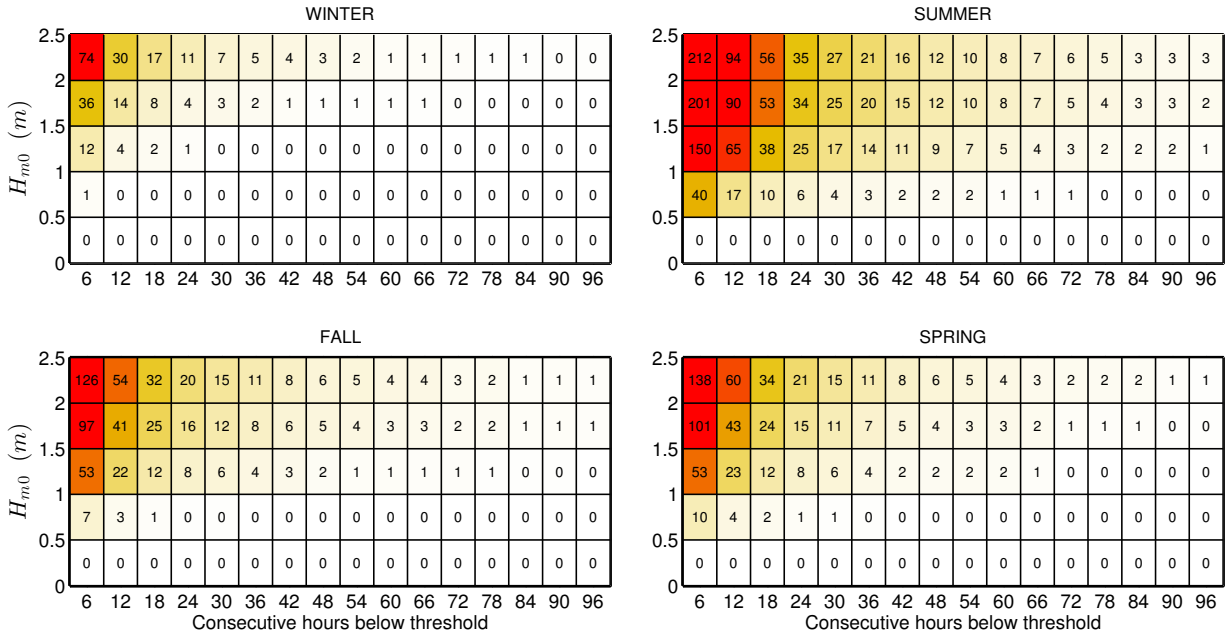

Figure 11: Average cumulative occurrences of wave height thresholds (weather windows) for each season at NETS with an additional restriction of U $<$ 15 mph.

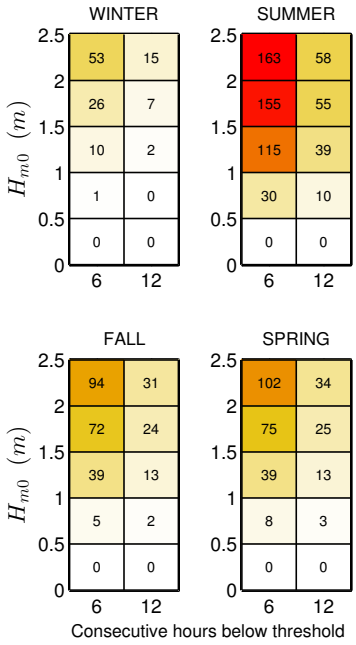

Figure 12: Average cumulative occurrences of wave height thresholds (weather windows) for 6- and 12-hour durations with $U < 15$ mph and only during daylight hours (5am – 10pm LST) at NETS.

3.4.5. Extreme Sea States

The modified IFORM was applied using NDBC 46050 data (see Table 1 for buoy information) to generate the 100-year environmental contour for NETS shown in Figure 13. Selected sea states along this contour are listed in Appendix A, Table 10. As stated in Section 1.2, environmental contours are used to determine extreme wave loads on marine structures and design these structures to survive extreme sea states of a given recurrence interval, typically 100-years. For NETS, the largest significant wave height estimated to occur every 100-years is over 17.3 m, and has an energy period of about 16.6 s. However, significant wave heights lower than 17.3 m, with energy period less than or greater than 16.6 s, listed in Table 10, could also compromise the survival of the WEC test device under a failure mode scenario in which resonance occurred between the incident wave and WEC device, or its subsystem. For comparison, 50- and 25-year return period contours are also shown in Figure 13. The largest significant wave height on the 50-year contour is 16.3 m with an energy period of about 16.4 s, and on the 25-year contour is 15.4 m and 16.1 s. It should be noted that conditions at the NDBC46050 buoy (at 128 m depth) may differ significantly from the conditions at the test site (at depths of 45-55 m).

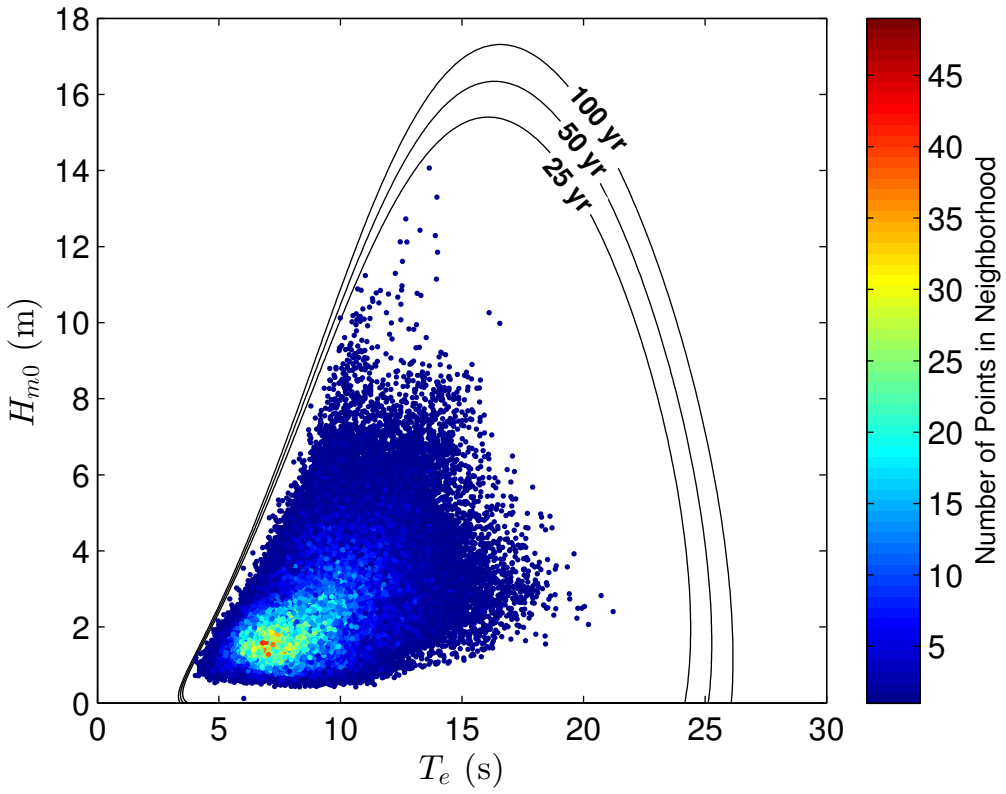

Figure 13: 100-year contour for NDBC 46050 (1996–2014).

3.4.6. Representative Wave Spectrum

All hourly discrete spectra measured at NDBC 46050 for the most frequently occurring sea states are shown in Figure 14. The most frequently occurring sea state, which is within the range 1.5 m $< H_{m0} <$ 2 m and 7 s $< T_e <$ 8 s, was selected from a JPD similar to Figure 6 in Section 3.4.1, but based on the NDBC 46050 buoy data. As a result, the JPD, and therefore the most common sea states, generated from buoy data are slightly different from that generated from hindcast data. For example, the most frequently occurring sea state for the JPD generated from hindcast data is in a H_{m0} bin 0.5 m lower (1 m $< H_m0 <$ 1.5 m), and one second higher on bounds for T_e (8 s $< T_e <$ 9 s). Often several sea states will occur at a very similar frequency, and therefore plots of hourly discrete spectra for several other sea states are also provided for comparison. Each of these plots includes the mean spectrum and standard wave spectra, including Bretschneider and JONSWAP, with default constants as described in Section 2.2.

For the purpose of this study, the mean spectrum is the 'representative' spectrum for each sea state, and the mean spectrum at the most common sea state, shown in Figure 14 (bottom-right plot), is considered the 'representative' spectrum at the site. The hourly spectra vary considerably about this mean spectrum, but this is partly reflective of the bin size chosen for H_{m0} and T_e. Comparisons of the representative spectra in all plots with the Bretschneider and JONSWAP spectra illustrate why modeled spectra with default constants, e.g., the shape parameter $\gamma = 3.3$ for the JONSWAP spectrum, should be used with caution. Using the constants provided in Section 2.2, the Bretschneider spectra are fair representations of the mean spectra in Figure 14, however it does not capture the bimodal nature of the spectra. The mean measured spectra is the best representation of the conditions, however, if these modeled spectra were to be used at this site, it is recommended that the constants undergo calibration against some mean spectrum, e.g., the representative spectrum constructed here. A better alternative may be to explore other methods or spectral forms to describe bimodal spectra (e.g., Mackay 2011) if it is known that the shape is not unimodal.

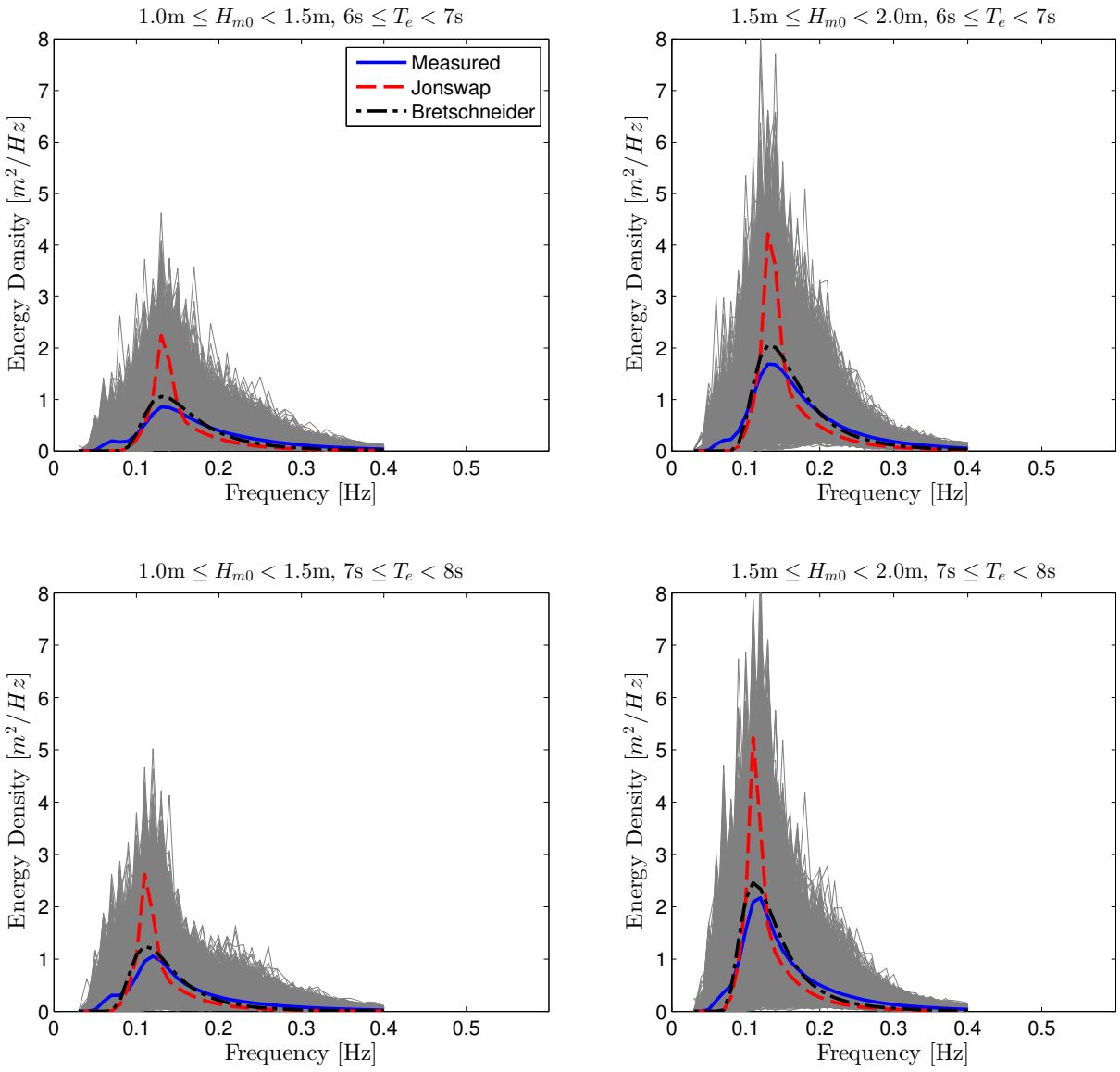

Figure 14: All hourly discrete spectra and the mean spectra measured at NDBC 46050 within the sea state listed above each plot. The JONSWAP and Bretschneider spectra are represented by red and black dotted lines, respectively.

4. U.S. NAVY WAVE ENERGY TEST SITE (WETS)

4.1. Site Description

The United States first grid-connected wave energy test site is being developed off the coast of the island of Oahu. The site, known as the U.S. Navy Wave Energy Test Site (WETS), is located on the windward side of the island at Marine Corps Base Hawaii (MCBH), at Kaneohe, as shown in Figure 15. The site infrastructure is being built by the U.S. Naval Facilities Engineering Command (NAVFAC) as a means of investigating the potential of wave energy to address the energy goals of the Navy. Through a cooperative effort between the Navy and the U.S. Department of Energy (DOE), the site will host companies seeking to test their pre-commercial WEC devices in an operational setting and advance their device transition readiness level. Now fully permitted and consisting of three berths, at water depths of 30 m (in place), 60 m, and 80 m (expected to be functional by July 2015), all within about 2 km of shore, the site will be capable of hosting point absorber and oscillating water column WEC devices up to a peak power of 1 MW.

The site is located in Hawaiian state waters at approximately 21.47 N, 157.75 W (Figure 15). The deep water mooring sites overlay a featureless sandy substrate on a slightly steeper slope (Department of the Navy 2014). Figure 16 shows the bathymetry near Mokapu and the surrounding area. The wave climate at the test site is dominated by swells from the North Pacific, which are more frequent in the winter, and year-round waves formed by the northeast trade winds, which peak in the summer months between May-October (Department of the Navy 2014). The wave environment at WETS is characterized by an annual average power flux of 10–15 kW/m, with a significant number of events exceeding 40 kW/m each year. Despite this reliable wave energy, quiet periods are likely throughout the year, providing year round access to WEC devices.

NAVFAC operates the site and handles the permitted berths, grid connection infrastructure, device-specific permits, and offers office space. Typically a Cooperative Research and Development Agreement (CRADA) or a Navy contract is set up.

The Hawaii National Energy Institute at the University of Hawaii (HNEI-UH) is working with NAVFAC and DOE to support efforts at WETS in three key areas: (1) independent WEC device performance analysis; (2) environmental impact monitoring; and, (3) outfitting of a site-dedicated at-sea support platform. Environmental monitoring consists of ongoing measurements and analysis of the device acoustic signature, device and cabling electromagnetic fields (EMF), and possible changes in the device/mooring-induced sediment transport, seawater chemistry, and the ecological environment. HNEI will independently assess the device performance through robust wave environment measurements using Waverider buoys and an ADCP, wave forecast modeling, comprehensive device power output monitoring, the creation of power matrices to characterize performance as a function of wave state, and regular diver and ROV inspections of the deployed devices and associated mooring and cabling infrastructure. An additional UH effort is aimed at utilizing the data from WETS

to advance geophysical fluid dynamics-based models of device performance to guide design

Figure 15: WETS is located on the northeast shore of Oahu, Hawaii near the Marine Corps Base Hawaii (MCBH). The site is 1–2 km off-shore in 30-80 m depth water and has one operational berth and two berths under construction. One National Data Buoy Center ocean buoy and one National Data Buoy Center meteorological station are close to the site (see Table 2). The Heeia Kea Small Boat Harbor is located in Kaneohe Bay and a boatyard is accessible in Honolulu, HI. The hindcast simulation used two points of reference as shown. Image modified from Google Earth (2014).

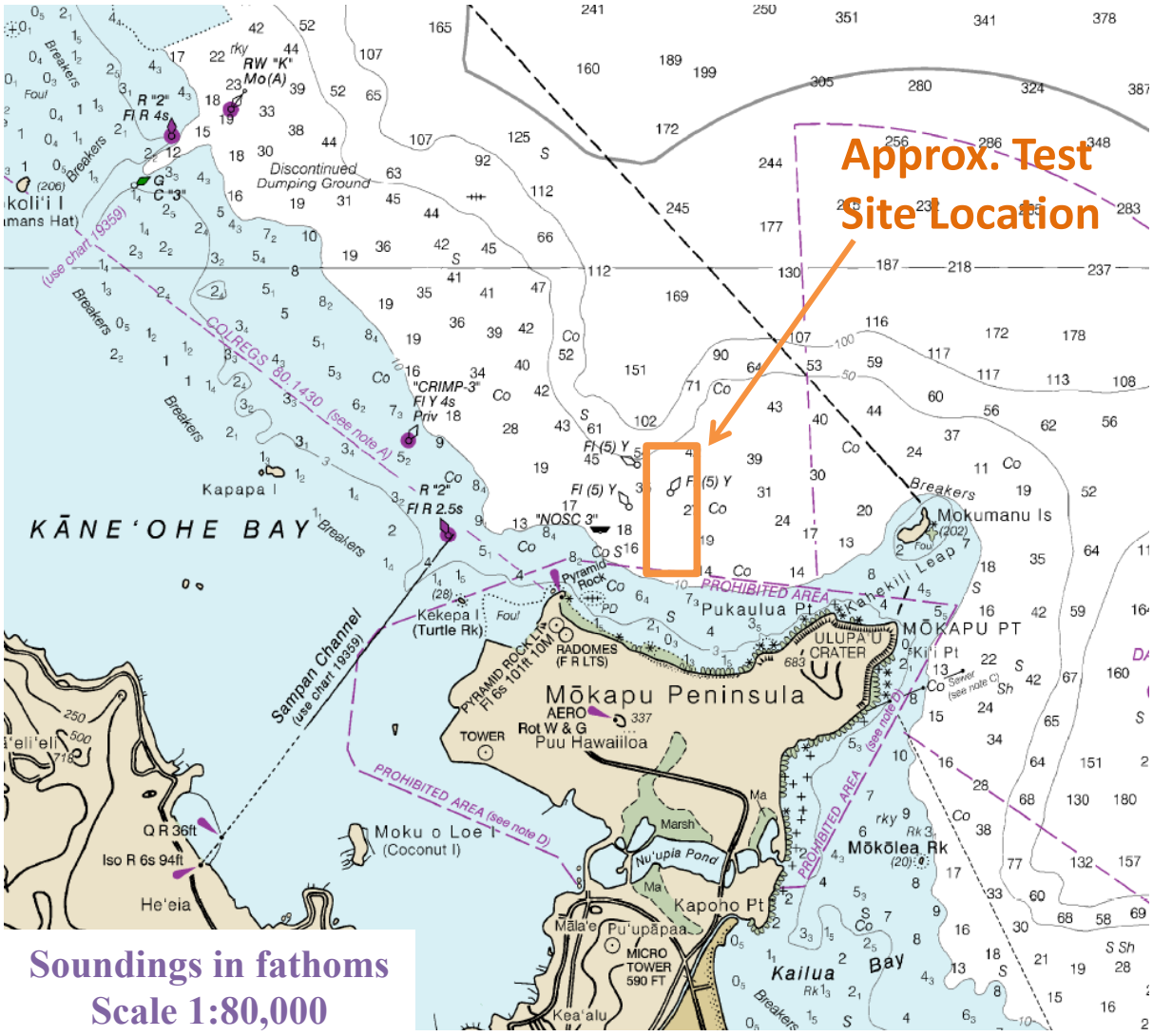

Figure 16: Nautical Chart of Mokapu Peninsula and surrounding area shows the gradually sloping bathymetry at WETS. Soundings in fathoms (1 fathom = 1.8288 m). Image modified from nautical chart #19357 (Office of Coast Survey 2013).

4.2. WEC Testing Infrastructure

4.2.1. Mooring Berths

There is one mooring berth at WETS and two under construction (Figure 17). The 30 m mooring berth uses a three point mooring system (a tri-moor configuration) with three sub-surface floats, two rock-bolted anchor bases and one gravity anchor. The mooring berth is fully functional and was used for testing a WEC device by Ocean Power Technologies between 2003 and 2011. Two deeper mooring berths at 60 m and 80 m are scheduled to be operational by July 2015. They also employ three point mooring systems and each utilizes three surface floats and three drag embedment anchors, with the majority of the mooring system components provided by the Navy, including the anchor, ground change, mooring chain, and surface buoy. Figure 18 shows a schematic of one of the three mooring legs for the 60 m and 80 m berths which were designed by Sound & Sea Technology.

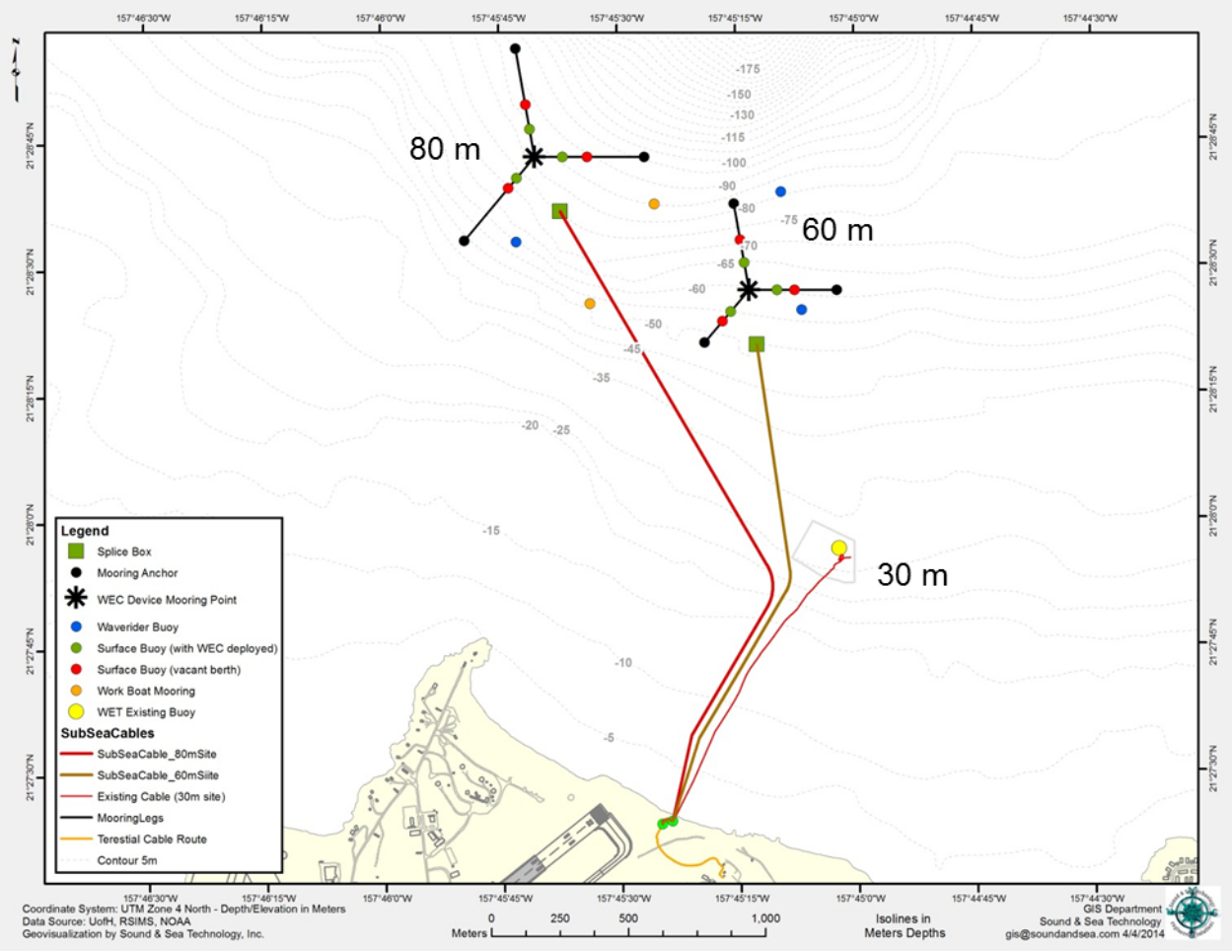

Figure 17: WETS mooring configuration and bathymetry map showing underwater cables and the three mooring sites at 30 m, 60 m, and 80 m depth (De Visser and Vega 2014).

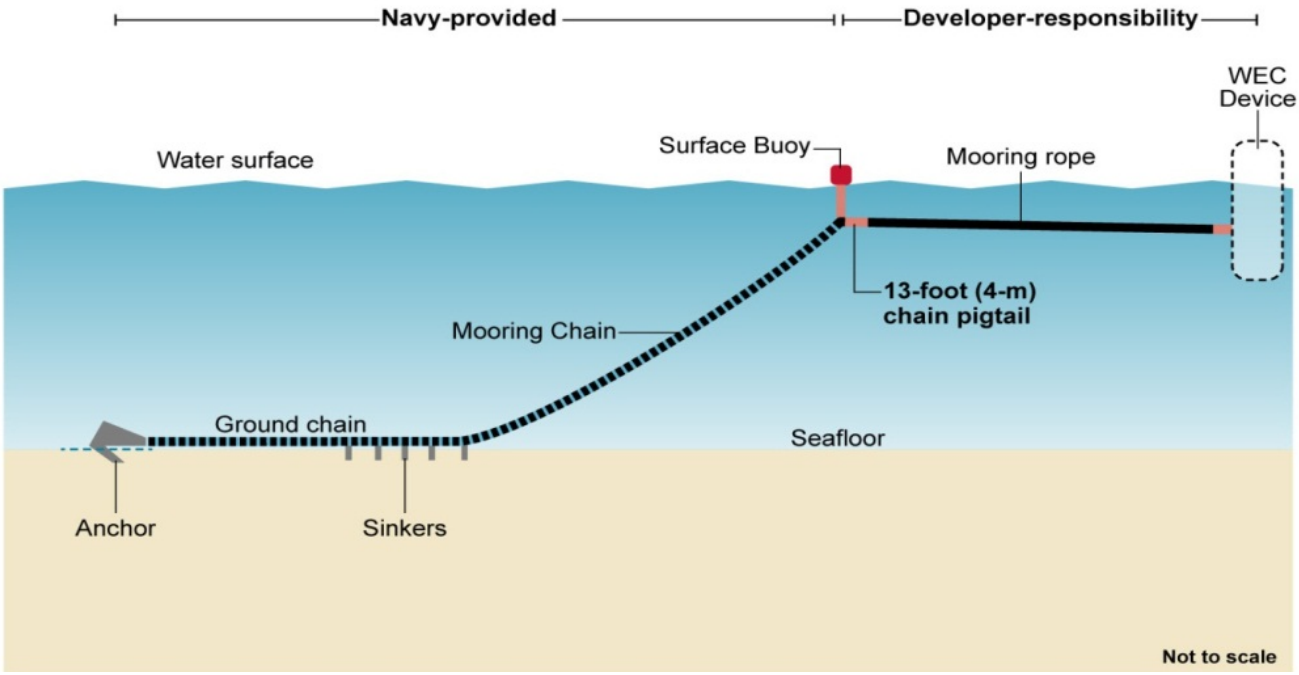

Figure 18: Sound & Sea Technology schematic of WETS 60 m and 80 m berths (De Visser and Vega 2014).

4.2.2. Electrical Grid Connection

WETS is a grid-accessible test site. An existing subsea cable with a maximum transmitting power of 250 kW at 4160 V services the 30 m mooring berth (De Visser and Vega 2014). Two additional cables are planned for installation by July 2015 to service the 60 m and 80 m mooring berths and will transmit up to 1 MW at 11,500 V (De Visser and Vega 2014).

4.2.3. Facilitating Harbor

To the West and to the East of WETS is Kaneohe Bay and Kailua Bay, respectively, which are both popular recreation destinations. For boat mooring, the Heeia Kea Small Boat Harbor (Waypoint #1 in Figure 15) offers 54 moorings, 21 berths and 3 boat ramps (State of Hawaii Division of Boating and Ocean Recreation 2014).

4.2.4. On-Shore Office Space

WETS is 1–2 km offshore of the Marine Corps Base Hawaii (MCBH), which encompasses the area of Mokapu Peninsula. Office space is available through MCBH (De Visser and Vega 2014).

4.2.5. Service Vessel and Engineering Boatyard

A key focus at WETS, by the Navy, DOE, and HNEI, is reducing the considerable costs to developers associated with at-sea testing of WEC devices. The regular device and mooring inspections mentioned above are an important aspect of this. Additionally, HNEI plans to contract with a local ocean engineering company to provide a self-propelled barge equipped with cranes and hyperbaric chamber, dive and ROV facilities, an A-frame, and workspaces for WEC developers and UH scientists/engineers (Vega, 2014). To reduce mobilization costs and shorten emergency response time, this platform will be kept at Heeia Kea Small Boat Harbor, a state marina within an hours transit from the site. Further, a limited amount of emergency maintenance response will be provided to tenants at WETS, furthering HNEIs ability to fully document device reliability issues and develop operational and maintenance protocols for DOE and the Navy. In addition, several engineering boatyards are available in Honolulu Harbor with a variety of services available (Vega 2014).

4.2.6. Travel and Communication Infrastructure

The Honolulu International Airport is only a half hour drive from MCBH. Cellular phone coverage is adequate and consistent, and cell phones may be used on MCBH.

4.2.7. Met-Ocean Monitoring Equipment

Real-time meteorological and wave data are collected by two met-ocean buoys from the CDIP database, one on-shore meteorological station available through the Automated-Surface-Observing-System (ASOS) and one maintained by NOAA. Instrument and data specifications for this monitoring equipment are summarized in Table 2. Buoy data is accessible online at the CDIP databases. CDIP198 (NDBC 51207) (Figure 19 (a)) is located very close to the 80 m depth berth, and CDIP098 (NDBC 51202) (Figure 19 (b)) is located approximately 12 km southeast. On-shore, there is a meteorological station on MCBH near the site.

Figure 19: a) CDIP198 Waverider, b) CDIP098 Waverider (Coastal Data Information Program 2013).

Table 2: Wave monitoring equipment in close proximity to WETS.

Instrument Name (Nickname)	**CDIP198/ NDBC 51207**		**CDIP198/ NDBC 51202 (Mokapu Point, HI)**		**ASOS PHNG Kaneohe Bay Marine Corps Airfield**	**MOKH1 - 1612480 Mokuoloe, HI**
Type	Waverider Buoy		Waverider Buoy		Meteorological Station	Water Level Observation Network
Measured parameters	-std. met. data -spectral wave density data -spectral wave direction data		-std. met. data -spectral wave density data -spectral wave direction data		-wind dir & speed -barometric pressure -air temp -humidity	-wind dir & speed -gust -atmos press -air temp -water temp
Variables reported (includes derived variables)	*Std. Met.:* WVHT DPD APD MWD WTMP (30 min sampling period)	-Spectral Wave Density Spectral Wave direction (30 min sampling period)	*Std. Met.:* WVHT DPD APD MWD WTMP (30 min sampling period)	-Spectral Wave Density Spectral Wave direction (30 min sampling period)	WDIR WSPD (10 min sampling period) PRES ATMP 1 hour sampling period)	WDIR WSPD GST PRES ATMP WTMP (6 min sampling period)
Location	at WETS		directly east of Kailua Bay, 12 km southeast of WETS		Installed at MCBH, near the test site	on Coconut Island farther west into Kaneohe Bay than WETS)
Coordinates	21.477 N 157.753 W (21°28'39" N 157° 45'10"W)		21.417 N 157.668 W (21°25'1" N 157°40'4" W)		unknown	21.432 N 157.790 W (21°25'55" N 157°47'24" W)
Depth	81 m		82 m		unknown	-air temp height: 5.5 m above site elevation -anemometer height: 12.7 m above site elevation -barometer elev: 2.8 m above mean sea level
Data Start	10/27/2012		8/10/2000		unknown	6/25/2008
Data End	present		present		present	present
Period of Record	∼3 yrs		∼15 yrs		unknown	∼7 yrs
Owner/ Contact Person	Pacific Islands Ocean Observing System (PacIOOS) – "Data provided by Scripps" Data reported at http://cdip.ucsd.edu/?ximg=search&xsearch=198&xsearch_Dtype=Station_I		Pacific Islands Ocean Observing System (PacIOOS) – "Data provided by Scripps" Data reported at http://cdip.ucsd.edu/?ximg=search&xsearch=098&xsearch_type=Station_ID		http://www.aviationweather.gov/metar	NOAA Tides & Currents

4.2.8. Environmental Monitoring

Environmental conditions at WETS have been characterized by the Navy with support from HNEI. Background environmental data includes wave, current, and climate data, as well as bathymetry and sediment profiles (De Visser and Vega 2014). Environmental monitoring, provided by HNEI, consists of ongoing measurements and analysis of acoustics, electromagnetic fields (EMF), and ecological surveys (to determine possible changes in sediment transport, seawater chemical composition, and the ecological environment).

4.2.9. Permitting

The berths at the site are permitted for testing of generic point absorbers and oscillating water column (OWC) devices. Developers must individually complete device-specific categorical exclusion applications, and an Army Corp of Engineers permit.

4.3. Data Used

Researchers affiliated with the Hawaii National Marine Renewable Energy Center (HINMREC) at the University of Hawaii produced a 34 year hindcast dataset for the area offshore of Oahu (Li and Cheung 2014, Li et al. 2015). This hindcast is an improved version of that by Stopa et al. (2013). The 34 year dataset was used to calculate statistics of interest for the characterization. Note in Version 1 of this catalogue, only 10 years of the hindcast was available so data is updated to the full 34 years here. The hindcast data at two grid points (21.472 N, 157.747 W and 21.4775 N, 157.7526 W) for the 60 m "Kaneohe II" and 80 m "WETS" berths, respectively, were analyzed by UH (see Figure 15 and Figure 17 for location).

In addition to the hindcast data set, historical data from buoy NDBC 51202 was used to calculate estimates of extreme events because of its longer period of record (2001-2014). Historical data from buoy CDIP198/NDBC 51207 was used to calculate representative spectra because of its location at WETS. Wind data from CFSR was used, as explained in Section 2.3. A high resolution wind data set for the Hawaiian Islands (in addition to the global CFSR data set) was utilized in the hindcast by Li and Cheung (2014), and therefore monthly averages will be provided in Appendix B as well. As with the other sites, current data was downloaded from OSCAR. See Figures 15 and 20 for data locations.

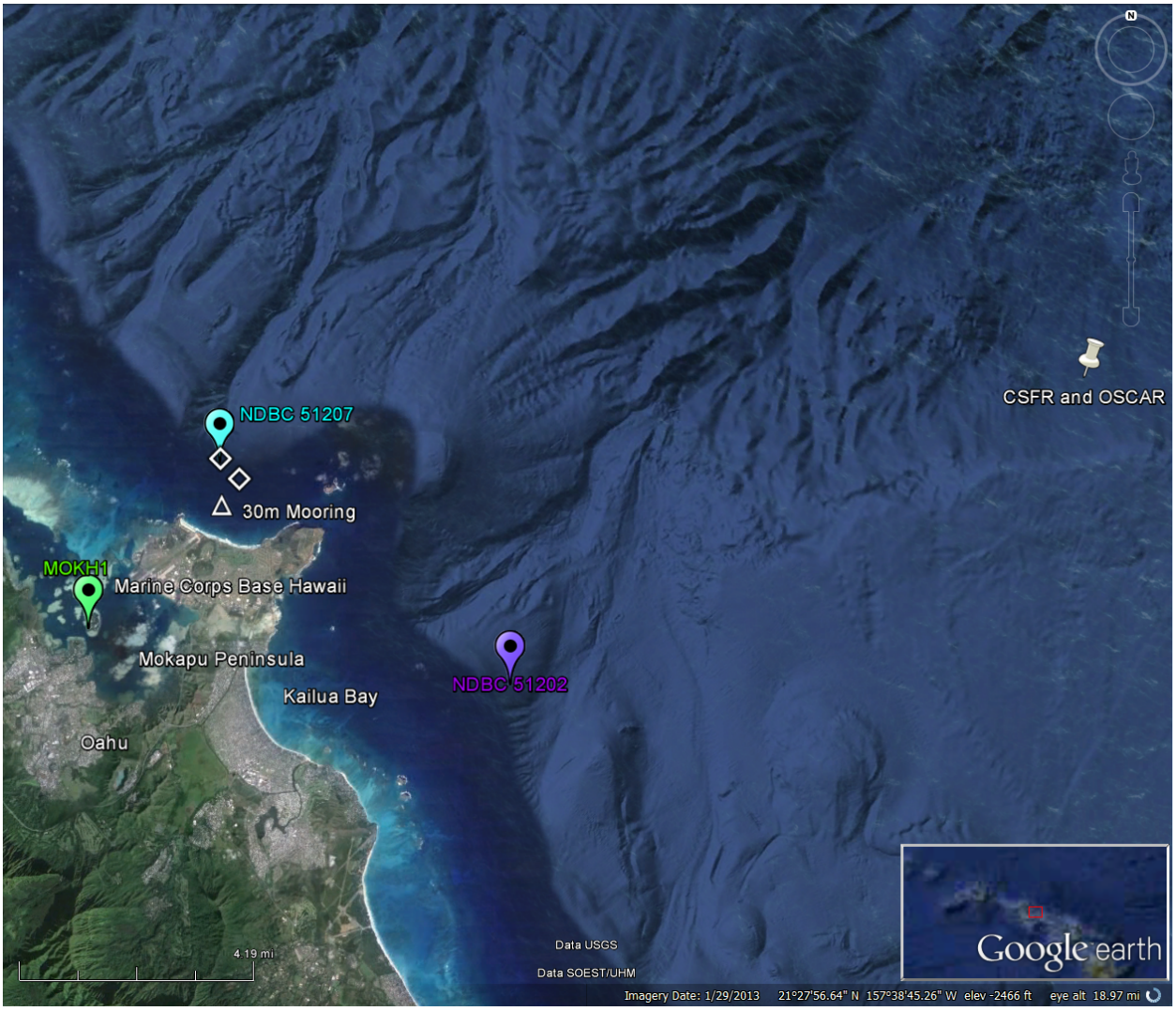

Figure 20: Two wave buoys and one met station surround the test site. The data points for OSCAR and CSFR overlap at 21.5 N, 157.5 W (Google Earth 2014).

4.4. Results

The following sections provide information on the joint probability of sea states, the variability of the IEC TS parameters, cumulative distributions, weather windows, extreme sea states, and representative spectra. This is supplemented by wave roses as well as wind and surface current data in Appendix B. The wind and surface current data provide additional information to help developers plan installation and operations & maintenance activities.

4.4.1. Sea States: Frequency of Occurrence and Contribution to Wave Energy

Joint probability distributions of the significant wave height, H_{m0}, and energy period, T_e, are shown in Figures 21 and 22. Figure 21 (top) shows the frequency of occurrence of each binned sea state and Figure 21 (bottom) shows the percentage contribution to the total

wave energy for "Kaneohe II" berth (60 m depth). The same information is shown for the "WETS" berth (80 m depth) in Figure 22. Figure 21 (top) and Figure 22 (top) indicate that the majority of sea states are within the range 1 m $< H_{m0} <$ 2.5 m and 5 s $< T_e <$ 11 s. WETS experiences a minimal amount of extreme sea states, which rarely exceed 5 m. The site is well suited for testing WECs at various scales, and testing the operation of WECs under normal sea states. Year-round testing occurs at WETS and the winter storms may be considered for survival testing for scaled devices (compared to a full-scale devices deployed in a higher energy location).

As mentioned in the methodology (Section 2.2), previous studies show that sea states with the highest occurrence do not necessarily correspond to those with the highest contribution to total wave energy, as is the case in Figure 21 and Figure 22. The total wave energy in an average year is 114,450 kWh/m at the Kaneohe II berth and 125,850 kWh/m at the WETS berth, which corresponds to an average annual omnidirectional wave power of 13.0 kW/m and 14.3 kW/m. The most frequently occurring sea state is within the range 1 m $< H_{m0} <$ 1.5 m and 6 s $< T_e <$ 7 s for Kaneohe II, and 1.5 m $< H_{m0} <$ 2 m and 6 s $< T_e <$ 7 s for WETS, while the sea state that contributes most to energy is within the range 1.5 m $< H_{m0} <$ 2 m and 7 s $< T_e <$ 8 s for both Kaneohe II and WETS. Several sea states occur at a similar frequency, and sea states within 1 m $< H_{m0} <$ 2 m and 6 s $< T_e <$ 8 s contribute a similar amount to energy.

Frequencies of occurrence and contributions to energy of less than 0.01% are considered negligible and are not shown for clarity. For example, the sea state within 0.5 m $< H_{m0} <$ 1 m and 13 s $< T_e <$ 14 s has an occurrence of 0.01%. The contribution to total energy, however, is only 0.007% and, therefore, does not appear in Figure 21 (bottom). Similarly, the sea state within 3 m $< H_{m0} <$ 3.5 m and 16 s $< T_e <$ 17 s has an occurrence of 0.003%, but the contribution to total energy is 0.02%.

Curves showing the mean, 5^{th} and 95^{th} percentiles of wave steepness, H_{m0}/δ, are also shown in Figure 21 and Figure 22. The mean wave steepness is 0.0175 ($\approx$1/57) at Kaneohe II and 0.0186 ($\approx$1/54) at WETS. The 95^{th} percentile is 0.0287 ($\approx$1/35) at Kaneohe II and 0.0303 ($\approx$1/33) at WETS.

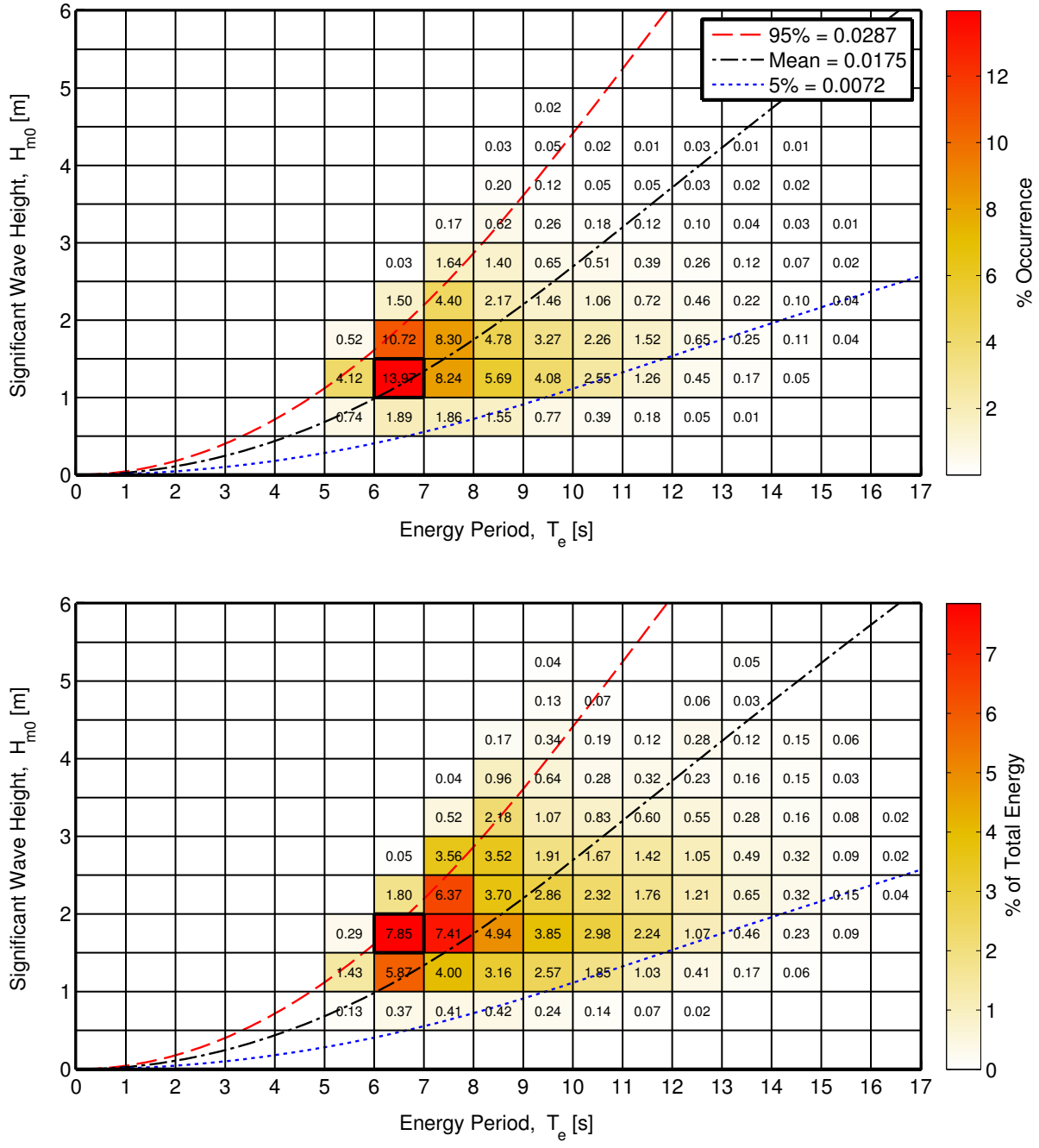

Figure 21: Joint probability distribution of sea states for the Kaneohe II berth (60 m depth). The top figure is frequency of occurrence and the bottom figure is percentage of total energy, where total energy in an average year is 114,450 kWh/m.

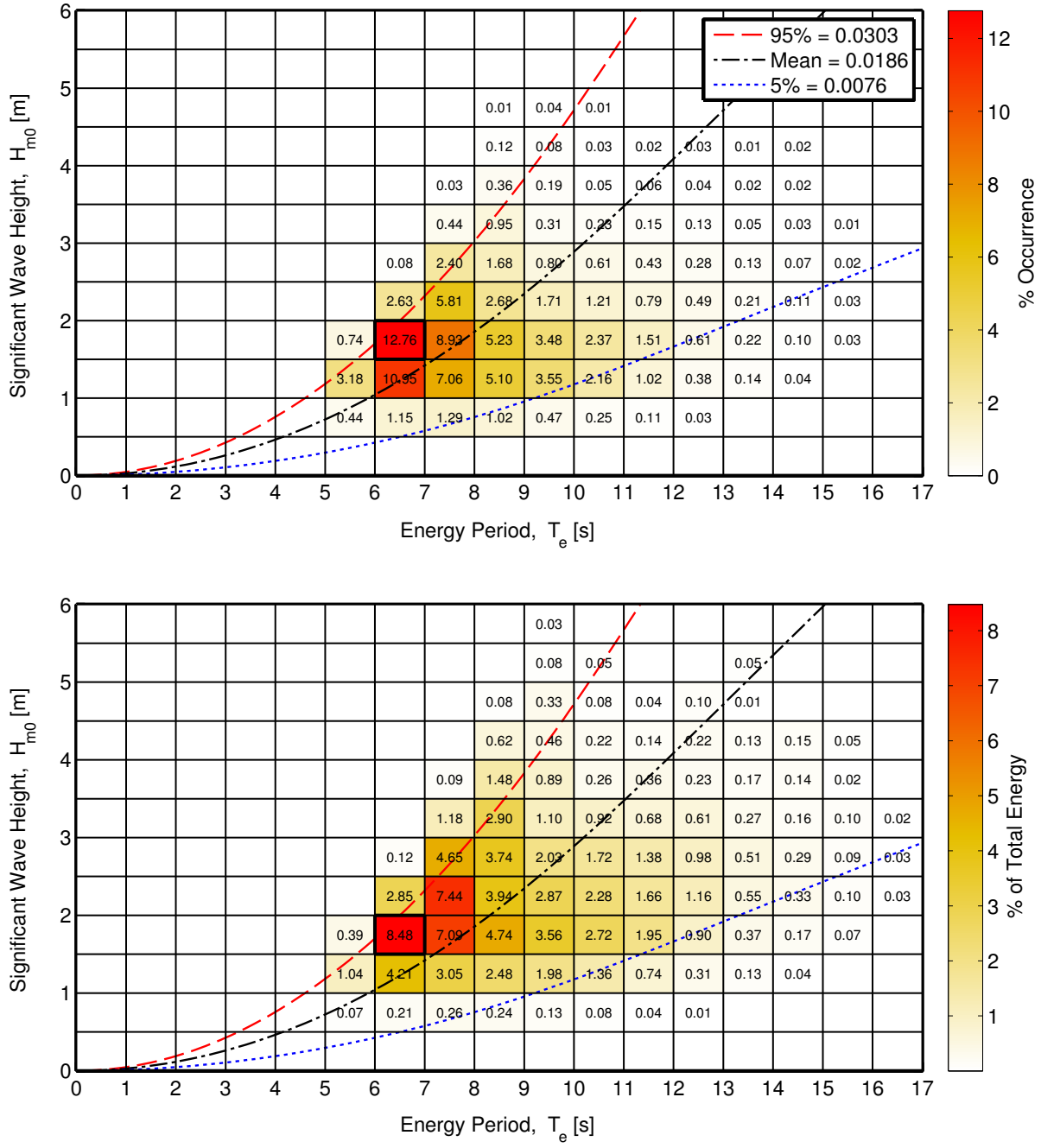

Figure 22: Joint probability distribution of sea states for the WETS berth (80 m depth). The top figure is frequency of occurrence and the bottom figure is percentage of total energy, where total energy in an average year is 125,850 kWh/m.

4.4.2. IEC TS Parameters

The monthly means of the six IEC TS parameters, along with the 5^{th} and 95^{th} percentiles, are shown in Figures 23 and 24. The values in the figures are summarized in Tables 13 and 14 in Appendix B.

Monthly means of the omnidirectional wave power, J, significant wave height, H_{m0}, and energy period, T_e, show the greatest seasonal variability compared to the other parameters. Values are largest and vary the most during the winter months. These observations are consistent with the relationship between wave power density, significant wave height and energy period, where wave power density, J, is proportional to the energy period, T_e, and the square of the significant wave height, H_{m0}.

The directionality coefficient (larger values indicate low directional spreading), is slightly larger in the summer, and it can be seen that the direction of maximum directionally resolved wave power (defined as the direction from which waves arrive in degrees clockwise from north), is most consistently from north/northeast during the summer, and varies more throughout the rest of the year. This is because summer months are dominated by wind waves from the northeast, while the winter months are made up of both wind waves and frequent swells from the North Pacific.

Seasonal variation of the spectral width, ϵ_0, is much less than the other parameters and barely discernable. Monthly means for ϵ_0 remain nearly constant between 0.35 and 0.4. In summary, the waves at both the Kaneohe II and WETS berths, from the perspective of monthly means, have a fairly consistent spectral width, are predominantly from the north/northeast, and exhibit a wave power that has a fairly narrow directional spread in the summer, and a wider directional spread in the winter.

Wave roses of wave power and significant wave height, presented in Appendix B, Figure 126 and Figure 127, also show the spread of direction of the maximum wave energy at WETS. The larger waves (with higher wave power), often come as swells from the North Pacific, while smaller waves usually come from the northeast as wind waves. Figure 126 shows two dominant wave direction sectors, northeast and approximately east-northeast (ENE). Along the predominant wave direction, which is northeast (45°), the omnidirectional wave power density is at or below 35 kW/m less than 25% of the time, and greater than 35 kW/m approximately 1-2% of the time. Along the ENE direction (60°), wave power density is at or below 35 kW/m about 25% of the time and rarely (about 1% of the time) exceeds 35 kW/m.

Note that the wave climate is made up of swells from the North and South Pacific and year-round wind waves from the northeast. Therefore the direction of maximum directionally resolved wave power may not fully describe the origin of the wave power (i.e., the combination of swells and year-round wind waves from slightly different directions).

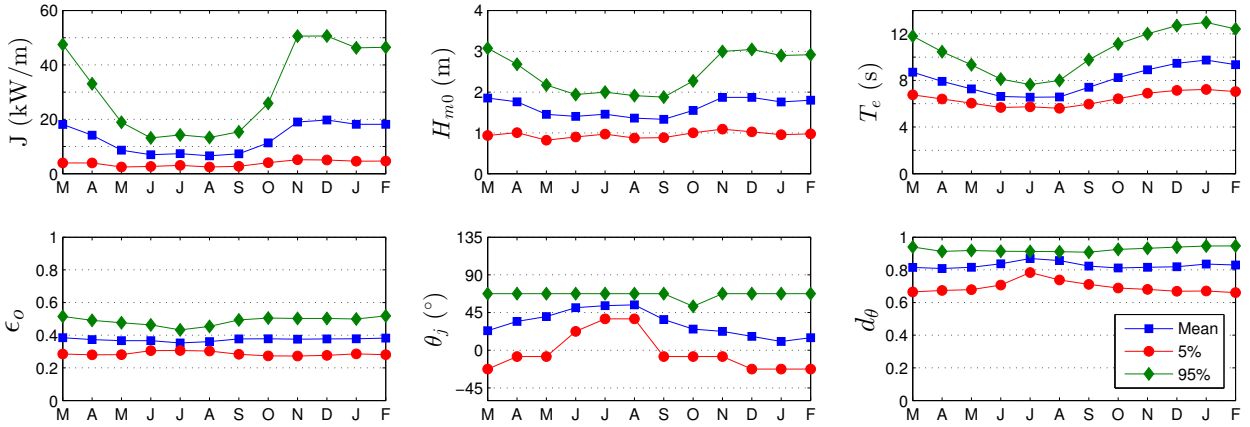

Figure 23: The average, 5^{th} and 95^{th} percentiles of the six parameters at Kaneohe II.

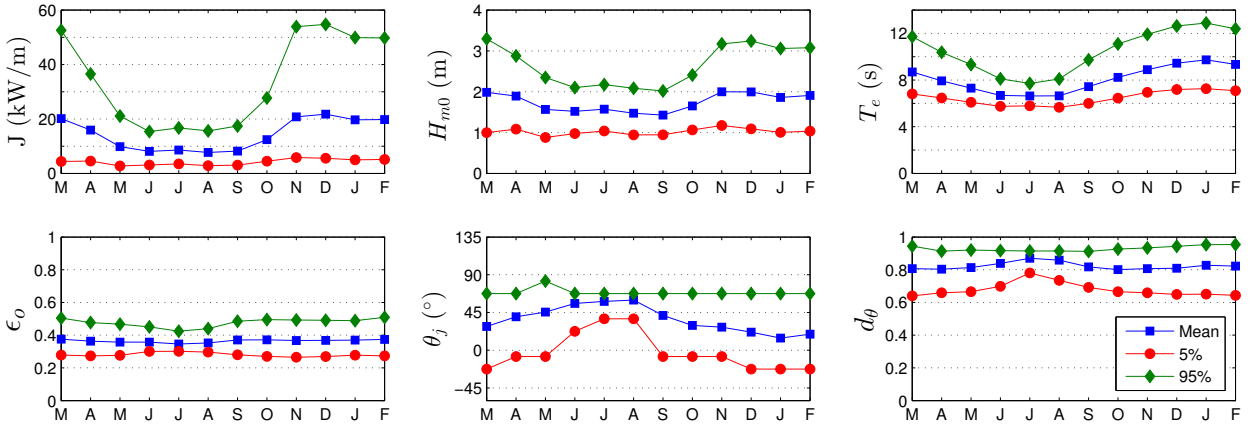

Figure 24: The average, 5^{th} and 95^{th} percentiles of the six parameters at WETS.

Monthly means, however, smear the significant variability of the six IEC parameters over small time intervals as shown in plots of the six IEC TS parameters at 1-hour intervals in Figure 25 for a representative year. While seasonal patterns described for Figures 23 and 24 are still evident, these plots show how sea states can vary abruptly at small time scales with sudden changes, e.g., jumps in the wave power as a result of a storm. Note that the data in Figure 25 is from NDBC 51207, co-located at the WETS 80 m berth.

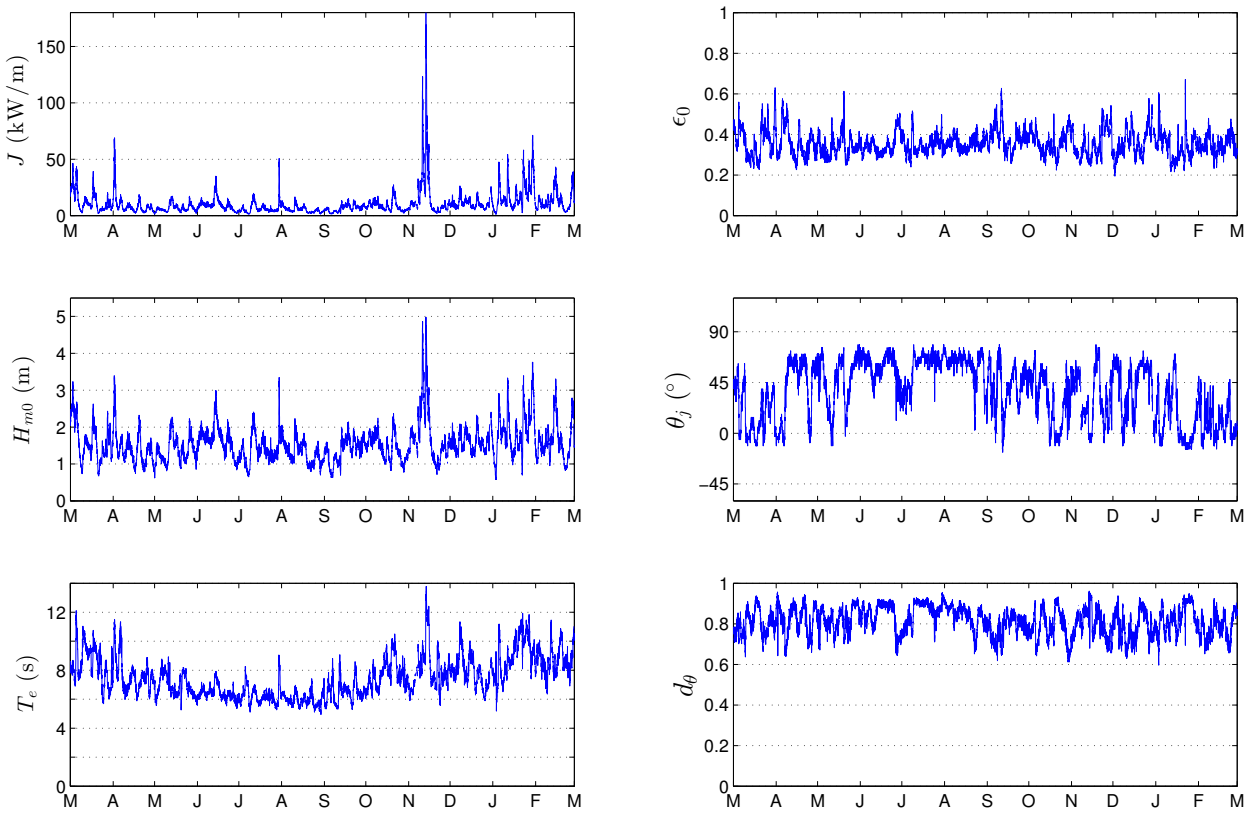

Figure 25: The six parameters of interest over a one-year period, March 2013 – February 2014 at NDBC 51207 co-located at the WETS 80 m berth.

4.4.3. Cumulative Distributions

Annual and seasonal cumulative distributions (a.k.a., cumulative frequency distributions) at WETS are shown in Figure 26. Note that spring is defined as March – May, summer is June – August, fall is September – November, and winter is December – February. The cumulative distributions are another way to visualize and describe the frequency of occurrence of individual parameters, such as H_{m0} and T_e. A developer could use cumulative distributions to estimate how often they can access the site to install or perform operations and maintenance based on their specific device, service vessels, and diving operation constraints. For example, if significant wave heights need to be less than or equal to 1 m for installation and recovery, according to Figure 26, this condition occurs about 5% of the time on average within a given year. If significant wave heights need to be less than or equal to 2 m for emergency maintenance, according to Figure 26, this condition occurs about 74% of the time on average within a given year. Cumulative distributions, however, do not account for the duration of a desirable sea state, or weather window, which is needed to plan deployment and servicing of a WEC device at a test site. This limitation is addressed with the construction of weather window plots in the next section.

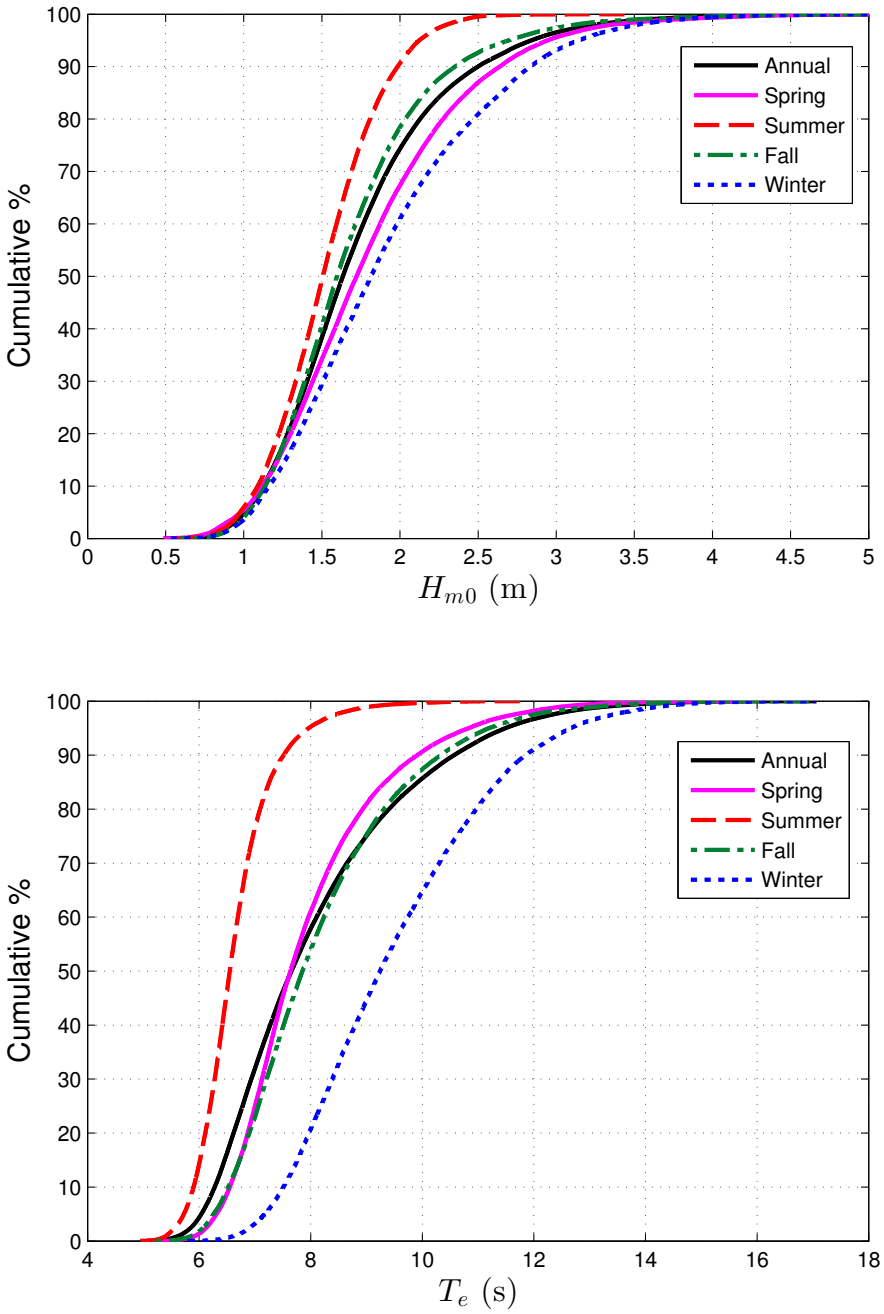

Figure 26: Annual and seasonal cumulative distributions of the significant wave height (top) and energy period (bottom) at WETS.

4.4.4. Weather Windows

Figure 27 shows the number of weather windows at WETS, when significant wave heights are at or below some threshold value for a given duration, for an averaged winter, spring, summer, and fall. In these plots, each occurrence lasts a duration that is some multiple of 6-hours. The minimum weather window is, therefore, 6-hours in duration, and the maximum

is 96-hours (4 days). The significant wave height threshold is the upper bound in each bin and indicates the maximum significant wave height experienced during the weather window. Note that the table is cumulative, so, for example, an occurrence of $H_{m0} \leq 1m$ for at least 42 consecutive hours in the fall is included in the count for 36 consecutive hours as well. In addition, one 12-hour window counts would count as two 6-hour windows. Although there are more occurrences of lower wave heights during the summer than winter (which corresponds to increased opportunities for deployment or operations and maintenance), the difference is not as significant at this site compared to others. The summer does have increased opportunities for deployment, however, it it still somewhat rare to find a longer weather window under 1 m. This is due to the consistent year-round trade winds. The timeseries in Figure 25 confirms that although wave heights remain fairly low in the summer (typically not exceeding 3 m), they rarely fall below 1 m. This also can be seen in Figure 24 where the 5^{th} percentile of H_{m0} remains near 1 m throughout the year.

Weather window plots provide useful information at test sites when planning schedules for deploying and servicing WEC test devices. For example, if significant wave heights need to be less than or equal to 1 m for at least 12 consecutive hours to service a WEC test device at WETS with a given service vessel, there would be, on average, nine weather windows in the summer, but only five in the winter. When wind speed is also considered, Figure 28 shows the average number of weather windows with the additional restriction of wind speed, $U < 15$ mph. Note that wind data was available from this hindcast, and was used herein (Ning and Cheung 2014), see Section B.4. For shorter durations (6- and 12-hour windows), daylight is necessary. Windows with $U < 15$ mph and only during daylight hours are shown in Figure 29. Daylight was estimated as 5am - 10pm Local Standard Time (LST).

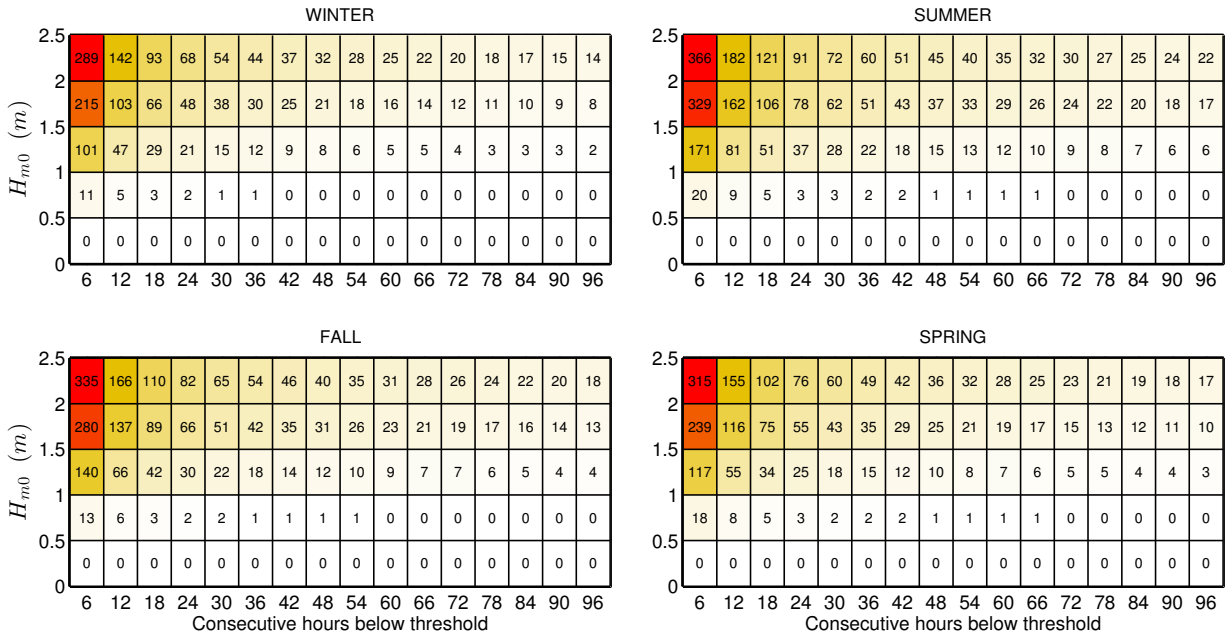

Figure 27: Average cumulative occurrences of wave height thresholds (weather windows) for each season at WETS. Winter is defined as December – February, spring as March – May, summer as June – August, and fall as September – November.

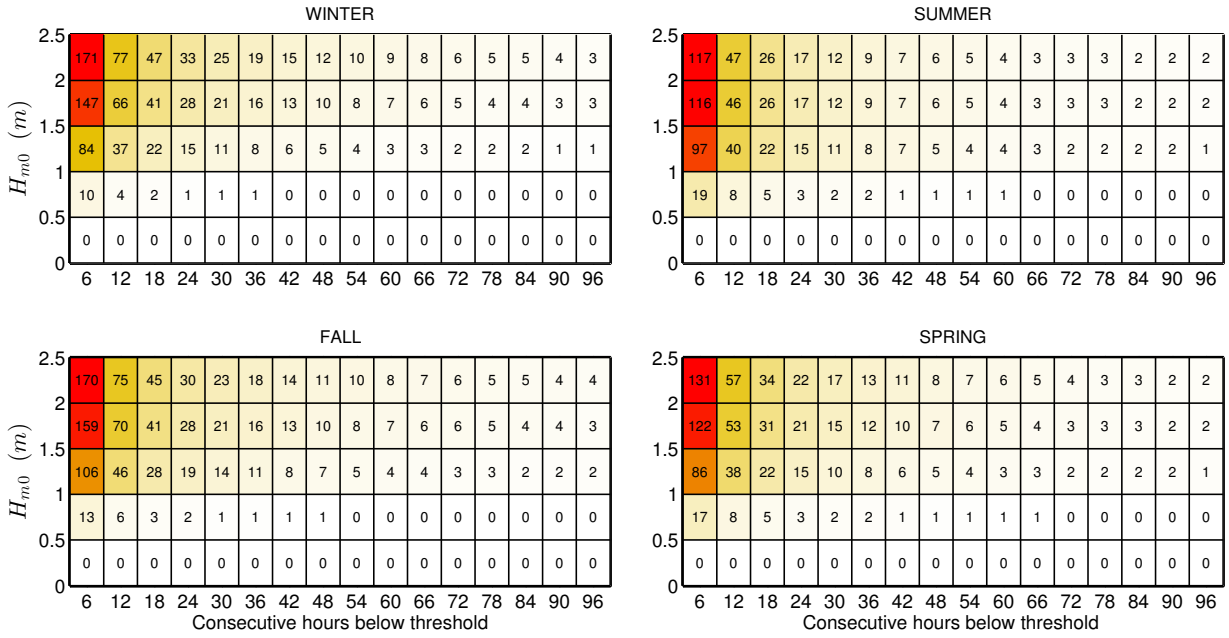

Figure 28: Average cumulative occurrences of wave height thresholds (weather windows) for each season at WETS with an additional restriction of $U < 15$ mph.

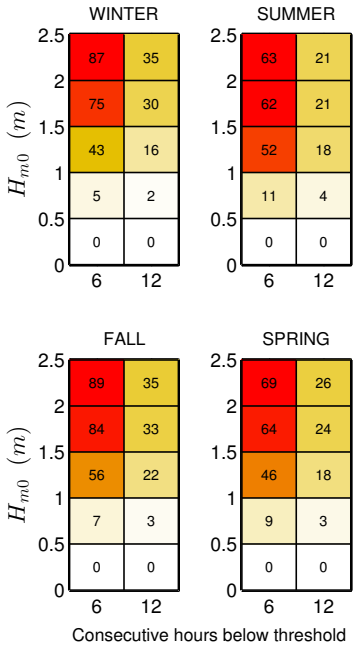

Figure 29: Average cumulative occurrences of wave height thresholds (weather windows) for 6- and 12-hour durations with $U < 15$ mph and only during daylight hours (5am - 10pm LST) at WETS.

4.4.5. Extreme Sea States

The modified IFORM was applied using CDIP098 / NDBC51202 to generate the 100-year environmental contour for WETS shown in Figure 30. Although there is a buoy co-located at WETS (CDIP198/NDBC51207), the period of record is only about three years, and therefore it was necessary to use a nearby buoy with a longer period of record (see Table 2 for buoy information). Selected sea states along this contour are listed in Appendix B, Table 15.

As stated in Section 1.2, environmental contours are used to determine extreme wave loads on marine structures and design these structures to survive extreme sea states of a given recurrence interval, typically 100-years. For WETS, the largest significant wave height estimated to occur every 100-years, is over 7.2 m, and has an energy period of about 13.0 s. However, significant wave heights lower than 7.2 m, with energy period less than or greater than 13 s, listed in Appendix B, Table 15, could also compromise the survival of the WEC test device under a failure mode scenario in which resonance occurred between the incident wave and WEC device, or its subsystem. For comparison, 50- and 25-year return period contours are also shown in Figure 30. The largest significant wave height on the 50-year contour is 6.9 m with an energy period of about 12.7 s, and on the 25-year contour is 6.6 m and 12.5 s. It should be noted that conditions at the NDBC51207 buoy may differ significantly from the conditions at the test site, even thought they are at similar depths, NDBC51202 is outside of Kaneohe Bay.

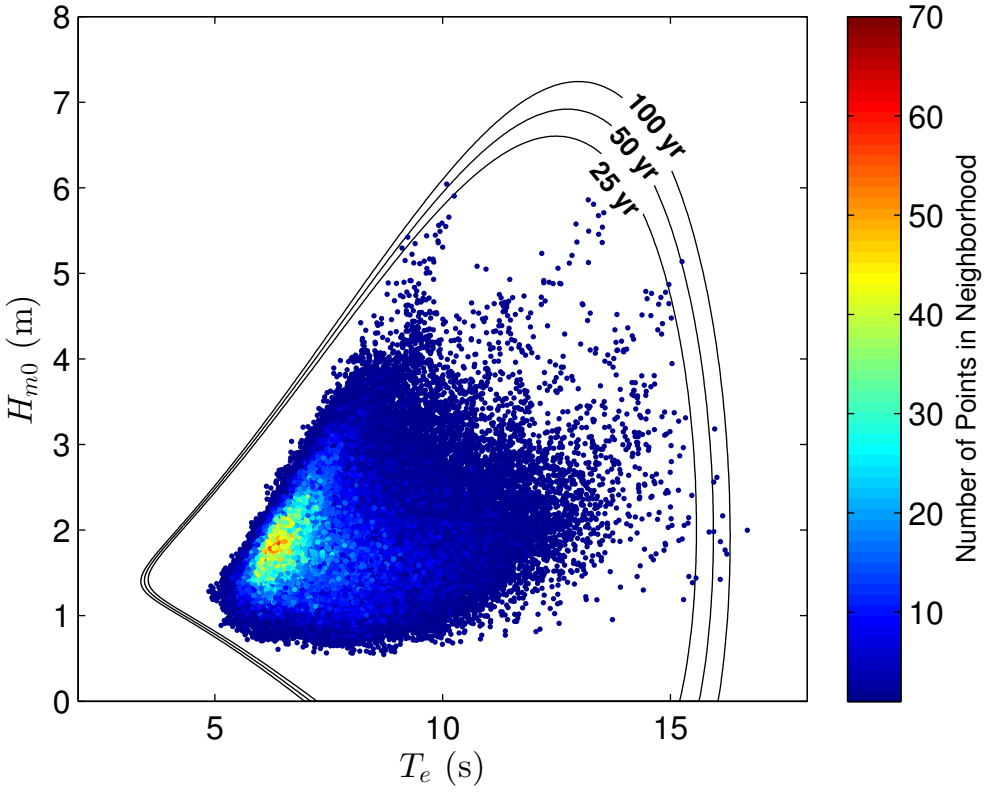

Figure 30: 100-year contour for CDIP098/NDBC51202 (2001 – 2014).

4.4.6. Representative Wave Spectrum

All hourly discrete spectra measured at CDIP198 / NDBC51207 for the most frequently occurring sea states are shown in Figure 31. The most frequently occurring sea state, which is within the range 1.5 m $< H_{m0} <$ 2 m and 6 s $< T_e <$ 7 s, was selected from a JPD similar to Figure 22 in Section 4.4.1, but based on the CDIP198 / NDBC51207 buoy data. As a result, the JPD, and therefore the most common sea states, generated from buoy data are sometimes slightly different from that generated from hindcast data. However for this case, at WETS, the most frequently occurring sea state for the JPD generated from hindcast data is in the same range for both T_e (6 s $< T_e <$ 7 s) and H_{m0} (1.5 m $< H_{m0} <$ 2 m). Often several sea states will occur at a very similar frequency, and therefore plots of hourly discrete spectra for several other sea states are also provided for comparison. Each of these plots includes the mean spectrum and standard wave spectra, including Bretschneider and JONSWAP, with default constants as described in Section 2.2.

For the purpose of this study, the mean spectrum is the 'representative' spectrum for each sea state, and the mean spectrum at the most common sea state, shown in Figure 31 (top-right plot), is considered the 'representative' spectrum at the site. The hourly spectra vary considerably about this mean spectrum, but this is partly reflective of the bin size chosen for H_{m0} and T_e. Comparisons of the representative spectra in all plots with the Bretschneider and JONSWAP spectra illustrate why modeled spectra with default constants, e.g., the shape parameter $\gamma = 3.3$ for the JONSWAP spectrum, should be used with caution. Using the constants provided in Section 2.2, the Bretschneider spectra are fair representations of the mean spectra in Figure 31. The mean measured spectra is the best representation of the conditions, however, if these modeled spectra were to be used at this site, it is recommended that the constants undergo calibration against some mean spectrum, e.g., the representative spectrum constructed here.

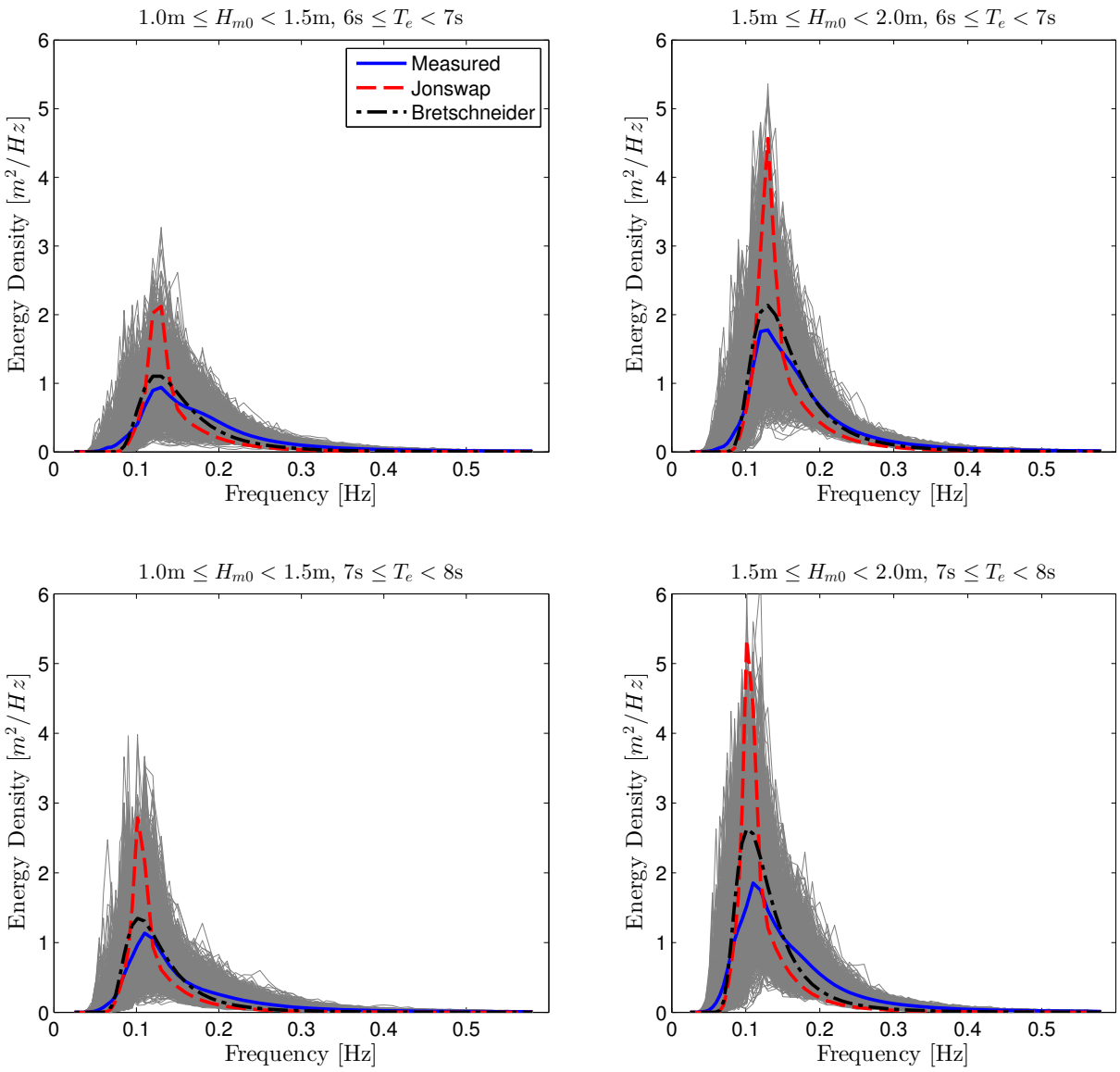

Figure 31: All hourly discrete spectra and the mean spectra measured at CDIP198 / NDBC 51207 within the sea state listed above each plot. The JONSWAP and Bretschneider spectra are represented by red and black dotted lines, respectively.

5. JENNETTE'S PIER WAVE ENERGY TEST CENTER

5.1. Site Description

Jennette's Pier, owned by the State of North Carolina and managed by the NC Aquarium Division, is a unique public facility that provides education and outreach including displays of experimental data and monitoring equipment. The University of North Carolina Coastal Studies Institute (UNC CSI) began a partnership with Jennette's Pier in 2004 to foster research, ocean energy device testing and monitoring, outreach, and education. Part of this partnership is the Jennette's Pier Wave Energy Test Center. The site was used for the first time in December 2011 by Resolute Marine Energy.

The Jennette's Pier Wave Energy Test Facility has two test berth locations, one approximately 80 m north of the pier structure at 6 m water depth (35.9119 N, 75.5933 W) that is called the 'nearshore berth' and one approximately 600 m east of the seaward end of the pier at 11 m depth (35.9123 N, 75.5863 W) that is called the 'offshore berth.' The seabed is sandy at both locations. Figure 33 shows the gently sloping bathymetry around the site, which consists of a wide shelf.

The wave climate at the test site varies seasonally, with calmer seas in the summer compared to more energetic seas in the winter. The wave environment at Jennette's Pier is characterized by an annual average power flux of about 6.08 kW/m at 12.6 m depth.

The nearby University of North Carolina (UNC) Coastal Studies Institute (CSI) offers a wide range of technical and testing infrastructure support services for WEC developers. Jennette's Pier has small scale, shallow water wave energy resources, and is suited for scaled devices.

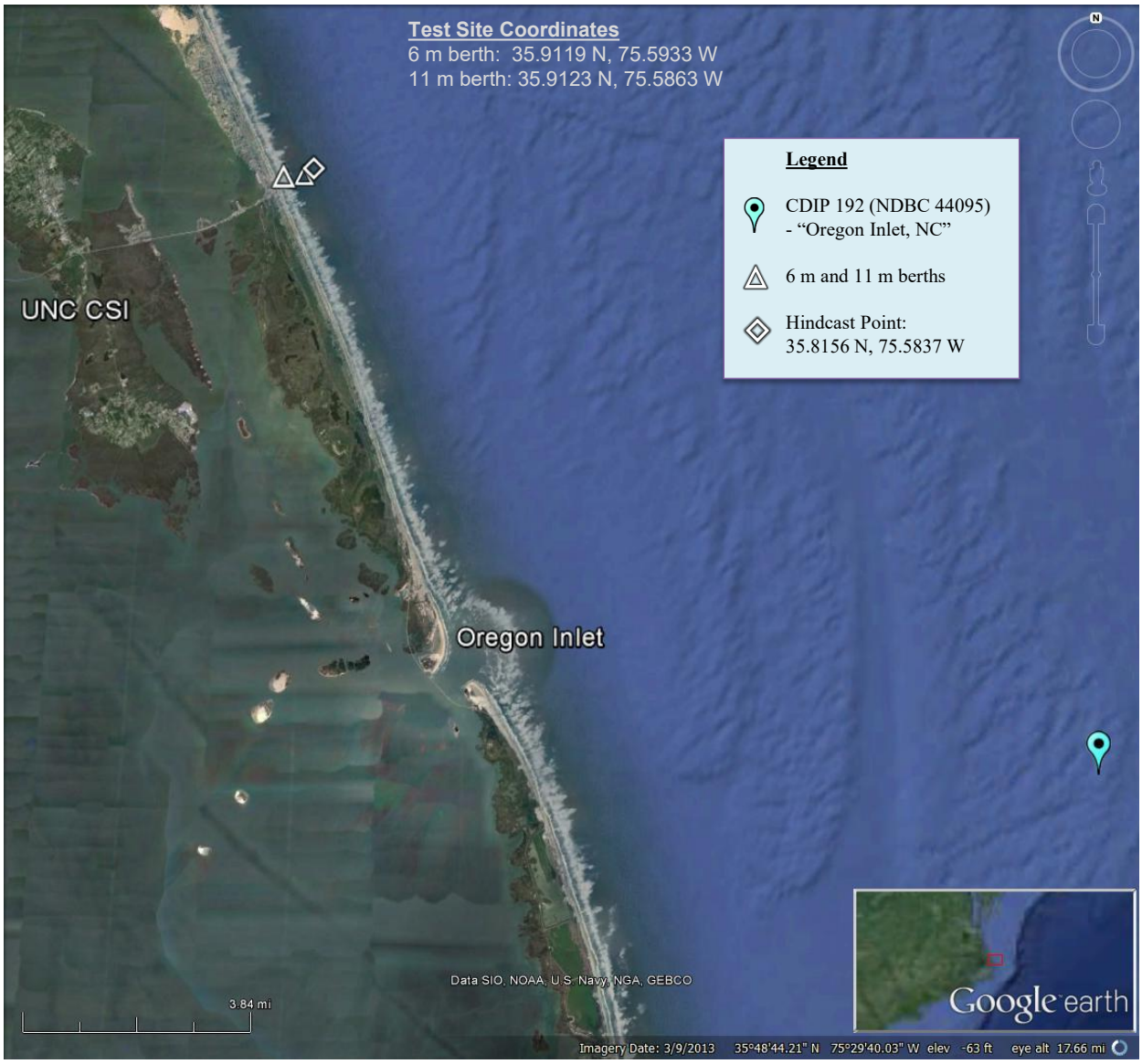

Figure 32: Jennette's Pier is located in the coastal waters of North Carolina in the town of Nags Head. The test site is 0.08 – 0.3 km off-shore in 6 – 11 m depth water. One National Data Buoy Center (NDBC) buoy is southeast of the site (see Table 3). The nearby UNC CSI is shown. Image modified from Google Earth (Google Earth 2015).

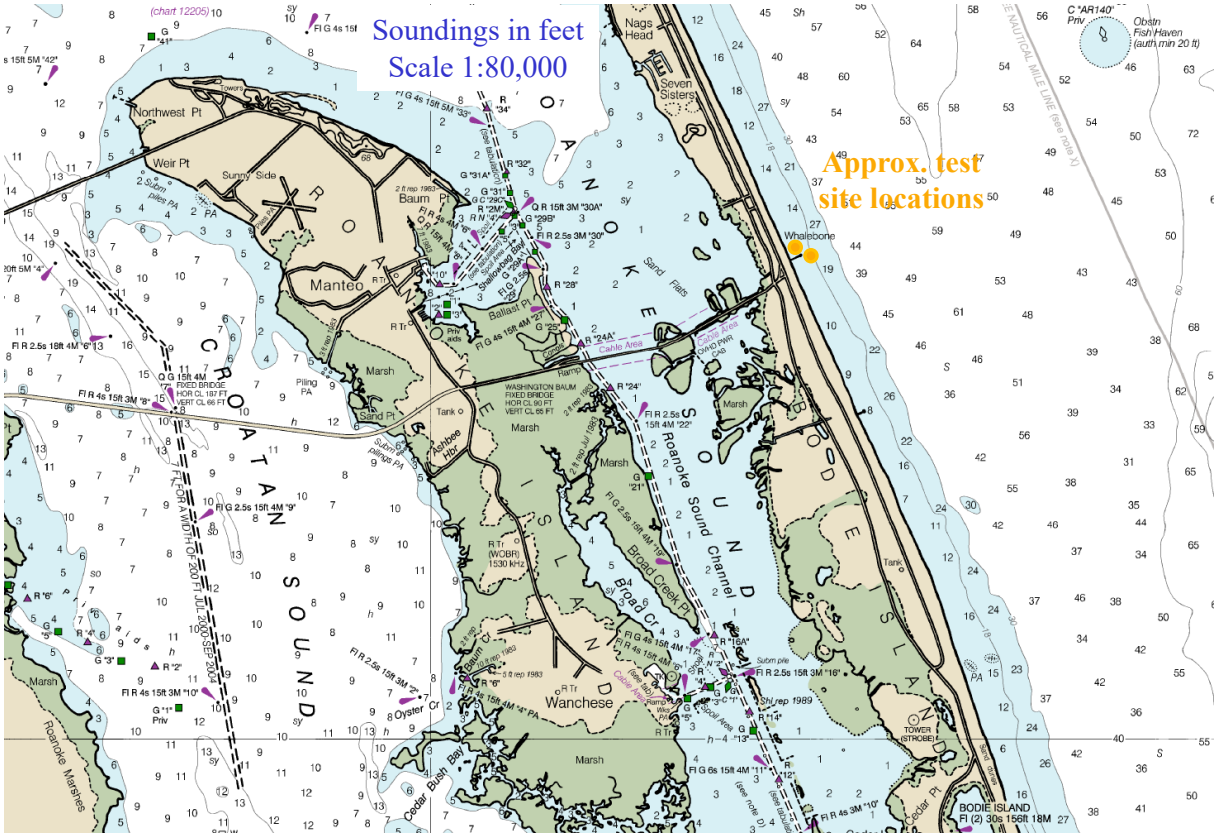

Figure 33: Nautical chart of Nags Head Island and the surrounding area shows the gradually sloping bathymetry off Jennette's Pier. Soundings in feet (1 foot = 0.3048 m). Image modified from nautical chart #12204 (Office of Coast Survey 2015).

5.2. WEC Testing Infrastructure

5.2.1. Mooring Berths

Moorings for wave energy devices will be temporary. Energy generated and monitoring instrumentation will be cabled to Jennette's Pier where there is a cable trough that protects cables running from the seabed to the research building at the seaward end of the pier and then to the pier house.

5.2.2. Electrical Grid Connection

Several renewable energy technologies are built into Jennette's Pier, including solar panels and three 10 kW wind turbines. The turbines are net metered and feed into the Pier substation (they do not feed into the grid). The Pier is exploring the possibility of similarly net metering wave energy devices tested at the site.

5.2.3. Facilitating Harbor

The Jennette's Pier Wave Energy Test Center can be accessed by boat via Oregon Inlet (∼10 miles from the Pier). Several harbors are within 10 miles of the inlet, including harbors and marinas at UNC CSI and Wanchese, from which service vessels and commercial divers are available. UNC CSI also has a Zodiac that can be beach-launched to support launch and recovery operations.

5.2.4. On-Shore Office Space

Office space is available for rent at UNC CSI, which is about 5 miles west of Jennette's Pier in Wanchese, NC. The Jennette's Pier research building is equipped with computers, which are cabled to the pier house. The pier house offers fiber optic connectivity, generator backup power, and a server that provides remote telemetric access to instrument data. In addition, the UNC CSI campus serves as a fiber hub for the MCNC NCREN network, resulting in upload and download speeds faster than T3 connections and latency of only 2 – 8 milliseconds.

5.2.5. Service Vessel and Engineering Boatyard Access

UNC CSI vessels are available for use, along with a vessel Captain, research technicians, and dive operations support for additional fees. Services from the UNC CSI fabrication shop including equipment rental and research equipment are available for a fee.

5.2.6. Travel and Communication Infrastructure

The Norfolk International Airport (ORF) is approximately a two hour drive from UNC CSI and Jennettes Pier. Raleigh Durham International Airport (RDU) is approximately a three hour drive from UNC CSI and Jennettes Pier. Cellular service offers consistent coverage; there are several Federal Communication Commission (FCC) registered cell phone towers located in and around Nags Head, NC.

5.2.7. Met-Ocean Monitoring Equipment

There is one Coastal Data Information Program (CDIP) buoy (Figure 34a) that measures and collects ocean data (see Figure 32 for location). There is also an Acoustic Wave and Current Gauge (AWAC) co-located at the 11 m berth (Figure 34b). Instrument and data specifications for this monitoring equipment are summarized in Table 3. Buoy data is accessible online at the CDIP and NDBC databases, and AWAC data is available through the U.S. Army Corps of Engineers Field Research Facility website. The land based meteorological station is north of the site. Other met stations are nearby with shorter periods of record. In addition, there are many measurements at Duck, NC (∼34 km northwest of Jennettes Pier), see Section 6.2.7.

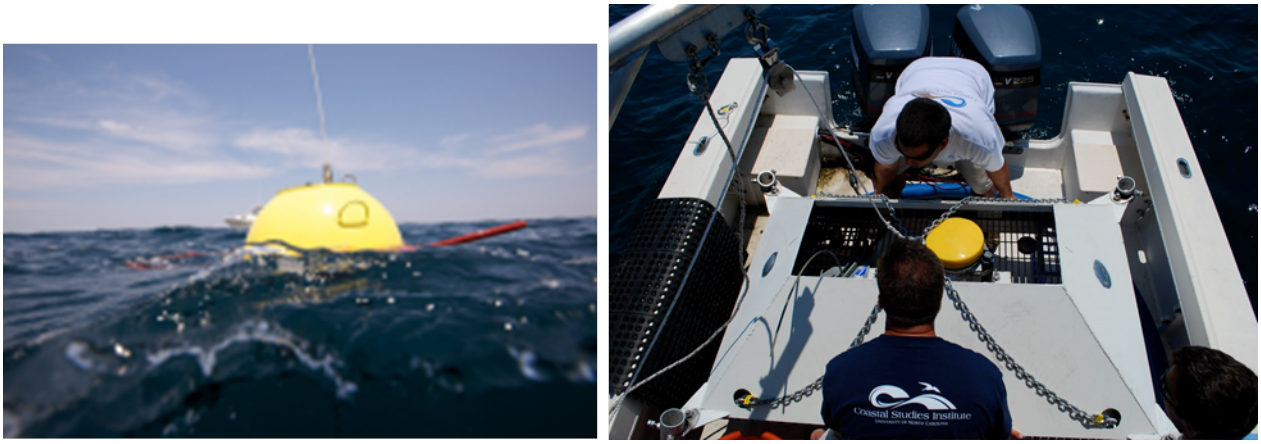

Figure 34: (a) CDIP 192 (NDBC 44095) located about 30 km southeast of the test site (Coastal Data Information Program 2013), (b) the AWAC being installed at the 11 m berth.

Table 3: Wave monitoring equipment in close proximity to Jennette's Pier.

Instrument Name (Nickname)	**NDBC 44095- CDIP 192 "Oregon Inlet, NC")**		**Jennette's Pier AWAC (awac05)**			**KNCNAGSH4**
Type	Waverider Buoy		Acoustic Wave and Current Gauge (AWAC)			Met station
Measured Parameters	-std. met. data -spectral wave density -spectral wave direction		-std. met. data -spectral wave density -spectral wave direction -current speed and direction			meteorological data
Variables reported, including derived variables (Sampling interval)	*Std Met.:* WVHT DPD APD MWD WTMP (30 min sampling period)	-Spectral Wave Density -Spectral Wave direction (30 min sampling period)	*Std Met.:* WVHT DPD MWD (1 hr sampling period)	-Spectral Wave Density -Spectral Wave direction (1 hr sampling period	-Longshore current speed -Cross-shore current speed (1 hr sampling period)	AirTemp DewPoint Pressure WDIR WSPD Humidity Precip (5 min sampling period)
Location	∼30 km southeast of Jennette's Pier; 7 miles off Oregon Inlet, NC		Co-located at 11 m berth			Nags Head, NC
Coordinates	35.750 N 75.330 W (35°45'0" N 75°19'48" W)		35.9123 N 75.5868 W (35°54.74' N 75°35.205' W)			35°56'54" N, 75°37'37" W
Depth	18.3 m		11.3 m			Elevation: 10 ft
Data Start	4/2012		consistent data since 9/2012 (sporadic data collection from 2009-2012)			11/25/2007
Data End	present		3/16/2014			present
Period of Record	∼3.5 yrs		∼1.5 yrs			∼8 yrs
Owner/ Contact Person	USACE, CDIP/UNC "Information Submitted by Scripps" http://cdip.ucsd.edu/themes/s?un=0&tz=UTC&pb=1&wp=0&hl=1&r=999&bl=s?d2=p70:s:128:st:1&d2=p9&u2=s:192:st:1 http://www.ndbc.noaa.gov/station_page.php?station=44095		Field Research Facility, Coastal Observations & Analysis Branch, US Army Corps of Engineers, Duck, North Carolina http://www.frf.usace.army.mil/awac05/realtime.shtml			National Weather Service; data available on wunderground.com http://www.wunderground.com/personal-weather-station/dashboard?ID=KNCNAGSH4

5.2.8. Environmental Monitoring

Jennettes Pier has the capability to monitor environmental conditions using CTDs (measuring Conductivity, Temperature, and pressure which can be related to Depth), water quality monitors, and an optical backscatter. Two Nortek Aquadopp current meters can be deployed with devices to measure the local wave and current environment. Two Multi-Electronique

hydrophones for passive acoustic monitoring can be deployed with devices as well. Photographic and videographic documentation of colonization and response of marine organisms to devices can be recorded by UNC CSI divers (open and closed circuit rebreather certified), ROVs, or stationary cameras. UNC CSI has extensive photography and videography capabilities via still cameras rated to up to 450 ft, Digital Cinema cameras for Ultra-HD capture at depths to 450 ft, GoPros rated to 1000 ft, and a Deepsea Power and Light 0.01 lux lighting, 170 degree field of view camera rated to almost 2000 m with 1100 ft of cable and a sea-light sphere capable of emitting 4000 lumens.

5.2.9. Permitting

The 6 m and 11 m test berths are permitted by the U.S. Army Corps of Engineers. Notice will be given to mariners via the Coast Guard when specific devices are tested. Information on berth leasing charges, personnel fees, equipment hire, etc., can be requested from Jennettes Pier or UNC CSI. A well-defined work plan must be submitted 60 days before the proposed start date, and settled on 30 days before operations begin. The Jennettes Pier Operations Committee must approve the work plan prior to the research partner beginning operations. Operations must be respectful to the recreational use of Jennettes Pier, and peak season for public activities is April – October.

5.3. Data used

Researchers at the UNC CSI produced a 31 year hindcast dataset for the area offshore of North Carolina (UNC CSI 2015). This dataset was used to calculate statistics of interest for the wave resource characterization at the Jennette's Pier and USACE FRF sites. The hindcast data at the grid point shown in Figure 32.

In addition to the hindcast data set, historical data from AWAC05 was used to calculate representative spectra. Because the AWAC05 only has consistent data for about three years, historical data from a USACE FRF waverider buoy (NDBC 44056 / CDIP 433) was used to calculate extreme sea states. Wind data was available from a met station on-shore. However, to be consistent with the other sites, Climate Forecast System Reanalysis (CFSR) winds were used, as explained in Section 2.3. As with the other sites, current data was downloaded from OSCAR. See Figures 32 and 35 for data locations.

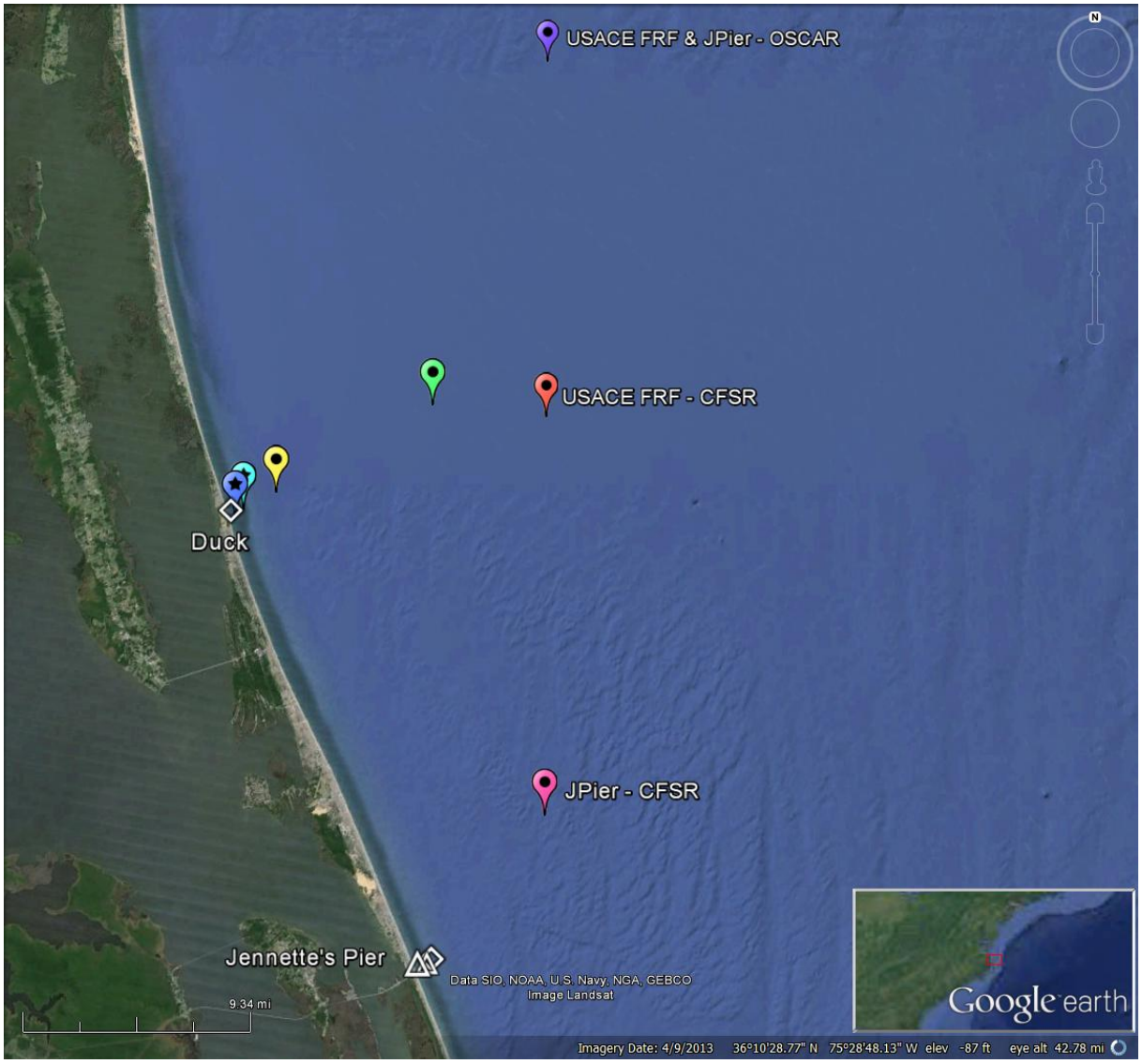

Figure 35: Jennette's Pier & USACE FRF (see Chapter 6) location map showing CSFR wind and OSCAR surface current data points (Google Earth 2015).

5.4. Results

The following sections provide information on the joint probability of sea states, the variability of the IEC TS parameters, cumulative distributions, weather windows, extreme sea states, and representative spectra. This is supplemented by wave roses as well as wind and surface current data in Appendix C. The wind and surface current data provide additional information to help developers plan installation and operations & maintenance activities.

5.4.1. Sea States: Frequency of Occurrence and Contribution to Wave Energy

Joint probability distributions of the significant wave height, H_{m0}, and energy period, T_e, are shown in Figure 36. Figure 36 (top) shows the frequency of occurrence of each binned sea state and Figure 36 (bottom) shows the percentage contribution to the total wave energy. Figure 36 (top) indicates that the majority of sea states are within the range 0 m $< H_{m0} <$ 2 m and 4 s $< T_e <$ 9 s. Jennette's Pier experiences a minimal amount of extreme sea states, which rarely exceed 5 m. The site is well suited for testing WECs at smaller scales, especially those that are bottom mounted because the depth is only 11 m at the 'offshore berth.'

As mentioned in the methodology (Section 2.2), previous studies show that sea states with the highest frequencies of occurrence do not necessarily correspond to those with the highest contribution to total wave energy. The total wave energy in an average year is about 53,300 kWh/m, which corresponds to an average annual omnidirectional wave power of 6.08 kW/m. The most frequently occurring sea state is within the range 0.5 m $< H_{m0} <$ 1 m and 5 s $< T_e <$ 6 s, while the sea state that contributes most to energy is within the range 1.5 m $< H_{m0} <$ 2 m and 6 s $< T_e <$ 7 s. Several sea states occur at a similar frequency, and sea states within 0.5 m $< H_{m0} <$ 3 m and 5 s $< T_e <$ 10 s contribute a similar amount to energy.

Frequencies of occurrence and contributions to energy of less than 0.01% are considered negligible and are not shown for clarity. For example, the sea state within 0 m $< H_{m0} <$ 0.5 m and 9 s $< T_e <$ 10 s has an occurrence of 0.03%. The contribution to total energy, however, is only 0.004% and, therefore, does not appear in Figure 36 (bottom). Similarly, the sea state within 6 m $< H_{m0} <$ 6.5 m and 10 s $< T_e <$ 11 s has an occurrence of 0.0001%, but the contribution to total energy is 0.05%.

Curves showing the mean, 5^{th} and 95^{th} percentiles of wave steepness, H_{m0}/λ, are also shown in Figure 36. The mean wave steepness at the Jennette's Pier site is 0.0180 ($\approx 1/56$), and the 95^{th} percentile is about 1/29.

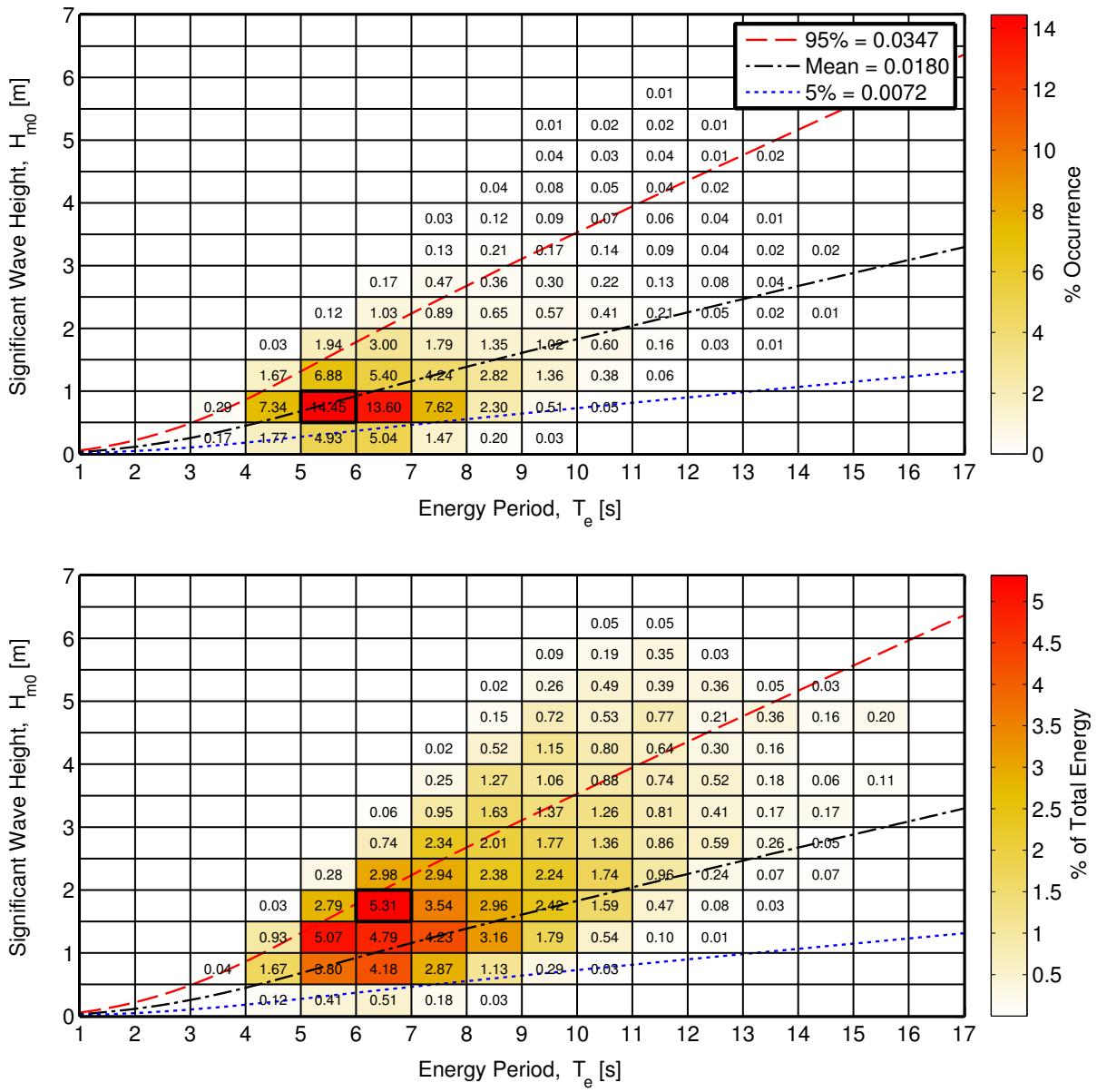

Figure 36: Joint probability distribution of sea states for the Jennette's Pier site. The top figure is frequency of occurrence and the bottom figure is percentage of total energy, where total energy in an average year is 53,300 kWh/m.

5.4.2. IEC TS Parameters

The monthly means of the six IEC TS parameters, along with the 5^{th} and 95^{th} percentiles, are shown in Figure 37. The months, March – February, are labeled with the first letter (e.g., March is M). The values in the figure are summarized in Table 18 in Appendix C.

Monthly means of the significant wave height, H_{m0}, and the omnidirectional wave power density, J, show the greatest seasonal variability compared to the other parameters. Values are smallest and vary the least during the summer months, while the rest of the year is

fairly consistent. The same trend is observed for the monthly mean energy period, T_e, but its variation is less pronounced. These observations are consistent with the relationship between wave power density, significant wave height and energy period, where wave power density, J, is proportional to the energy period, T_e, and the square of the significant wave height, H_{m0}.

The direction of maximum directionally resolved wave power is typically from the east at $\sim 90°$ during the summer and from east/northeast at $\sim 70°$ during the rest of the year. Seasonal variations of the remaining parameters, ϵ_0 and d_θ, are much less than J, H_{m0}, T_e, and θ_J, and are barely discernable. Monthly means for spectral width, ϵ_0, remain nearly constant at ~ 0.34. Similarly, monthly means for the directionality coefficient, d_θ, remains at ~ 0.87. In summary, the waves at the Jennette's Pier site, from the perspective of monthly means, have a fairly consistent spectral width, are predominantly from the east / northeast, and exhibit a wave power that has a narrow directional spread.

Wave roses of wave power and significant wave height, presented in Appendix C, Figure 132 and 133, also show the predominant direction of the wave energy at the Jennette's Pier site, which is east, with frequent but small shifts to the north. Figure 132 shows two dominant wave direction sectors, east (at 90°) and east/northeast (ENE) at 60°. Along the predominant wave direction, 90°, the omnidirectional wave power density is at or below 35 kW/m about 22% of the time, and greater than 35 kW/m about 0.37% of the time. Along the east/northeast direction (60°), wave power density is at or below 35 kW/m about 18% of the time, and greater than 35 kW/m about 1% of the time.

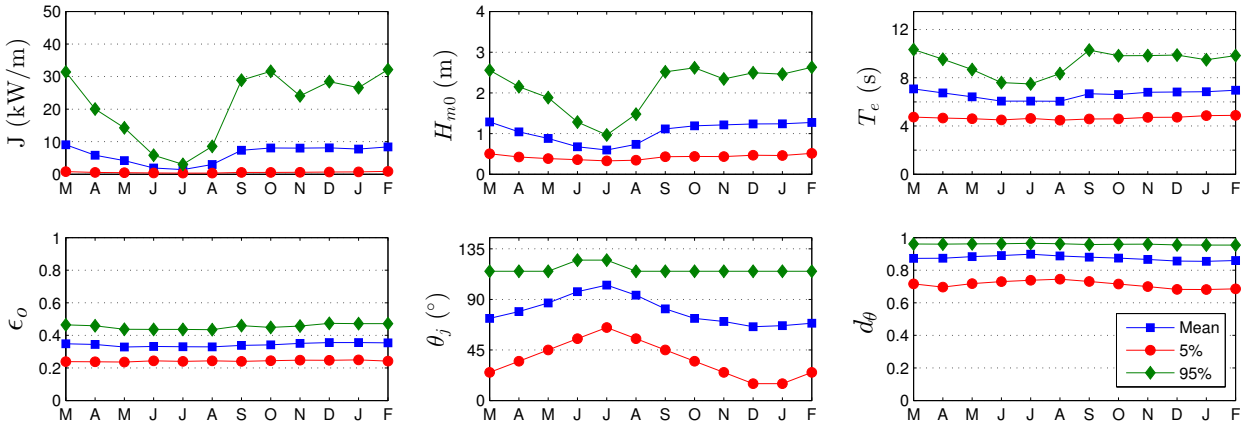

Figure 37: The average, 5^{th} and 95^{th} percentiles of the six parameters at the Jennette's Pier site.

Monthly means, however, smear the significant variability of the six IEC parameters over small time intervals as shown in plots of the parameters at 1-hour intervals in Figure 38 for a representative year. While seasonal patterns described for Figure 37 are still evident, these plots show how sea states can vary abruptly at small time scales with sudden changes, e.g., jumps in the wave power as a result of a storm.

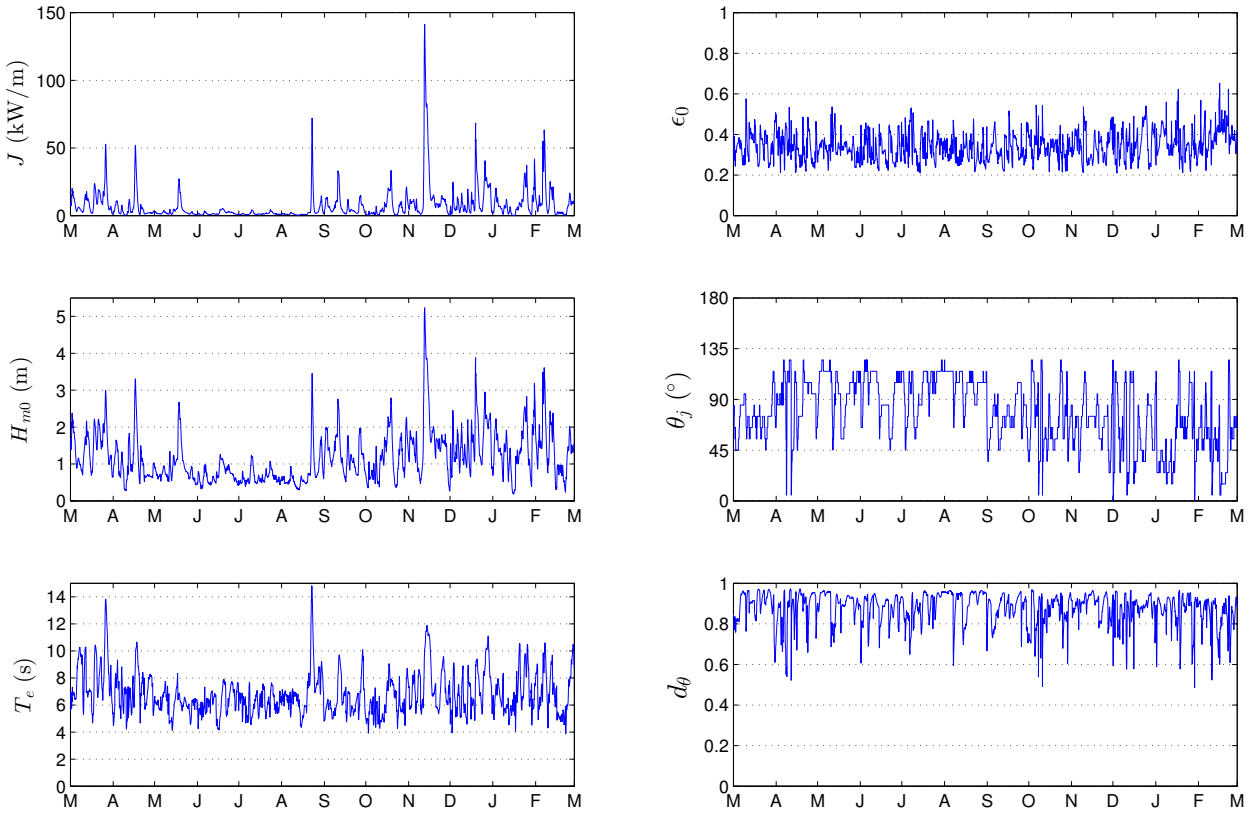

Figure 38: The six parameters of interest over a one-year period, March 2009 – February 2010 at the Jennette's Pier site.

5.4.3. Cumulative Distributions

Annual and seasonal cumulative distributions (a.k.a., cumulative frequency distributions) are shown in Figure 39. Note that spring is defined as March - May, summer as June - August, fall as September - November, and winter as December - February. The cumulative distributions are another way to visualize and describe the frequency of occurrence of individual parameters, such as H_{m0} and T_e. A developer could use cumulative distributions to estimate how often they can access the site to install or perform operations and maintenance based on their specific device, service vessels, and diving operation constraints. For example, if significant wave heights need to be less than or equal to 1 m for installation and recovery, according to Figure 39, this condition occurs about 60% of the time on average within a given year. If significant wave heights need to be less than or equal to 2 m for emergency maintenance, according to Figure 39, this condition occurs nearly 93% of time on average within a given year. Cumulative distributions, however, do not account for the duration of a desirable sea state, or weather window, which is needed to plan deployment and servicing of a WEC device at a test site. This limitation is addressed with the construction of weather window plots in the next section.

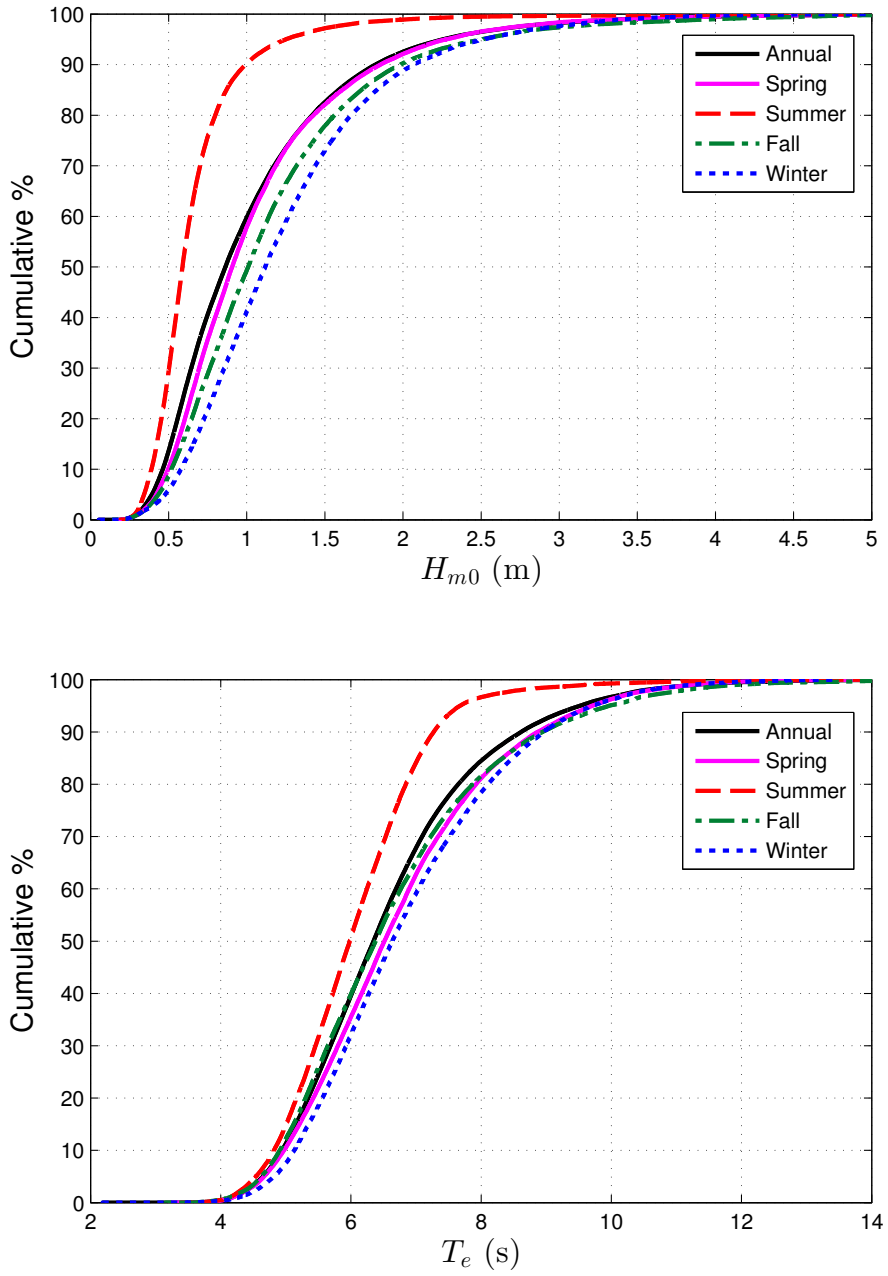

Figure 39: Annual and seasonal cumulative distributions of the significant wave height (top) and energy period (bottom) at the Jennette's Pier site.

5.4.4. Weather Windows

Figure 40 shows the number of weather windows at the Jennette's Pier site, when significant wave heights are at or below some threshold value for a given duration, for an average winter, spring, summer and fall. In these plots, each occurrence lasts a duration that is some multiple of 6-hours. The minimum weather window is, therefore, 6-hours in duration, and the maximum is 96-hours (4 days). The significant wave height threshold is the upper

bound in each bin and indicates the maximum significant wave height experienced during the weather window. Note that the table is cumulative, so, for example, an occurrence of $H_{m0} \leq 0.5$ m for at least 66 consecutive hours in the fall is included in the count for 60 consecutive hours as well. In addition, one 12-hour window counts would count as two 6-hour windows. It is clear that there are significantly more occurrences of lower significant wave heights during the summer than winter, which corresponds to increased opportunities for deployment or operations and maintenance.

Weather window plots provide useful information at test sites when planning schedules for deploying and servicing WEC test devices. For example, if significant wave heights need to be less than or equal to 0.5 m for at least 12 consecutive hours to service a WEC test device at the Jennette's Pier site with a given service vessel, there would be, on average, forty-six weather windows in the summer, but only seven in the winter. When wind speed is also considered, Figure 41 shows the average number of weather windows with the additional restriction of wind speed, $U < 15$ mph. The local winds (which are not necessarily driving the waves) are used in these weather windows, and are given in Appendix C.4. That wind data was not available from the hindcast, so data from CFSR was used (see Section 2.3, Appendix C.4). For shorter durations (6- and 12-hour windows), daylight is necessary. Windows with $U < 15$ mph and only during daylight hours are shown in Figure 42. Daylight was estimated as 5am – 10pm Local Standard Time (LST).

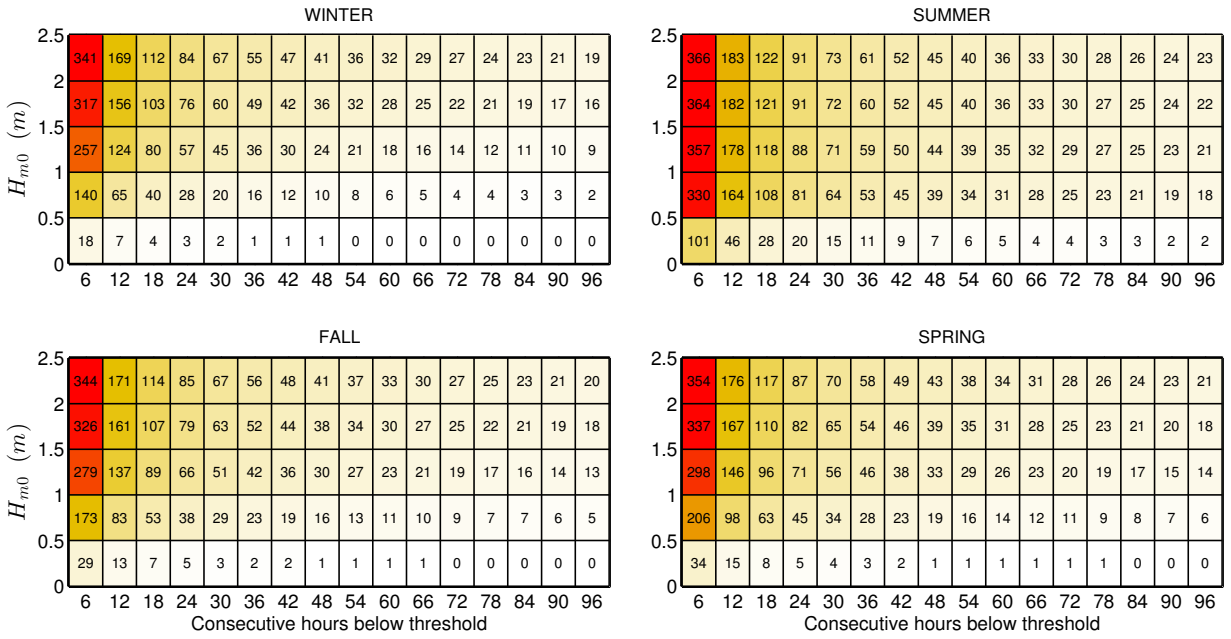

Figure 40: Average cumulative occurrences of wave height thresholds (weather windows) for each season at the Jennette's Pier site. Winter is defined as December – February, spring as March – May, summer as June – August, and fall as September – November.

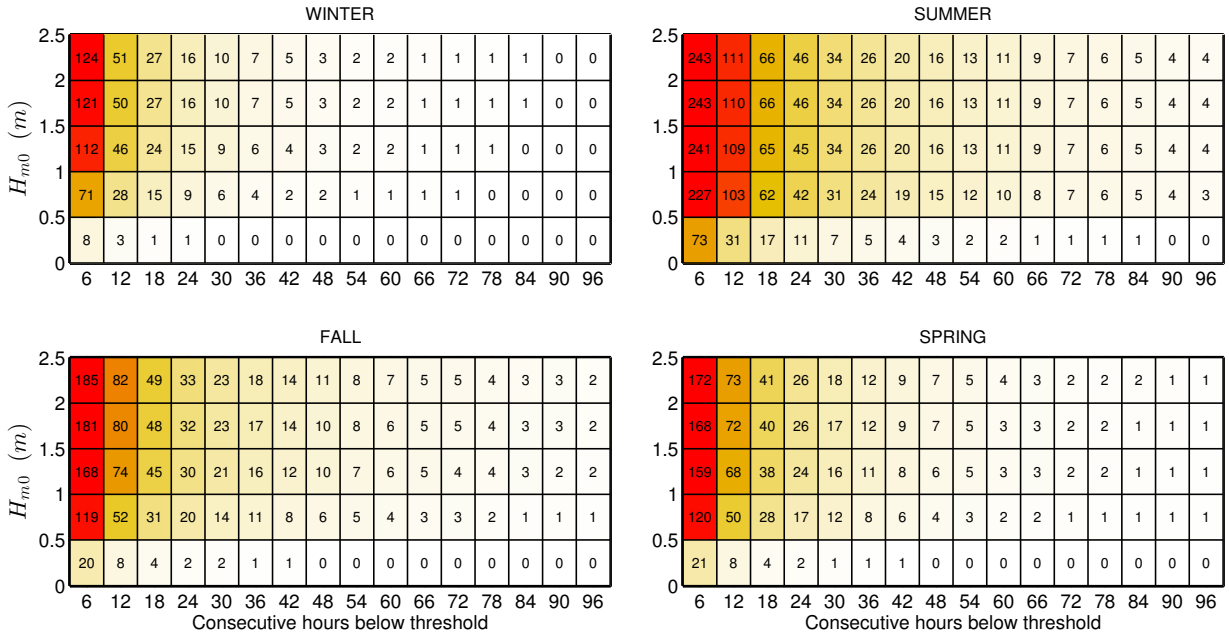

Figure 41: Average cumulative occurrences of wave height thresholds (weather windows) for each season at the Jennette's Pier site with an additional restriction of U < 15 mph.

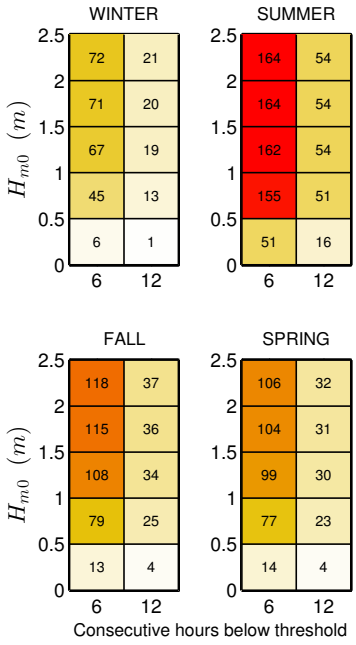

Figure 42: Average cumulative occurrences of wave height thresholds (weather windows) for 6- and 12-hour durations with $U < 15$ mph and only during daylight hours (5am – 10pm LST) at the Jennette's Pier site.

5.4.5. Extreme Sea States

As mentioned in 2.2, the way IFORM and the modified IFORM are currently implemented, they do not work well for datasets whose variables (H_{m0} and T_e) are bimodally distributed. The NDBC 44056 dataset is not well suited for IFORM, and therefore only the extreme significant wave height is estimated here using extreme value theory.

The generalized extreme value distribution (GEV) was fit to the annual significant wave height maximum in order to generate estimates of extreme values under the annual maximum method (AMM) (Rugerio et al. 2010). The peak over threshold (POT) method was also applied to the entire dataset in order to generate estimates of extreme values based on significant wave height exceedances over a certain threshold. Based on the application of this method as described by Ruggerio et al. (2010), the 99.5^{th} percentile of significant wave height was used as a threshold value. These methods were applied using the WAFO matlab toolbox (Brodtkorb et al. 2000). The bootstrapping method (Efron and Tibshirani 1993) was applied in order to generate a 95% confidence interval around the CDFs derived using both of the extreme value distribution methods utilized in this analysis.

The 100-year H_{m0} is estimated as 7.55 m and 8.46 m using the GEV and POT methods, respectively, as shown in Figures 43 and 44. The 10-, 25-, and 50-year values are shown in the figures. It should be noted that conditions at the NDBC44056 buoy (at 17 m depth) may differ significantly from the conditions at the test site berths (at 6 m and 11 m depths).

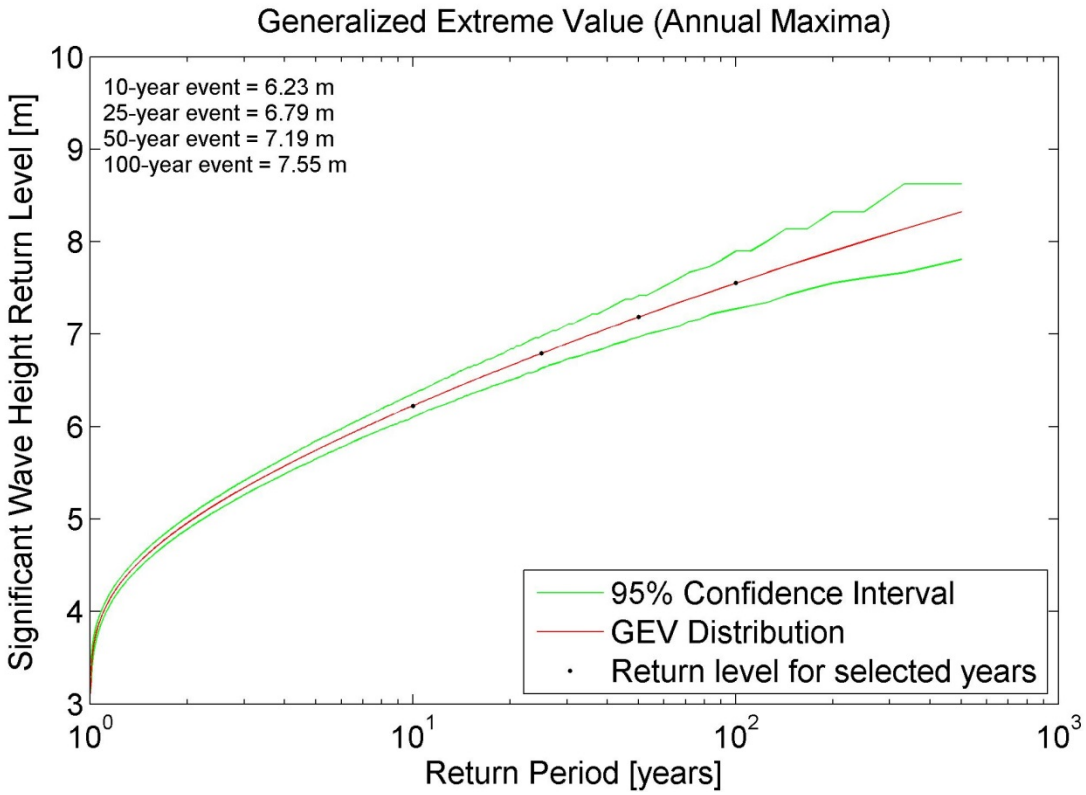

Figure 43: The generalized extreme values distribution was fit to annual maximum of significant wave height from NDBC44056 to generate estimates of extreme values. The 95% confidence interval is shown as well.

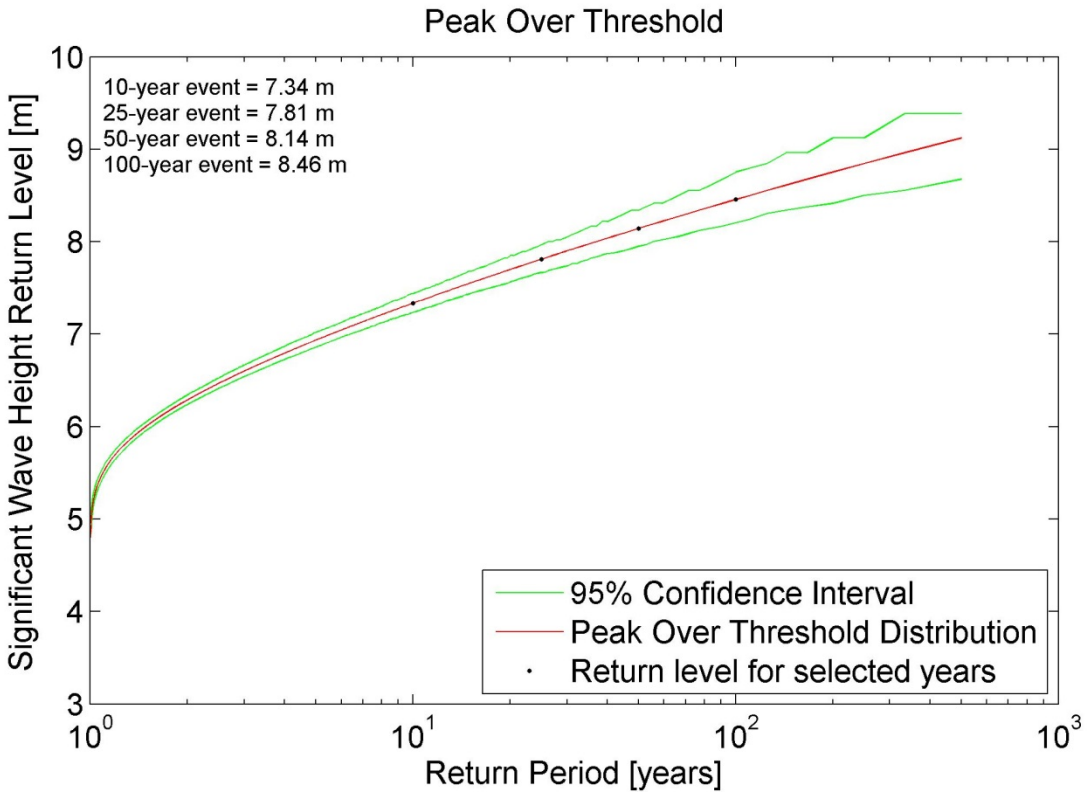

Figure 44: The peak over thresholds method was used with a threshold value of the 99.5^{th} percentile of significant wave height from NDBC44056. The 95% confidence interval is shown as well.

5.4.6. Representative Wave Spectrum

All hourly discrete spectra measured at AWAC05 for the most frequently occurring sea states are shown in Figure 45. The most frequently occurring sea state, which is within the range 0.5 m $< H_{m0} <$ 1 m and 7 s $< T_e <$ 8 s, was selected from a JPD similar to Figure 36 in Section 5.4.1, but based on the AWAC05 data. As a result, the JPD, and therefore the most common sea states, generated from the measured wave data are slightly different from that generated from hindcast data. For example, the most frequently occurring sea state for the JPD generated from hindcast data is in the same range for H_{m0} (0.5 m $< H_{m0} <$ 1 m), but two seconds lower on bounds for T_e (5 s $< T_e <$ 6 s). Often several sea states will occur at a very similar frequency, and therefore plots of hourly discrete spectra for several other sea states are also provided for comparison. Each of these plots includes the mean spectrum and standard wave spectra, including Bretschneider and JONSWAP, with default constants as described in Section 2.2.

For the purpose of this study, the mean spectrum is the 'representative' spectrum for each sea state, and the mean spectrum at the most common sea state, shown in Figure 45 (bottom-left plot), is considered the 'representative' spectrum at the site. The hourly spectra vary considerably about this mean spectrum, but this is partly reflective of the bin size chosen for H_{m0} and T_e. Comparisons of the representative spectra in all plots with the Bretschneider

and JONSWAP spectra illustrate why modeled spectra with default constants, e.g., the shape parameter $\gamma = 3.3$ for the JONSWAP spectrum, should be used with caution. Using the constants provided in Section 2.2, the Bretschneider spectra are, at best, fair representations of the mean spectra in Figure 59. There is some evidence of bimodal spectra in the four sea states displayed, which is not captured by the modeled spectra. The mean measured spectra is the best representation of the conditions, however, if these modeled spectra were to be used at this site, it is recommended that the constants undergo calibration against some mean spectrum, e.g., the representative spectrum constructed here. A better alternative may be to explore other methods or spectral forms to describe bimodal spectra (e.g., Mackay 2011) if it is known that the shape is not unimodal.

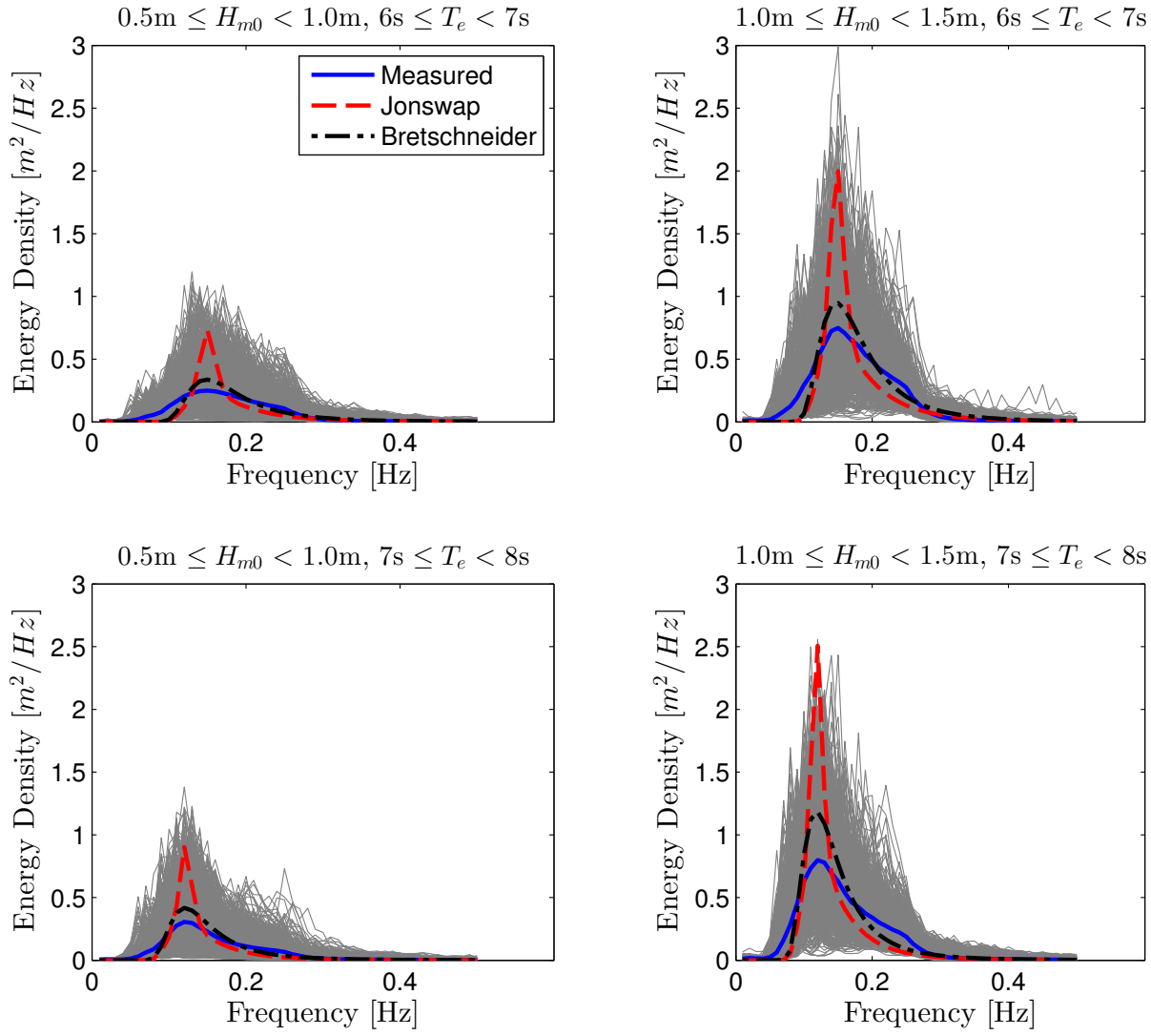

Figure 45: All hourly discrete spectra and the mean spectra measured at AWAC05 within the sea state listed above each plot. The JONSWAP and Bretschneider spectra are represented by red and black dotted lines, respectively.

6. U.S. ARMY CORPS OF ENGINEERS (USACE) FIELD RESEARCH FACILITY (FRF)

6.1. Site Description

The Field Research Facility (FRF) located on the Atlantic Ocean in Duck, NC was established by the U.S. Army Corps of Engineers in 1977 as part of the Coastal and Hydraulics Laboratory to support the Corps coastal engineering research requirements. The facility consists of a 560 m (1840-ft) long research pier, a main office building, field support buildings, and a 40 m (130-ft) observation tower. Since its creation, the FRF has maintained a comprehensive, long-term monitoring program of the coastal ocean including waves, tides, currents, local meteorology, and the concomitant beach response. The monitoring program is supported by a small, highly skilled field staff and several unique vehicles that permit successful operations in the turbulent surf zone.

At the site, the bathymetry is gently sloping, and the sea bed is sandy. Figure 47 shows the bathymetry around the site, and consists of a wide shelf. For the purpose of this catalogue, hindcast data at 36.1858 N, 75.7486 W at 4.8 m depth was used to represent the site. The wave climate at the test site varies seasonally, with calmer seas in the summer compared to more energetic seas in the winter. The wave environment at USACE FRF is characterized by an annual average power flux of about 3.29 kW/m at 4.8 m depth.

The USACE FRF offers a wide range of technical and testing infrastructure support services for WEC developers. The site has small scale, shallow water wave energy resources, and can accommodate scaled devices. The research pier can serve as a cable conduit through the surf zone to locations on land.

The FRF was utilized as an off-grid WEC test site in 2012 by Resolute Marine Energy (RME). RME located their device approximately 25 m south of the pier and in 6 m water depth. The FRF is capable of deploying devices past the pier in state waters. Locations past the pier would have higher wave power compared to the data presented in this chapter at 4.8 m depth, and presumably wave characteristics would be similar to the Jennette's Pier Wave Energy Converter Test Facility in Chapter 5, which uses hindcast data in 12.6 m depth and is $\sim$34 km southeast of the FRF.

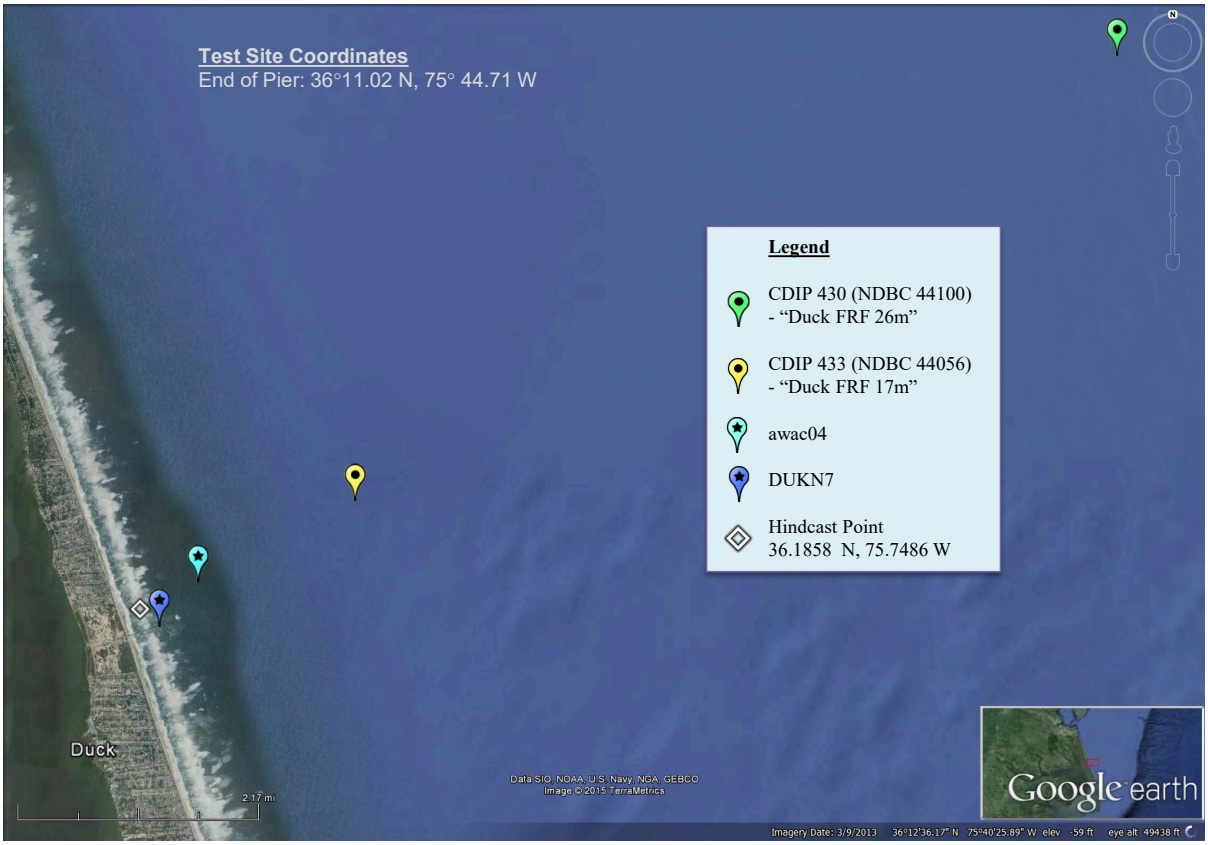

Figure 46: The USACE FRF is located in the coastal waters of North Carolina in the town of Duck. Three buoys, one AWAC, and one water level observation network close to the site are shown (see Table 4). Image modified from Google Earth (Google Earth 2015).

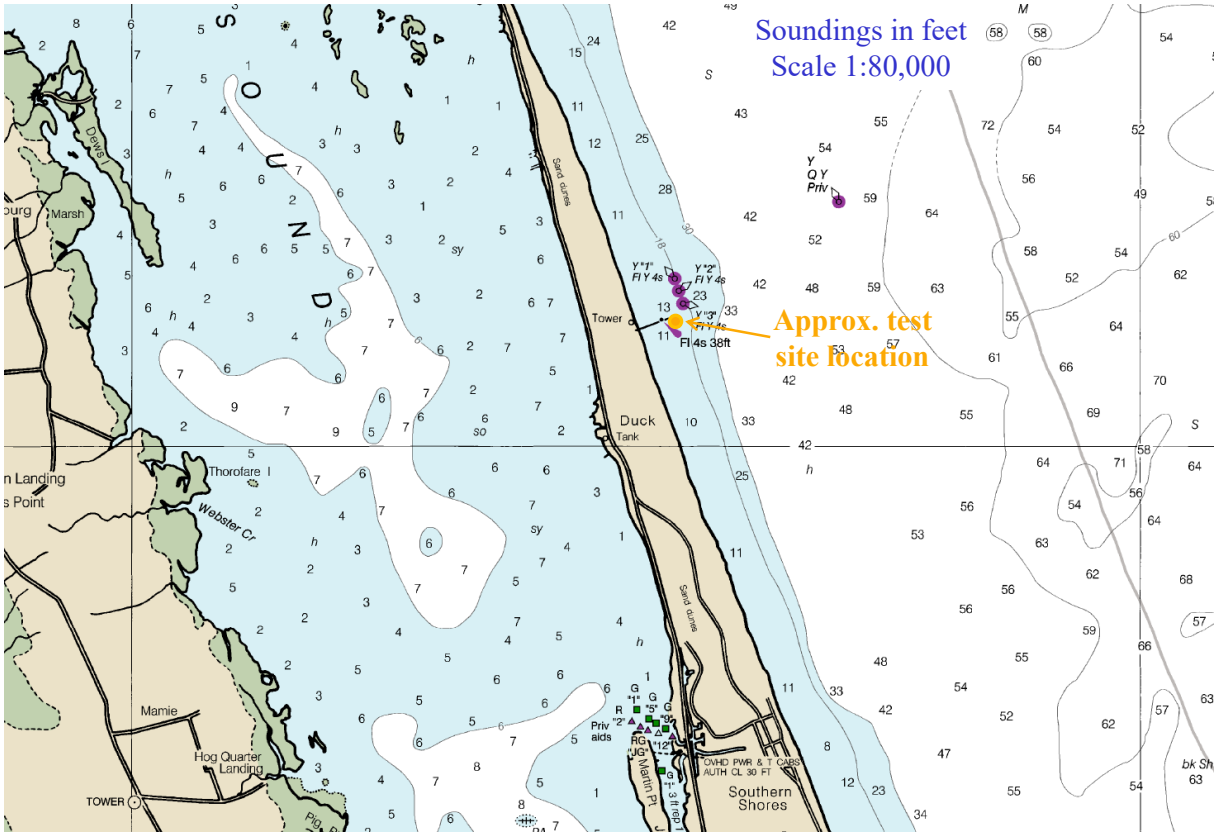

Figure 47: Nautical chart of Duck, NC and the surrounding area shows the gradually sloping bathymetry off Duck Pier. Soundings in feet (1 foot = 0.3048 m). Image modified from nautical chart #12204 (Office of Coast Survey 2015). End of Pier Coordinates: 36°11.02 N, 75°44.71 W.

6.2. WEC Testing Infrastructure

6.2.1. Mooring Berths

Mooring systems are not provided and would need to be installed according to the developer's design (FRF staff have extensive experience deploying moored equipment at this site). Energy generated and monitoring instrumentation will be cabled to the FRF communications trailer located at the seaward end of the pier or along the pier to a landward location.

6.2.2. Electrical Grid Connection

There are no special provisions for interfacing with the electrical grid (for the purpose of exporting power).

During the RME experiment, access to the grid was provided via a 3 phase outlet located on the pier. Their wave-driven generator was an induction machine (off-the-shelf induction motor driven as a generator) and was "plugged in" to this outlet. A load bank was setup to

absorb any additional power generated to eliminate the export of power. The combination of their generator and load bank "looked" to the grid as a conventional motor consisting of a "real" load component (kW) equal to the net of generator output and load bank absorption, as well as a "reactive component" (kVAR) to excite the field of the generator. The load power factor was probably not less than 80%.

All aspects of the power flow to the grid connection were measured via a multi-function power transducer supplied by Ohio Semitronics. Measurements included real power, reactive power, apparent power (vector sum of real and reactive components) and power factor = real/apparent. The line-line voltages and line currents were also monitored. As a protective measure the system was provided with a frequency transducer and programmed to disconnect the apparatus in the event of an unusual deviation from 60 Hz.

6.2.3. Facilitating Harbor

The USACE FRF can be accessed by boat via Oregon Inlet (∼30 miles from the Pier). Several harbors are within 10 miles of the inlet, including harbors and marinas at UNC CSI and Wanchese, from which service vessels and commercial divers are available. ARMY Lighter Amphibious Resupply Cargo (LARC) vessels are also available at the FRF. These 10.6 m amphibious crafts are capable of driving off the beach and operating on the ocean within 3 nm of the coast.

6.2.4. On-Shore Office Space

Office space is available at the FRF although schedule dependent.

6.2.5. Service Vessel and Engineering Boatyard Access

A USACE FRF vessel and amphibious craft are available for support, along with a vessel Captain, research technicians, and dive operations support for additional fees.

6.2.6. Travel and Communication Infrastructure

The Norfolk International Airport (ORF) is approximately a one and a half hour drive from the USACE FRF. Raleigh Durham International Airport (RDU) is approximately a three and a half hour drive from the USACE FRF. Cellular service offers consistent coverage; there are several Federal Communication Commission (FCC) registered cell phone towers located in and around Duck, NC.

6.2.7. Met-Ocean Monitoring Equipment

There are many instruments located near the USACE FRF site. The most prominent ones are listed here, and additional information can be found on the FRF website. There is one National Buoy Data Center (NDBC) buoy (Figure 48(a)) that measures and collects ocean

data, along with two CDIP buoys (Figure 48(b)) operated by the USACE FRF. There is an AWAC just northeast of the end of the pier, and a water level observation network on the pier (see Figure 46 for location). Instrument and data specifications for this monitoring equipment are summarized in Table 4. As noted above, not all measurements are listed here, and it is recommended to check the FRF website (http://www.frf.usace.army.mil/frf_data.shtml) for all available data. In addition, there are several measurements nearby at Jennettes Pier, NC (∼34 km southeast of the FRF), see Section 5.2.7.

Figure 48: (a) NDBC 44014 located 93 km northeast of the test site (National Data Buoy Center 2015), (b) CDIP 430 located 15 km northeast of the site (Field Research Facility, 2015).

Table 4: Wave monitoring equipment in close proximity to the USACE FRF.

Instrument Name (Nickname)	**NDBC 44014 ("Virginia Beach")**			**NDBC 44100 - CDIP 430 - ("Duck FRF 26m, NC")**		**NDBC 44056 - CDIP 433 ("Duck FRF 17m, NC")**	
Type	3-meter discus buoy			Waverider Buoy		Waverider Buoy	
Measured parameters	-std. met. data -continuous winds -spectral wave density -spectral wave direction			-std. met. data -spectral wave density -spectral wave direction		-std. met. data -spectral wave density -spectral wave direction	
Variables reported, including derived variables (Sampling interval)	*Std Met.:* WDIR WSPD GST WVHT DPD APD PRES ATMP WTMP (1 hr sampling period)	*Contin. Winds:* WDIR WSPD GDR GST GTIME (10 min sampling period)	-Spectral Wave Density -Spectral Wave direction (1 hr sampling period)	*Std Met.:* WVHT DPD APD MWD WTMP (30 min sampling period)	-Spectral Wave Density -Spectral Wave direction (30 min sampling period)	*Std Met.:* WVHT DPD APD MWD WTMP (30 min sampling period)	-Spectral Wave Density -Spectral Wave direction (30 min sampling period)
Location	∼93 km northeast of the end of FRF Duck Pier			∼15 km northeast of the end of FRF Duck Pier		∼3 km northeast of the end of FRF Duck Pier	
Coordinates	36.611 N 74.842 W (36°36'41" N 74°50'31" W)			36°15.461 N 75°35.479 W (36°15'27.66" N 75°35'28.74" W)		36.200 N 75.714 W (36° 11.993N 75°42.843W)	
Depth	47.6 m			26 m		17.4 m	
Data Start	std met: 10/1/1990 contin winds: 12/31/2002 spect wave dens: 01/23/1996 spect wave dir: 04/14/1998			5/22/2008		spectral wave data: 1987 directional spectra: 1997	
Data End	present			present		present	
Period of Record	std met: ∼25 yrs contin winds: ∼13 yrs spect wave dens: ∼20 yrs spect wave dir: ∼17 yrs			∼7 yrs		spectral data: ∼28 yrs directional spectra: ∼18 yrs	
Owner / Contact Person	Funding provided by the US Army Corps of Engineers, Coastal Hydraulics Laboratory Owned and maintained by National Data Buoy Center http://www.ndbc.noaa.gov/station_history.php?station=44014			Field Research Facility, Coastal Observations & Analysis Branch, US Army Corps of Engineers, Duck, North Carolina http://www.frf.usace.army.mil/wvrdr430/archive.shtml http://cdip.ucsd.edu/?units=metric&tz=UTC&pub=public&map_stati=1,2,3&nav=historic&sub=data&stn=430&stream=p1		Field Research Facility, Coastal Observations & Analysis Branch, US Army Corps of Engineers, Duck, North Carolina http://www.frf.usace.army.mil/wvrdr630/realtime.shtml http://cdip.ucsd.edu/?units=metric&tz=UTC&pub=public&map_stati=1,2,3&nav=recent&sub=observed&stn=433&stream=p1&xitem=info	

Instrument Name (Nickname)	**11m AWAC (awac04) – Duck Field Research Facility**			**DUKN7 - 8651370 - Duck Pier, NC**
Type	Acoustic Wave and Current Gauge (AWAC)			Water Level Observation Network
Measured parameters	std. met. data spectral wave density spectral wave direction current speed and direction			wind dir & speed gust pressure air temperature water temperature
Variables reported, including derived variables (Sampling interval)	*Std Met.:* WVHT DPD MWD (1 hr sampling period)	Spectral Wave Density Spectral Wave direction (1 hr sampling period)	Longshore current speed Cross-shore current speed (1 hr sampling period)	WDIR WSPD GST PRES ATMP WTMP (6 min sampling period)
Location	∼0.8 km northeast of the end of FRF Duck Pier			on FRF Duck Pier
Coordinates	36.189 N 75.739 W (36°11.36' N 75°44.36' W)			36.183 N 75.747 W (36°11'1" N 75°44'44" W)
Depth	11.4 m			site elevation: 7.7 m above mean sea level air temp height: 8 m above site elevation anemometer height: 9.9 m above site elevation barometer elev: 9.1 m above mean sea level
Data Start	6/1/2008			7/1/2008
Data End	Currently down plans to restore data collect are underway			present
Period of Record	∼7.5 yrs			∼7.5 yrs
Owner / Contact Person	Field Research Facility, Coastal Observations & Analysis Branch, US Army Corps of Engineers, Duck, North Carolina http://www.nortekusa.com/usa/news/real-time-awac-data-from-duck-field-research-facility http://www.frf.usace.army.mil/awac04/realtime.shtml			NOAA's National Ocean Service, Tides & Currents http://www.ndbc.noaa.gov/station_page.php?station=dukn7 http://www.wunderground.com/MAR/buoy/DUKN7.html?

6.2.8. Environmental Monitoring

No monitoring has been required in previous deployments and tests.

6.2.9. Permitting

The site is permitted by the U.S. Army Corps of Engineers. Notice will be given to mariners via the Coast Guard when specific devices are tested.

6.3. Data used

Researchers at the UNC CSI produced a 31 year hindcast dataset for the area offshore of North Carolina (UNC CSI 2015). This dataset was used to calculate statistics of interest for the wave resource characterization at the Jennette's Pier and USACE FRF sites. The hindcast data at the grid point shown in Figure 46.

In addition to the hindcast data set, historical data from AWAC04 was used to calculate representative spectra. Because the AWAC04 only has data for about seven years, historical data from a USACE FRF waverider buoy (NDBC 44056 / CDIP 433) was used to calculate extreme sea states. Wind data was available from a water level observation network on the USACE FRF Duck pier. However, to be consistent with the other sites, Climate Forecast System Reanalysis (CFSR) winds were used, as explained in Section 2.3. As with the other sites, current data was downloaded from OSCAR. See Figures 46 and 49 for data locations.

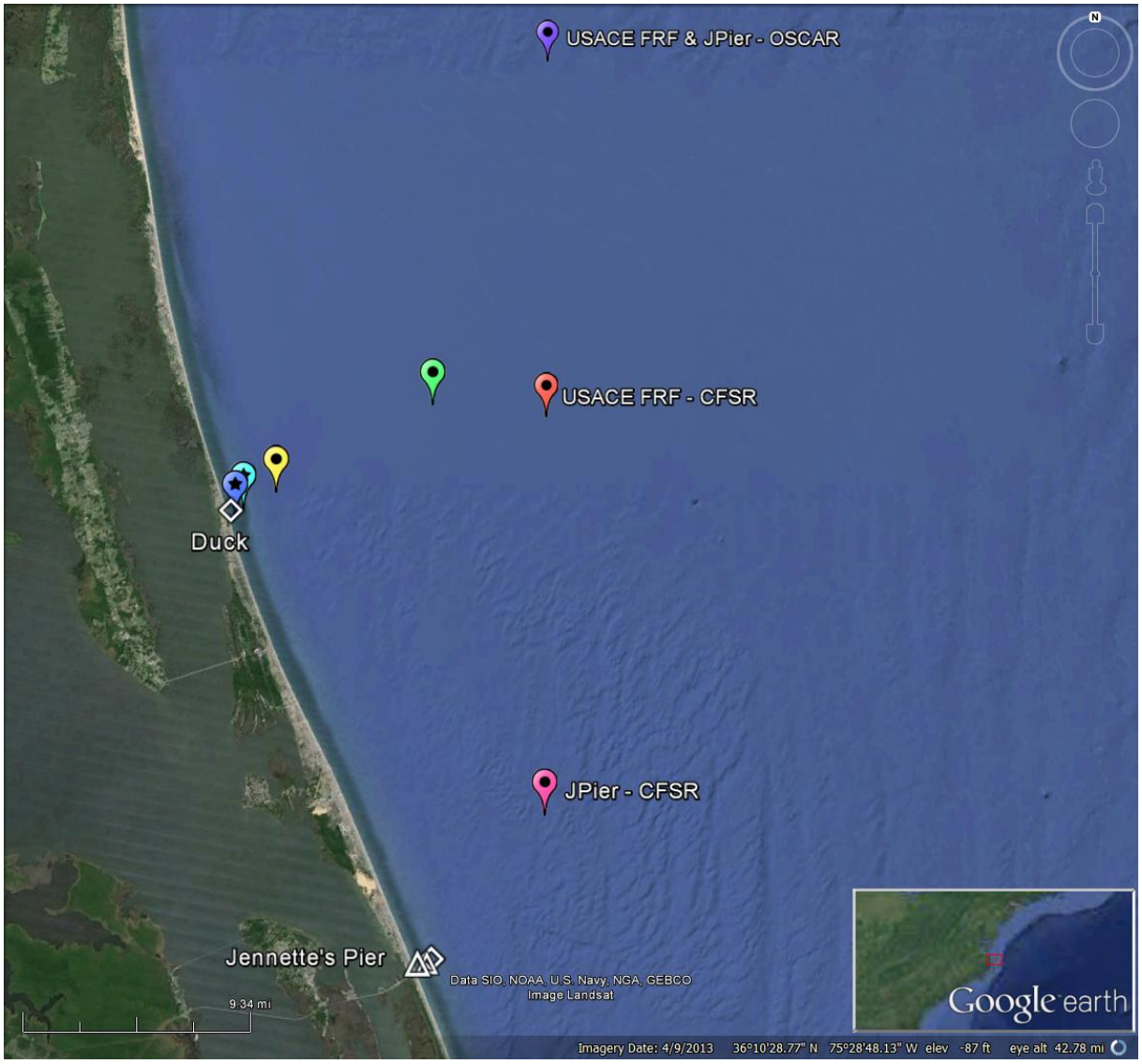

Figure 49: Jennette's Pier (see Chapter 5) & USACE FRF location map showing CSFR wind and OSCAR surface current data points (Google Earth 2015).

6.4. Results

The following sections provide information on the joint probability of sea states, the variability of the IEC TS parameters, cumulative distributions, weather windows, extreme sea states, and representative spectra. This is supplemented by wave roses as well as wind and surface current data in Appendix D. The wind and surface current data provide additional information to help developers plan installation and operations & maintenance activities.

6.4.1. Sea States: Frequency of Occurrence and Contribution to Wave Energy

Joint probability distributions of the significant wave height, H_{m0}, and energy period, T_e, are shown in Figure 50. Figure 50 (top) shows the frequency of occurrence of each binned sea state and Figure 50 (bottom) shows the percentage contribution to the total wave energy. Figure 50 (top) indicates that the majority of sea states are within the range 0 m $< H_{m0}$ $<$ 2 m and 4 s $< T_e <$ 9 s; very few occurrences of H_{m0} greater than 3 m occur because the data is taken from a depth of 4.8 m. The site is well suited for testing WECs at smaller scales, especially those that are bottom mounted because the depths only reach about 25 m at the end of the pier.

As mentioned in the methodology (Section 2.2), previous studies show that sea states with the highest frequencies of occurrence do not necessarily correspond to those with the highest contribution to total wave energy. The total wave energy in an average year is 28,815 kWh/m, which corresponds to an average annual omnidirectional wave power of 3.29 kW/m. The most frequently occurring sea state is within the range 0.5 m $< H_{m0} <$ 1 m and 5 s $< T_e$ $<$ 6 s, while the sea state that contributes most to energy is within the range 1 m $< H_{m0}$ $<$ 1.5 m and 5 s $< T_e <$ 6 s. Several sea states occur at a similar frequency, and sea states within 0.5 m $< H_{m0} <$ 2 m and 5 s $< T_e <$ 8 s contribute a similar amount to energy.

Frequencies of occurrence and contributions to energy of less than 0.01% are considered negligible and are not shown for clarity. For example, the sea state within 0 m $< H_{m0} <$ 0.5 m and 2 s $< T_e <$ 3 s has an occurrence of 0.03%. The contribution to total energy, however, is only 0.002% and, therefore, does not appear in Figure 50 (bottom). Similarly, the sea state within 2.5 m $< H_{m0} <$ 3 m and 15 s $< T_e <$ 16 s has an occurrence of 0.001%, but the contribution to total energy is 0.01%.

Curves showing the mean, 5^{th} and 95^{th} percentiles of wave steepness, H_{m0}/λ, are also shown in Figure 50. The mean wave steepness at the USACE FRF site is 0.0221 ($\approx 1/45$), and the 95^{th} percentile is about 1/24.

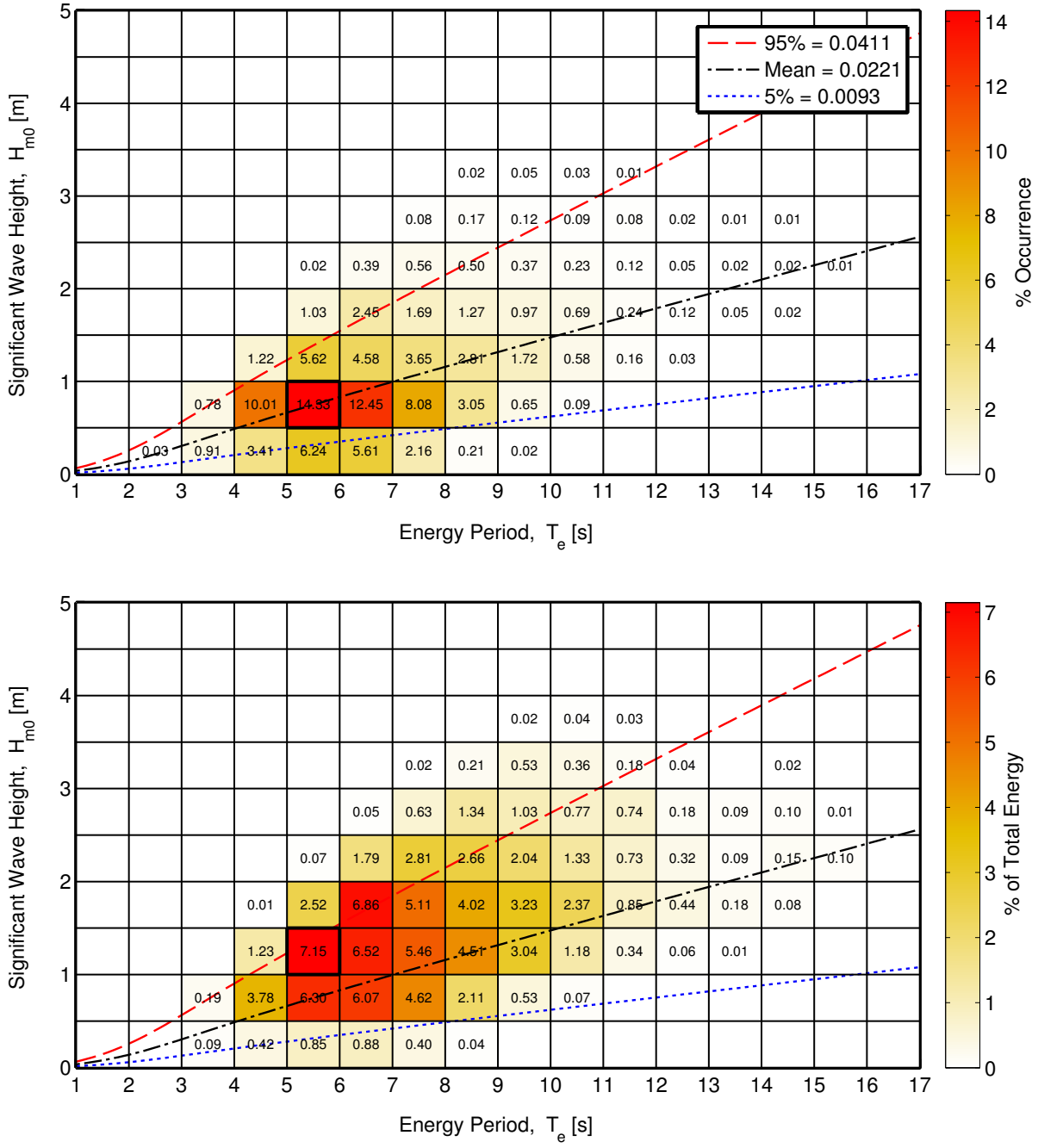

Figure 50: Joint probability distribution of sea states for the USACE FRF site. The top figure is frequency of occurrence and the bottom figure is percentage of total energy, where total energy in an average year is 28,815 kWh/m.

6.4.2. IEC TS Parameters

The monthly means of the six IEC TS parameters, along with the 5^{th} and 95^{th} percentiles, are shown in Figure 51. The months, March – February, are labeled with the first letter (e.g., March is M). The values in the figure are summarized in Table 23 in Appendix D.

Monthly means of the significant wave height, H_{m0}, and the omnidirectional wave power density, J, show the greatest seasonal variability compared to the other parameters. Values are smallest and vary the least during the summer months, while the rest of the year is fairly consistent. The same trend is observed for the monthly mean energy period, T_e, but its variation is less pronounced. These observations are consistent with the relationship between wave power density, significant wave height and energy period, where wave power density, J, is proportional to the energy period, T_e, and the square of the significant wave height, H_{m0}.

The direction of maximum directionally resolved wave power is typically from the east at $\sim 90°$ during the summer and from east/northeast at $\sim 70°$ during the rest of the year. Seasonal variations of the remaining parameters, ϵ_0 and d_θ, are much less than J, H_{m0}, T_e, and θ_J, and are barely discernable. Monthly means for spectral width, ϵ_0, remain nearly constant at ~ 0.37. Similarly, monthly means for the directionality coefficient, d_θ, remains at ~ 0.9. In summary, the waves at the USACE FRF site, from the perspective of monthly means, have a fairly consistent spectral width, are predominantly from the east / northeast, and exhibit a wave power that has a narrow directional spread.

Wave roses of wave power and significant wave height, presented in Appendix D, Figure 138 and 139, also show the predominant direction of the wave energy at the USACE FRF site, which is east, with frequent but small shifts to the north. Figure 138 shows two dominant wave direction sectors, east (at 90°) and east/northeast (ENE) at 60°. Along the predominant wave direction, 90°, the omnidirectional wave power density is at or below 35 kW/m about 35% of the time, but greater than 35 kW/m about 0.02% of the time. Along the east/northeast direction (60°), wave power density is at or below 35 kW/m about 23% of the time, and greater than 35 kW/m about 0.04% of the time.

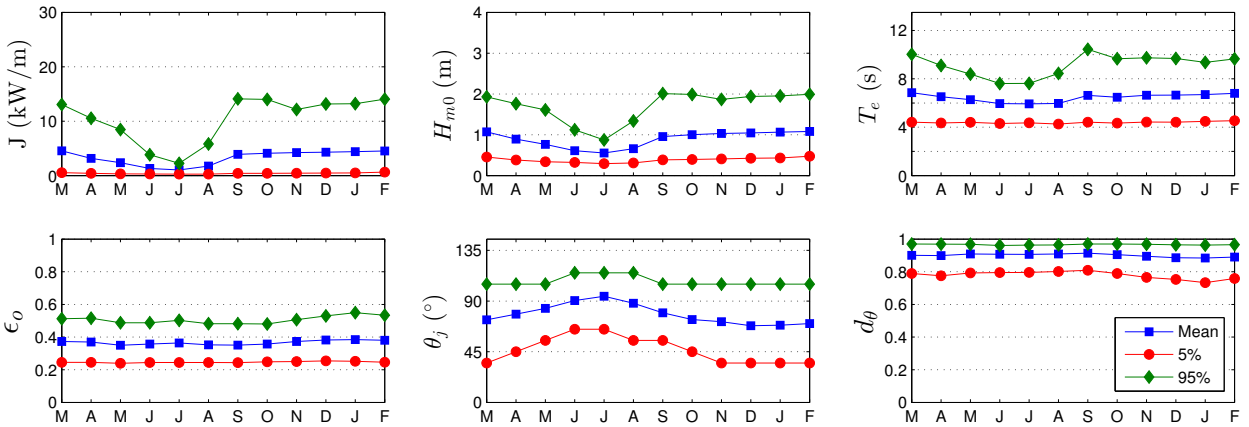

Figure 51: The average, 5^{th} and 95^{th} percentiles of the six parameters at the USACE FRF site.

Monthly means, however, smear the significant variability of the six IEC parameters over small time intervals as shown in plots of the parameters at 1-hour intervals in Figure 52 for a representative year. While seasonal patterns described for Figure 51 are still evident, these

plots show how sea states can vary abruptly at small time scales with sudden changes, e.g., jumps in the wave power as a result of a storm.

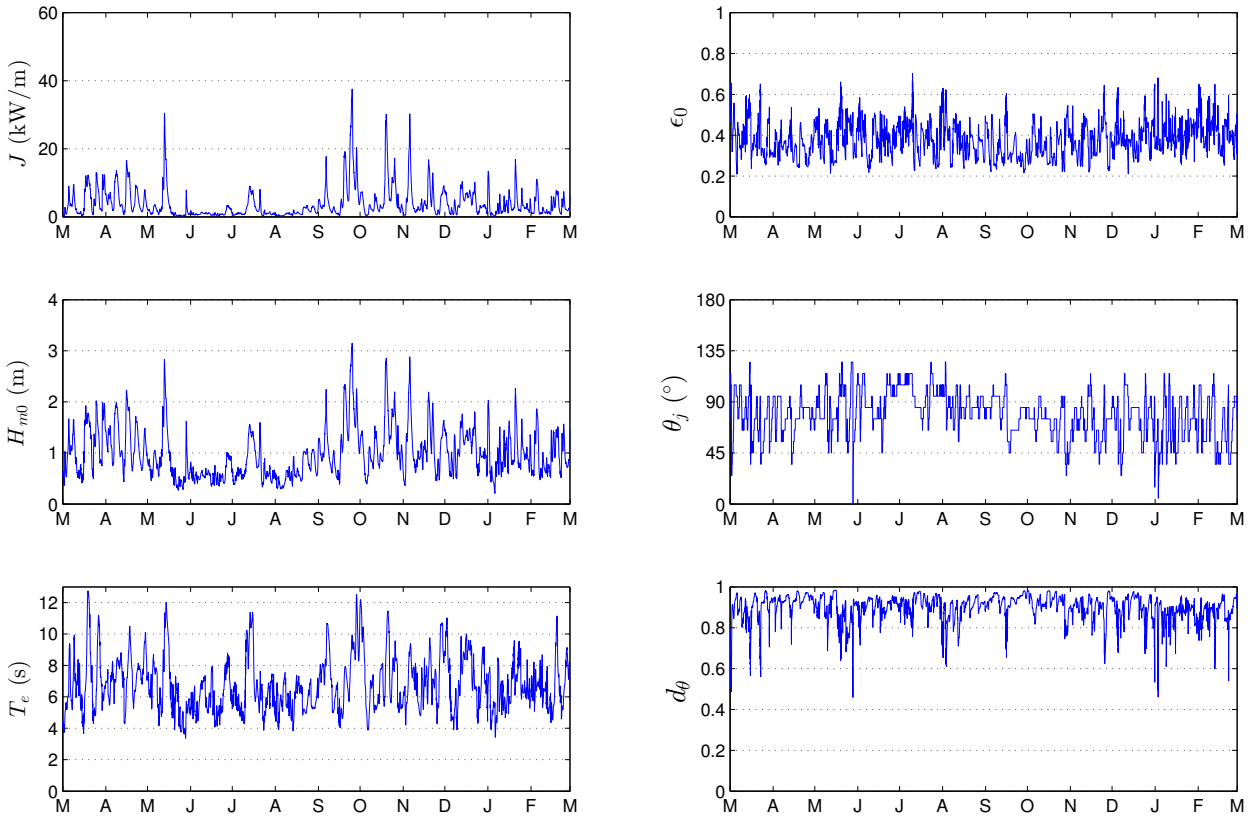

Figure 52: The six parameters of interest over a one-year period, March 2008 – February 2009 at the USACE FRF site.

6.4.3. Cumulative Distributions

Annual and seasonal cumulative distributions (a.k.a., cumulative frequency distributions) are shown in Figure 53. Note that spring is defined as March May, summer as June - August, fall as September - November, and winter as December - February. The cumulative distributions are another way to visualize and describe the frequency of occurrence of individual parameters, such as H_{m0} and T_e. A developer could use cumulative distributions to estimate how often they can access the site to install or perform operations and maintenance based on their specific device, service vessels, and diving operation constraints. For example, if significant wave heights need to be less than or equal to 1 m for installation and recovery, according to Figure 53, this condition occurs about 68% of the time on average within a given year. If significant wave heights need to be less than or equal to 2 m for emergency maintenance, according to Figure 53, this condition occurs nearly 97% of time on average within a given year. Cumulative distributions, however, do not account for the duration of a desirable sea state, or weather window, which is needed to plan deployment and servicing of a WEC device at a test site. This limitation is addressed with the construction of weather

window plots in the next section.

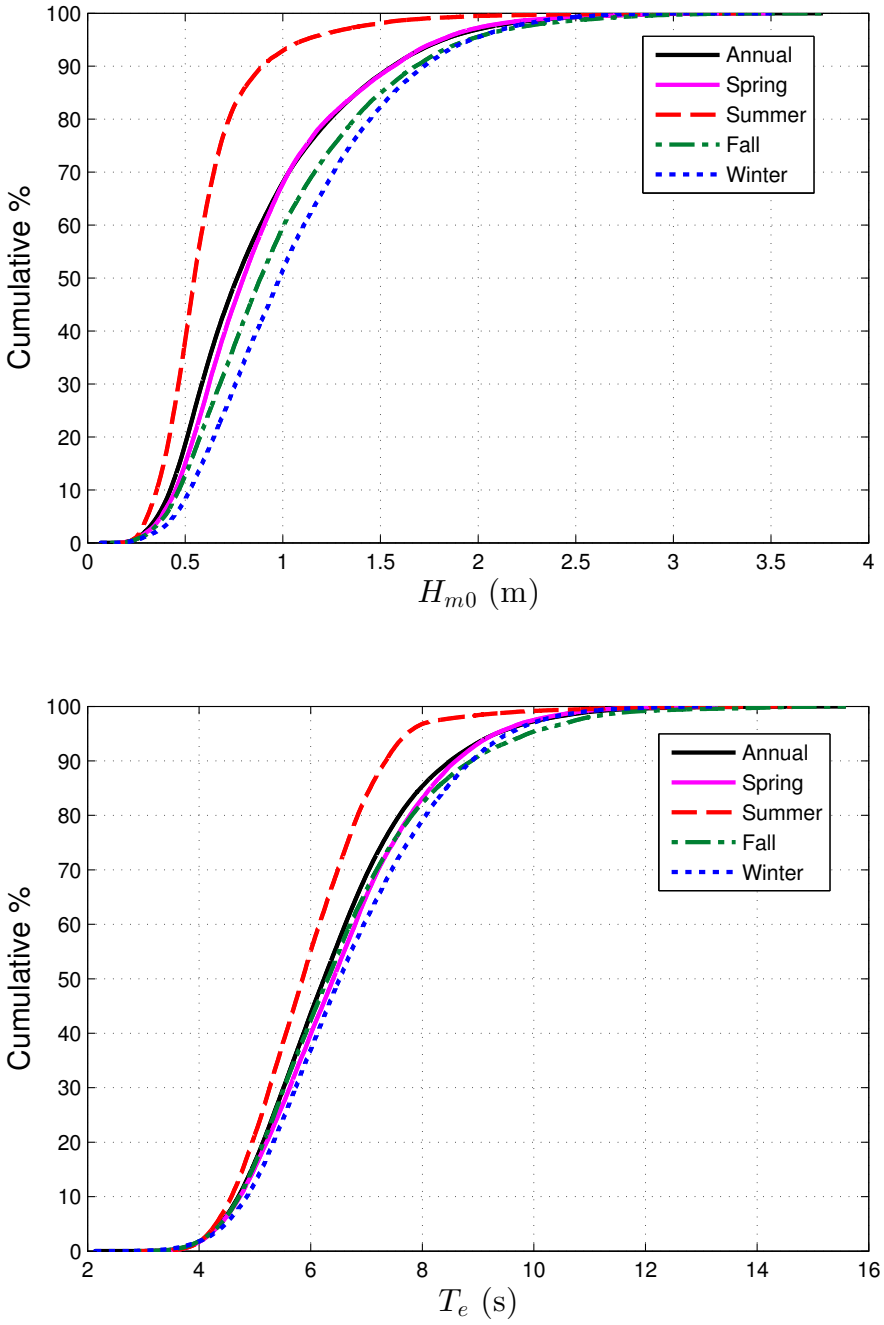

Figure 53: Annual and seasonal cumulative distributions of the significant wave height (top) and energy period (bottom) at the USACE FRF site.

6.4.4. Weather Windows

Figure 54 shows the number of weather windows at the USACE FRF site, when significant wave heights are at or below some threshold value for a given duration, for an average

winter, spring, summer and fall. In these plots, each occurrence lasts a duration that is some multiple of 6-hours. The minimum weather window is, therefore, 6-hours in duration, and the maximum is 96-hours (4 days). The significant wave height threshold is the upper bound in each bin and indicates the maximum significant wave height experienced during the weather window. Note that the table is cumulative, so, for example, an occurrence of $H_{m0} \leq 0.5$ m for at least 66 consecutive hours in the fall is included in the count for 60 consecutive hours as well. In addition, one 12-hour window counts would count as two 6-hour windows. It is clear that there are significantly more occurrences of lower significant wave heights during the summer than winter, which corresponds to increased opportunities for deployment or operations and maintenance.

Weather window plots provide useful information at test sites when planning schedules for deploying and servicing WEC test devices. For example, if significant wave heights need to be less than or equal to 0.5 m for at least 12 consecutive hours to service a WEC test device at the USACE FRF site with a given service vessel, there would be, on average, sixty weather windows in the summer, but only ten in the winter. When wind speed is also considered, Figure 55 shows the average number of weather windows with the additional restriction of wind speed, $U < 15$ mph. The local winds (which are not necessarily driving the waves) are used in these weather windows, and are given in Appendix D.4. That wind data was not available from the hindcast, so data from CFSR was used (see Section 2.3, Appendix D.4). For shorter durations (6- and 12-hour windows), daylight is necessary. Windows with $U < 15$ mph and only during daylight hours are shown in Figure 56. Daylight was estimated as 5am – 10pm Local Standard Time (LST).

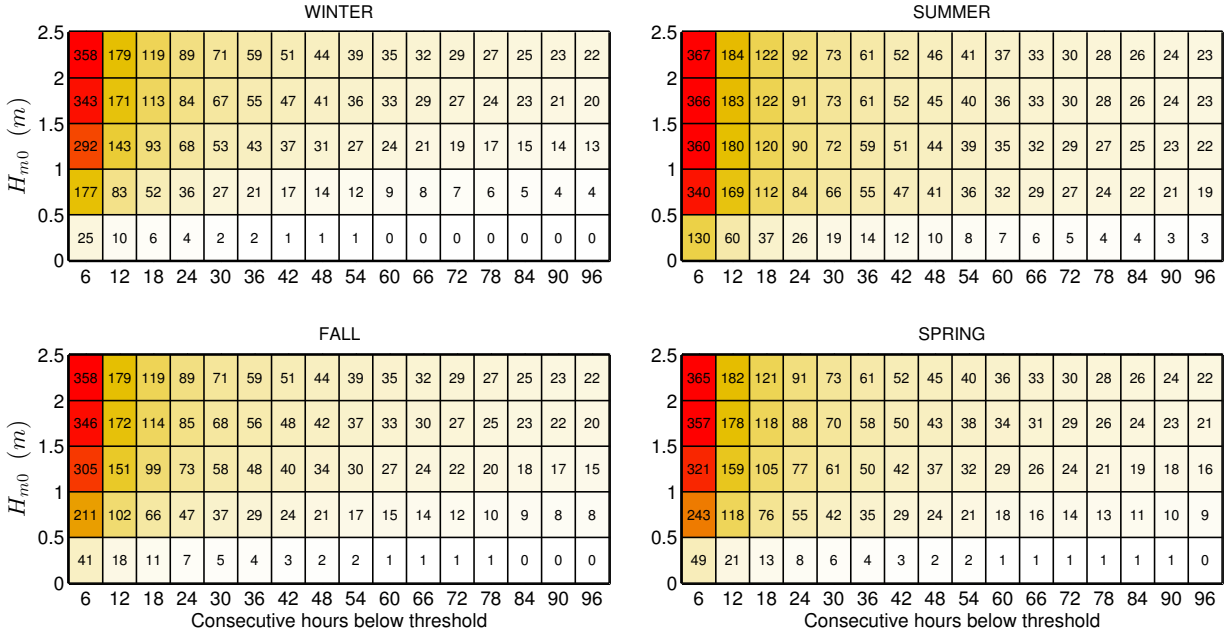

Figure 54: Average cumulative occurrences of wave height thresholds (weather windows) for each season at the USACE FRF site. Winter is defined as December – February, spring as March – May, summer as June – August, and fall as September – November.

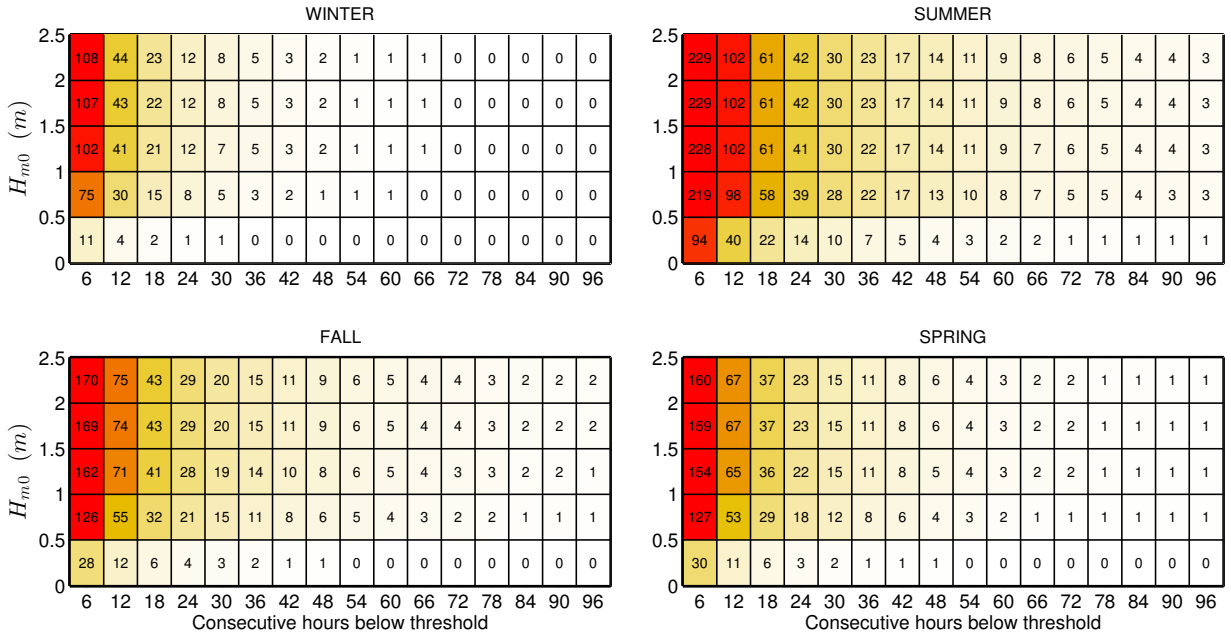

Figure 55: Average cumulative occurrences of wave height thresholds (weather windows) for each season at the USACE FRF site with an additional restriction of U < 15 mph.

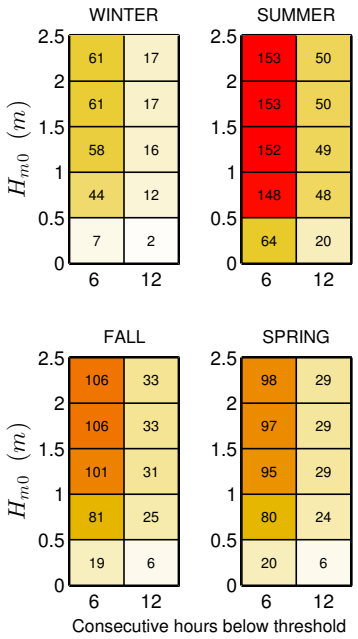

Figure 56: Average cumulative occurrences of wave height thresholds (weather windows) for 6- and 12-hour durations with $U < 15$ mph and only during daylight hours (5am – 10pm LST) at the USACE FRF site.

6.4.5. Extreme Sea States

As mentioned in 2.2, the way IFORM and the modified IFORM are currently implemented, they do not work well for datasets whose variables (H_{m0} and T_e) are bimodally distributed. The NDBC 44056 dataset is not well suited for IFORM, and therefore only the extreme significant wave height is estimated here using extreme value theory. Note this is the same dataset used for the Jennette's Pier site, but the text and figures are repeated here for completeness.

The generalized extreme value distribution (GEV) was fit to the annual significant wave height maximum in order to generate estimates of extreme values under the annual maximum method (AMM) (Rugerio et al. 2010). The peak over threshold (POT) method was also applied to the entire dataset in order to generate estimates of extreme values based on significant wave height exceedances over a certain threshold. Based on the application of this method as described by Ruggerio et al. (2010), the 99.5th percentile of significant wave height was used as a threshold value. These methods were applied using the WAFO matlab toolbox (Brodtkorb et al. 2000). The bootstrapping method (Efron and Tibshirani 1993) was applied in order to generate a 95% confidence interval around the CDFs derived using both of the extreme value distribution methods utilized in this analysis.

The 100-year H_{m0} is estimated as 7.55 m and 8.46 m using the GEV and POT methods, respectively, as shown in Figures 57 and 58. The 10-, 25-, and 50-year values are shown in the figures. It should be noted that conditions at the NDBC44056 buoy (at 17 m depth) are a good representative of locations available for testing, but for the location of the hindcast data (at 4.8 m depth) conditions may differ significantly.

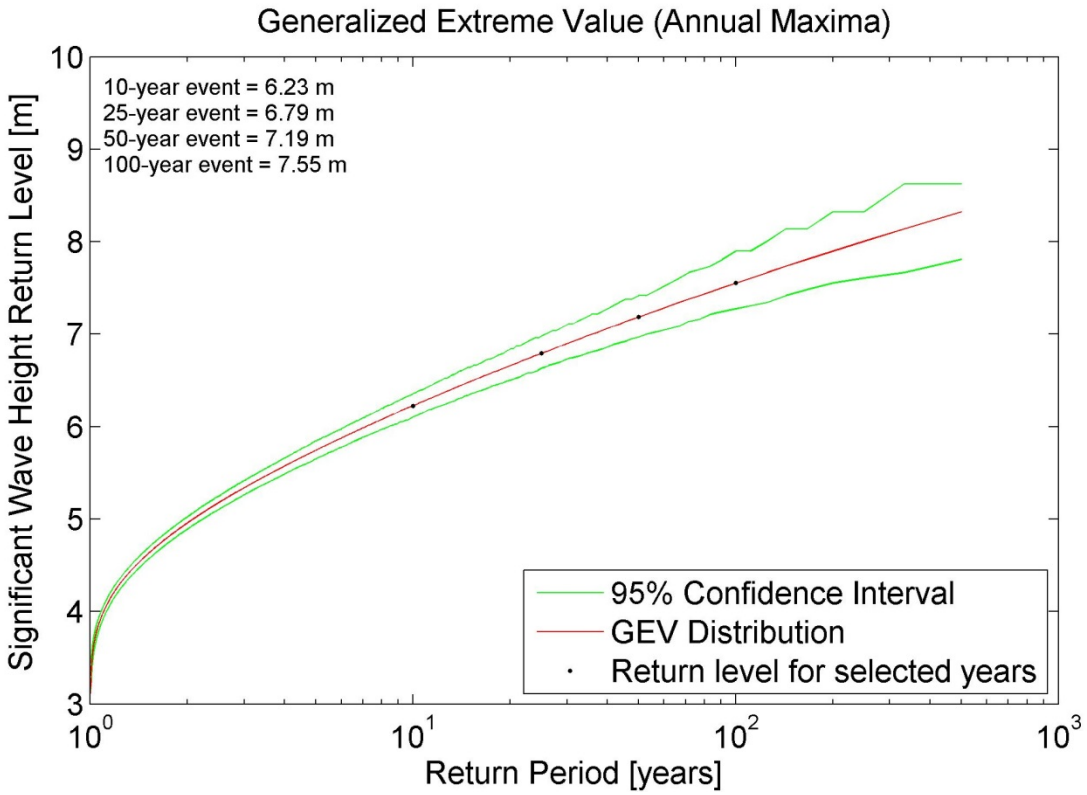

Figure 57: The generalized extreme values distribution was fit to annual maximum of significant wave height from NDBC44056 to generate estimates of extreme values. The 95% confidence interval is shown as well.

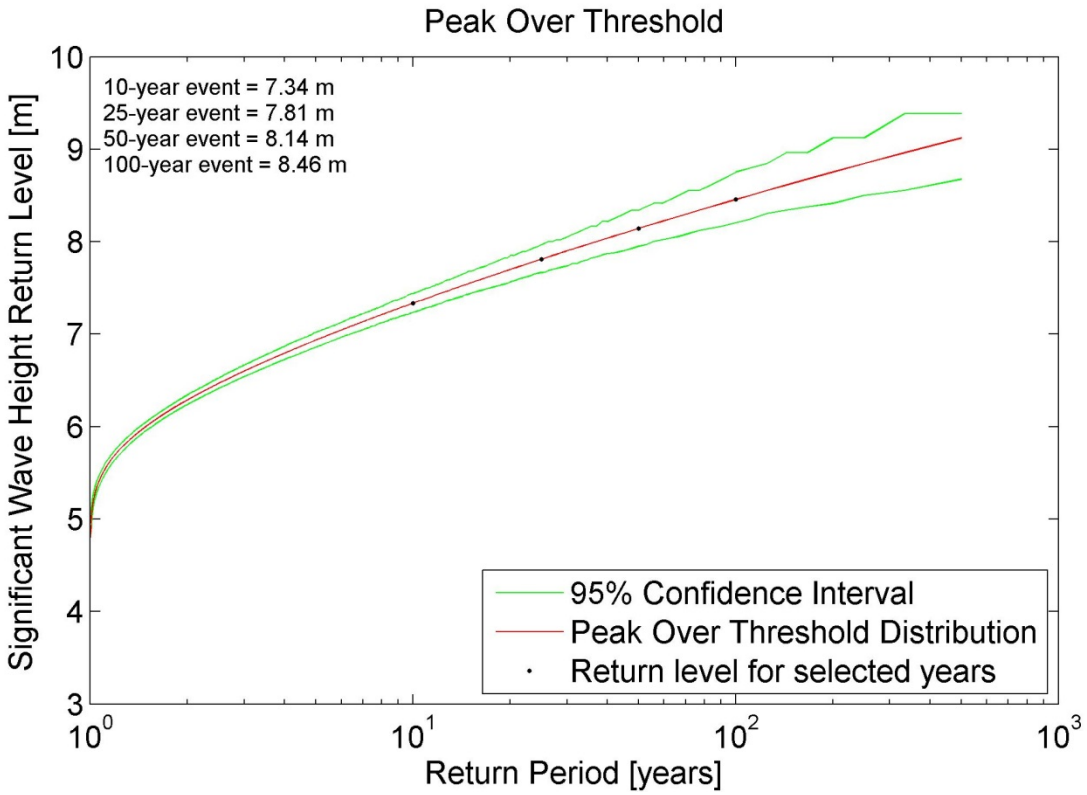

Figure 58: The peak over thresholds method was used with a threshold value of the 99.5th percentile of significant wave height from NDBC44056. The 95% confidence interval is shown as well.

6.4.6. Representative Wave Spectrum

All hourly discrete spectra measured at AWAC04 for the most frequently occurring sea states are shown in Figure 59. The most frequently occurring sea state, which is within the range 0.5 m $< H_{m0} <$ 1 m and 7 s $< T_e <$ 8 s, was selected from a JPD similar to Figure 50 in Section 6.4.1, but based on the AWAC04 data. As a result, the JPD, and therefore the most common sea states, generated from the measured wave data are slightly different from that generated from hindcast data. For example, the most frequently occurring sea state for the JPD generated from hindcast data is in the same range for H_{m0} (0.5 m $< H_{m0} <$ 1 m), but two seconds lower on bounds for T_e (5 s $< T_e <$ 6 s). Often several sea states will occur at a very similar frequency, and therefore plots of hourly discrete spectra for several other sea states are also provided for comparison. Each of these plots includes the mean spectrum and standard wave spectra, including Bretschneider and JONSWAP, with default constants as described in Section 2.2.

For the purpose of this study, the mean spectrum is the 'representative' spectrum for each sea state, and the mean spectrum at the most common sea state, shown in Figure 59 (bottom-left plot), is considered the 'representative' spectrum at the site. The hourly spectra vary considerably about this mean spectrum, but this is partly reflective of the bin size chosen for H_{m0} and T_e. Comparisons of the representative spectra in all plots with the Bretschneider

and JONSWAP spectra illustrate why modeled spectra with default constants, e.g., the shape parameter $\gamma = 3.3$ for the JONSWAP spectrum, should be used with caution. Using the constants provided in Section 2.2, the Bretschneider spectra are, at best, fair representations of the mean spectra in Figure 59. There is some evidence of bimodal spectra in the four sea states displayed, which is not captured by the modeled spectra. The mean measured spectra is the best representation of the conditions, however, if these modeled spectra were to be used at this site, it is recommended that the constants undergo calibration against some mean spectrum, e.g., the representative spectrum constructed here. A better alternative may be to explore other methods or spectral forms to describe bimodal spectra (e.g., Mackay 2011) if it is known that the shape is not unimodal.

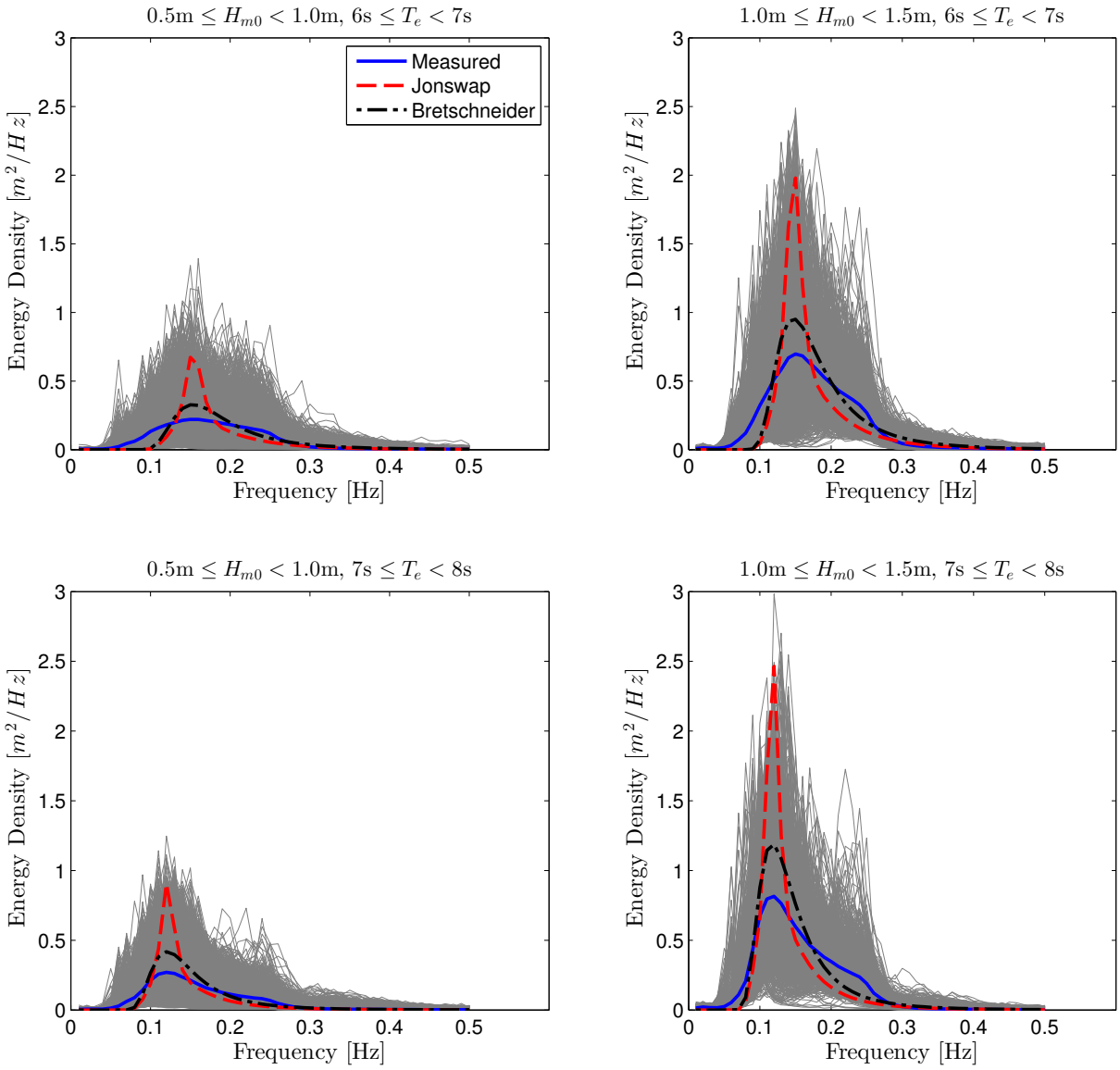

Figure 59: All hourly discrete spectra and the mean spectra measured at AWAC04 within the sea state listed above each plot. The JONSWAP and Bretschneider spectra are represented by red and black dotted lines, respectively.

7. PACIFIC MARINE ENERGY TEST CENTER (PMEC): LAKE WASHINGTON TEST SITE

7.1. Site Description

As described in the PMEC NETS chapter, the Pacific Marine Energy Center (PMEC) is the name of the Northwest National Marine Renewable Energy Centers (NNMREC) marine energy converter testing facilities located in the Pacific Northwest region. NNMREC is a Department of Energy funded entity designed to facilitate development of marine renewable energy technology. Ultimately PMEC will facilitate testing a broad range of technologies being produced by the marine energy industry (NNMREC 2014). The Lake Washington Test Site is an off-grid WEC test site that became operational in 2012. The most recent location used in winter 2012/2013 by Oscilla Power (Nair et al. 2013) will be designated the test location for the purpose of this catalogue. As shown in Figure 60, the Lake Washington site is at 47.6795 N, 122.2305 W. This site was chosen due to the long fetch from predominant southerly winds in winter and because the location is clear from barge traffic. Other locations in the lake may be available for testing, and it is encouraged to contact PMEC for recommendations.

The Lake Washington site is located in the northern portion of Lake Washington, northeast of Seattle, WA. At the test site, the water depth is approximately 51 m, the bathymetry is gently sloping, and the lake bed consists of soft mud. Figure 61 shows the bathymetry in the lake. The wave climate at the test site varies seasonally, with calmer conditions in the summer due to weak northerly winds, and more energetic conditions in the winter due to strong southerly winds. The wave climate is event driven by local winds, and there are periods of very low waves (nearly zero wave power) throughout the year. The wave environment at Lake Washington is characterized by an annual average power flux of about 0.04 kW/m.

NNMREC offers a wide range of technical and testing infrastructure support services for WEC developers. Lake Washington has small scale ('nursery') wave energy resources, and can accommodate scaled, prototype devices.

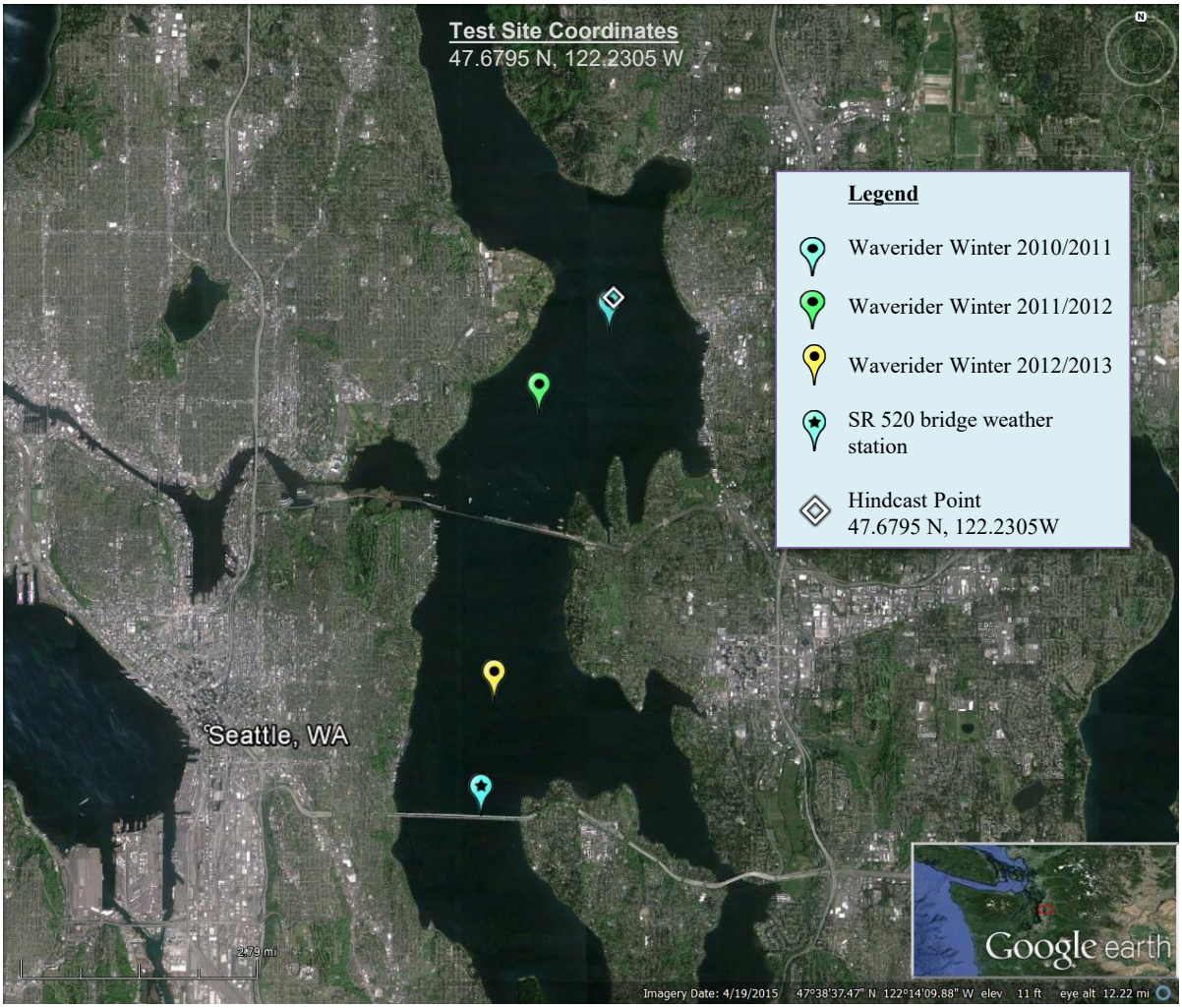

Figure 60: PMEC Lake Washington is located in the northern portion of Lake Washington northeast of Seattle. The test site is approximately 1.2 km off-shore in 56 m depth water. The fetch for predominant southerly winds in winter is about 5 km (from the Route 520 bridge). A Waverider buoy was deployed by APL-UW in three locations for short durations (see Table 5). Image modified from Google Earth (Google Earth 2015).

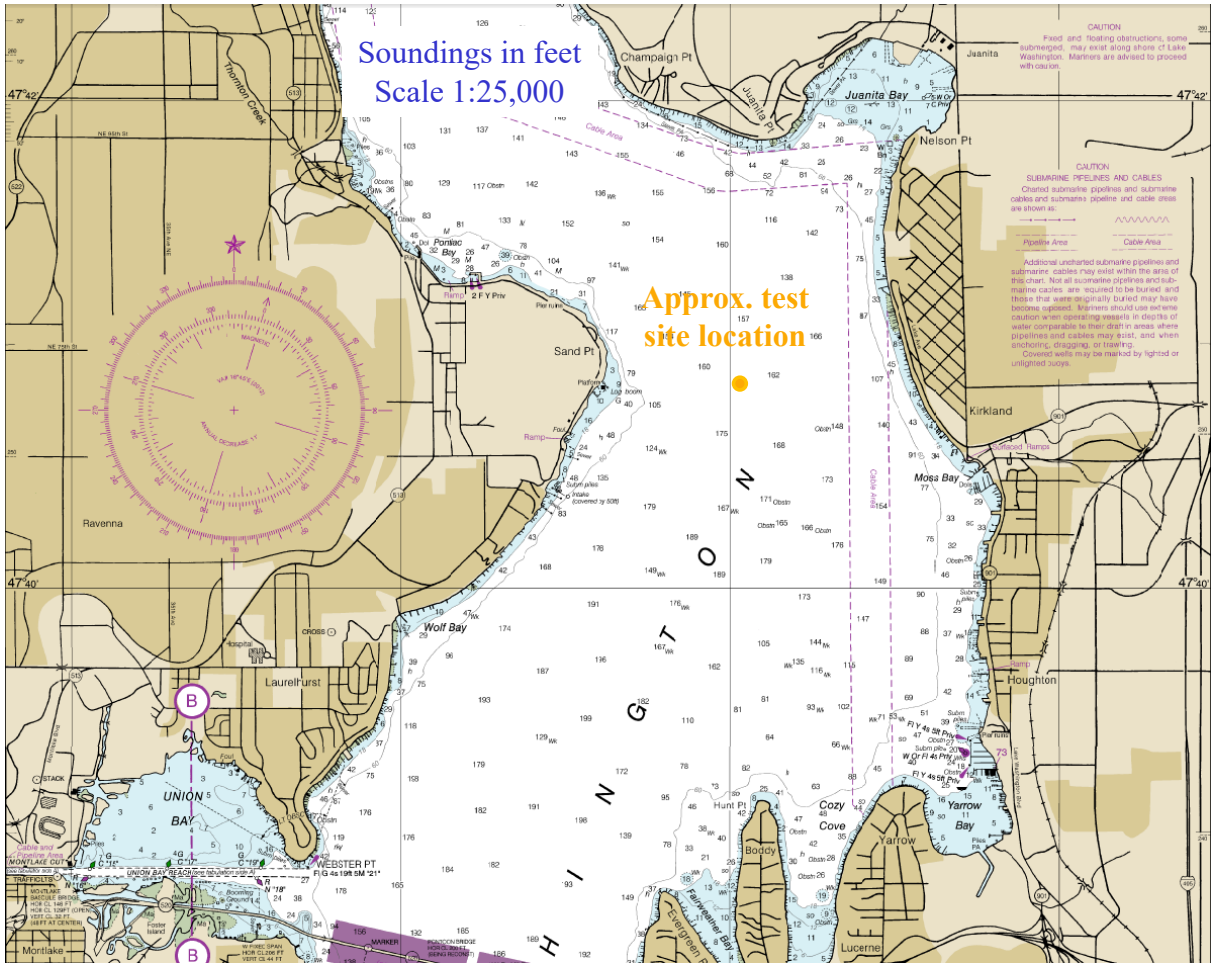

Figure 61: Nautical chart of part of Lake Washington shows the gradually sloping bathymetry around the test site. Soundings in feet (1 foot = 0.3048 m). Image modified from nautical chart #18447 (Office of Coast Survey 2012).

7.2. WEC Testing Infrastructure

7.2.1. Mooring Berths

PMEC Lake Washington does not have any mooring berths permanently installed. A temporary mooring system designed by the Advanced Physics Laboratory at the University of Washington (APL-UW) was used in the winter 2012/2013 testing (Nair et al. 2013).

7.2.2. Electrical Grid Connection

There is currently no electrical grid connection at PMEC Lake Washington, because it is a nursery / demonstration site. Testing typically consists of 'proof of concept' and is not ready for grid connection.

7.2.3. Facilitating Harbor

The APL dock facility is located 5 km east of Lake Washington, in Portage Bay at the western edge of the UW campus. The dock facility has room for staging, moorage for the APL vessels, and a 3 ton hoist.

7.2.4. On-Shore Office Space

Seattle is on the west side of Lake Washington, and several smaller cities are on the other surrounding sides. There is office space for rent as part of the APL "Collaboratory" in 909 Boat St, immediately adjacent to the APL dock facility.

7.2.5. Service Vessel and Engineering Boatyard Access

No dedicated service vessel is available at this time. The APL has a fleet of research vessels which can be reserved up to nine months in advance. The R/V Jack Robertson is the flagship at 56' LOA and with a 3 ton A-frame capacity. The R/V Henderson 54' LOA is a barge suitable to long-term operations (moored on the Lake for round-the-clock operations). Several smaller vessels are available.

In addition, private service vessels for hire are available in the Seattle area, from Foss Tugs, Norseman Maritime, Pacific Fisherman, and Island Tug & Towing.

7.2.6. Travel and Communication Infrastructure

Seattle-Tacoma International Airport (SEA) is in SeaTac, Washington, about 20 minutes south of downtown Seattle. Cellular service offers consistent coverage; there are several Federal Communication Commission (FCC) registered cell phone towers in and around Seattle, Washington.

7.2.7. Met-Ocean Monitoring Equipment

There were three separate deployments of a Waverider buoy by the Applied Physics Lab, at the University of Washington (APL-UW). Each deployment lasted for a few months and was located at different locations in the lake, each time at approximately 60 m depth. The first two locations corresponded to locations of interest for other wave projects (D'Asaro et al. 2014, Thomson et al. 2009). The third deployment of the APL-UW Waverider is less than a kilometer from the designated wave energy test site location used in winter 2012/2013. In addition, APL-UW has conducted numerous shorter deployments of SWIFT buoys to study the fetch dependence and whitecaps along the lake (Thomson 2012). There is also a monitoring buoy operated by King County that reports meteorological data. Instrument and data specifications for this monitoring equipment are summarized in Table 5. UW buoy data can be obtained from Jim Thomson by request, and King County wind data is available online. There are no NDBC buoys in Lake Washington.

Figure 62: Waverider buoy deployed by the University of Washington located less than 1 km from the test site.

Table 5: Wave monitoring equipment in close proximity to PMEC Lake Washington.

Instrument Name (Nickname)	**University of Washington Waverider - Deployment 1**		**University of Washington Waverider - Deployment 2**		**University of Washington Waverider - Deployment 3**	
Type	Waverider buoy		Waverider buoy		Waverider buoy	
Measured parameters	-std. met. data -spectral wave density -spectral wave direction		-std. met. data -spectral wave density -spectral wave direction		-std. met. data -spectral wave density -spectral wave direction	
Variables reported, including derived variables (Sampling interval)	*Std Met.:* WVHT DPD APD MWD (30 min sampling period)	-Spectral Wave Density -Spectral Wave direction (30 min sampling period)	*Std Met.:* WVHT DPD APD MWD (30 min sampling period)	-Spectral Wave Density -Spectral Wave direction (30 min sampling period)	*Std Met.:* WVHT DPD APD MWD (30 min sampling period)	-Spectral Wave Density -Spectral Wave direction (30 min sampling period)
Location	∼2.8 km southwest of the designated test site		∼8 km south/southwest of the designated test site		∼0.7 km south of the designated test site	
Coordinates	47.6582 N 122.2498 W (47°39'29.52" N 122°14'59.28" W)		47.6097 N 122.2615 W (47°36'34.97" N 122°15'40.69" W)		47.6733 N 122.2313 W (47°40'23.88" N 122°13'52.68" W)	
Depth	62 m		62 m		62 m	
Data Start	11/18/2010		10/25/2011		12/22/2012	
Data End	3/15/2011		1/11/2012		3/14/2013	
Period of Record	∼4 months		∼2.5 months		∼3 months	
Owner / Contact Person	University of Washington; contact Jim Thomson jthomson@apl.washington.edu		University of Washington; contact Jim Thomson jthomson@apl.washington.edu		University of Washington; contact Jim Thomson jthomson@apl.washington.edu	

Instrument Name (Nickname)	**King County Lake Washington Buoy**	**Washington State Department of Transportation SR 520**
Type	Monitoring buoy	Weather station
Measured parameters	Meteorological data	Meteorological data
Variables reported, including derived variables (Sampling interval)	AirTemp Pressure WDIR WSPD Humidity Precip Solar radiation (1 hr sampling period)	AirTemp Pressure WDIR WSPD Humidity (5 min sampling period)
Location	In the center of Lake Washington	On SR 520 bridge
Coordinates	47.6122 N 122.254 W	
Depth	-anemometer height: ∼2 m	
Data Start	1/1/2008	10/31/2007
Data End	present	present
Period of Record	∼7 yrs	∼8 yrs
Owner / Contact Person	King County; data available on https://green2.kingcounty.gov/lake-buoy/Data.aspx	Washington State Department of Transportation; data available on http://www.wsdot.wa.gov/traffic/bridges/WeatherHistory.aspx?bridge=SR+520

7.2.8. Environmental Monitoring

No monitoring has been required in previous deployments and tests.

7.2.9. Permitting

Each test requires its own permits. Everything works through the WA Joint Aquatic Resources Permit Application (JARPA), which is a single document used to request all permits. Previous deployments/tests have been required to avoid "fish windows", nominally the spring time.

7.3. Data used

Coast & Harbor produced a 10 year hindcast dataset for the Lake Washington site (Coast and Harbor 2015). This dataset was used to calculate parameters of interest for the characterization at this site. The hindcast data at the grid point shown in Figure 60 was analyzed.

In addition to the hindcast data set, short term data from a buoy deployment by APL-UW was used to calculate representative spectra. Because the buoy deployments were short term (less than a year), it was necessary to use hindcast data to calculated the extreme significant wave height. Wind data was available from the Washington State Department of Transportation weather station located on the SR 520 bridge south of the site. Climate Forecast System Reanalysis (CFSR) winds were only available over land near Lake Washington, and were not considered reliable data sources for wind on the lake, as mentioned in Section 2.3. In addition, OSCAR data is not available at this location, and no current measurements are available. Therefore the wind data from the SR 520 bridge was used for wind statistics, and to estimate surface current speeds (see Appendix E.5), so unfortunately this site cannot be consistent with the other sites in this manner.

7.4. Results

The following sections provide information on the joint probability of sea states, the variability of the IEC TS parameters, cumulative distributions, weather windows, extreme sea states, and representative spectra. This is supplemented by wave roses as well as wind and surface current data in Appendix E . The wind and surface current data provide additional information to help developers plan installation and operations & maintenance activities.

7.4.1. Sea States: Frequency of Occurrence and Contribution to Wave Energy

Joint probability distributions of the significant wave height, H_{m0}, and energy period, T_e, are shown in Figure 63. Figure 63 (top) shows the frequency of occurrence of each binned sea state and Figure 63 (bottom) shows the percentage contribution to the total wave energy. Note that because the waves are much smaller at this site compared to others in the catalogue, the JPD was broken into smaller bin ranges (0.1 m for H_{m0} and 0.2 s for T_e). Figure 63 (top)

indicates that the majority of sea states are within the range 0 m $< H_{m0} <$ 0.4 m and 1 s $< T_e <$ 2.2 s. A narrow range of sea states are experienced at the Lake Washington site, because they consist only of locally generated wind waves. The site is well suited for performing proof of concept testing for WECs at the beginning stages, and has scaled resources but relatively deep water ($\sim$50 m).

As mentioned in the methodology (Section 2.2), previous studies show that sea states with the highest frequencies of occurrence do not necessarily correspond to those with the highest contribution to total wave energy. The total wave energy in an average year is 177 kWh/m, which corresponds to an average annual omnidirectional wave power of 0.04 kW/m. The most frequently occurring sea state is within the range 0 m $< H_{m0} <$ 0.1 m and 1 s $< T_e <$ 1.2 s, while the sea state that contributes most to energy is within the range 0.4 m $< H_{m0} <$ 0.5 m and 2.2 s $< T_e <$ 2.4 s. Several sea states occur at a similar frequency, and sea states within 0.2 m $< H_{m0} <$ 0.5 m and 1.6 s $< T_e <$ 2.4 s contribute a similar amount to energy.

Frequencies of occurrence and contributions to energy of less than 0.01% are considered negligible and are not shown for clarity. For example, the sea state within 0.9 m $< H_{m0} <$ 1 m and 3 s $< T_e <$ 3.2 s contributes 0.23% to energy, but has an occurrence of only 0.007%, therefore it does not appear in Figure 63 (top).

Curves showing the mean, 5^{th} and 95^{th} percentiles of wave steepness, H_{m0}/λ, are also shown in Figure 63. The mean wave steepness at the Lake Washington site is 0.0463 ($\approx 1/22$), and the 95^{th} percentile is approximately 1/18.

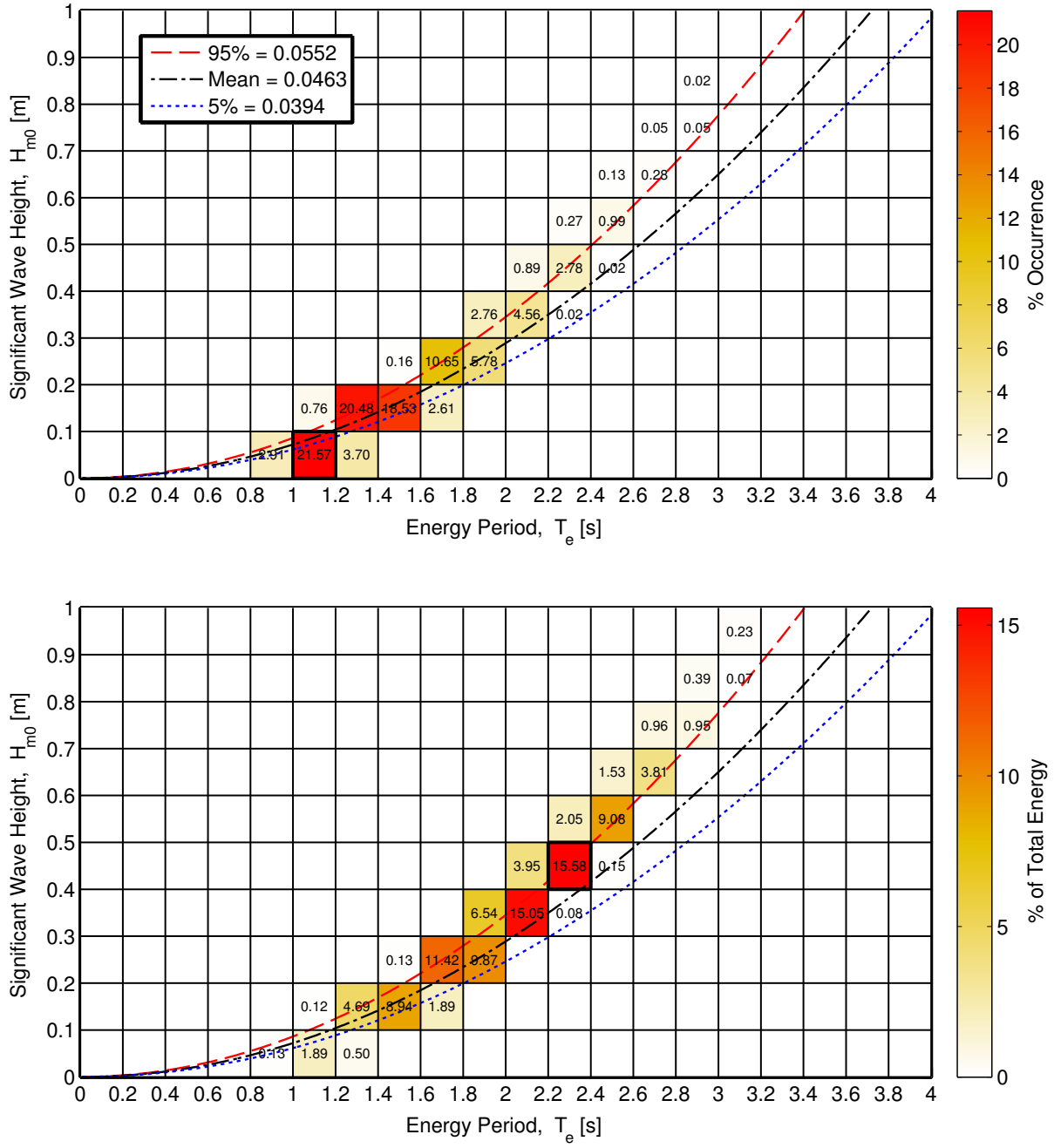

Figure 63: Joint probability distribution of sea states for Lake Washington. The top figure is frequency of occurrence and the bottom figure is percentage of total energy, where total energy in an average year is 177 kWh/m.

7.4.2. IEC TS Parameters

The monthly means of the six IEC TS parameters, along with the 5^{th} and 95^{th} percentiles, are shown in Figure 64. The months, March – February, are labeled with the first letter (e.g., March is M). The values in the figure are summarized in Table **??** in Appendix E.

Monthly means of the significant wave height, H_{m0}, and the omnidirectional wave power density, J, show the greatest seasonal variability compared to the other parameters. Values are largest and vary the most during the winter months. The same trend is observed for the monthly mean energy period, T_e, but its variation is less pronounced. These observations are consistent with the relationship between wave power density, significant wave height and energy period, where wave power density, J, is proportional to the energy period, T_e, and the square of the significant wave height, H_{m0}.

The direction of maximum directionally resolved wave power is typically from the south at $\sim 180°$, with some variaton in the mean in the summer months. There are frequent shifts of the direction to the north near 0° / 360°, which causes the 5th and 95th percentiles to be so wide. In some of the spring and fall months, the 5th percentile of direction changes because the northerly wind (and therefore waves) occur less often. The mean directionality coefficient is very consistent throughout the year, however, there are instances of lower d_θ in the summer (signified by the drop in the 5th percentile). Seasonal variation of the spectral width is indiscernible and appears to be nearly contant throughout the year at 0.24. In summary, the waves at the Lake Washington site, from the perspective of monthly means, have a fairly consistent spectral width, are predominantly from the south, and exhibit a wave power that has a narrow directional spread.

Wave roses of wave power and significant wave height, presented in Appendix E, Figures 144 and 145, also show the predominant direction of the wave energy at the Lake Washington site, which is south, with frequent shifts to the north/northeast. Figure 144 shows two dominant wave direction sectors, south (at 180°) and south/southwest (SSW) at 210°. Along the predominant wave direction, 180°, the omnidirectional wave power density is at or below 0.35 kW/m about 12% of the time, and greater than 0.35 kW/m nearly 0.2% of the time. Along the south/southwest direction (210°), wave power density is at or below 0.35 kW/m almost 8% of the time, and greater than 0.35 kW/m about 0.2% of the time.

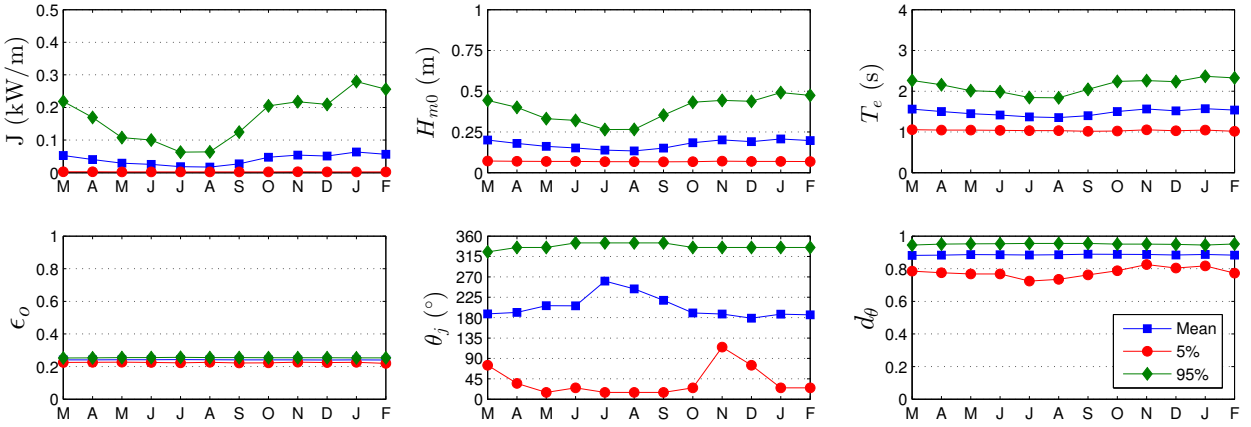

Figure 64: The average, 5^{th} and 95^{th} percentiles of the six parameters at the Lake Washington site.

Monthly means, however, smear the significant variability of the six IEC parameters over

small time intervals as shown in plots of the parameters at 1-hour intervals in Figure 65 for a representative year. While seasonal patterns described for Figure 64 are still evident, these plots show how sea states can vary abruptly at small time scales with sudden changes, e.g., jumps in the wave power as a result of a storm. The frequent shifts in wind direction are also evident in this figure.

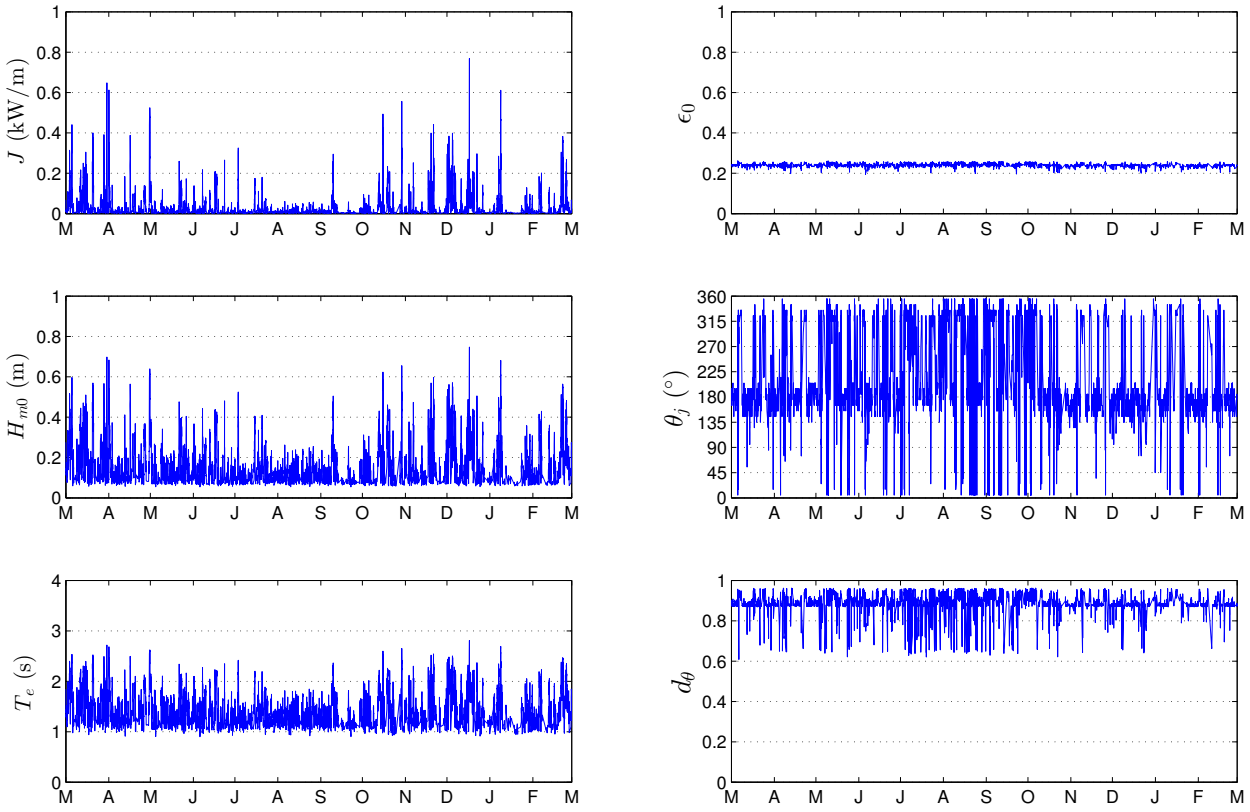

Figure 65: The six parameters of interest over a one-year period, March 2013 – February 2014 at the Lake Washington site.

7.4.3. Cumulative Distributions

Annual and seasonal cumulative distributions (a.k.a., cumulative frequency distributions) are shown in Figure 66. Note that spring is defined as March – May, summer as June – August, fall as September – November, and winter as December – February. The cumulative distributions are another way to visualize and describe the frequency of occurrence of individual parameters, such as H_{m0} and T_e. A developer could use cumulative distributions to estimate how often they can access the site to install or perform operations and maintenance based on their specific device, service vessels, and diving operation constraints. For example, if significant wave heights need to be less than or equal to 0.1 m for installation and recovery, according to Figure 66, this condition occurs nearly 28% of the time on average within a given year. If significant wave heights need to be less than or equal to 0.2 m for emergency maintenance, according to Figure 66, this condition occurs about 71% of time on average

within a given year. Cumulative distributions, however, do not account for the duration of a desirable sea state, or weather window, which is needed to plan deployment and servicing of a WEC device at a test site. This limitation is addressed with the construction of weather window plots in the next section.

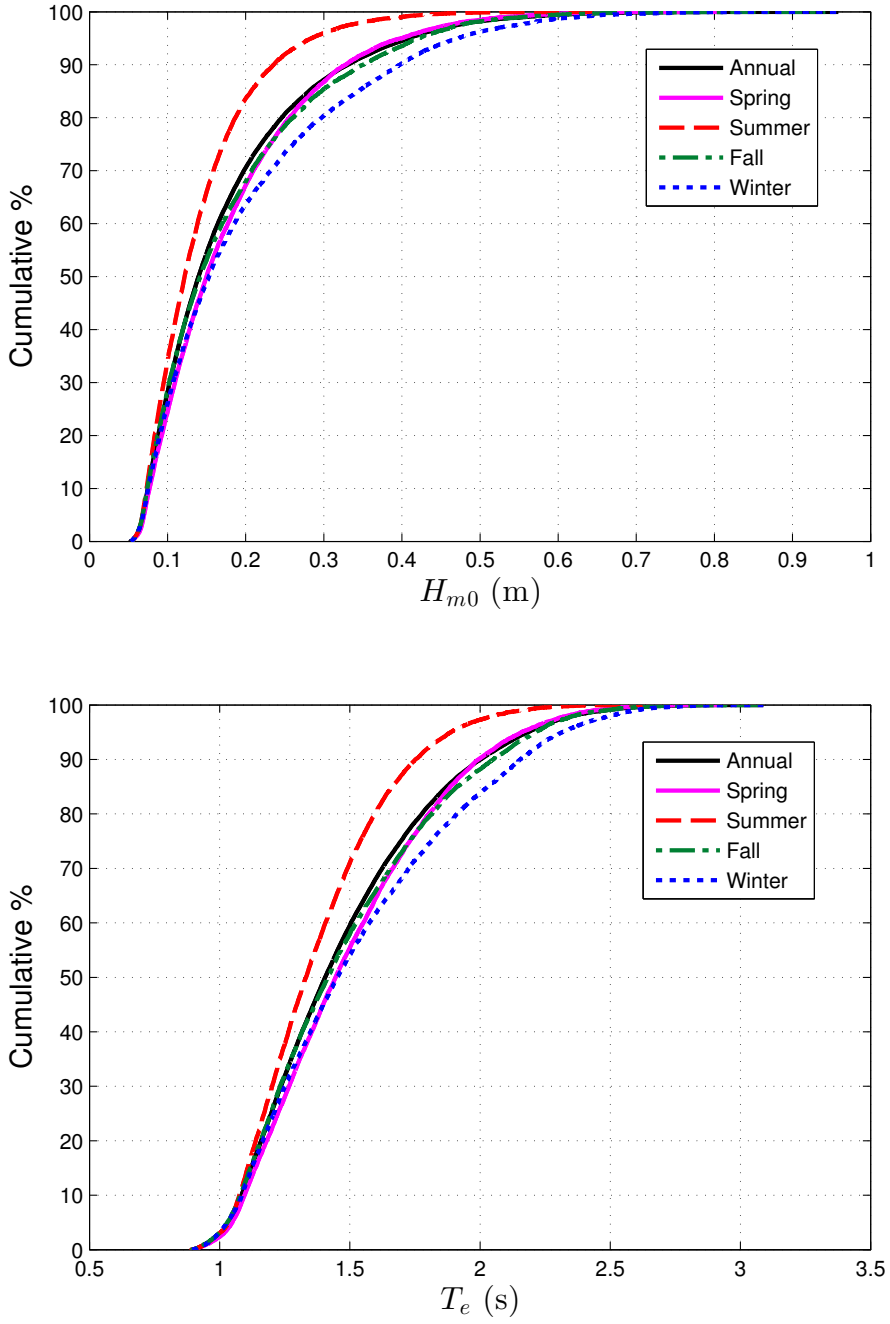

Figure 66: Annual and seasonal cumulative distributions of the significant wave height (top) and energy period (bottom) at the Lake Washington site.

7.4.4. Weather Windows

Figure 67 shows the number of weather windows at the Lake Washington site, when significant wave heights are at or below some threshold value for a given duration, for an average winter, spring, summer and fall. In these plots, each occurrence lasts a duration that is some multiple of 6-hours. The minimum weather window is, therefore, 6-hours in duration, and the maximum is 96-hours (4 days). The significant wave height threshold is the upper bound in each bin and indicates the maximum significant wave height experienced during the weather window. Note that the table is cumulative, so, for example, an occurrence of $H_{m0} \leq 0.2$ m for at least 72 consecutive hours in the fall is included in the count for 66 consecutive hours as well. In addition, one 12-hour window counts would count as two 6-hour windows. There are more occurrences of lower significant wave heights during the summer than winter, which typically corresponds to increased opportunities for deployment or operations and maintenance. For this particular test site, however, waves are so low during the summer that winter is a more likely deployment period because the frequent winter storms provide sufficient wave activity, but there are still many calm periods in the winter which would allow for deployment and maintenance (Nair et al. 2013).

Weather window plots provide useful information at test sites when planning schedules for deploying and servicing WEC test devices. For example, if significant wave heights need to be less than or equal to 0.2 m for at least 12 consecutive hours to service a WEC test device at the Lake Washington site with a given service vessel, there would be, on average, thirty-five weather windows in the winter. When wind speed is also considered, Figure 68 shows the average number of weather windows with the additional restriction of wind speed, $U < 15$ mph. The local winds (which for this site, do drive the waves) are used in these weather windows, and are given in Appendix E.4. That wind data was obtained from the SR 520 bridge weather station (see Section 2.3, Appendix E.4). For shorter durations (6- and 12-hour windows), daylight is necessary. Windows with $U < 15$ mph and only during daylight hours are shown in Figure 69. Daylight was estimated as 5am – 10pm Local Standard Time (LST).

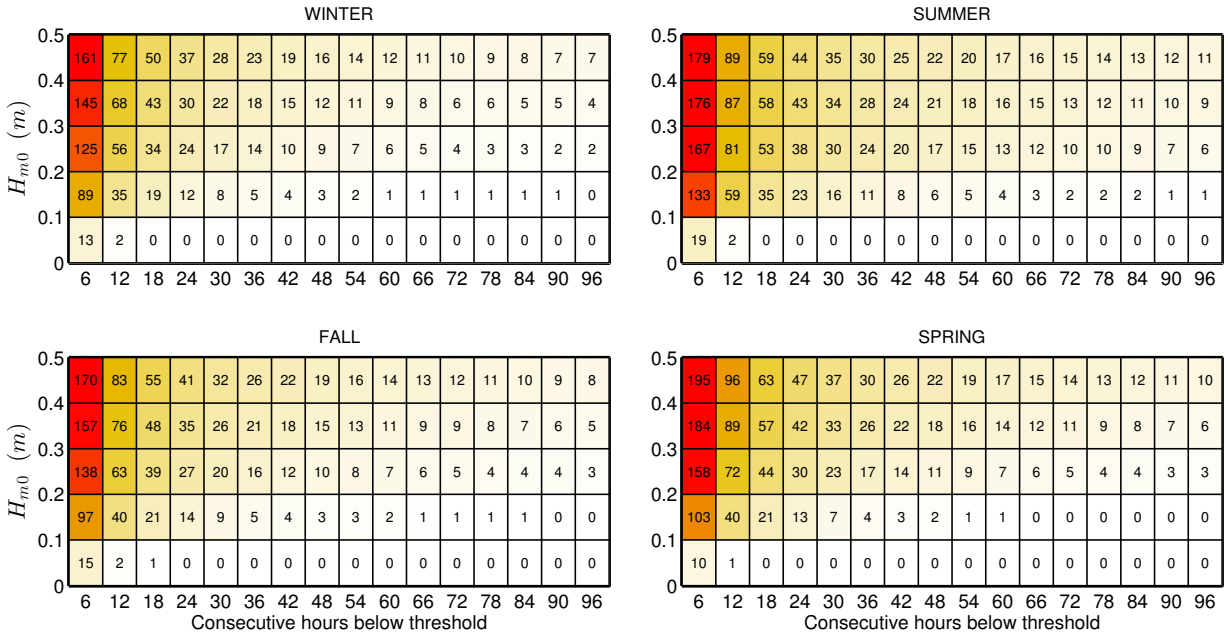

Figure 67: Average cumulative occurrences of wave height thresholds (weather windows) for each season at the Lake Washington site. Winter is defined as December – February, spring as March – May, summer as June – August, and fall as September – November.

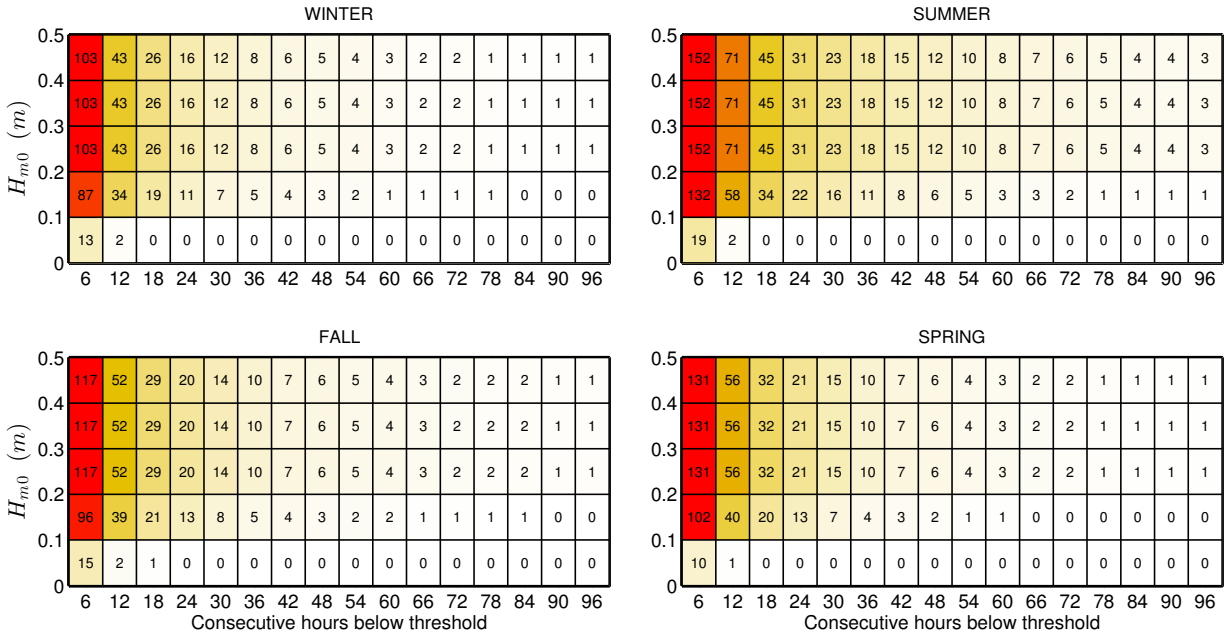

Figure 68: Average cumulative occurrences of wave height thresholds (weather windows) for each season at the Lake Washington site with an additional restriction of U $<$ 15 mph.

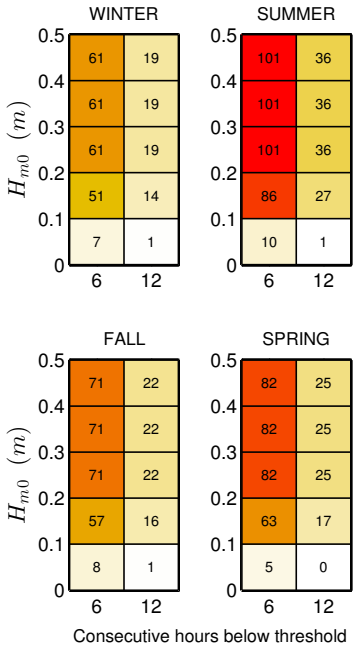

Figure 69: Average cumulative occurrences of wave height thresholds (weather windows) for 6- and 12-hour durations with $U < 15$ mph and only during daylight hours (5am – 10pm LST) at the Lake Washington site.

7.4.5. Extreme Sea States

Measured wave data at Lake Washington consists only of very short term deployment periods (less than a year), and is not an appropriate dataset for extreme sea state estimation. Hindcast data is therefore used for this site. In addition, as mentioned in 2.2, the Lake Washington dataset is not well suited for IFORM because the distribution is so narrow (see Figure 63) due to the waves being short fetched wind waves; so only the extreme significant wave height is estimated here using extreme value theory.

The generalized extreme value distribution (GEV) was fit to the annual significant wave height maximum in order to generate estimates of extreme values under the annual maximum method (AMM) (Rugerio et al. 2010). The peak over threshold (POT) method was also applied to the entire dataset in order to generate estimates of extreme values based on significant wave height exceedances over a certain threshold. Based on the application of this method as described by Ruggerio et al. (2010), the 99.5th percentile of significant wave height was used as a threshold value. These methods were applied using the WAFO matlab toolbox (Brodtkorb et al. 2000). The bootstrapping method (Efron and Tibshirani 1993) was applied in order to generate a 95% confidence interval around the CDFs derived using both of the extreme value distribution methods utilized in this analysis.

The 100-year H_{m0} is estimated as 1.13 m and 1.04 m using the GEV and POT methods, respectively, as shown in Figures 70 and 71. The 10-, 25-, and 50-year values are shown in the figures.

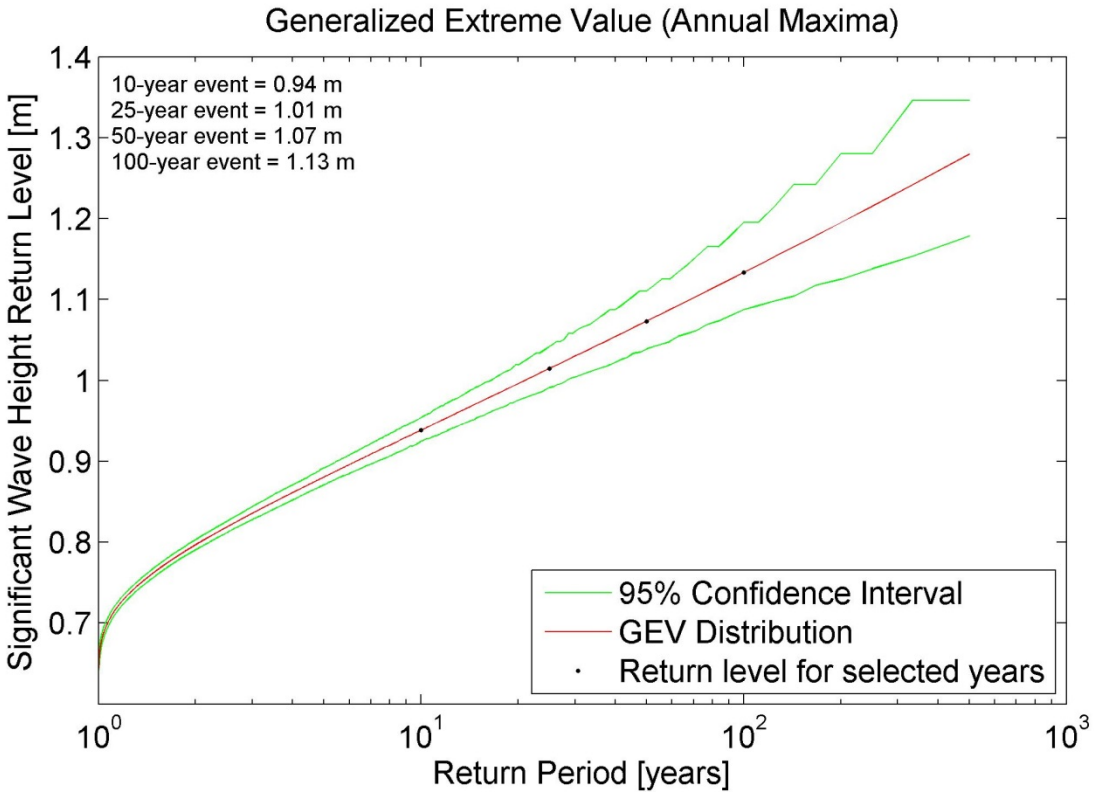

Figure 70: The generalized extreme values distribution was fit to annual maximum of significant wave height from the hindcast dataset to generate estimates of extreme values. The 95% confidence interval is shown as well.

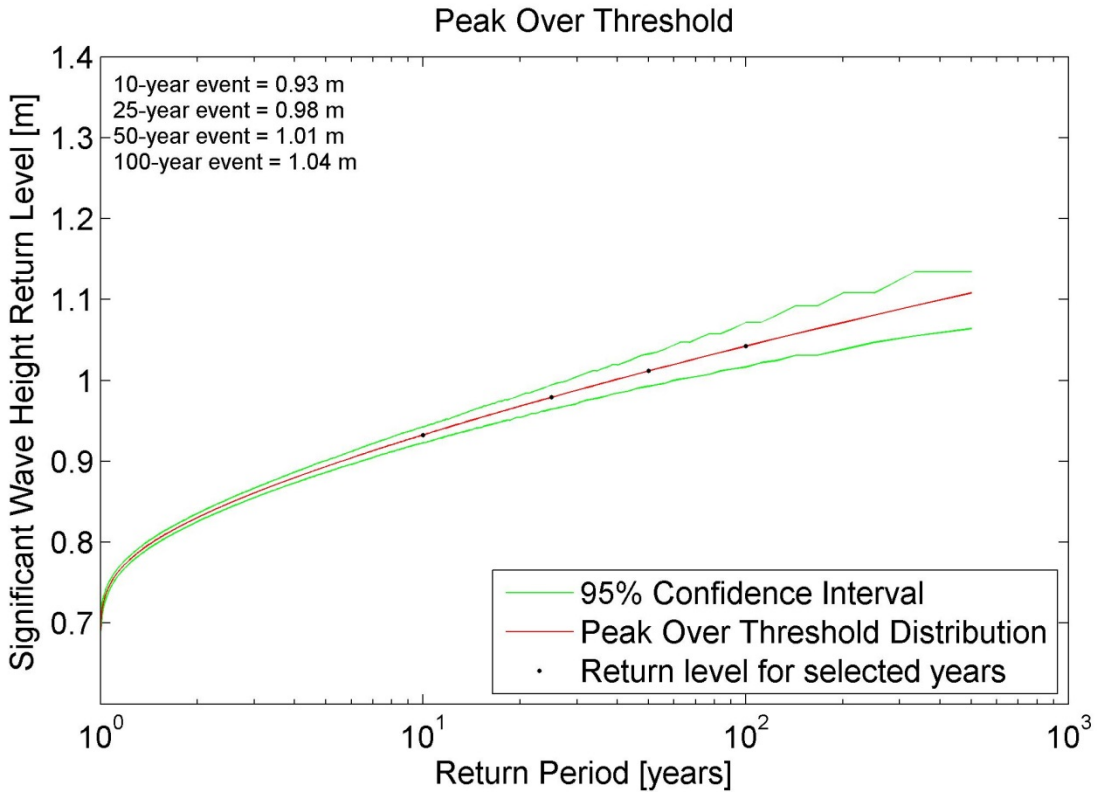

Figure 71: The peak over thresholds method was used with a threshold value of the 99.5th percentile of significant wave height from the hindcast dataset. The 95% confidence interval is shown as well.

7.4.6. Representative Wave Spectrum

All hourly discrete spectra from the hindcast data for the most frequently occurring sea states are shown in Figure 72. Note that typically measured data is used in this catalogue, however, for this site, the measured data was very short term, and not representative of a full year. The most frequently occurring sea state, which is within the range 0 m $< H_{m0} <$ 0.1 m and 1 s $< T_e <$ 1.2 s, was selected from the hindcast JPD in Figure 63 in Section 7.4.1. Often several sea states will occur at a very similar frequency, and therefore a plot of hourly discrete spectra for one other sea state is also provided for comparison. Each of these plots includes the mean spectrum and standard wave spectra, including Bretschneider and JONSWAP, with default constants as described in Section 2.2.

For the purpose of this study, the mean spectrum is the 'representative' spectrum for each sea state, and the mean spectrum at the most common sea state, shown in Figure 72 (left plot), is considered the 'representative' spectrum at the site. The hourly spectra vary somewhat about this mean spectrum, but this is partly reflective of the bin size chosen for H_{m0} and T_e. Comparisons of the representative spectra in all plots with the Bretschneider and JONSWAP spectra illustrate why modeled spectra with default constants, e.g., the shape parameter $\gamma =$ 3.3 for the JONSWAP spectrum, should be used with caution. Using the constants provided in Section 2.2, the Bretschneider spectra are fair representations of the mean spectra in

Figure 72. If available, mean measured spectra (with a period of record of at least one year) would be the best representation of the conditions. In this case, the mean simulated spectra are considered the best representation, although short term measurements are still informative. If modeled standard spectra (Bretschneider or JONSWAP) were to be used at this site, it is recommended that the constants undergo calibration against some mean spectrum, e.g., the representative spectrum constructed here.

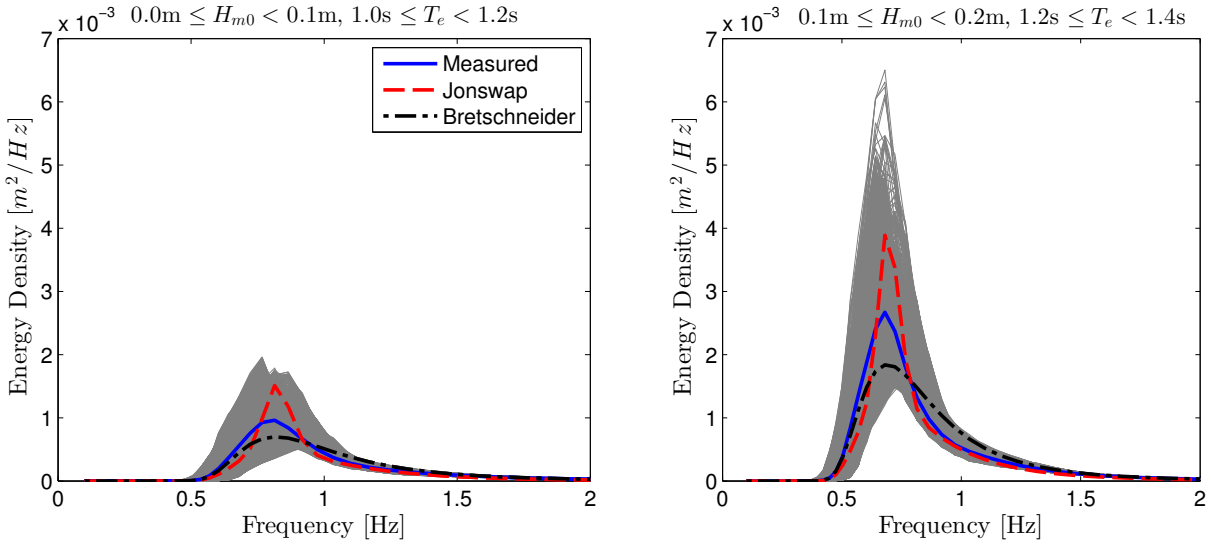

Figure 72: All hourly discrete spectra and the mean spectra from the hindcast dataset within the sea state listed above each plot. The JONSWAP and Bretschneider spectra are represented by red and black dotted lines, respectively.

8. PACIFIC MARINE ENERGY TEST CENTER (PMEC): SOUTH ENERGY TEST SITE (SETS)

8.1. Site Description

As described in the PMEC NETS chapter, the Pacific Marine Energy Center (PMEC) is the name of the Northwest National Marine Renewable Energy Centers (NNMREC) marine energy converter testing facilities located in the Pacific Northwest region. NNMREC is a Department of Energy funded entity designed to facilitate development of marine renewable energy technology. Ultimately PMEC will facilitate testing a broad range of technologies being produced by the marine energy industry (NNMREC 2015). NNMREC is currently in the permitting phase of developing a utility-scale, grid-accessible test site, the South Energy Test Site (SETS), which is planned to be operational in 2017. As shown in Figure 73, SETS will encompass an area of 2-square nautical mile (roughly 6.9 square kilometers) in the Outer Continental Shelf (outside state waters), centered at approximately 44.567 N, 124.229 W. Four grid-connected test berths, each with its own subsea cable, are planned.

SETS is located near the City of Newport, Oregon and Yaquina Bay. At the test site, the water depth is approximately 58-75 m (32-41 fathoms), the bathymetry is gently sloping, and the sea bed is predominantly sandy. Figure 74 shows the bathymetry surrounding the test site. The wave climate at the test site varies seasonally, with calmer seas in the summer compared to more energetic seas in the winter. The wave environment at SETS is characterized by an annual average power flux of about 40.7 kW/m, including a number of events with significant wave heights exceeding 7 m each winter.

NNMREC offers a wide range of technical and testing infrastructure support services for WEC developers as discussed in the PMEC NETS chapter. SETS has full scale wave energy resources, and will be able to accommodate utility scale devices and small arrays. NNMREC would like testing at this facility to allow certification to IEEE and other international standards, and ideally some of the devices will provide power to the local grid (NNMREC 2015), although this will depend on getting the necessary approvals and many other factors.

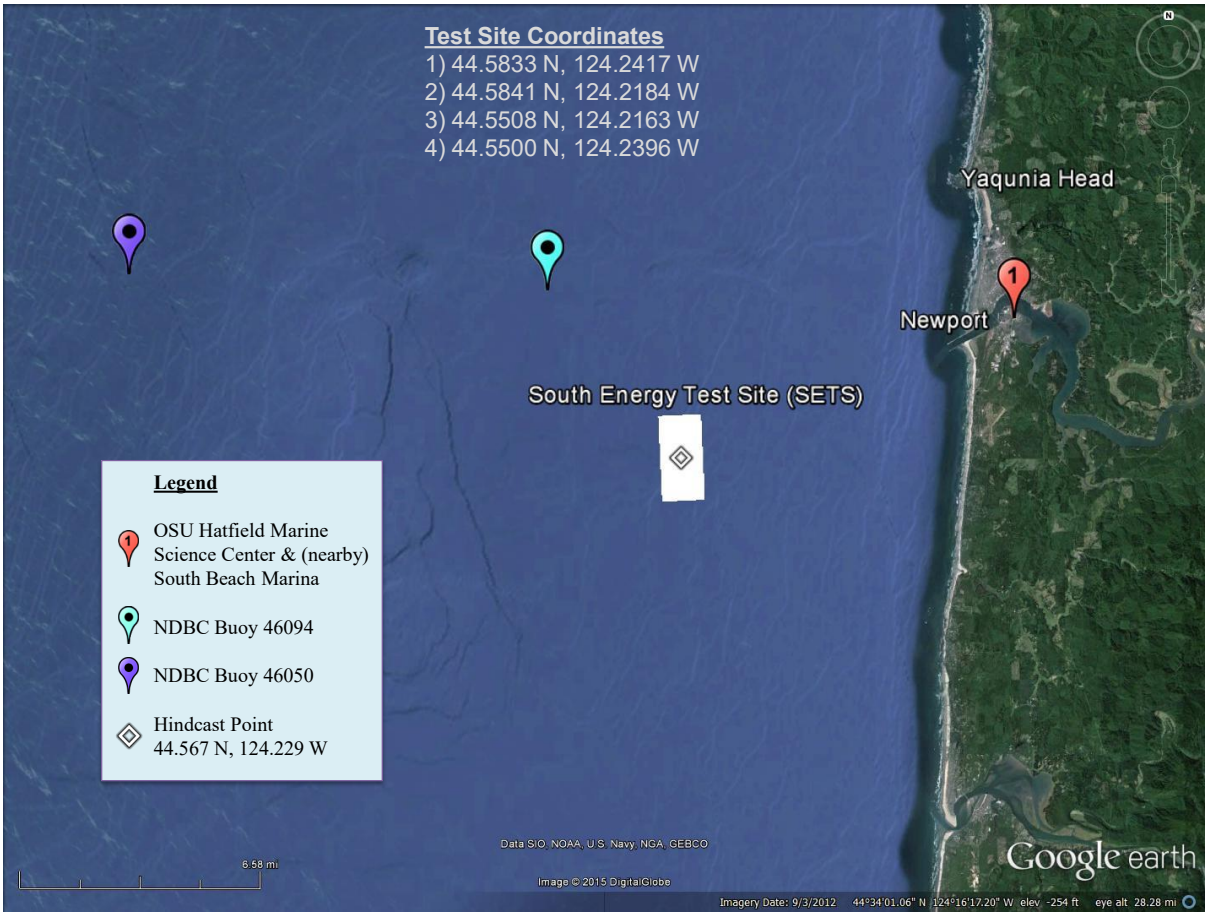

Figure 73: SETS is located in the coastal waters of Oregon near the City of Newport. The test site is approximately 11–13 km off-shore in 58–75 m depth water. One National Data Buoy Center (NDBC) ocean buoy and one NDBC meteorological station are close to the site (see Table 6). The South Beach Marina, Port of Toledo Yaquina Boatyard, and OSU Hatfield Marine Science Center offer services valuable for WEC testing. The point of reference for the hindcast simulation is in the center of SETS. Image modified from Google Earth (Google Earth 2015).

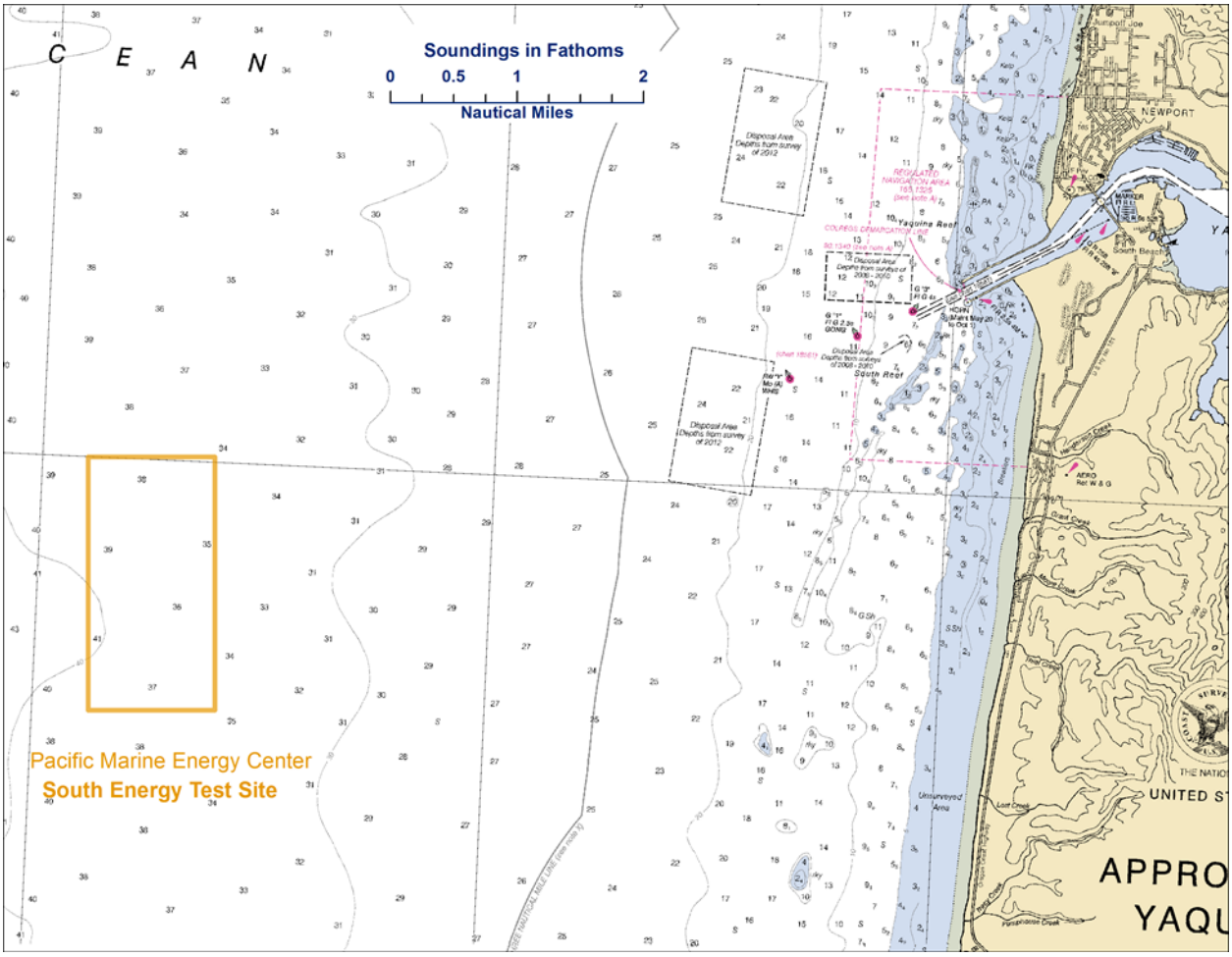

Figure 74: Nautical chart of Yaquina Head and surrounding area shows the gradually sloping bathymetry around SETS. Soundings in fathoms (1 fathom = 1.8288 m). Image modified from nautical chart #18561 (Office of Coast Survey 2011).

8.2. WEC Testing Infrastructure

8.2.1. Mooring Berths

SETS is planned to be permitted to test up to twenty WECs concurrently so that small arrays can be tested. Mooring systems will not be provided and would need to be installed according to the developer's design. Three- to four-point anchoring layouts are commonly used, but NNMREC is researching the feasibility of single point moorings. WEC testing can be done year around, and devices will likely be in the site for multiple years.

8.2.2. Electrical Grid Connection

SETS will be a utility scale grid connected facility. Four-grid connected test berths with their own buried subsea cable are planned. In addition to transmitting energy, the subsea cable will also be capable of transmitting performance and environmental data to an onshore

control center.

8.2.3. Facilitating Harbor

SETS is approximately 13 km south/southwest of the entrance to Yaquina Bay, the mouth of the Yaquina River. The South Beach Marina is located near the outlet of Yaquina Bay and offers year-round boat mooring (near Waypoint #1 in Figure 73).

8.2.4. On-Shore Office Space

The fishing and tourist City of Newport, Oregon, where approximately ten thousand people live, is on the north side of Yaquina Bay (U.S. Census Bureau 2012). Meeting rooms and temporary office space through PMEC are planned to be available following the completion of SETS.

8.2.5. Service Vessel and Engineering Boatyard Access

No dedicated service vessel is available at this time, but following the completion of SETS, more resources may be available through PMEC. Service vessels for hire are likely available in the Newport/Toledo area. The Port of Toledos Yaquina Boatyard (Waypoint #2 in Figure 73) services boats and provides space for self-service. Yaquina Boatyard hauls boats up to 300 tons and has capabilities that include steel fabrication, carpentry, painting, haul-out, and project management (Port of Toledo 2014).

8.2.6. Travel and Communication Infrastructure

Portland International Airport (PDX) is a two and a half hour drive from Newport, Oregon. Eugene Airport is located closer and is a one hour and forty minute drive. Cellular service offers consistent coverage; three Federal Communication Commission (FCC) registered cell phone towers are located in and around Newport, Oregon.

8.2.7. Met-Ocean Monitoring Equipment

A buoy for measuring waves and currents is currently deployed for a 1 year period. Data may be available from OSU after deployment completion. NNMREC plans to deploy instrumentation in each berth when devices are testing. Specific instrumentation will depend on the device. If the site is empty of WECs under test, it is planned that one monitoring device will be deployed at all times.

In addition, there are two National Buoy Data Center (NDBC) buoys that measure and collect ocean data and one NDBC station reporting meteorological data (see Figure 73 for location). Instrument and data specifications for this monitoring equipment are summarized in Table 6. Buoy data is accessible online at the NDBC database. NDBC 46050 (Stonewall Bank) is located 25 km northwest of the test site and provides spectral wave data. NDBC

46094 (NH-10) is slightly closer to the site at about 9 km northwest and reports standard ocean wave data (Figure 75 (a)). The land based meteorological station is situated directly on the shoreline (Figure 75 (b)).

Figure 75: (a) Moored buoy NDBC 46094 located 9 km northwest of the test site, (b) meteorological station NWPO3 on the coastline 15 km northeast of the test site (National Data Buoy Center 2014).

Table 6: Wave monitoring equipment in close proximity to SETS. Note this is the same equipment provided for NETS in Table 1.

Instrument Name (Nickname)	**NDBC Station 46094 (also called NH-10)**	**NDBC Station 46050 (Stonewall Bank)**			**NWPO3**	
Type	Moored buoy	3-meter discus buoy			C-MAN station (MARS payload)	
Measured parameters	-std. met. data -continuous winds -sea surface temp, salinity, density -current measurements	-std. met. data -continuous winds -spectral wave density -spectral wave direction			-std. met. data -continuous winds	
Variables reported, including derived variables (Sampling interval)	*Std Met.:* WDIR WSPD BAR ATMP (10 min sampling period)	*Std Met.:* WDIR WSPD GST WVHT DPD APD PRES ATMP WTMP (1 hr sampling period)	*Contin. Winds:* WDIR WSPD GDR GST GTIME (10 min sampling period)	-Spectral Wave Density -Spectral Wave direction (1 hr sampling period)	*Std Met.:* WD WSPD GST BAR ATMP DEWP (1 hr sampling period)	*Contin. Winds:* WDIR WSPD GDR GST GTIME (10 min sampling period)
Location	directly west of Newport, 9 km northwest of SETS	20 nm (nautical miles, 1 nm = 1.852 km) directly west of Newport, 25 km northwest of SETS			on the shoreline, near Newport, 15 km northeast of SETS	
Coordinates	44.633 N 124.304 W (44°38'0" N 124°18'13" W)	44.639 N 124.534 W (44°38'20" N 124°32'2" W)			44.613 N 124.067 W (44°36'48" N 124°4'0" W)	
Depth	-depth: 81 m -air temp 2.5 m above site -anemometer 3 m above site	-depth: 128 m -air temp: 4 m above water -anemometer: 5 m above water -barometer: sea level -sea temp depth: 0.6 m below water			-site: 9.1 m above sea level -air temp: 6.4 m above site -anemometer: 9.4 m above site -barometer: 11 m above sea level	
Data Start	2/5/2007	-std met: 11/16/1991 -contin winds: 09/07/1997 -spect wave dens: 01/01/1996 -spect wave dir: 03/05/2008			-std met: 1/10/1985 -contin winds: 1/12/1997	
Data End	present; several winters missing data	present			present	
Period of Record	∼8.5 yrs	-std met: ∼24 yrs -contin winds: ∼18 yrs -spect wave dens: ∼20 yrs -spect wave dir: ∼7.5 yrs			std met: ∼31 yrs contin winds: ∼19 yrs	
Owner / Contact Person	Oregon Coastal Ocean Observing System/ National Data Buoy Center	National Data Buoy Center			National Data Buoy Center	

8.2.8. Environmental Monitoring

Environmental conditions have been characterized at the site by Oregon State University, NOAA, and NNMREC. The information gathered includes baseline measurements of benthic habitat and organisms, marine mammal populations, and acoustics (Batten 2013). Developers can contract with NNMREC to monitor environmental effects of WEC deployments during testing. Required environmental monitoring of WEC deployments is yet to be determined, and will depend on permitting.

8.2.9. Permitting

NNMREC is in the process of permitting. More information will be available once SETS is completed.

8.3. Data used

Researchers at the Northwest National Marine Renewable Energy Center (NNMREC) produced a 7 year hindcast dataset for the area offshore of Oregon (García-Medina et al. 2014) in order to complement the study of temporal and spatial variability in the wave resource over the Pacific Northwest region by Lenee-Bluhm et al.(2011). This dataset was used to calculate statistics of interest for the wave resource characterization at SETS. The hindcast data at the grid point in the center of SETS was analyzed (see Figure 73). Although a 10 year hindcast would be preferred, García-Medina et al. (2014) showed that the probability density function (PDF) of significant wave height from their hindcast compared to NDBC 46029 buoy data were in agreement up to $\sim$7 m, and, therefore, the hindcast is at least representative of the twenty-seven years of buoy operation, 1985 – 2011.

In addition to the hindcast data set, historical data from buoy NDBC 46050 was used to calculate extreme sea states and representative spectra. Wind data was available from NDBC 46050 and a Coastal-Marine Automated Network (C-MAN) station, NWPO3 located just on-shore. However, to be consistent with the other sites, Climate Forecast System Reanalysis (CFSR) winds were used, as explained in Section 2.3. As with the other sites, current data was downloaded from OSCAR. See Figures 73 and 76 for data locations.

Figure 76: SETS location map showing the CFSR wind and OSCAR surface current data points, and NDBC buoy locations (Google Earth 2015).

8.4. Results

The following sections provide information on the joint probability of sea states, the variability of the IEC TS parameters, cumulative distributions, weather windows, extreme sea states, and representative spectra. This is supplemented by wave roses as well as wind and surface current data in Appendix F . The wind and surface current data provide additional information to help developers plan installation and operations & maintenance activities.

8.4.1. Sea States: Frequency of Occurrence and Contribution to Wave Energy

Joint probability distributions of the significant wave height, H_{m0}, and energy period, T_e, are shown in Figure 77. Figure 77 (top) shows the frequency of occurrence of each binned sea state and Figure 77 (bottom) shows the percentage contribution to the total wave energy. Figure 77 (top) indicates that the majority of sea states are within the range 1 m $< H_{m0} <$ 3.5 m and 7 s $< T_e <$ 11 s; but a wide range of sea states are experienced at SETS, including extreme sea states caused by severe storms where H_{m0} exceeded 7.5 m. The site is well suited for testing WECs at various scales, including full-scale WECs, and testing the operation of WECs under normal sea states. Although the occurrence of an extreme sea state for survival testing of a full scale WEC is unlikely during a normal test period, the SETS wave climate offers opportunities for survival testing of scaled model WECs.

As mentioned in the methodology (Section 2.2), previous studies show that sea states with the highest frequencies of occurrence do not necessarily correspond to those with the highest contribution to total wave energy. The total wave energy in an average year is 350,391 kWh/m, which corresponds to an average annual omnidirectional wave power of 40.7 kW/m. The most frequently occurring sea state is within the range 1.5 m $< H_{m0} <$ 2 m and 8 s $< T_e <$ 9 s, while the sea state that contributes most to energy is within the range 3.5 m $< H_{m0} <$ 4 m and 10 s $< T_e <$ 11 s. Several sea states occur at a similar frequency, and sea states within 2 m $< H_{m0} <$ 5 m and 9 s $< T_e <$ 11 s contribute a similar amount to energy.

Frequencies of occurrence and contributions to energy of less than 0.01% are considered negligible and are not shown for clarity. For example, the sea state within 0.5 m $< H_{m0} <$ 1 m and 5 s $< T_e <$ 6 s has an occurrence of 0.02%. The contribution to total energy, however, is only 0.001% and, therefore, does not appear in Figure 77 (bottom). Similarly, the sea state within 8.5 m $< H_{m0} <$ 9 m and 13 s $< T_e <$ 14 s has an occurrence of 0.005%, but the contribution to total energy is 0.07%.

Curves showing the mean, 5^{th} and 95^{th} percentiles of wave steepness, H_{m0}/λ, are also shown in Figure 77. The mean wave steepness at SETS is 0.0166 ($\approx 1/60$), and the 95^{th} percentile is approximately 1/34.

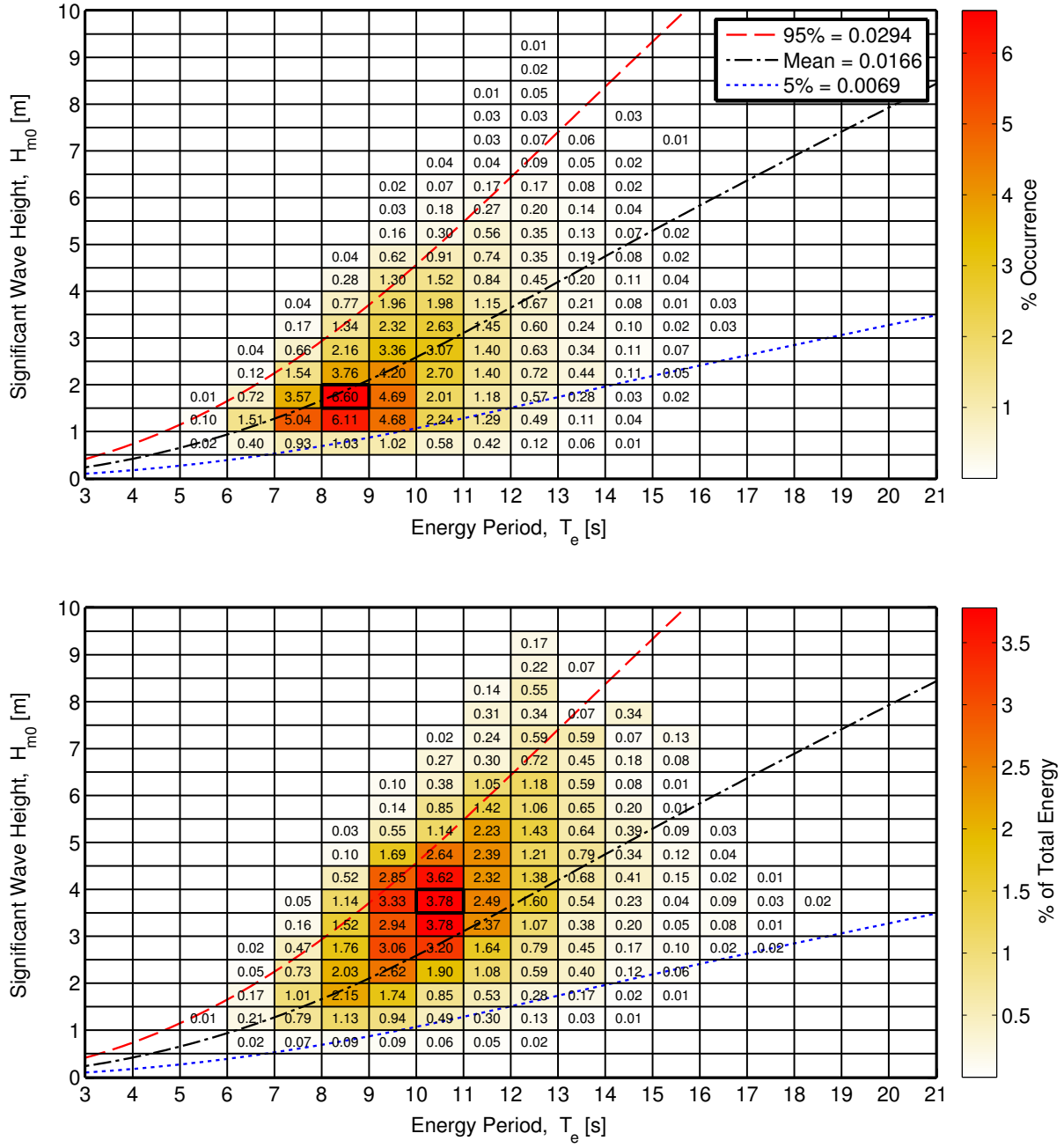

Figure 77: Joint probability distribution of sea states for SETS. The top figure is frequency of occurrence and the bottom figure is percentage of total energy, where total energy in an average year is 350,291 kWh/m.

8.4.2. IEC TS Parameters

The monthly means of the six IEC TS parameters, along with the 5^{th} and 95^{th} percentiles, are shown in Figure 78. The months, March – February, are labeled with the first letter (e.g., March is M). The values in the figure are summarized in Table **??** in Appendix F.

Monthly means of the significant wave height, H_{m0}, and the omnidirectional wave power density, J, show the greatest seasonal variability compared to the other parameters. Values are largest and vary the most during the winter months. The same trend is observed for the monthly mean energy period, T_e, but its variation is less pronounced. These observations are consistent with the relationship between wave power density, significant wave height and energy period, where wave power density, J, is proportional to the energy period, T_e, and the square of the significant wave height, H_{m0}.

Slight seasonal variation in the spectral width, ϵ_0, can be seen, where the spectral width is smaller in the winter, and has greater variation in the summer. The direction of maximum directionally resolved wave power, θ_J, is fairly consistent throughout the year from west, and slight variation throughout the year can be seen but it does not seem to correspond directly to season. Some seasonal variability of the directionality coefficient, d_θ, is evident, with lower values and more variation in the summer. In summary, the waves at SETS, from the perspective of monthly means, have a fairly consistent spectral width, although narrower in the winter, are predominantly from the west, and exhibit a wave power that has a narrow directional spread, especially in the winter.

Wave roses of wave power and significant wave height, presented in Appendix F, Figure 150 and 151, also show the predominant direction of the wave energy at SETS, which is west, with frequent but small shifts to the north and occasional but small shifts to the south. Figure 150 shows two dominant wave direction sectors, west (at 270°) and west/northwest (WNW) at 285°. Along the predominant wave direction, 285°, the omnidirectional wave power density is at or below 35 kW/m about 19% of the time, but greater than 35 kW/m nearly 15% of the time. Along the west direction (270°), wave power density is at or below 35 kW/m about 18% of the time, and greater than 35 kW/m about 11% of the time.

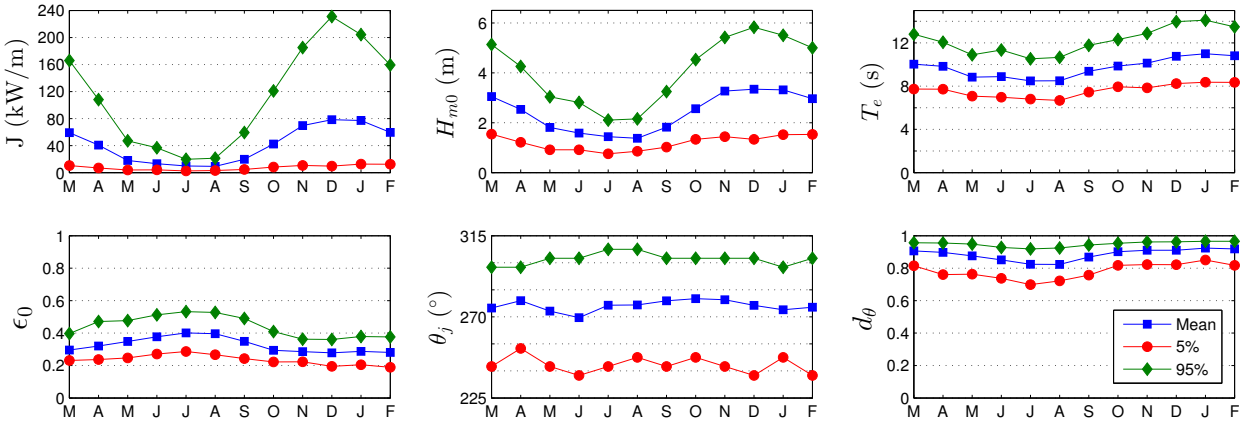

Figure 78: The average, 5^{th} and 95^{th} percentiles of the six parameters at SETS.

Monthly means, however, smear the significant variability of the six IEC parameters over small time intervals as shown in plots of the parameters at 1-hour intervals in Figure 79 for a representative year. While seasonal patterns described for Figure 78 are still evident, these plots show how sea states can vary abruptly at small time scales with sudden changes, e.g.,

jumps in the wave power as a result of a storm.

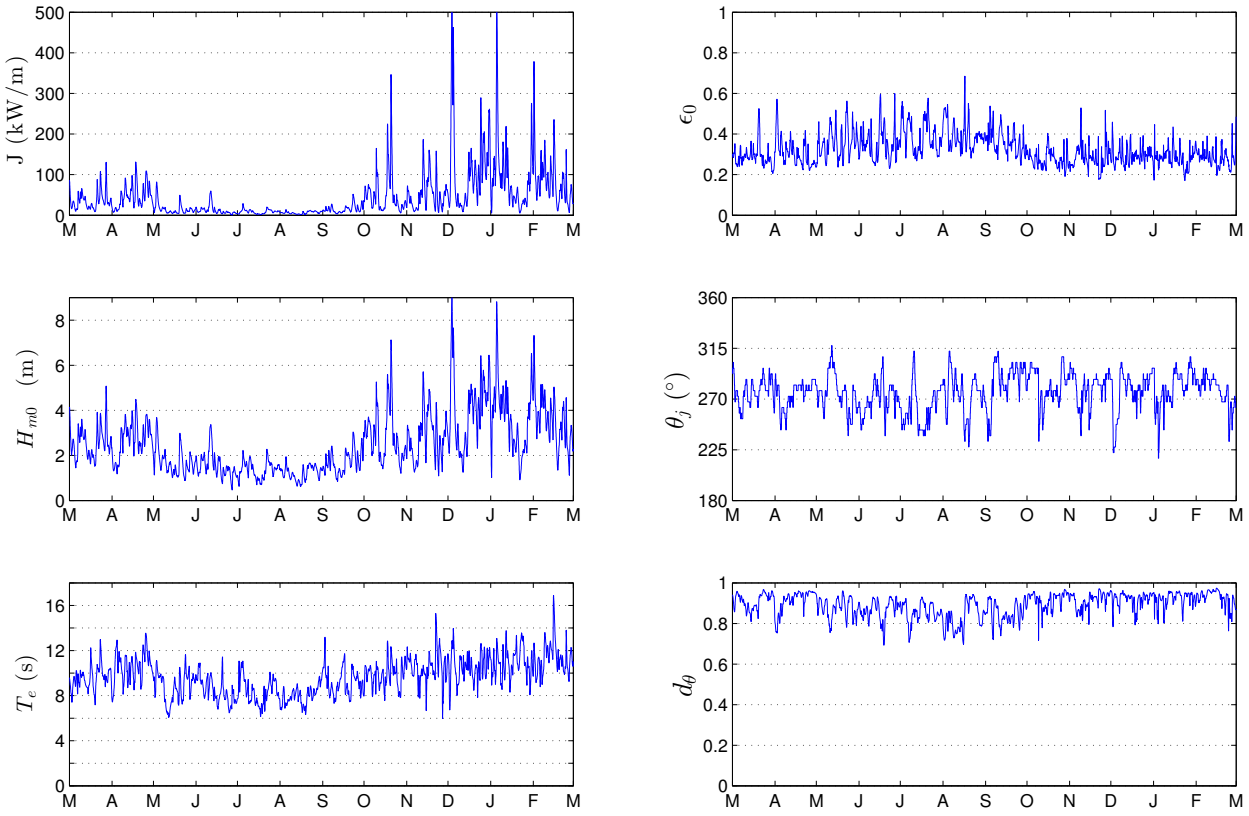

Figure 79: The six parameters of interest over a one-year period, March 2007 – February 2008 at SETS.

8.4.3. Cumulative Distributions

Annual and seasonal cumulative distributions (a.k.a., cumulative frequency distributions) are shown in Figure 80. Note that spring is defined as March – May, summer as June – August, fall as September – November, and winter as December – February. The cumulative distributions are another way to visualize and describe the frequency of occurrence of individual parameters, such as H_{m0} and T_e. A developer could use cumulative distributions to estimate how often they can access the site to install or perform operations and maintenance based on their specific device, service vessels, and diving operation constraints. For example, if significant wave heights need to be less than or equal to 1 m for installation and recovery, according to Figure 80, this condition occurs about 4.6% of the time on average within a given year. If significant wave heights need to be less than or equal to 2 m for emergency maintenance, according to Figure 80, this condition occurs about 46% of time on average within a given year. Cumulative distributions, however, do not account for the duration of a desirable sea state, or weather window, which is needed to plan deployment and servicing of a WEC device at a test site. This limitation is addressed with the construction of weather window plots in the next section.

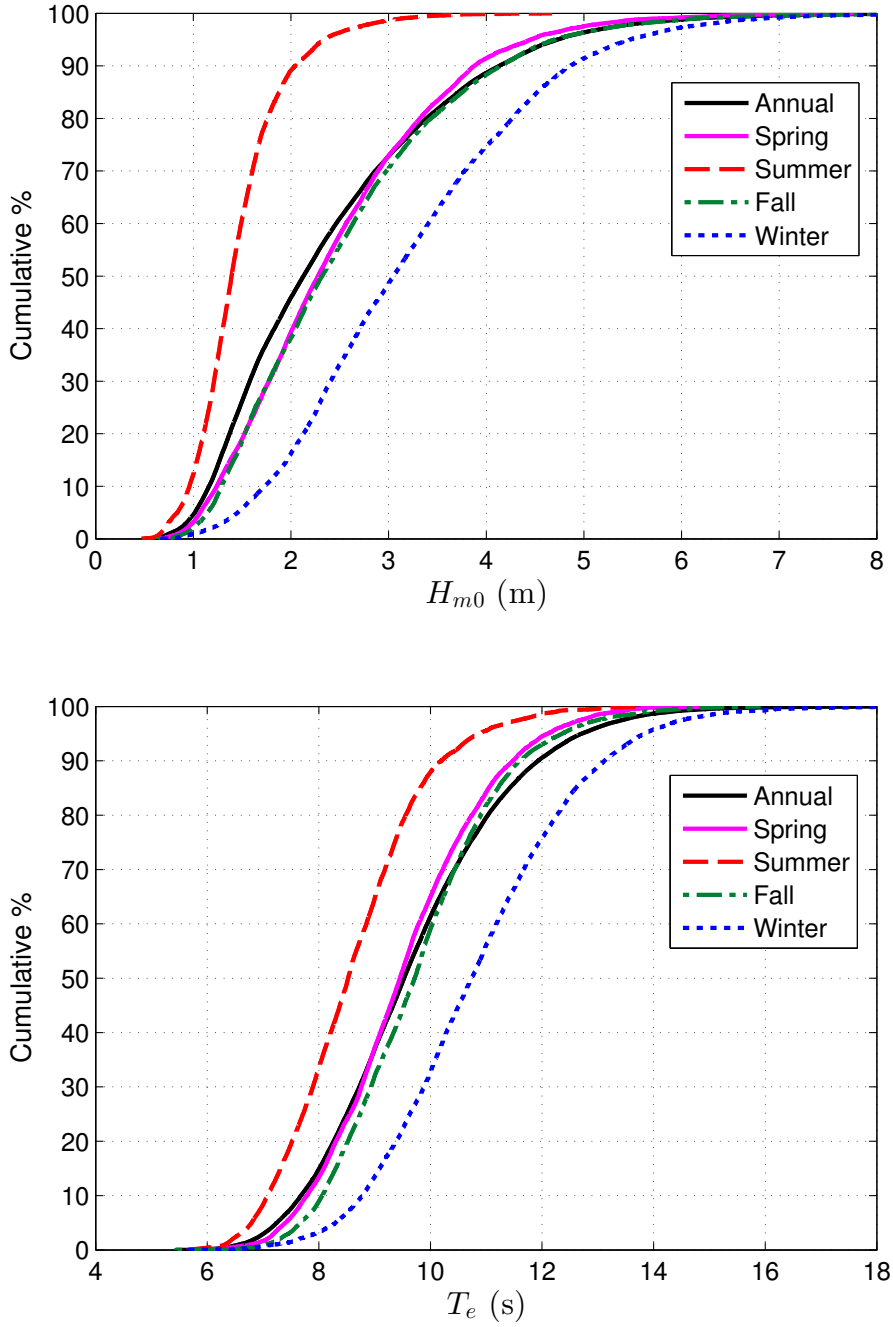

Figure 80: Annual and seasonal cumulative distributions of the significant wave height (top) and energy period (bottom) at SETS.

8.4.4. Weather Windows

Figure 81 shows the number of weather windows at SETS, when significant wave heights are at or below some threshold value for a given duration, for an average winter, spring, summer and fall. In these plots, each occurrence lasts a duration that is some multiple of 6-hours. The minimum weather window is, therefore, 6-hours in duration, and the maximum

is 96-hours (4 days). The significant wave height threshold is the upper bound in each bin and indicates the maximum significant wave height experienced during the weather window. Note that the table is cumulative, so, for example, an occurrence of $H_{m0} \leq 1$ m for at least 30 consecutive hours in the fall is included in the count for 24 consecutive hours as well. In addition, one 12-hour window counts would count as two 6-hour windows. It is clear that there are significantly more occurrences of lower significant wave heights during the summer than winter, which corresponds to increased opportunities for deployment or operations and maintenance.

Weather window plots provide useful information at test sites when planning schedules for deploying and servicing WEC test devices. For example, if significant wave heights need to be less than or equal to 1 m for at least 12 consecutive hours to service a WEC test device at SETS with a given service vessel, there would be, on average, nineteen weather windows in the summer, but only one in the winter. When wind speed is also considered, Figure 82 shows the average number of weather windows with the additional restriction of wind speed, $U < 15$ mph. The local winds (which are not necessarily driving the waves) are used in these weather windows, and are given in Appendix F.4. That wind data was not available from the hindcast, so data from CFSR was used (see Section 2.3, Appendix F.4). For shorter durations (6- and 12-hour windows), daylight is necessary. Windows with $U < 15$ mph and only during daylight hours are shown in Figure 83. Daylight was estimated as 5am – 10pm Local Standard Time (LST).

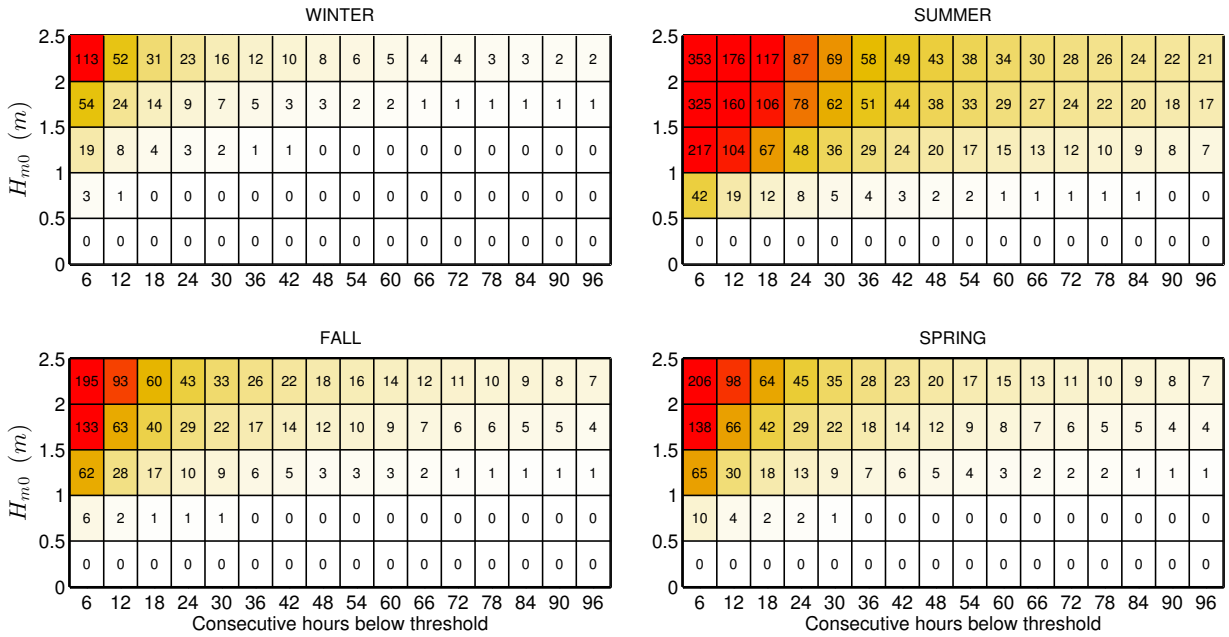

Figure 81: Average cumulative occurrences of wave height thresholds (weather windows) for each season at SETS. Winter is defined as December – February, spring as March – May, summer as June – August, and fall as September – November.

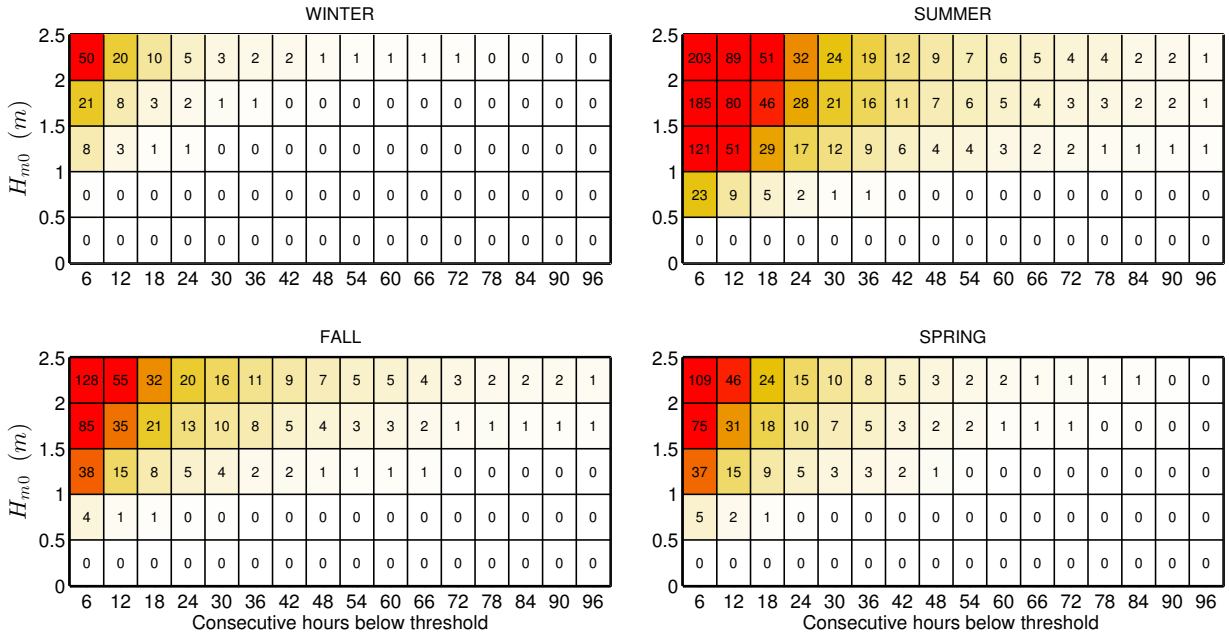

Figure 82: Average cumulative occurrences of wave height thresholds (weather windows) for each season at SETS with an additional restriction of U $<$ 15 mph.

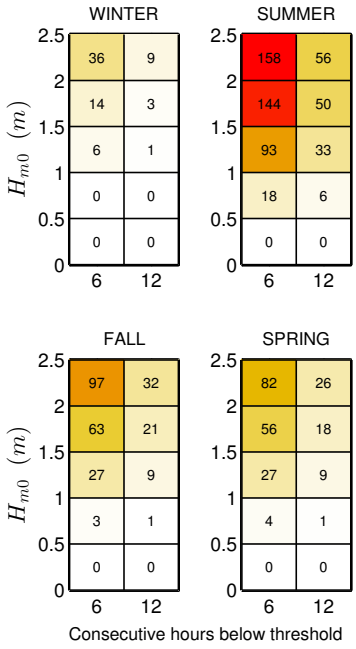

Figure 83: Average cumulative occurrences of wave height thresholds (weather windows) for 6- and 12-hour durations with $U < 15$ mph and only during daylight hours (5am – 10pm LST) at SETS.

8.4.5. Extreme Sea States

The modified IFORM was applied using NDBC 46050 data (see Table 6 for buoy information) to generate the 100-year environmental contour for SETS shown in Figure 84. Note this is the same data set used for NETS, but for completeness, the text and figure are repeated here. Selected sea states along this contour are listed in Appendix F, Table 34. As stated in Section 1.2, environmental contours are used to determine extreme wave loads on marine structures and design these structures to survive extreme sea states of a given recurrence interval, typically 100-years. For SETS, the largest significant wave height estimated to occur every 100-years is over 17.3 m, and has an energy period of about 16.6 s. However, significant wave heights lower than 17.3 m, with energy period less than or greater than 16.6 s, listed in Table 34, could also compromise the survival of the WEC test device under a failure mode scenario in which resonance occurred between the incident wave and WEC device, or its subsystem. For comparison, 50- and 25-year return period contours are also shown in Figure 84. The largest significant wave height on the 50-year contour is 16.3 m with an energy period of about 16.4 s, and on the 25-year contour is 15.4 m and 16.1 s. It should be noted that conditions at the NDBC46050 buoy (at 128 m depth) may differ significantly from the conditions at the test site (at depths of 58-75 m).

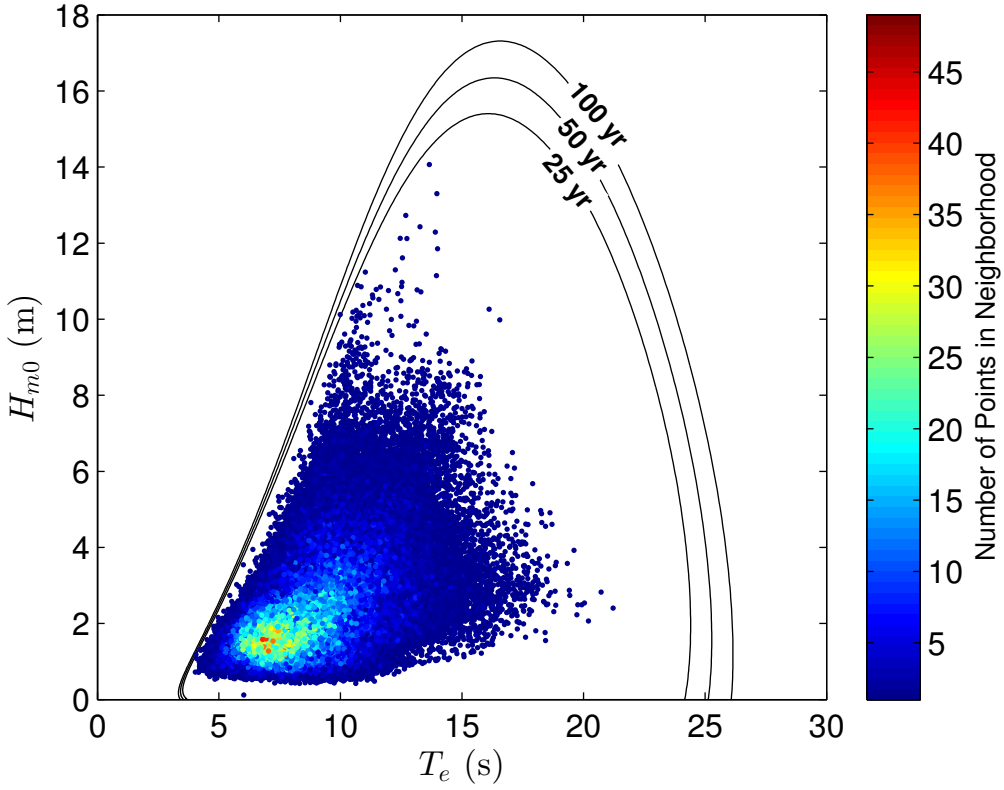

Figure 84: 100-year contour for NDBC 46050 (1996–2014).

8.4.6. Representative Wave Spectrum

All hourly discrete spectra measured at NDBC 46050 for the most frequently occurring sea states are shown in Figure 85. Note this is the same data set used for NETS, but for completeness, the text and figure are repeated here. The most frequently occurring sea state, which is within the range 1.5 m $< H_{m0} <$ 2 m and 7 s $< T_e <$ 8 s, was selected from a JPD similar to Figure 77 in Section 8.4.1, but based on the NDBC 46050 buoy data. As a result, the JPD, and therefore the most common sea states, generated from buoy data are slightly different from that generated from hindcast data. For example, the most frequently occurring sea state for the JPD generated from hindcast data is in the same range for H_{m0} (1.5 m $< H_m0 <$ 2 m), but one second higher on bounds for T_e (8 s $< T_e <$ 9 s). Often several sea states will occur at a very similar frequency, and therefore plots of hourly discrete spectra for several other sea states are also provided for comparison. Each of these plots includes the mean spectrum and standard wave spectra, including Bretschneider and JONSWAP, with default constants as described in Section 2.2.

For the purpose of this study, the mean spectrum is the 'representative' spectrum for each sea state, and the mean spectrum at the most common sea state, shown in Figure 85 (bottom-right plot), is considered the 'representative' spectrum at the site. The hourly spectra vary considerably about this mean spectrum, but this is partly reflective of the bin size chosen for H_{m0} and T_e. Comparisons of the representative spectra in all plots with the Bretschneider and JONSWAP spectra illustrate why modeled spectra with default constants, e.g., the shape parameter $\gamma = 3.3$ for the JONSWAP spectrum, should be used with caution. Using the constants provided in Section 2.2, the Bretschneider spectra are fair representations of the mean spectra in Figure 85, however it does not capture the bimodal nature of the spectra. The mean measured spectra is the best representation of the conditions, however, if these modeled spectra were to be used at this site, it is recommended that the constants undergo calibration against some mean spectrum, e.g., the representative spectrum constructed here. A better alternative may be to explore other methods or spectral forms to describe bimodal spectra (e.g., Mackay 2011) if it is known that the shape is not unimodal.

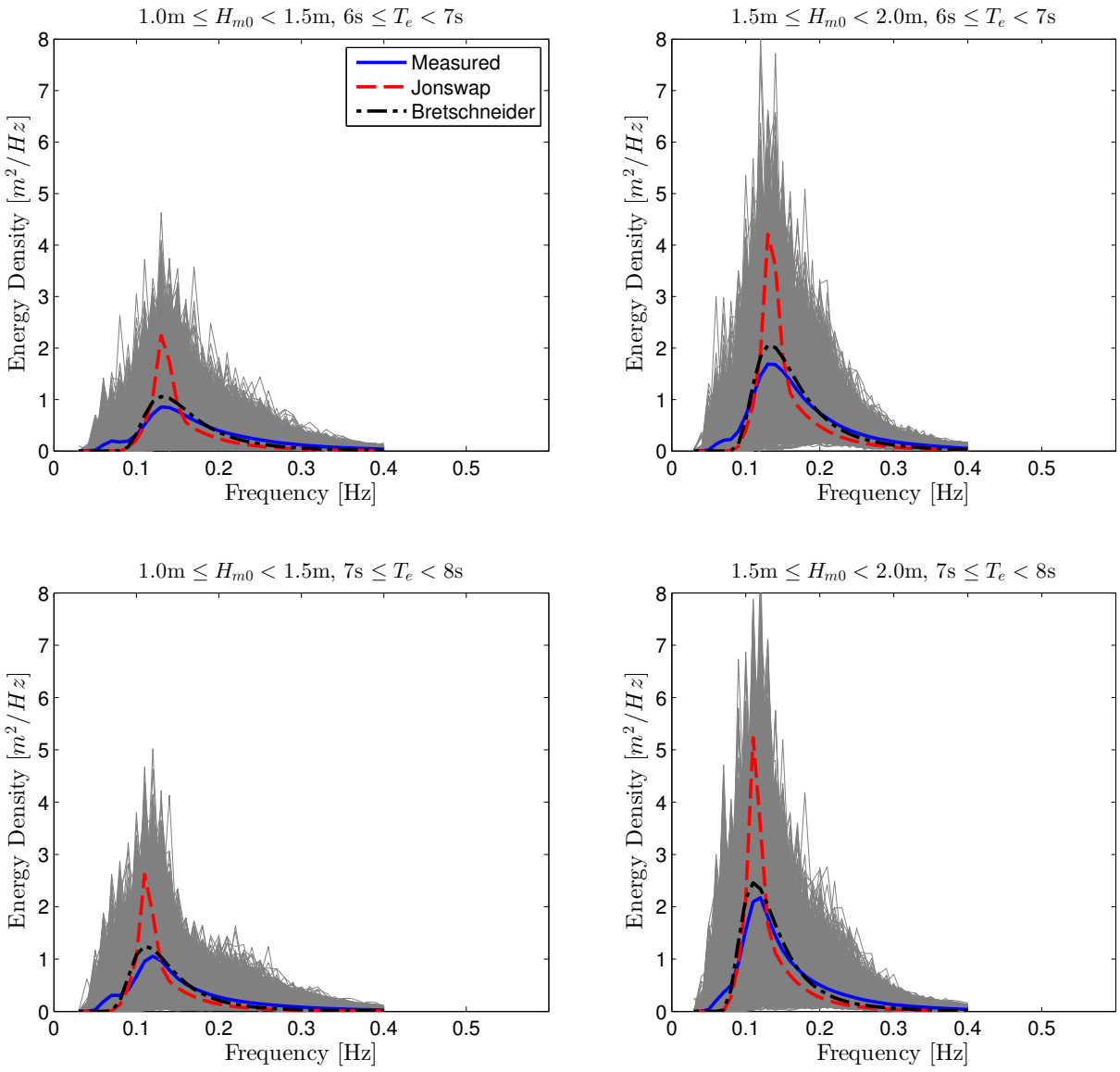

Figure 85: All hourly discrete spectra and the mean spectra measured at NDBC 46050 within the sea state listed above each plot. The JONSWAP and Bretschneider spectra are represented by red and black dotted lines, respectively.

9. CALWAVE PROPOSED CENTRAL COAST WEC TEST SITE AT VANDENBERG AIR FORCE BASE (VAFB)

9.1. Site Description

The California Wave Energy Test Center (CalWave) Feasibility Study evaluated offshore test sites along the California coast for establishment of a national wave energy testing facility (Williams et al. 2015). The project originally considered two candidate areas, one offshore of Humboldt Bay, which is described in Chapter 9, and another Central Coast site offshore of Vandenberg Air Force Base (VAFB). The project down selected to VAFB due to its accessibility to shore-side support infrastructure and supply chain, among other reasons. At VAFB, there are currently five siting at sea alternatives (locations) and three shore site alternatives. Two offshore sites, and one shore site, are most favorable and are considered in the Conceptual Design Scenario. The "South Base" shore location is considered as the Notional Shore Site design case. Therefore, in this catalogue, the wave statistics will be presented at both offshore alternatives. As shown in Figure 86, the two Vandenberg siting options each consist of four berths centered at approximately 34.521 N, 120.689 W for the 'South' site and 34.4851 N, 120.6024 W for the 'South by Southeast' site in the Outer Continental Shelf (outside state waters). See the CalWave report (Williams et al. 2015) for additional figures of the site. The seafloor footprint would be constrained to an area of about four square nautical miles. There are also two infrastructure scenarios that will be considered in 2016: (a) using an existing offshore oil and gas platform and on shore infrastructure, or (b) construction of new submarine power cables. If the CalWave Test Center continues to be funded, it is assumed that testing could begin in 2021.

The Central Coast site is located near Vandenberg Air Force Base and the City of Lompoc, California. At the South site, the water depth is approximately 71-109 m (38.8-59.6 fathoms), and at the South by Southeast site, the water depth is approximately 66-102 m (36.1-55.8 fathoms). The bathymetry in general is gently sloping near the potential 'South' and 'South by Southeast' berths, and then drops off to deeper water to the southeast. The sea bed is predominantly sandy, with rocky outcroppings. Figure 87 shows the bathymetry surrounding the test site. The wave climate at the test site varies seasonally, with calmer seas in the summer compared to more energetic seas in the winter. The wave environment at Vandenberg is characterized by an annual average power flux of about 39.9 kW/m at the South site and 31.4 kW/m at the South by Southeast site, including a number of events with significant wave heights exceeding 5 m each winter.

The CalWave Team plans to offer a wide range of technical and testing infrastructure included and optional support services for WEC developers. Vandenberg has full scale wave energy resources, and is planned to be appropriate for mature technologies, at Technical Readiness Level (TRL) 7-9 WECs, which are approaching full-scale, grid-connected operation. The BOEM lease blocks being considered would enable use of up to four berths in the South and South-by-Southeast alternatives, and will allow a broad range of test conditions for the

purpose of populating a WEC power matrix. Cables would land at the South Base site near Vandenberg Dock. Once WECs are proven, commercial site alternatives are available in the vicinity to power offshore oil platforms that are presently using diesel generators.

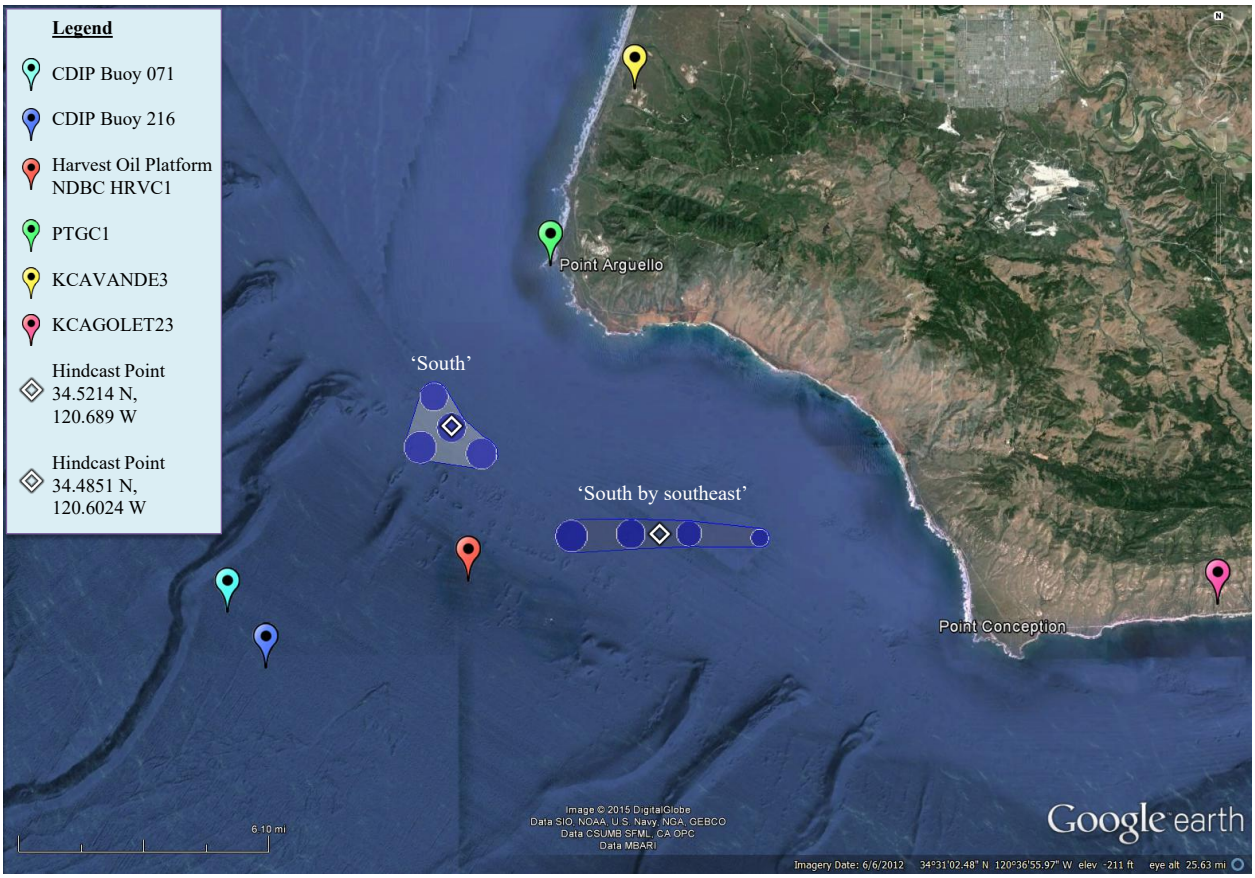

Figure 86: Two of the potential Vandenberg test site areas, 'South', and 'South by Southeast' (SSE), are located on the coast of California near the city of Lompoc and Vandenberg Air Force Base. The South site is approximately 6-9 km off-shore in 71-109 m depth water (38.8-59.6 fathoms) and the South by Southeast site is approximately 6-11 km off-shore in 66-102 m depth water (36.1-55.8 fathoms). No berthing infrastructure exists at this time, however four potential berths at each site are signified by the blue circles. Two Coastal Data Information Program (CDIP) ocean buoys, and several National Weather Service (NWS) meteorological stations are close to the test site. The points of reference for the hindcast simulation data presented in this chapter are shown. Image modified from Google Earth (2015).

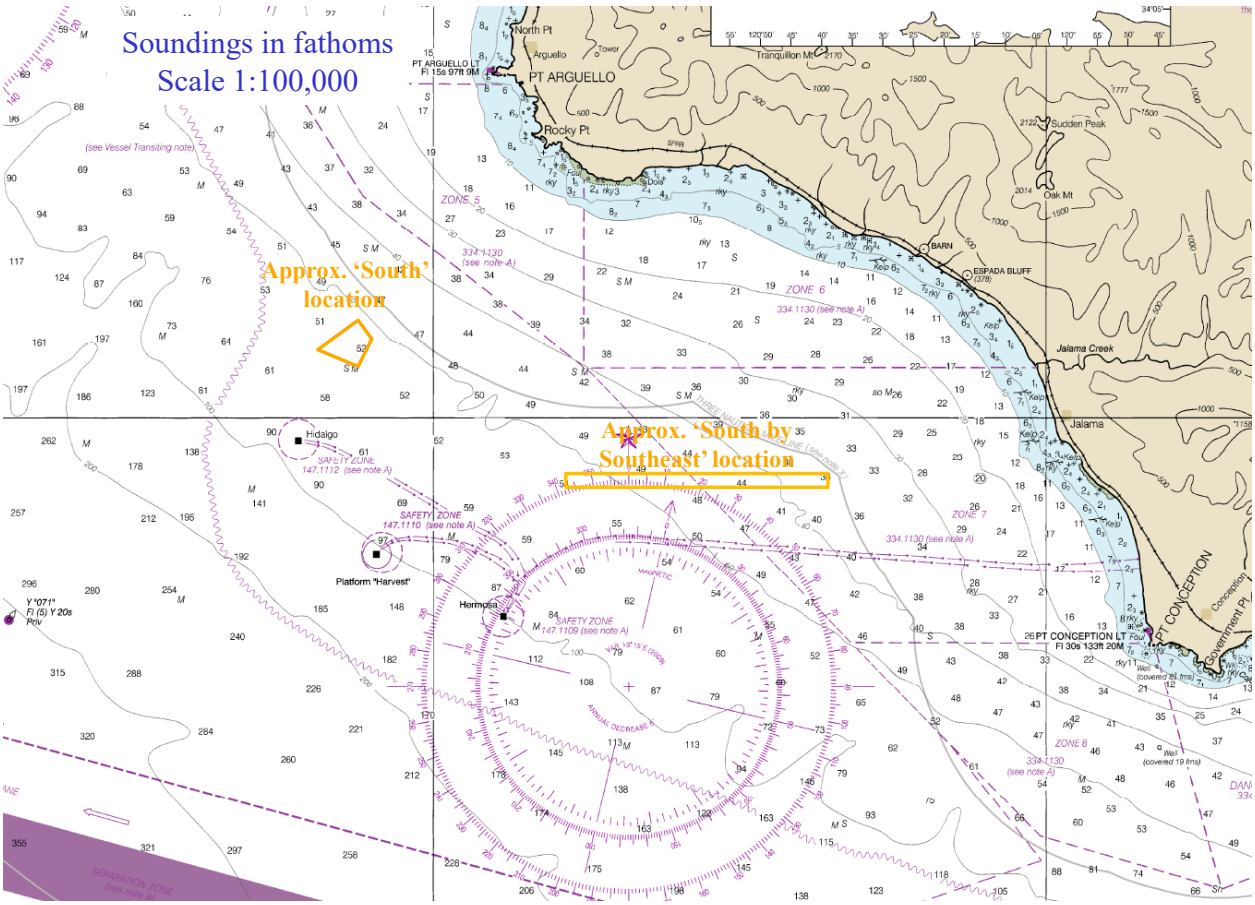

Figure 87: Nautical chart of the Vandenberg area offshore of Point Arguello and Point Conception shows the general bathymetry around the proposed test site. Soundings in fathoms (1 fathom = 1.8288 m). Image modified from nautical chart #18721 (Office of Coast Survey 2015).

9.2. WEC Testing Infrastructure

9.2.1. Mooring Berths

Four deep water berths are planned at either the South or South by Southeast locations. CalWave will be designed for WEC developers to provide key equipment optimized for their device, including the mooring and anchoring, umbilical, and power conditioning equipment. Alternatives for future expansion are available for deeper sites and shallow/mid-depth sites.

9.2.2. Electrical Grid Connection

The Conceptual Design includes four (4) "home run" cables from sea to shore, rated at 10 MW at 25 kV, plus a spare cable for a total of five (5) cables. Cables will land on VAFB at the notional "South Base" location and connect to a Department of Defense (DOD) grid

that is supplied by PG&E. Initially CalWave will connect with the Vandenberg distribution local grid at 12 kV, with an upgrade path to 70 kV.

9.2.3. Facilitating Harbor

Port Hueneme is the only deep water harbor between Los Angeles and the San Francisco Bay area, and is about 70 nm (∼130 km) from Vandenberg Dock and supports the offshore oil and gas industry. This facility can host very large vessels, and houses large cranes, dockside storage facilities and marine operations services for the oil and gas industry. Cal Poly Pier in Port San Luis and Port San Luis Boatyard are both approximately 24 nm (∼44 km) from Vandenberg Dock. Ellwood Pier is about 37 nm (∼69 km), Santa Barbara Harbor is about 54 nm (∼100 km), and Casitas Pier in Carpentaria is about 58 nm (∼107 km) from Vandenberg Dock. The Cojo Anchorage, on the sheltered side of Point Conception, is routinely used as a staging location by the offshore industry. More information and figures can be found in the CalWave report (Williams et al. 2015).

9.2.4. On-Shore Office Space

CalWave has focused on a notional shore station facility at the 'South Base' location, which would be appropriate for either the South or South by Southeast test site alternatives. This shore station facility is adjacent to Vandenberg Dock on Vandenberg AFB, and is planned to have two modular buildings, with on-site space for WEC developers. The Shore Station includes an area for modular power conditioning equipment to be provided by WEC developers. The Vandenberg Dock area, which is located at the former U.S. Coast Guard Surf Station, next to the shore station, is a potential location for office functions, on a not-to-interfere basis. This potential shore station would host key personnel and WEC developer staff during test operations.

9.2.5. Service Vessel and Engineering Boatyard Access

Capable shore side infrastructure is readily available near the project area due to a long history of oil services construction and operations in the area. Facilities include heavy lift floating cranes (offshore rated) and dockside cranes, and a variety of work boats and other vessels including large work vessels and cable lay equipment, remotely operated vehicles, and automated underwater vehicles. More detailed information is in Williams et al. 2015.

9.2.6. Travel and Communication Infrastructure

There are several airports in the area. The Santa Barbara Municipal Airport (SBA) is 38.2 miles southeast of Lompoc, and the Los Angeles International Airport (LAX) is 126.7 miles southeast of Lompoc. The Santa Maria Pub/Capt G Allan Hancock Field Airport (SMX) is 18 miles north of Lompoc. There are several Federal Communication Commission (FCC) registered cell towers located in and around Lompoc, CA, and cell phones may be used on VAFB, although coverage varies by location on-base.

9.2.7. Met-Ocean Monitoring Equipment

Real-time meteorological and wave data are collected by two met-ocean buoys and four meteorological stations. Instrument and data specifications for this monitoring equipment are summarized in Table 7. Buoy data is accessible online at the CDIP and NDBC databases. CDIP071 (NDBC 46218) is located approximately 15 km southwest of the test site, and CDIP216 (NDBC 46257) was recently deployed nearby. There is a water level observation network on the Harvest Oil Platform, just south of the site. There are several meteorological stations onshore.

Figure 88: (a) Waverider buoy CDIP071 / NDBC46218 located about 15 km southwest of test site (National Data Buoy Center 2015). (b) C-MAN Station PTGC1 located about 10 km north of test site (National Data Buoy Center 2015).

Table 7: Wave monitoring equipment in close proximity to the VAFB proposed test site.

Instrument Name (Nickname)	**CDIP071 / NDBC46218 - ("Harvest, CA")**		**CDIP216 / NDBC46257 ("Harvest Southeast, CA)**		**HRVC1 - 9411406 - Harvest Oil Platform, CA**
Type	Waverider Buoy		Waverider Buoy		Water Level Observation Network
Measured parameters	-std. met. data -spectral wave density data -spectral wave direction data		-std. met. data -spectral wave density data -spectral wave direction data		-barometric pressure -air temp
Variables reported, including derived variables (Sampling interval)	*Std. Met.:* WVHT DPD APD MWD WTMP (30 min)	-Spectral Wave Density -Spectral Wave Direction (30 min)	*Std. Met.:* WVHT DPD APD MWD WTMP (30 min)	-Spectral Wave Density -Spectral Wave Direction (30 min)	PRES ATMP (6 min sampling period)
Location	∼15 km southwest of site		∼15 km southwest of site		Just south of the site
Coordinates	34.454 N 120.782 W (34°27'14.4" N 120°46'55.2" W)		34.439 N 120.766 W (34°26'20.4" N 120°45'57.6" W)		34.469 N 120.682 W (34°28'9" N 120°40'55" W)
Depth	548.6 m		576.1 m		-air temp height: 30 m above site elevation -barometer elev: 26.1 m mean sea level
Data Start	3/19/1998 (additional short deployment in Dec 1995 - Mar 1996)		7/9/2015		3/1/2013
Data End	present		present		present
Period of Record	∼17.5 yrs		< 1 yr		∼2.5 yrs
Owner / Contact Person	NOAA – "Information Submitted by Scripps" http://cdip.ucsd.edu/themes/s?pb=1&u2=s:071:st:1&d2=p9		NOAA – "Information Submitted by Scripps" http://cdip.ucsd.edu/?nav=historic&sub=data&stn=216&stream=p1&xitem=info		NOAA's National Ocean Service http://www.ndbc.noaa.gov/station_history.php?station=hrvc1

Instrument Name (Nickname)	**PTGC1**		**KCAVANDE3**	**KCAGOLET23**
Type	C-MAN station (MARS payload)		Met station	Met station
Measured parameters	-std. met. data -continuous winds		Meteorological data	Meteorological data
Variables reported, including derived variables (Sampling interval)	*Std Met.:* WD WSPD GST BAR ATMP DEWP (1 hr sampling period)	*Contin. Winds:* WDIR WSPD GDR GST GTIME (10 min sampling period)	AirTemp DewPoint Pressure WDIR WSPD Humidity Precip (5 min)	AirTemp DewPoint Pressure WDIR WSPD Humidity Precip Solar Radiation UV Index (5 min)
Location	$\sim$ 10 km north of the site, on shoreline		SpaceX Launch Complex 4 Office	Goleta, CA
Coordinates	34.577 N 120.648 W (34°34'36" N 120°38'54" W)		34.637 N 120.613 W (34°38'13.2" N, 120°36'46.8" W)	34.461 N 120.371 W (34°27'39.6" N 120°22'15.6" W)
Depth	-site: 32.3 m above sea level -air temp: 9.1 m above site -anemometer: 9.4 m above site -barometer: 33.5 m above sea level		Elevation: 305 ft	Elevation: 98 ft
Data Start	-std met: 4/23/1984 -contin winds: 4/26/1997		1/19/2012	6/19/2015
Data End	present		present	present
Period of Record	std met: $\sim$31.5 yrs contin winds: $\sim$18.5 yrs		$\sim$3.5 yrs	$<$ 1 yr
Owner / Contact Person	National Data Buoy Center http://www.ndbc.noaa.gov/station_history.php?station=ptgc1		National Weather Service; data download wunderground.com	National Weather Service; data download wunderground.com

9.2.8. Environmental Monitoring

Environmental conditions have not been assessed at the Vandenberg Site, although a summary of potential environmental studies that may be needed are in Williams et al. 2015. When CalWave receives the next phase of funding, they will further characterize the site.

9.2.9. Permitting

No permits have been obtained as of 2015. CalWave has leveraged the lessons-learned from PG&E's WaveConnect Program and has investigated most aspects of the permitting process at this stage. A high level screening analysis to identify critical issues in the process has been ongoing. The information found so far from this process can be found in Williams et al. 2015.

9.3. Data used

Humboldt State University (part of the CalWave team) produced a 10 year hindcast dataset for the various siting alternative locations offshore of Vandenberg Air Force Base (Williams et al. 2015). This dataset was used to calculate parameters of interest for the characterization at the two locations presented for the CalWave central coast site. The hindcast data at the grid points shown in Figure 86 were analyzed.

In addition to the hindcast data set, historical data from buoy CDIP071 / NDBC 46218 was used to calculate estimates of extreme events and representative spectra. As with the other sites, CFSR wind data and OSCAR current data were used. See Figures 86 and 89 for data locations.

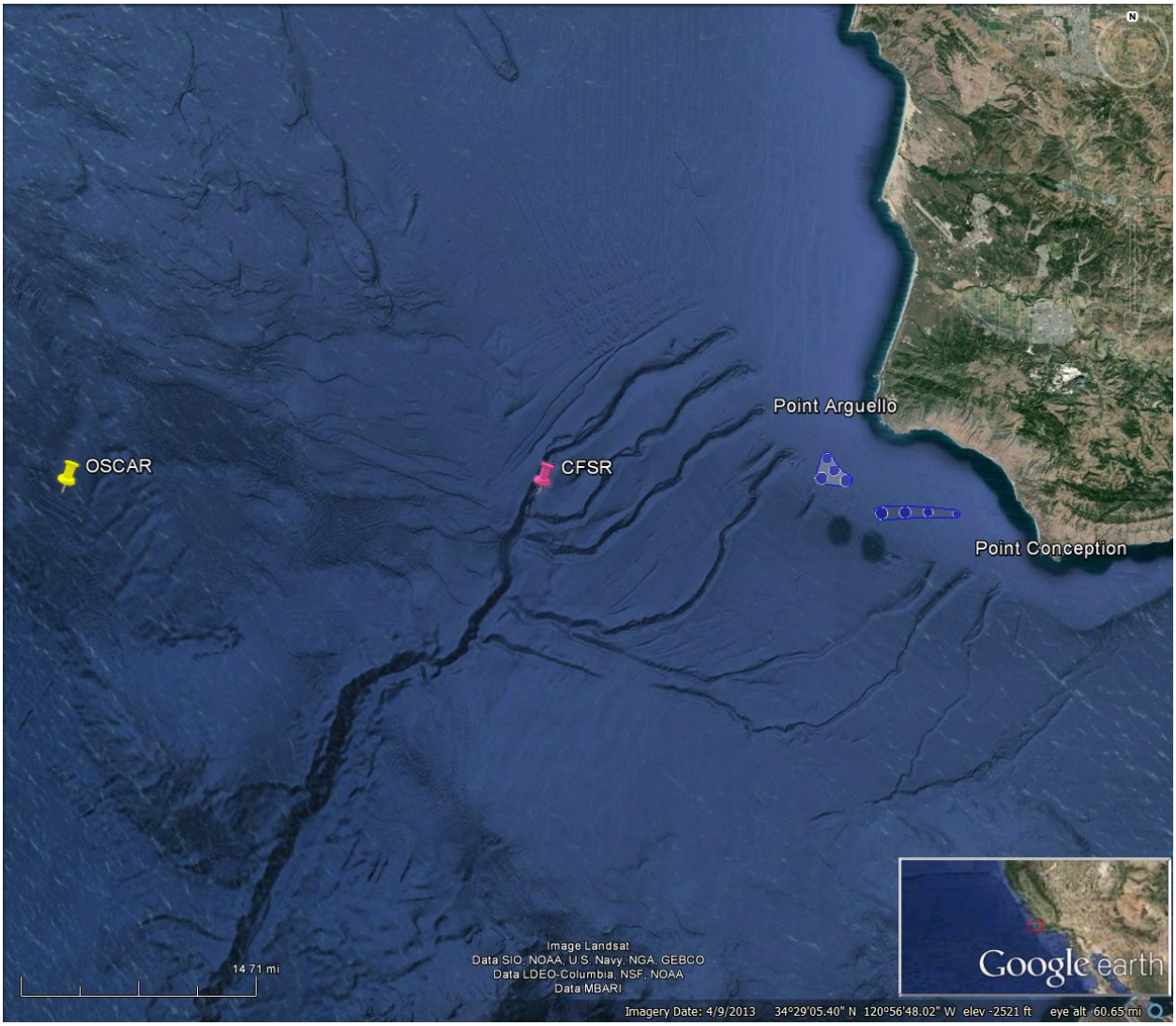

Figure 89: The catalogue test site locations in relation to OSCAR surface current and CSFR wind data points (Google Earth 2015).

9.4. Results

The following sections provide information on the joint probability of sea states, the variability of the IEC TS parameters, cumulative distributions, weather windows, extreme sea states, and representative spectra. This is supplemented by wave roses as well as wind and surface current data in Appendix G. The wind and surface current data provide additional information to help developers plan installation and operations & maintenance activities.

9.4.1. Sea States: Frequency of Occurrence and Contribution to Wave Energy

Joint probability distributions of the significant wave height, H_{m0}, and energy period, T_e, are shown in Figures 90 and 91. Figure 90 (top) shows the frequency of occurrence of each binned sea state and Figure 90 (bottom) shows the percentage contribution to the total wave energy for the South location. The same information is shown for the SSE location in 91. Figure 90 and Figure 91 (top) indicate that the majority of sea states are within the range 1.5 m $< H_{m0} <$ 3.5 m and 6 s $< T_e <$ 13 s; but a wide range of sea states are experienced at the Vandenberg site, including extreme sea states caused by severe storms where H_{m0} exceeded 6 m. The site is well suited for testing WECs at various scales, including full-scale WECs, and testing the operation of WECs under normal sea states. This would also be a desirable site for commercial deployment. Although the occurrence of an extreme sea state for survival testing of a full scale WEC is unlikely during a normal test period, the Vandenberg site wave climate offers opportunities for survival testing of scaled model WECs.

As mentioned in the methodology (Section 2.2), previous studies show that sea states with the highest occurrence do not necessarily correspond to those with the highest contribution to total wave energy, as is the case in Figures 90 and 91. The total wave energy in an average year at the South location is about 352,980 kWh/m, which corresponds to an average annual omnidirectional wave power of 39.9 kW/m. The total average wave energy in an average year at the SSE location is about 277,660 kWh/m, which corresponds to an average annual omnidirectional wave power of 31.4 kW/m. The most frequently occurring sea state is within the range 2 m $< H_{m0} <$ 2.5 m and 10 s $< T_e <$ 11 s for both the South and SSE locations, while the sea state that contributes most to energy is within the range 3 m $< H_{m0} <$ 3.5 m and 12 s $< T_e <$ 13 s for the South location and within the range 2.5 m $< H_{m0} <$ 3 m and 11 s $< T_e <$ 12 s for the SSE location. Several sea states occur at a similar frequency, and sea states within 2 m $< H_{m0} <$ 4 m and 10 s $< T_e <$ 13 s contribute a similar amount to energy.

Frequencies of occurrence and contributions to energy of less than 0.01% are not shown in the figure for clarity. For example, the sea state within 0.5 m $< H_{m0} <$ 1 m and 4 s $< T_e <$ 5 s has an occurrence of 0.04% for the South location. The contribution to total energy, however, is only 0.002% and, therefore, does not appear in Figure 90 (bottom). Similarly, the sea state within 7.5 m $< H_{m0} <$ 8 m and 16 s $< T_e <$ 17 s has an occurrence of 0.003%, but the contribution to total energy is 0.05%.

Curves showing the mean, 5^{th} and 95^{th} percentiles of wave steepness, H_{m0}/γ, are also shown in Figures 90 and 91. The mean wave steepness is 0.0150 ($\approx$1/67) at the South location,

and 0.0142 (≈1/70) at the SSE location. The 95^{th} percentile is 0.0323 (≈1/31) at the South and 0.0312 (≈1/32) at the SSE location.

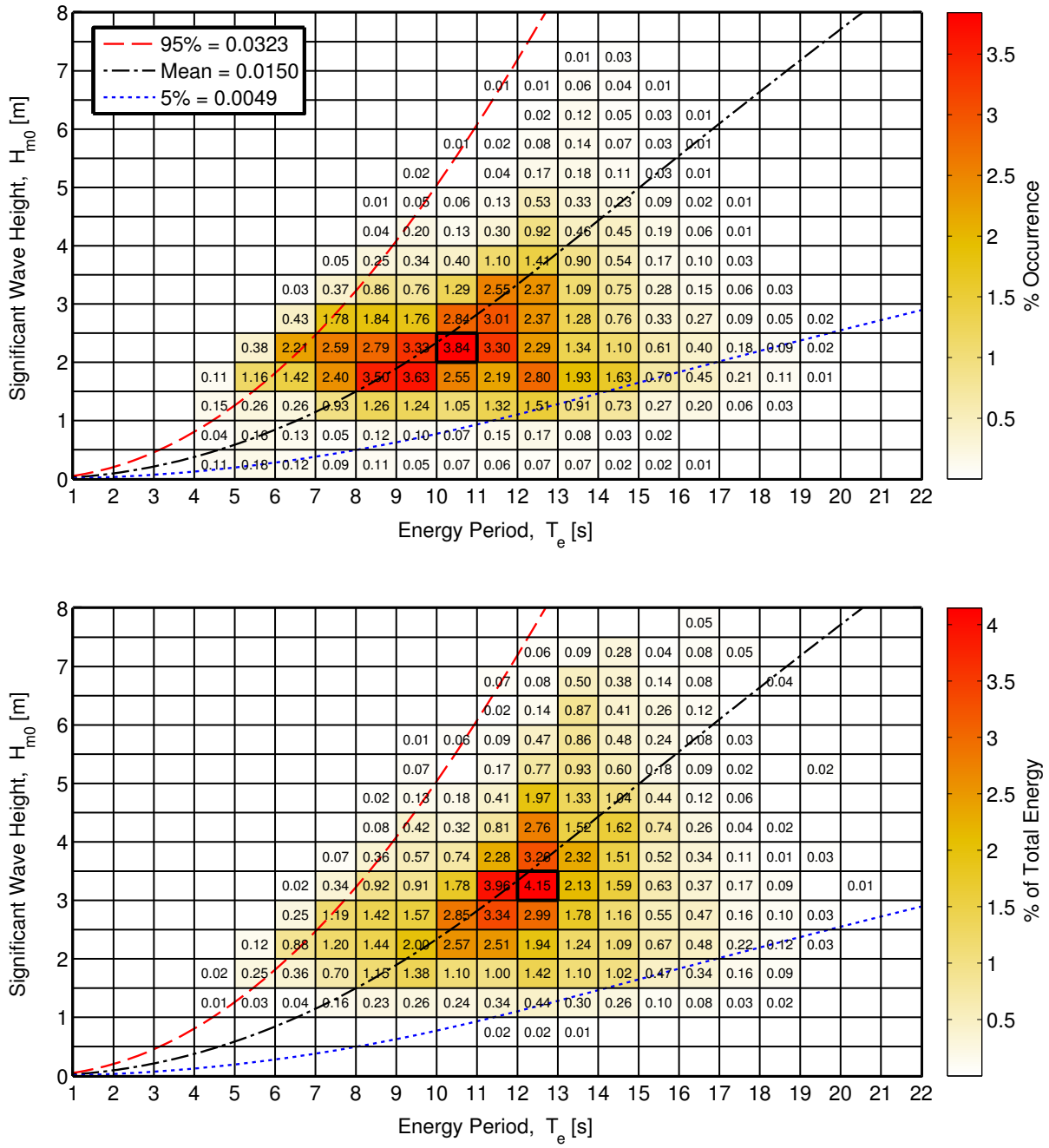

Figure 90: Joint probability distribution of sea states for the South Vandenberg site. The top figure is frequency of occurrence and the bottom figure is percentage of total energy, where total energy in an average year is 352,980 kWh/m.

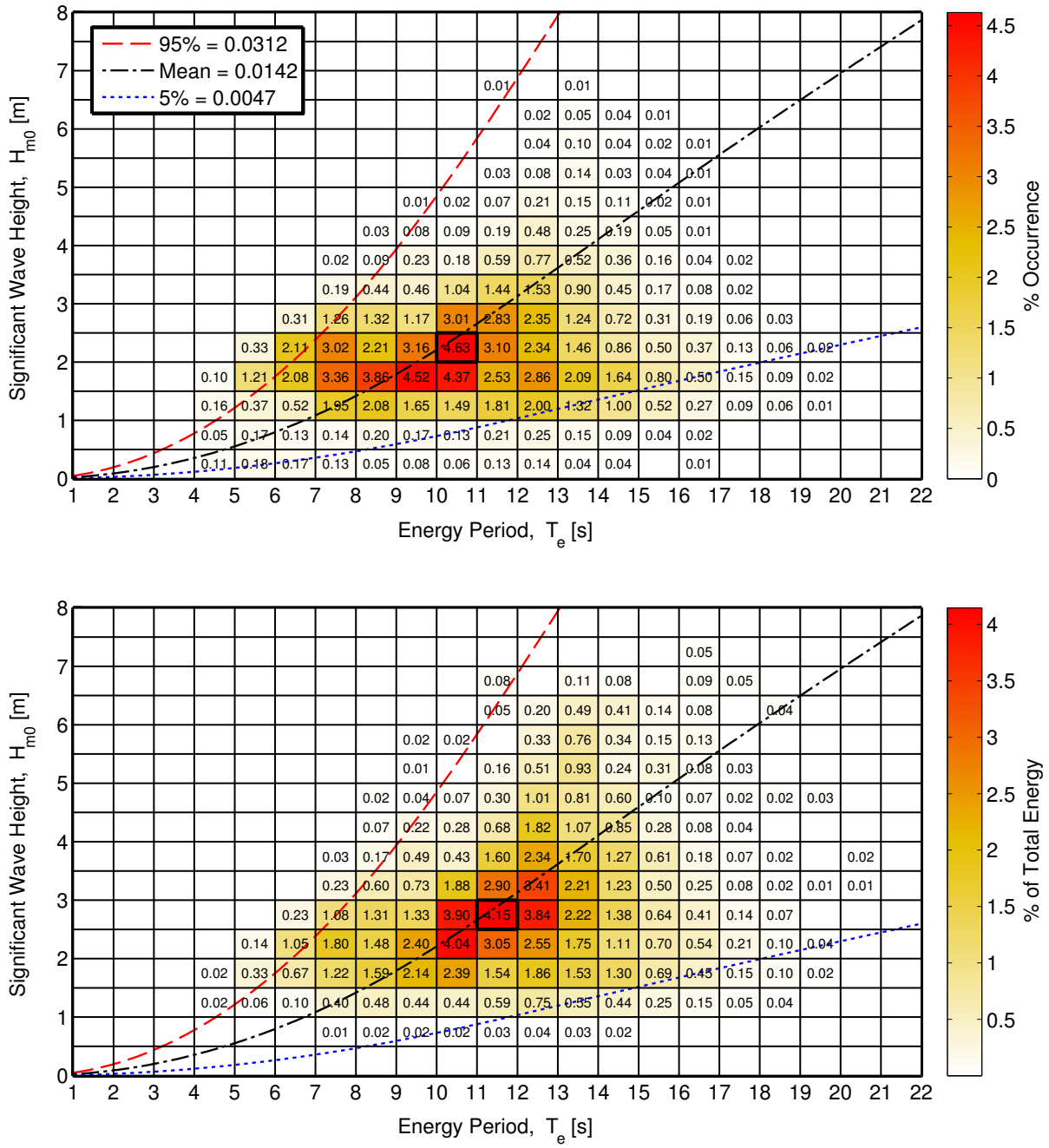

Figure 91: Joint probability distribution of sea states for the SSE Vandenberg site. The top figure is frequency of occurrence and the bottom figure is percentage of total energy, where total energy in an average year is 277,660 kWh/m.

9.4.2. IEC TS Parameters

The monthly means of the six IEC TS parameters, along with the 5^{th} and 95^{th} percentiles, are shown in Figures 92 and 93. The months, March - February, are labeled with the first letter (e.g., March is M). The values in the figure are summarized in Tables 37 and 38 in

Appendix G.

Monthly means of the significant wave height, H_{m0}, and the omnidirectional wave power density, J, show the greatest seasonal variability compared to the other parameters. Values are largest and vary the most during the winter months. The same trend is observed for the monthly mean energy period, T_e, but its variation is less pronounced. These observations are consistent with the relationship between wave power density, significant wave height and energy period, where wave power density, J, is proportional to the energy period, T_e, and the square of the significant wave height, H_{m0}.

The direction of maximum directionally resolved wave power is very consistent in the winter from west/northwest, and during the rest of the year has frequent shifts to the south, signified by the drop in the 5^{th} percentile. Seasonal variations of the remaining parameters, ϵ_0 and d_θ, are much less than J, H_{m0}, T_e, and θ_J, and are barely discernable. Monthly means for spectral width, ϵ_0, remain nearly constant at ~ 0.24. Similarly, monthly means for the directionality coefficient, d_θ, remain nearly constant at ~ 0.98. In summary, the waves at both the South and SSE locations at the Vandenberg site, from the perspective of monthly means, have a fairly consistent spectral width, are predominantly from the west/northwest, and exhibit a wave power that has a very narrow directional spread.

Wave roses of wave power and significant wave height, presented in Appendix G, Figures 156 - 159, also show the predominant direction of the wave energy at the Vandenberg site, which is west/northwest, with frequent shifts to the south. Figure G shows two dominant wave direction sectors, northwest (at 300°) and west/northwest (WNW) at 285°. At the South location, along the predominant wave direction, 300°, the omnidirectional wave power density is at or below 35 kW/m about 25% of the time, but greater than 35 kW/m nearly 15% of the time. Along the WNW direction (285°), wave power density is at or below 35 kW/m about 12% of the time, and greater than 35 kW/m about 17% of the time. At the SSE location, along the predominant wave direction, 300°, the omnidirectional wave power density is at or below 35 kW/m about 31% of the time, and greater than 35 kW/m about 6% of the time. Along the WNW direction (285°), wave power density is at or below 35 kW/m about 17% of the time, and greater than 35 kW/m about 16% of the time.

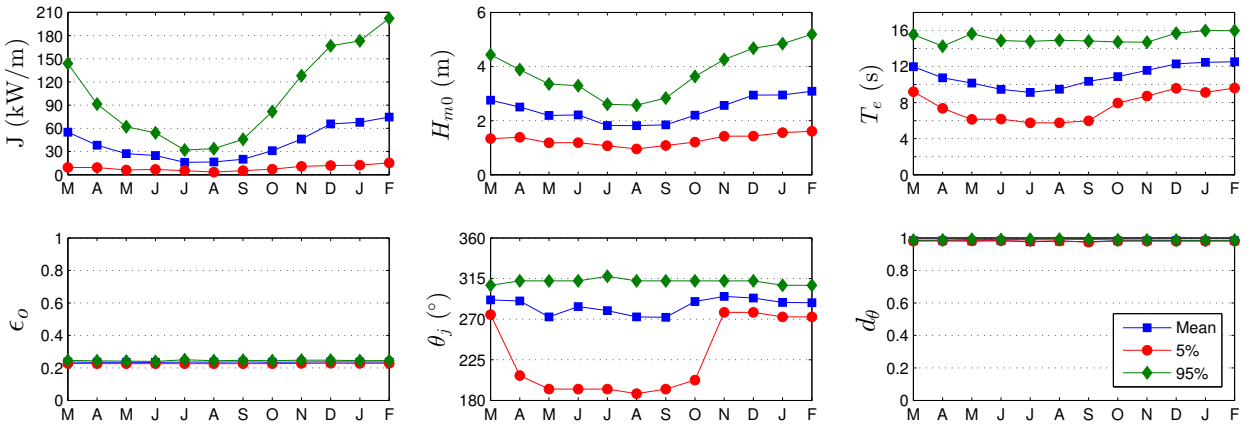

Figure 92: The average, 5^{th} and 95^{th} percentiles of the six parameters at the South Vandenberg site.

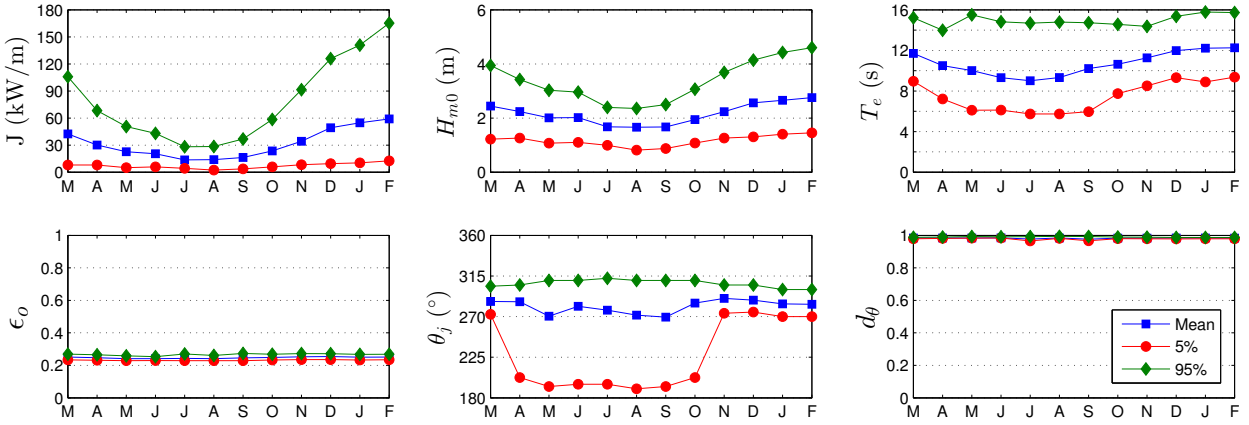

Figure 93: The average, 5^{th} and 95^{th} percentiles of the six parameters at the SSE Vandenberg site.

Monthly means, however, smear the significant variability of the six IEC parameters over small time intervals as shown in plots of the parameters at 1-hour intervals in Figures 94 and 95 for a representative year. While seasonal patterns described for Figures 92 and 93 are still evident, these plots show how sea states can vary abruptly at small time scales with sudden changes, e.g., jumps in the wave power as a result of a storm.

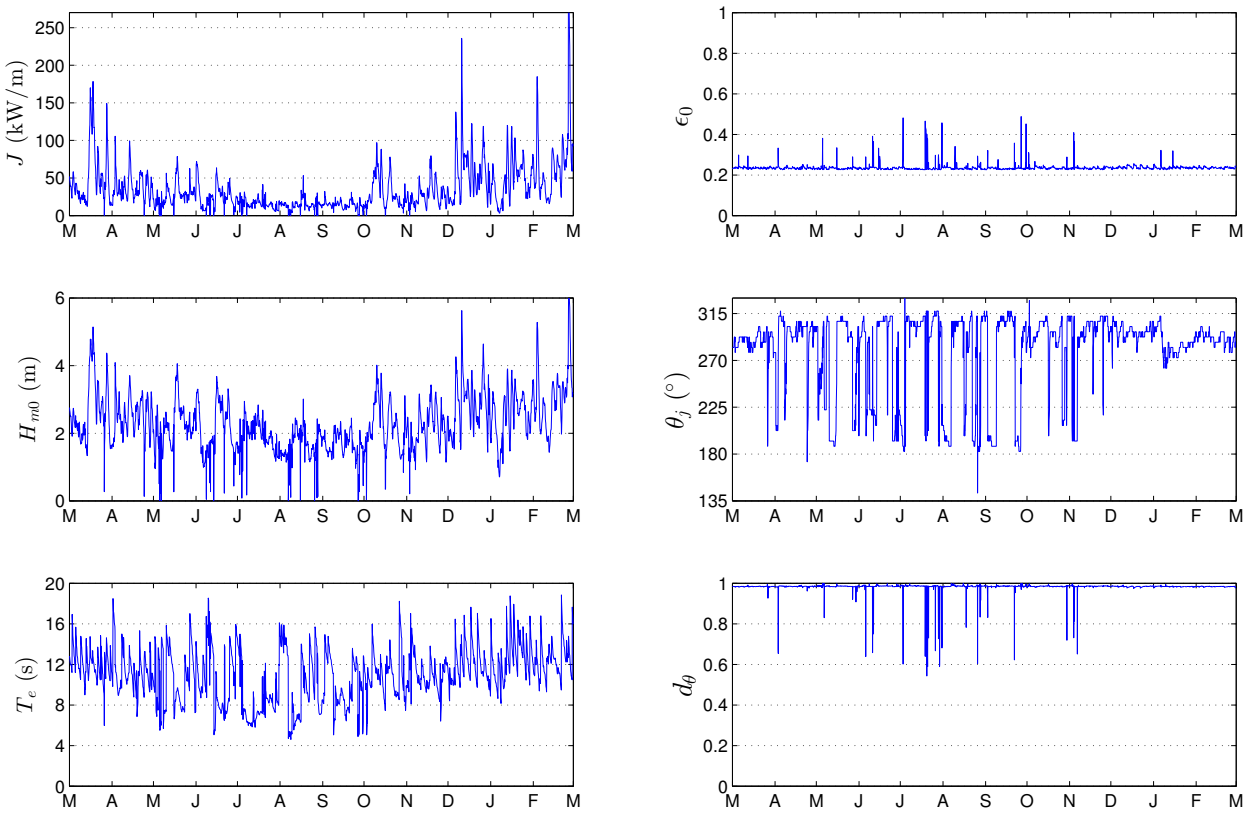

Figure 94: The six parameters of interest over a one-year period, March 2003 – February 2004 at the South Vandenberg site.

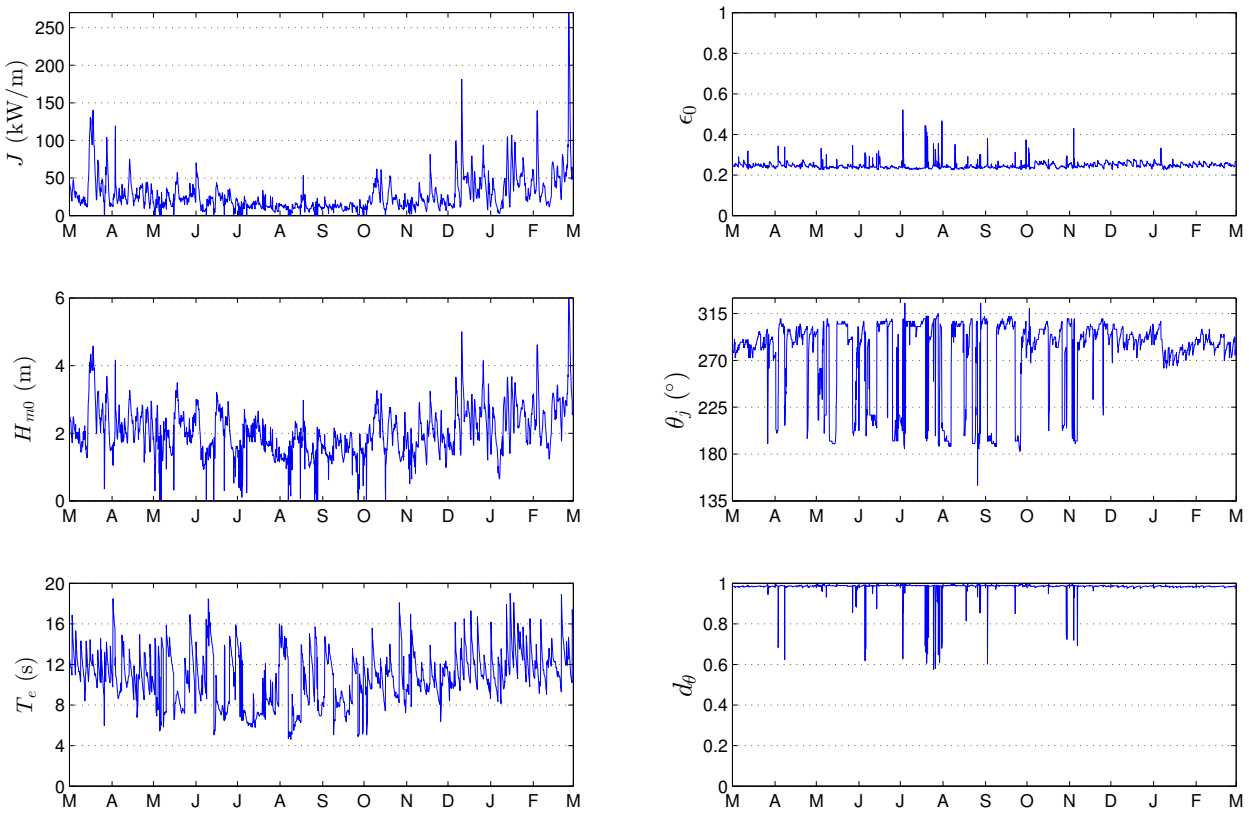

Figure 95: The six parameters of interest over a one-year period, March 2003 – February 2004 at the SSE Vandenberg site.

9.4.3. Cumulative Distributions

Annual and seasonal cumulative distributions (a.k.a., cumulative frequency distributions) are shown in Figures 96 and 97 for the South and SSE sites, respectively. Note that spring is defined as March – May, summer as June – August, fall as September – November, and winter as December – February. The cumulative distributions are another way to visualize and describe the frequency of occurrence of individual parameters, such as H_{m0} and T_e. A developer could use cumulative distributions to estimate how often they can access the site to install or perform operations and maintenance based on their specific device, service vessels, and diving operation constraints. For example, if significant wave heights need to be less than or equal to 1 m for installation and recovery, according to Figure 96, this condition occurs about 2% of the time on average within a given year. If significant wave heights need to be less than or equal to 2 m for emergency maintenance, according to Figure 96, this condition occurs about 37% of time on average within a given year. Cumulative distributions, however, do not account for the duration of a desirable sea state, or weather window, which is needed to plan deployment and servicing of a WEC device at a test site. This limitation is addressed with the construction of weather window plots in the next section.

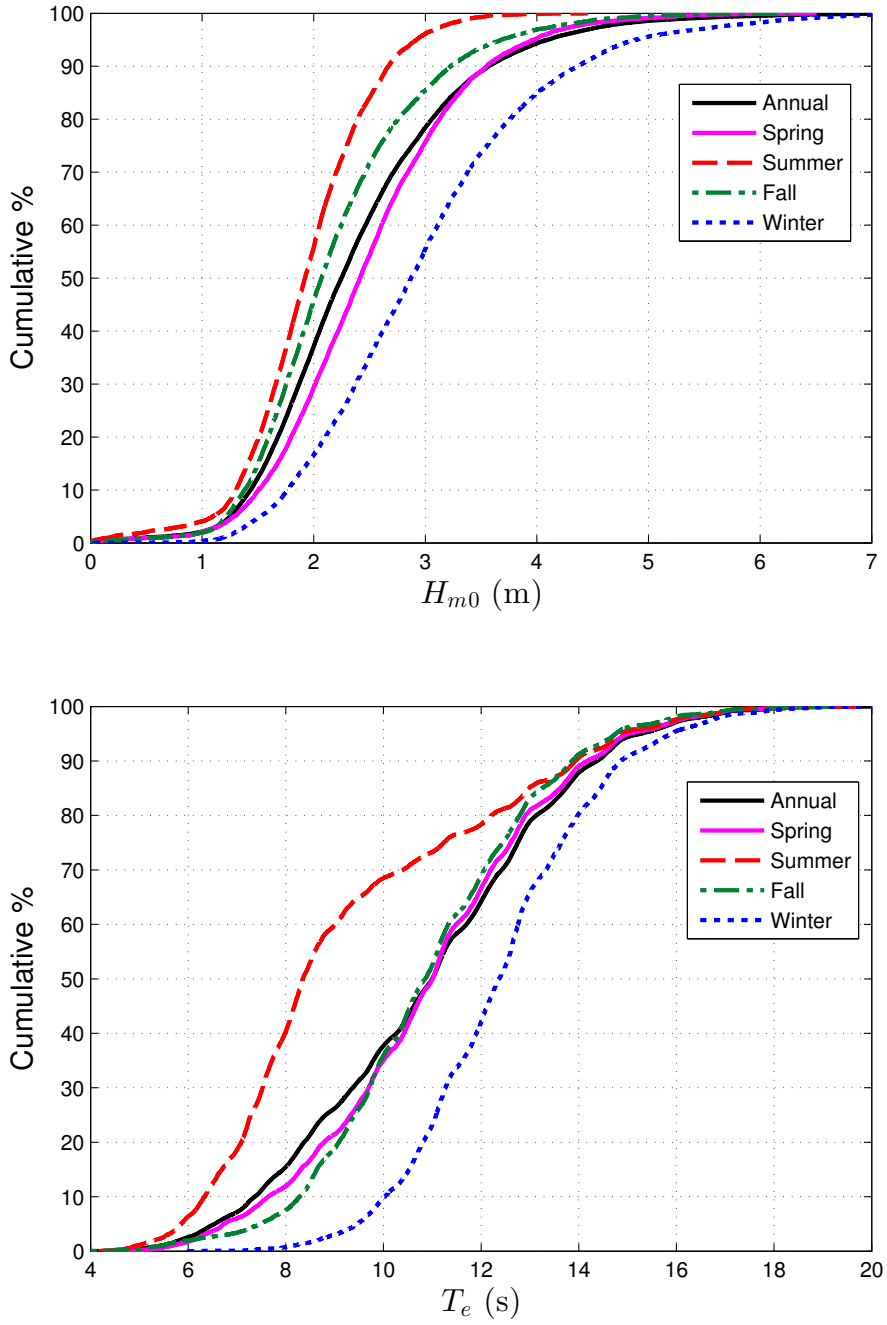

Figure 96: Annual and seasonal cumulative distributions of the significant wave height (top) and energy period (bottom) at the South Vandenberg site.

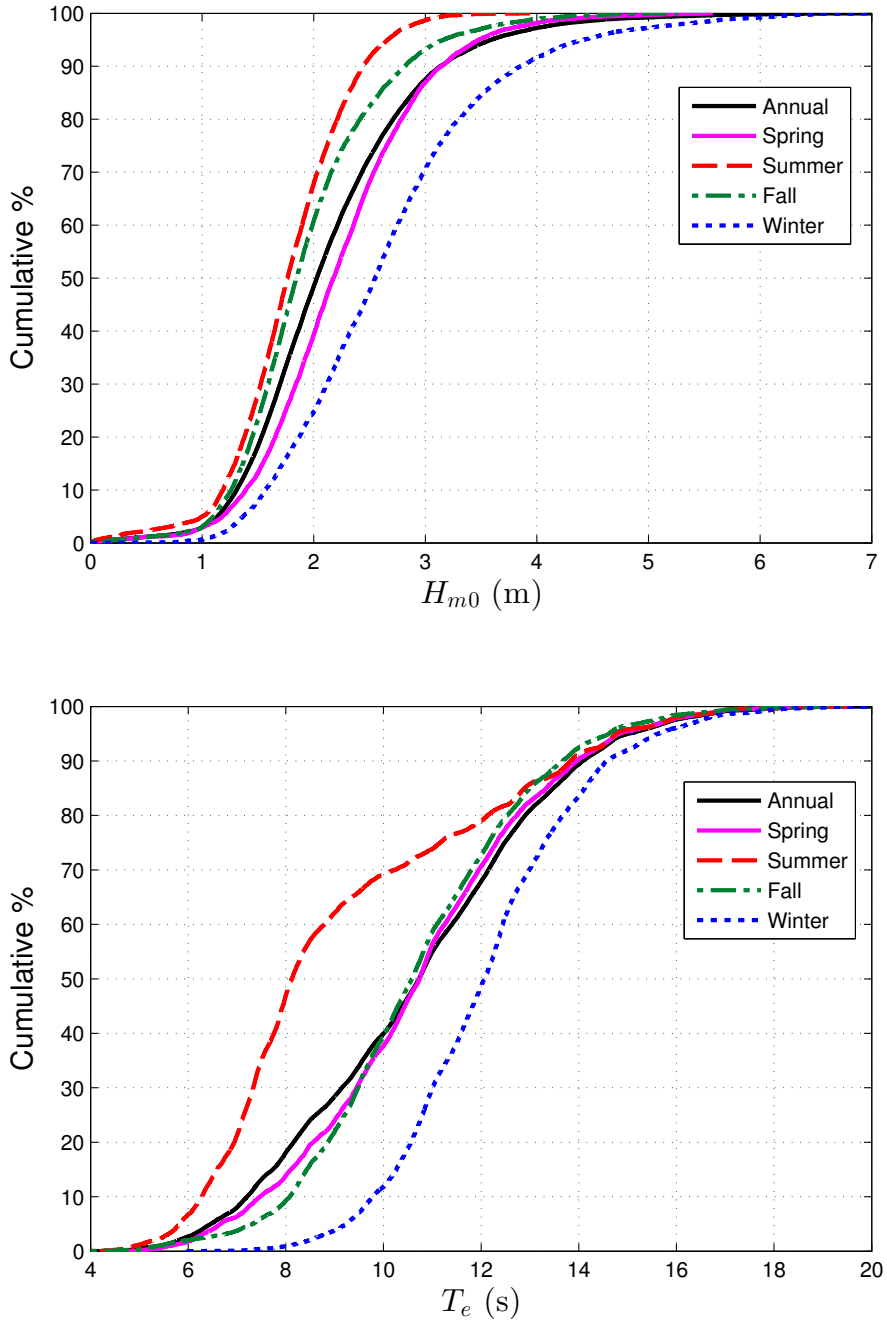

Figure 97: Annual and seasonal cumulative distributions of the significant wave height (top) and energy period (bottom) at the SSE Vandenberg site.

9.4.4. Weather Windows

Figures 98 and 101 show the number of weather windows at the South and SSE Vandenberg sites, when significant wave heights are at or below some threshold value for a given duration, for an average winter, spring, summer and fall. In these plots, each occurrence lasts a duration that is some multiple of 6-hours. The minimum weather window is, therefore,

6-hours in duration, and the maximum is 96-hours (4 days). The significant wave height threshold is the upper bound in each bin and indicates the maximum significant wave height experienced during the weather window. Note that the table is cumulative, so, for example, an occurrence of $H_{m0} \leq 1.5$ m for at least 78 consecutive hours in the fall is included in the count for 72 consecutive hours as well. In addition, one 12-hour window counts would count as two 6-hour windows. It is clear that there are more occurrences of lower significant wave heights during the summer than winter, which corresponds to increased opportunities for deployment or operations and maintenance.

Weather window plots provide useful information at test sites when planning schedules for deploying and servicing WEC test devices. For example, if significant wave heights need to be less than or equal to 1 m for at least 12 consecutive hours to service a WEC test device at the South Vandenberg site with a given service vessel, there would be, on average, two weather windows in the summer, but none in the winter. When wind speed is also considered, Figures 99 and 102 shows the average number of weather windows with the additional restriction of wind speed, $U < 15$ mph. The local winds (which are not necessarily driving the waves) are used in these weather windows, and are given in Appendix G.4. That wind data was not available from the hindcast, so data from CFSR was used (see Section 2.3, Appendix G.4). For shorter durations (6- and 12-hour windows), daylight is necessary. Windows with $U < 15$ mph and only during daylight hours are shown in Figures 100 and 103. Daylight was estimated as 5am – 10pm Local Standard Time (LST).

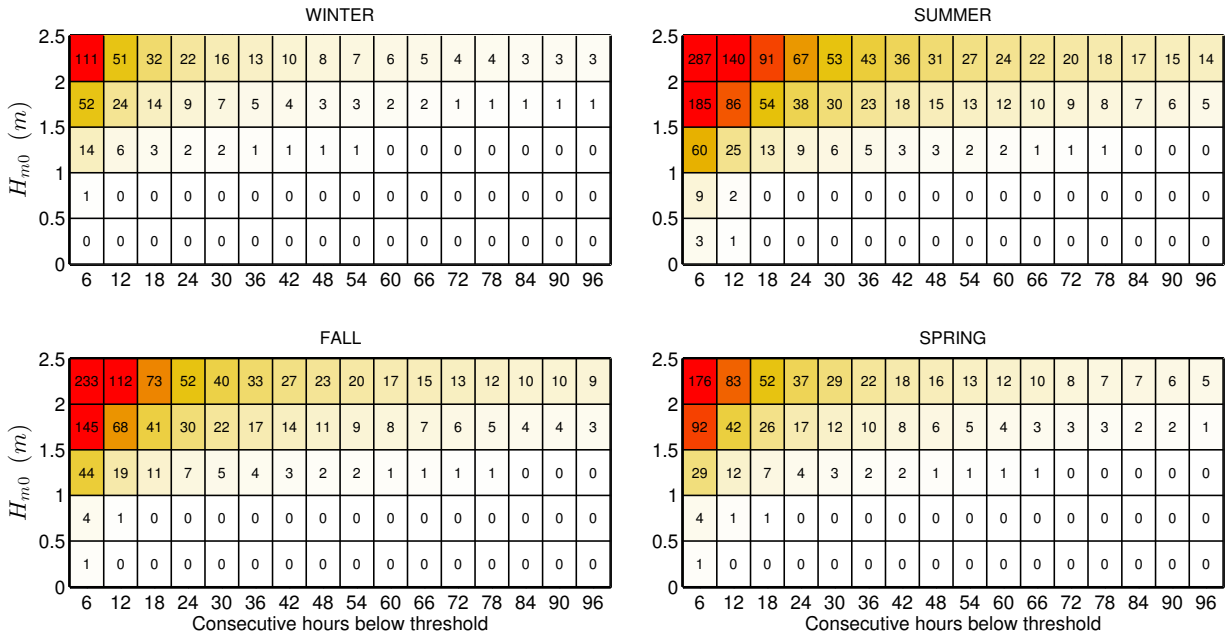

Figure 98: Average cumulative occurrences of wave height thresholds (weather windows) for each season at the South Vandenberg site. Winter is defined as December – February, spring as March – May, summer as June – August, and fall as September – November.

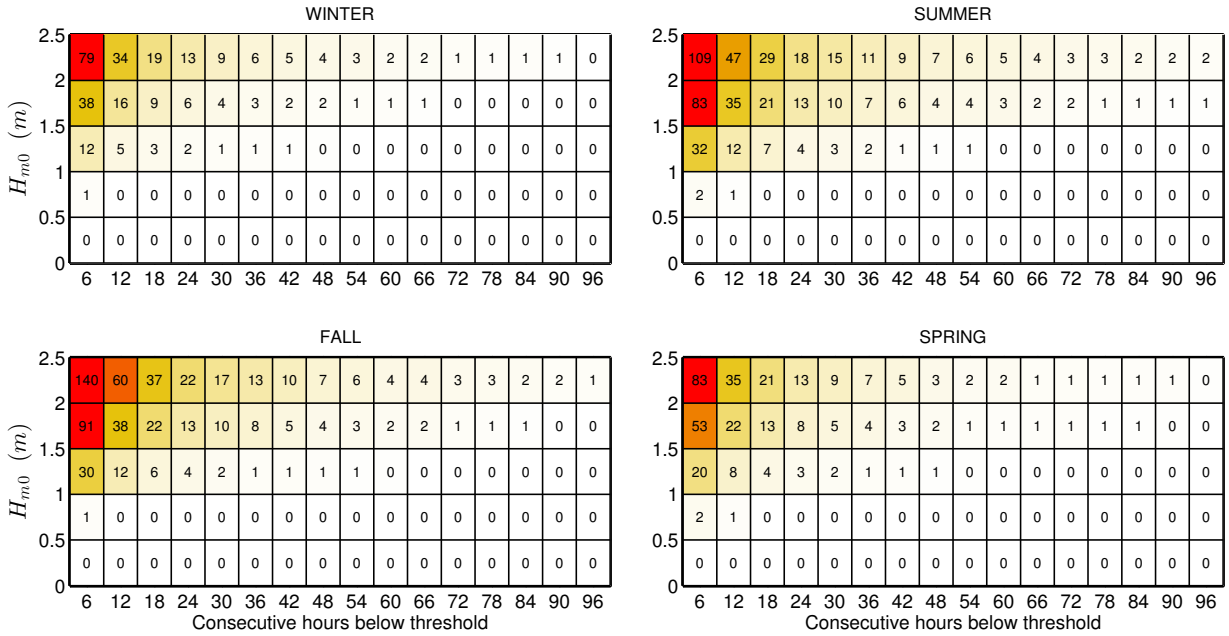

Figure 99: Average cumulative occurrences of wave height thresholds (weather windows) for each season at the South Vandenberg site with an additional restriction of U $<$ 15 mph.

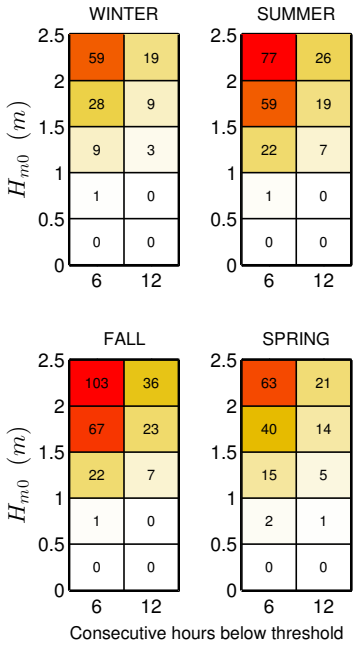

Figure 100: Average cumulative occurrences of wave height thresholds (weather windows) for 6- and 12-hour durations with $U < 15$ mph and only during daylight hours (5am – 10pm LST) at the South Vandenberg site.

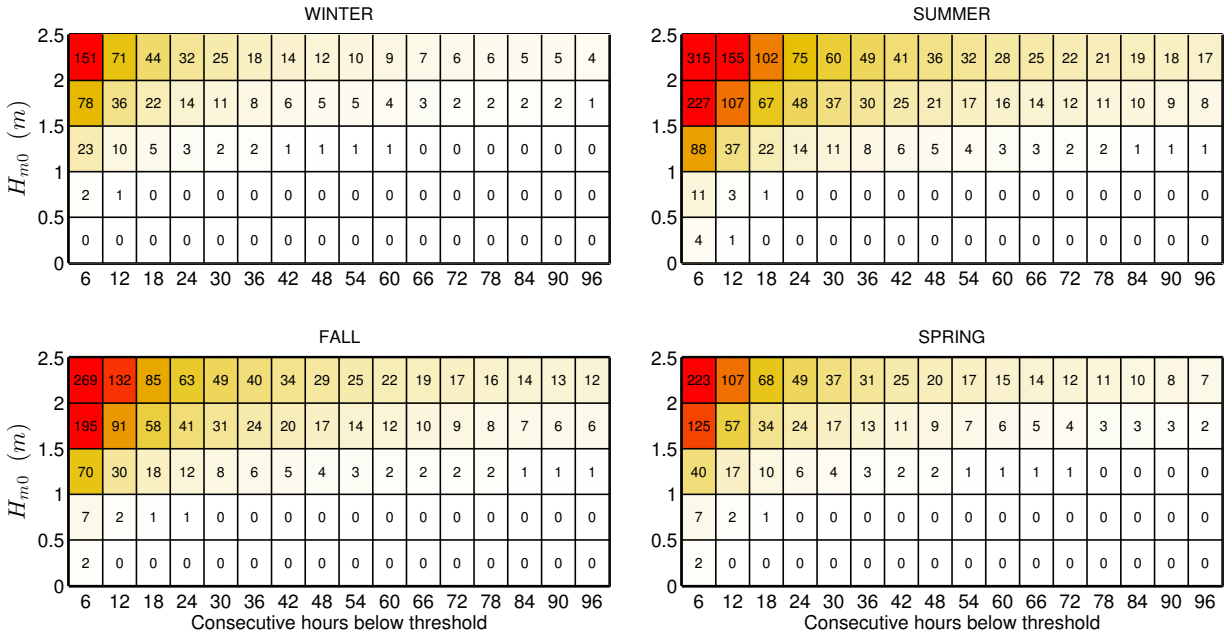

Figure 101: Average cumulative occurrences of wave height thresholds (weather windows) for each season at the SSE Vandenberg site. Winter is defined as December – February, spring as March – May, summer as June – August, and fall as September – November.

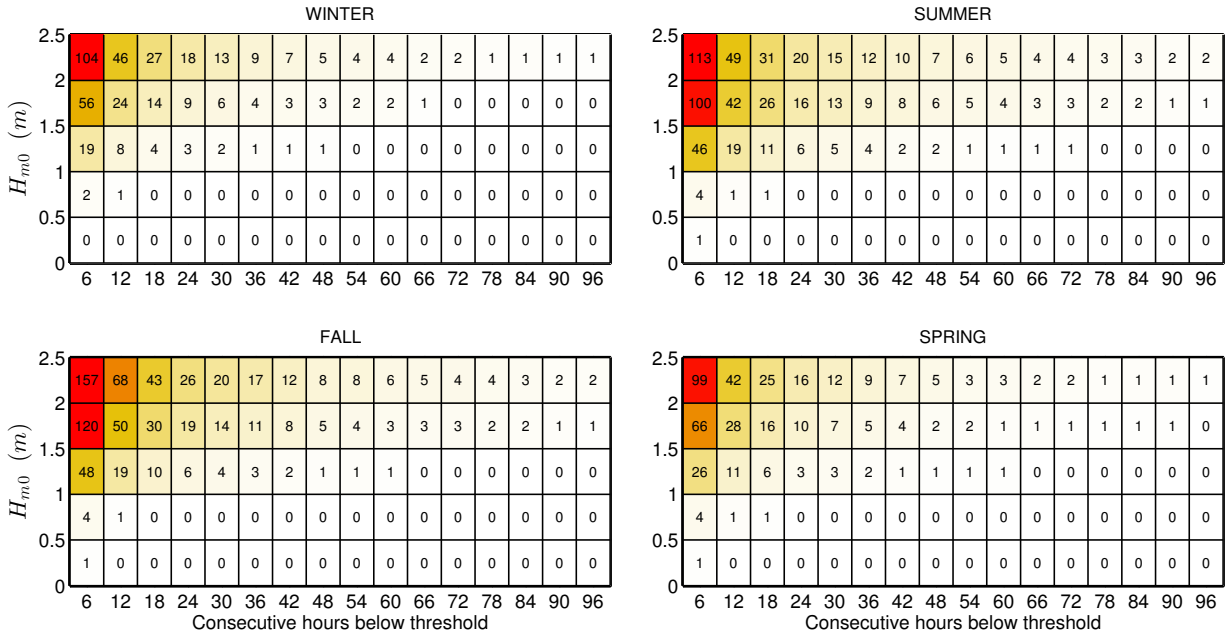

Figure 102: Average cumulative occurrences of wave height thresholds (weather windows) for each season at the SSE Vandenberg site with an additional restriction of U $<$ 15 mph.

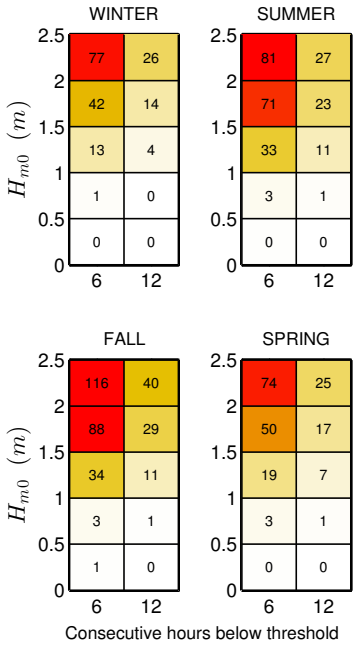

Figure 103: Average cumulative occurrences of wave height thresholds (weather windows) for 6- and 12-hour durations with $U < 15$ mph and only during daylight hours (5am – 10pm LST) at the SSE Vandenberg site.

9.4.5. Extreme Sea States

As mentioned in 2.2, the way IFORM and the modified IFORM are currently implemented, they do not work well for datasets whose variables (H_{m0} and T_e) are bimodally distributed. The CDIP071 / NDBC 46218 dataset is not well suited for IFORM, and therefore only the extreme significant wave height is estimated here using extreme value theory.

The generalized extreme value distribution (GEV) was fit to the annual significant wave height maximum in order to generate estimates of extreme values under the annual maximum method (AMM) (Rugerio et al. 2010). The peak over threshold (POT) method was also applied to the entire dataset in order to generate estimates of extreme values based on significant wave height exceedances over a certain threshold. Based on the application of this method as described by Ruggerio et al. (2010), the 99.5th percentile of significant wave height was used as a threshold value. These methods were applied using the WAFO matlab toolbox (Brodtkorb et al. 2000). The bootstrapping method (Efron and Tibshirani 1993) was applied in order to generate a 95% confidence interval around the CDFs derived using both of the extreme value distribution methods utilized in this analysis.

The 100-year H_{m0} is estimated as 9.98 m and 9.63 m using the GEV and POT methods, respectively, as shown in Figures 104 and 105. The 10-, 25-, and 50-year values are shown in the figures. It should be noted that conditions at the NDBC46218 buoy (at a depth on the order of 500 m) may differ significantly from the conditions at the test site (at depths on the order of 100 m).

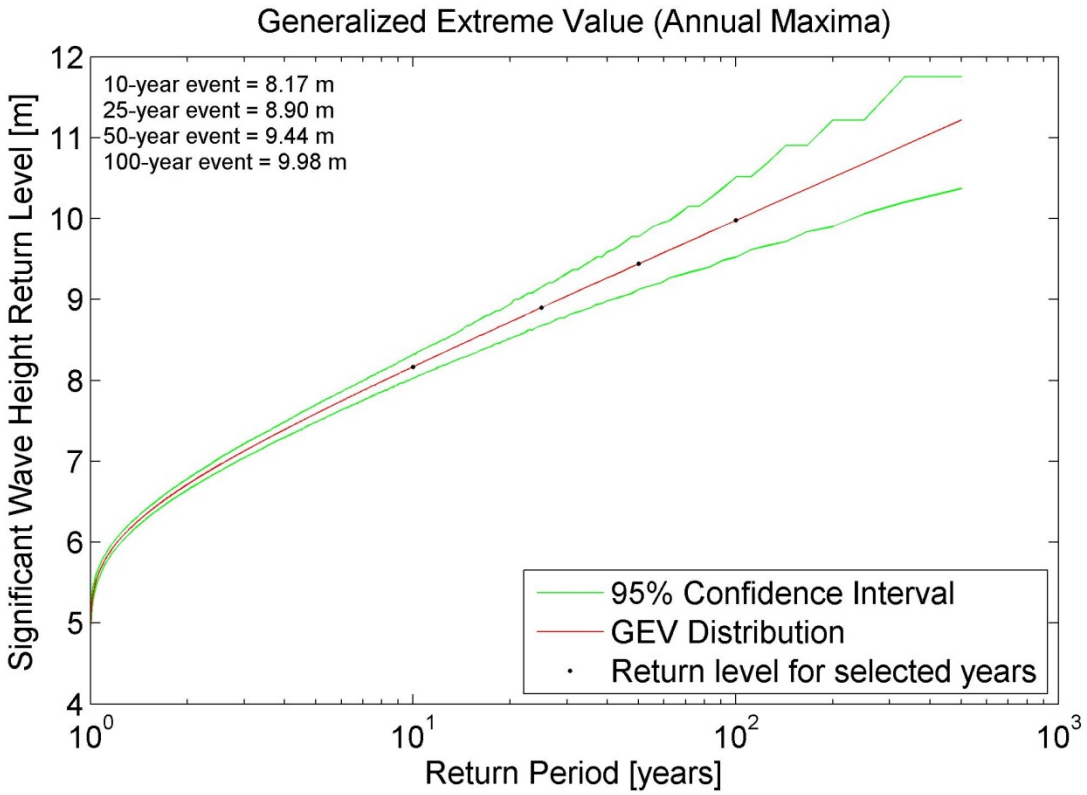

Figure 104: The generalized extreme values distribution was fit to annual maximum of significant wave height from NDBC46218 to generate estimates of extreme values. The 95% confidence interval is shown as well.

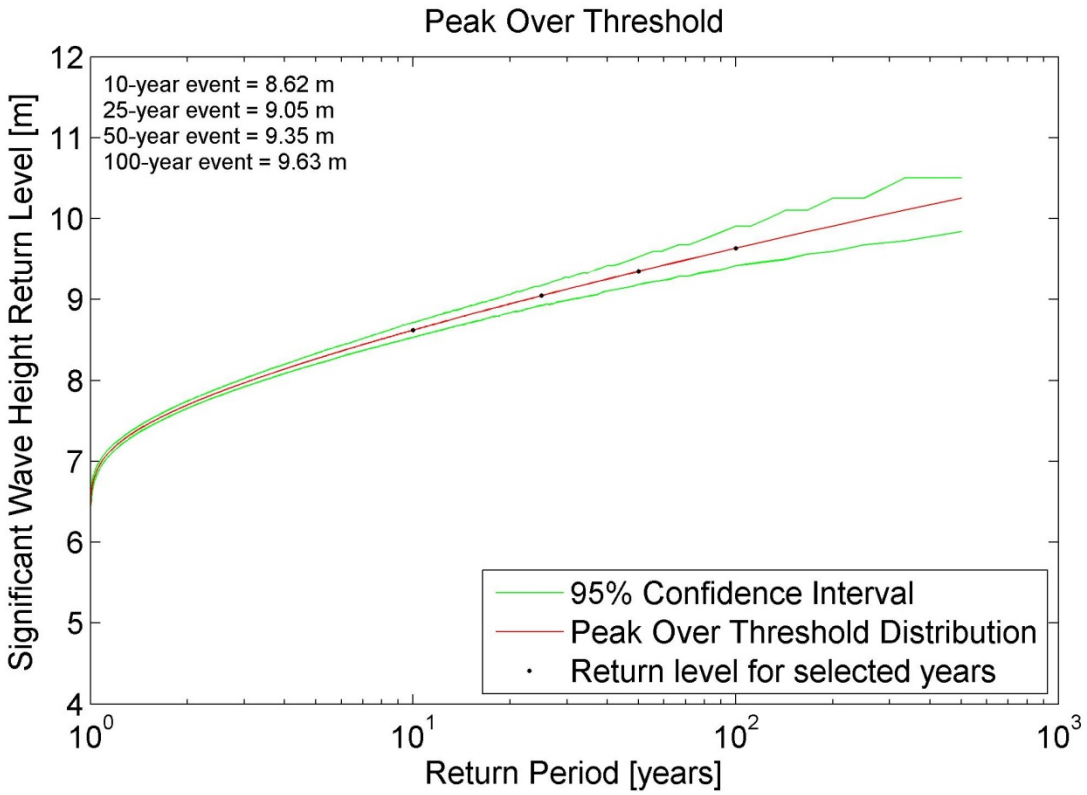

Figure 105: The peak over thresholds method was used with a threshold value of the 99.5th percentile of significant wave height from NDBC46218. The 95% confidence interval is shown as well.

9.4.6. Representative Wave Spectrum

All hourly discrete spectra measured at CDIP071 / NDBC46218 for the most frequently occurring sea states are shown in Figure 106. The most frequently occurring sea state, which is within the range 1.5 m $< H_{m0} <$ 2 m and 8 s $< T_e <$ 9 s, was selected from a JPD similar to Figures 90 & 91 in Section 9.4.1, but based on the NDBC 46218 buoy data. As a result, the JPD, and therefore the most common sea states, generated from buoy data are slightly different from that generated from hindcast data. For example, the most frequently occurring sea state for the JPD generated from hindcast data is 0.5 m higher on bounds for H_{m0} (2 m $< H_m0$ ¡ 2.5 m), and two seconds higher on bounds for T_e (10 s $< T_e <$ 11 s). Often several sea states will occur at a very similar frequency, and therefore plots of hourly discrete spectra for several other sea states are also provided for comparison. Each of these plots includes the mean spectrum and standard wave spectra, including Bretschneider and JONSWAP, with default constants as described in Section 2.2.

For the purpose of this study, the mean spectrum is the 'representative' spectrum for each sea state, and the mean spectrum at the most common sea state, shown in Figure 106 (bottom-left plot), is considered the 'representative' spectrum at the site. The hourly spectra vary considerably about this mean spectrum, but this is partly reflective of the bin size chosen for H_{m0} and T_e. Comparisons of the representative spectra in all plots with the Bretschneider

and JONSWAP spectra illustrate why modeled spectra with default constants, e.g., the shape parameter $\gamma = 3.3$ for the JONSWAP spectrum, should be used with caution. Using the constants provided in Section 2.2, the Bretschneider spectra are, at best, fair representations of the mean spectra in Figure 106, and it does not capture the bimodal nature of the spectra. The mean measured spectra is the best representation of the conditions, however, if these modeled spectra were to be used at this site, it is recommended that the constants undergo calibration against some mean spectrum, e.g., the representative spectrum constructed here. A better alternative would be to explore other methods or spectral forms to describe bimodal spectra (e.g., Mackay 2011) if it is known that the shape is not unimodal.

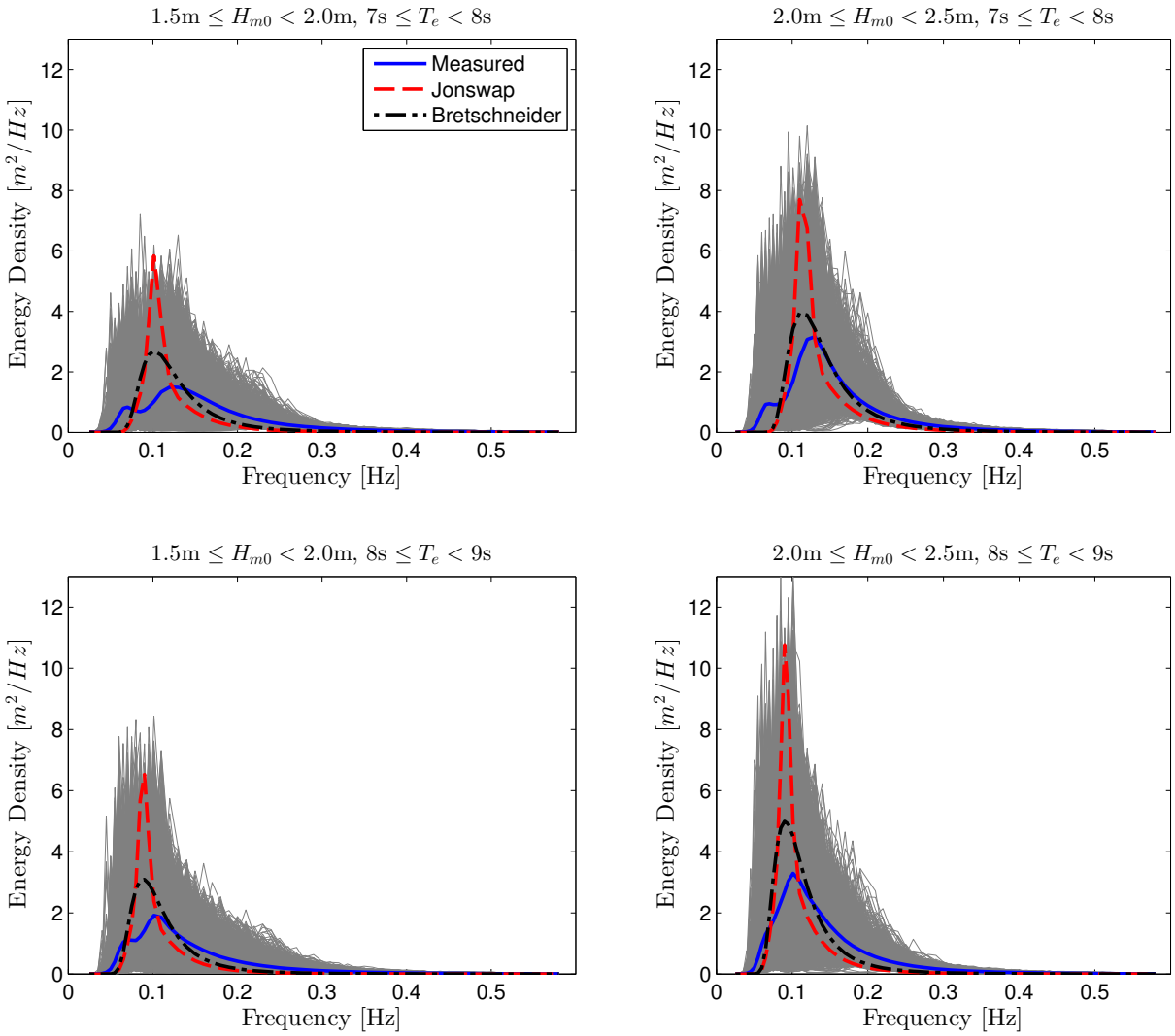

Figure 106: All hourly discrete spectra and the mean spectra measured at CDIP071 / NDBC 46218 within the sea state listed above each plot. The JONSWAP and Bretschneider spectra are represented by red and black dotted lines, respectively.

10. HUMBOLDT BAY, CALIFORNIA: POTENTIAL WEC TEST SITE

10.1. Site Description

For the purpose of this catalogue, the potential WEC site offshore of Humboldt Bay, referred to herein as the Humboldt Site, is located at 40.8418 N, 124.2477 W. As seen in Figure 107, the Humboldt Site lies in the footprint of the former Pacific Gas & Electrics (PG&E) pilot project test bed, the Humboldt WaveConnect (HWC), which was located in state waters to potentially ease permitting restrictions. PG&E considered this location for a WEC testing facility during the years 2008 – 2011 (Dooher et al. 2011). PG&E chose this test bed location based on numerous considerations, and the motivation for HWCs site placement is available in more detail in PG&Es Final Report (Dooher et al. 2011).

The Humboldt Site is approximately 9 km north/northwest of Humboldt Bay near the city of Eureka in Humboldt County, California (Figure 107). The site is at 45 m depth and lies over a sedimentary shelf consisting of sand and clay. As seen in Figure 108, the deployment site features a gently sloping seabed without many irregularities such as canyons that could disturb the local wave field (Dooher et al. 2011). The sediment and bathymetry are well suited for subsea cable burial and anchoring (Dooher et al. 2011).

The wave climate at the test site varies seasonally, with calmer seas in the summer compared to more energetic seas in the winter. The wave environment at the site is characterized by an annual average power flux of about 32.2 kW/m, including a number of events with significant wave heights exceeding 7 m each winter.

This site is not as developed as some of the other sites in this catalogue, but it has the basic infrastructure needed to support WEC testing. The surrounding area offers port facilities, an electrical substation on shore, and an abundance of high quality met-ocean data.

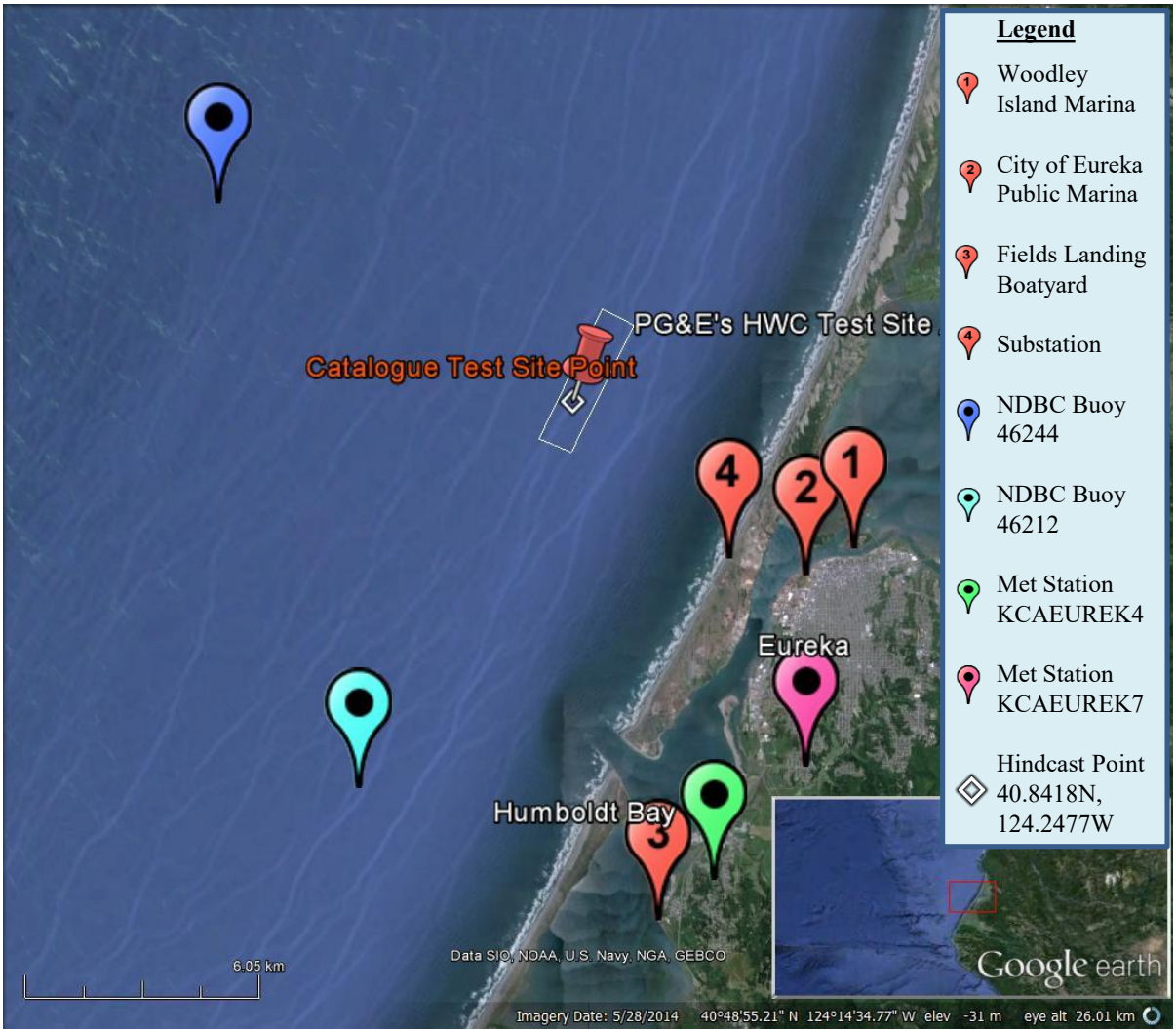

Figure 107: The proposed Humboldt Site is located on the coast of California near the city of Eureka. The test site is 5-6 km off-shore in 45 m depth water (~25 fathoms). No berthing or ocean infrastructure exist at this time. A future grid connection could be established at the existing substation. Two National Data Buoy Center (NDBC) ocean buoys and two National Weather Service (NWS) meteorological stations are close to the test site. The Woodley Island Marina and the City of Eureka Public Marina are located in Humboldt Bay and boatyard access is available at the Fields Landing Boatyard. The point of reference for the hindcast simulation is the primary coordinate for the proposed test site. Image modified from Google Earth (2014).

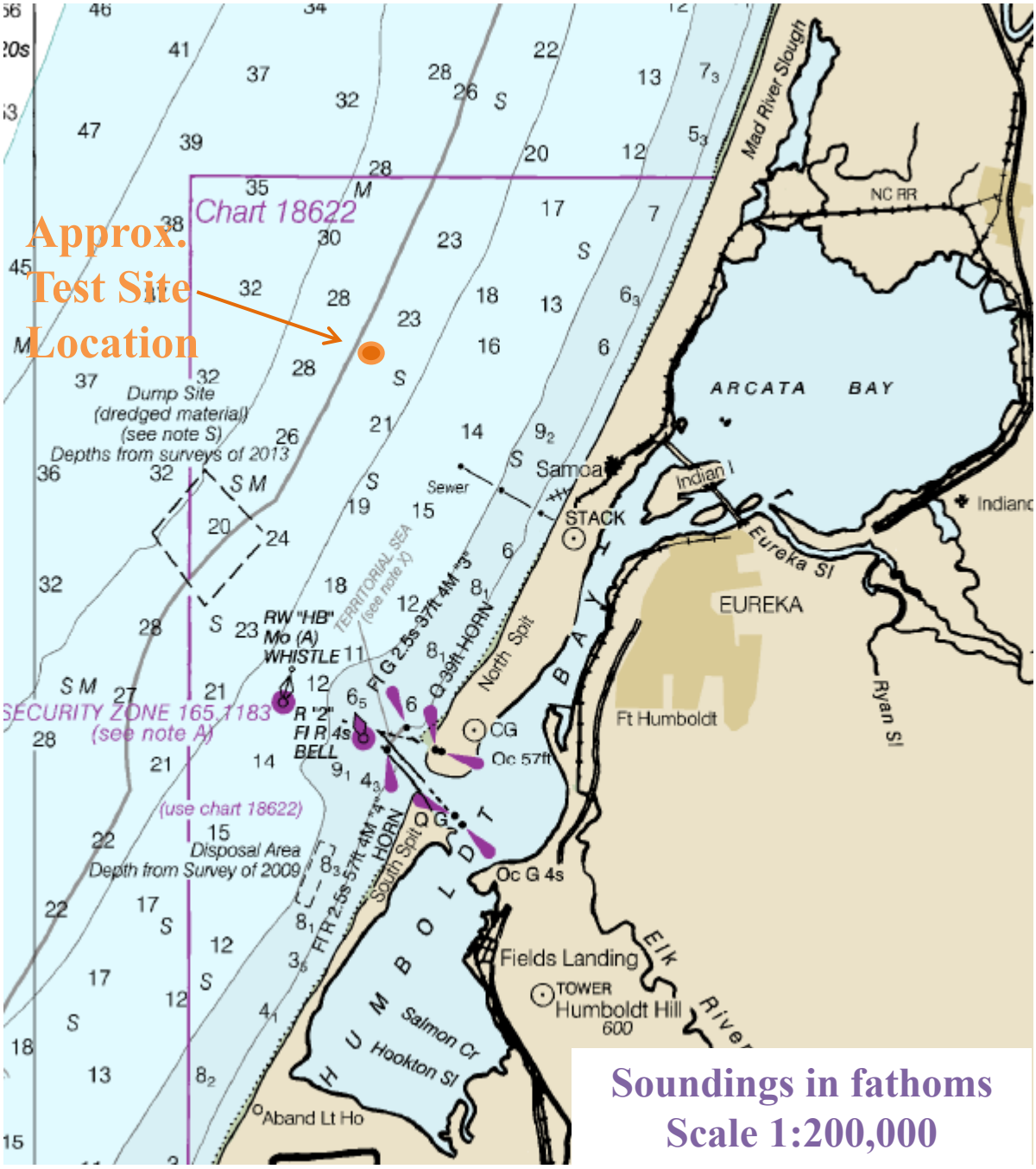

Figure 108: Nautical chart of Humboldt Bay and surrounding area shows the general bathymetry around the proposed test site. Sounds in fathoms (1 fathom = 1.8288 m). For a detailed map of Humboldt Bay, see Nautical chart #18622 (Office of Coast Survey 2013). Image modified from nautical chart #18620 (Office of Coast Survey 2012).

10.2. WEC Testing Infrastructure

10.2.1. Mooring Berths

As a potential test site, the Humboldt Site has no mooring berths installed or planned.

10.2.2. Electrical Grid Connection

There is currently no grid connection at the Humboldt Site. Future projects, however, may take advantage of the substation onshore directly landward of the test site (Waypoint #4 in Figure 107). The 60 kV PG&E Fairhaven Substation has three 60 kV lines connected to it, the highest of which accommodates 41 MW. The nearby former pulp mill facility also has a substation that interconnects to the same 60 kV transmission lines and is capable of accommodating 30 MW.

10.2.3. Facilitating Harbor

The port nearest to the test site is located within Humboldt Bay, which is the only deep-water port on California's North Coast (Department of Transportation 2012). For boat mooring, there are two options in Humboldt Bay near the city of Eureka: the Woodley Island Marina (Waypoint #1 in) and the City of Eureka Public Marina (Waypoint #2 in Figure 107).

10.2.4. On-Shore Office Space

10.2.5. Service Vessel and Engineering Boatyard Access

No dedicated service vessel is available at this time. Boats may be serviced at Fields Landing Boatyard (Waypoint #3 in Figure 107). This boatyard serves small to commercial-sized fishing boats with a travel lift. Repairs are made by the owner or hired external personnel. There may be companies such as Englund Marine & Industrial Supply Co. that can provide additional engineering services.

10.2.6. Travel and Communication Infrastructure

The Arcata/Eureka Airport services the Humboldt Bay area. The airport has several flights per day. Cellular phone service is available with moderate to full coverage.

10.2.7. Met-Ocean Monitoring Equipment

Real-time meteorological and wave data are collected by three met-ocean buoys and two meteorological stations. Instrument and data specifications for this monitoring equipment are summarized in Table 8. Buoy data is accessible online at the CDIP and NDBC databases. CDIP168 (NDBC46244) is operational and located approximately 8 km west of the test site. NDBC 46022 (Figure 109 (a)), approximately 30 km southwest of the site, has been offline

for repair and is expected to be operational in the fall of 2014. CDIP128 (NDBC 46212) (Figure 109 (b)) is approximately 12 km from the test site, but was decommissioned in 2013. In addition to the met/ocean buoys, there are two land based meteorological stations located in Eureka, California.

Figure 109: (a) Discus buoy NDBC46022 located 30 km from site, (b) Waverider buoy CDIP128/NDBC46212 located 12 km south of test site (National Data Buoy Center 2014).

Table 8: Wave monitoring equipment in close proximity to the Humboldt proposed test site.

Instrument Name (Nickname)	**CDIP128/ NDBC46212 - ("South Spit")**		**NDBC46022 (LLNR 500 / "Buoy 22")**			**CDIP168 / NDBC46244 - ("North Spit")**	
Type	Waverider Buoy		3-meter discus buoy			Waverider Buoy	
Measured parameters	-std. met. data -spectral wave density data -spectral wave direction data		-std. met. data -continuous winds data -spectral wave density data -spectral wave direction data (only from 2007-2010)			-std. met data -spectral wave density data -spectra wave directional data	
Variables reported, including derived variables (Sampling interval)	*Std. Met.:* WVHT DPD APD MWD WTMP (30 min)	-Spectral Wave Density -Spectral Wave Direction (30 min)	*Std. Met.:* WDIR WSPD GST WVHT DPD APD PRES ATMP WTMP (1 hr)	*Contin. Winds:* WDIR WSPD GDR GST GTIME (10 min)	-Spectral Wave Density -Spectral Wave Direction (1 hr)	*Std. Met.:* WDIR WSPD GST WVHT DPD APD PRES ATMP WTMP (30 min)	-Spectral Wave Density -Spectral Wave Direction (30 min)
Location	12 km South of site, 6.5 km West of Humboldt Bay entrance		30 km West/Southwest of Test site			8 km West of Test Site	
Coordinates	40.753 N 124.313 W (40°45'12" N 124°18'48" W)		40.724 N 124.578 W (40°43'25" N 124°34'41" W)			40.888 N 124.356 W (40°53'18" N 124°21'22" W)	
Depth	40 m		674.8 m			114 m	
Data Start	1/22/2004		-wave data: 1982 -spectral wave data: 01/01/1996 -directional spectra: 06/01/2007			2/9/2010	
Data End	4/3/2013		-11/13/2013 -dir. spectra ended 2/19/2010 -will be redeployed 8/2014			present	
Period of Record	∼9 yrs		-wave data: ∼32 yrs -spectral data: ∼18 yrs -directional spectra: ∼4 yrs			∼5.5 yrs	
Owner/ Contact Person	NOAA– "Information Submitted by Scripps" http://cdip.ucsd.edu/?nav=recent&sub=observed&stn=128&xitem=info&stream=p1		National Data Buoy Center http://www.ndbc.noaa.gov/station_page.php?station=46022			NOAA– "Information Submitted by Scripps" http://cdip.ucsd.edu/?ximg=search&xsearch=168&xsearch_ type=Station_ID	

Instrument Name (Nickname)	**KCAEUREK4**	**KCAEUREK7**
Type	Met station	Met Station
Measured parameters	Meteorological Data	Meteorological Data
Variables reported, including derived variables (Sampling interval)	AirTemp DewPoint Pressure WDIR WSPD Humidity (5 min)	AirTemp DewPoint Pressure WDIR WSPD Humidity Precip (5 min)
Location	Humboldt Hill, Eureka, CA	Herrick Hill, Eureka, CA
Coordinates	40.732 N 124.205 W (40° 43' 54" N, 124° 12' 17" W)	40.758 N 124.177 W
Depth	Elev.: 85 ft	Elev.: 102 ft
Data Start	3/7/2008	3/15/2011
Data End	present	present
Period of Record	∼6.5 yrs	∼3.5 yrs
Owner/ Contact Person	National Weather Service; data download wunderground.com	National Weather Service; data download wunderground.com

10.2.8. Environmental Monitoring

Environmental conditions have not been assessed at the Humboldt Site, and although some environmental studies were conducted as part of an environmental site assessment (ESA) for the HWC project site, the ESA was never completed (Dooher et al. 2011). PG&E partnered with Redwood Sciences Lab, Klamath Bird Observatory, and Humboldt State University (HSU) for their ESA related studies. Several ESA related studies reached completion including a marine life study conducted by Dr. Dawn Goley at HSU (Dooher et al. 2011: Appendix HSU E), a sediment dynamics study (Dooher et al. 2011: Appendix HSU C) and site placement in relation to local fishing economics study (Dooher et al. 2011: Appendix HSU D, Appendix HSU B). Future projects must further characterize the site and be responsible for environmental monitoring of the WEC device.

10.2.9. Permitting

The Humboldt Site has no federal, state or local permits to operate as a WEC test site. Future efforts to permit the Humboldt Site will require a substantial investment through the NEPA process, including outreach to various stakeholders, required permits for testing in California state waters, the development of an environmental impact report and monitoring, and adaptive management plans. The time required for this process is unknown and developers should be prepared for significant time uncertainty.

Although future projects must devote a significant effort to permitting at Humboldt Bay, developers can leverage the lessons learned from the HWC project site to ease the process. PG&E states in their report that they hope that their experiences may be informative for future test site developers and help future projects avoid some of the struggles they faced (Dooher et al. 2011). PG&E was issued preliminary permits for the HWC project site in 2008 through the Federal Energy Regulatory Commission (FERC), but a Pilot Project Licensing Process (PPLP) was never obtained (Dooher et al. 2011). Of all the obstacles, uncertainty regarding the expected impact of WEC devices on the environment was a major challenge in obtaining the permit. This uncertainty was partly due to the lack of specific information concerning WEC technologies to be tested at PG&Es site, and also the relative lack of understanding about the marine environment at the site. More information about PG&Es HWC project can be found in their final report, which is available from the Office of Science and Technical Information at http://www.osti.gov/scitech/biblio/1032845 (report ID 1032845).

10.3. Data used

Researchers at Sandia National Laboratories produced a 10 year hindcast dataset for the area offshore of Humboldt Bay, CA (Dallman et al. 2014). This dataset was used to calculate parameters of interest for the characterization at this site. The hindcast data at the grid point shown in Figure 110 was analyzed.

In addition to the hindcast data set, historical data from buoy CDIP128/NDBC 46212 was

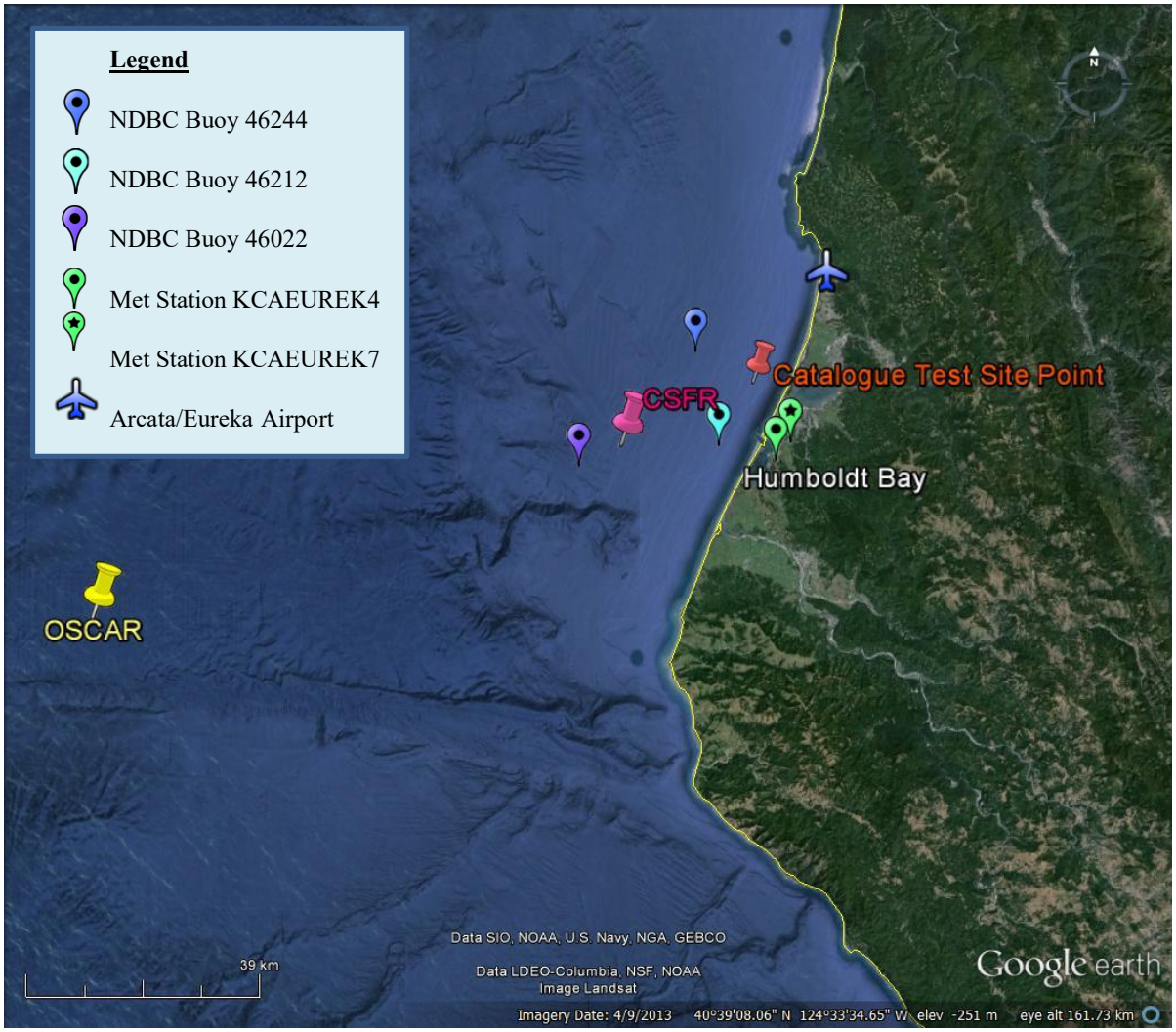

Figure 110: The catalogue test site location in relation to NDBC Buoys, OSCAR surface current data points, CSFR wind data points, and the nearest airport (Google Earth 2014).

10.4. Results

The following sections provide information on the joint probability of sea states, the variability of the IEC TS parameters, cumulative distributions, weather windows, extreme sea states, and representative spectra. This is supplemented by wave roses as well as wind and surface current data in Appendix H. The wind and surface current data provide additional information to help developers plan installation and operations & maintenance activities.

10.4.1. Sea States: Frequency of Occurrence and Contribution to Wave Energy

Joint probability distributions of the significant wave height, H_{m0}, and energy period, T_e, are shown in Figure 111. Figure 111 (top) shows the frequency of occurrence of each binned sea state and Figure 111 (bottom) shows the percentage contribution to the total wave energy. Figure 111 (top) indicates that the majority of sea states are within the range 1 m $< H_{m0} <$ 3.5 m and 6 s $< T_e <$ 11 s; but a wide range of sea states are experienced at the Humboldt Site, including extreme sea states caused by severe storms where H_{m0} exceeded 7 m. The site is well suited for testing WECs at various scales, including full-scale WECs, and testing the operation of WECs under normal sea states. This would also be a desirable site for commercial deployment. Although the occurrence of an extreme sea state for survival testing of a full scale WEC is unlikely during a normal test period, the Humboldt Site wave climate offers opportunities for survival testing of scaled model WECs.

As mentioned in the methodology (Section 2.2), previous studies show that sea states with the highest occurrence do not necessarily correspond to those with the highest contribution to total wave energy. The total wave energy in an average year is 282,600 kWh/m, which corresponds to an average annual omnidirectional wave power of 32.2 kW/m. The most frequently occurring sea state is within the range 1.5 m $< H_{m0} <$ 2 m and 6 s $< T_e <$ 7 s, while the sea state that contributes most to energy is within the range 3 m $< H_{m0} <$ 3.5 m and 10 s $< T_e <$ 11 s. Several sea states occur at a similar frequency, and sea states within 2 m $< H_{m0} <$ 4.5 m and 9 s $< T_e <$ 12 s contribute a similar amount to energy.

Frequencies of occurrence and contributions to energy of less than 0.01% are not shown in the figure for clarity. For example, the sea state within 0.5 m $< H_{m0} <$ 1 m and 4 s $< T_e <$ 5 s has an occurrence of 0.02%. The contribution to total energy, however, is only 0.001% and, therefore, does not appear in Figure 111 (bottom). Similarly, the sea state within 8 m $< H_{m0} <$ 8.5 m and 13 s $< T_e <$ 14 s has an occurrence of 0.007%, but the contribution to total energy is 0.11%.

Curves showing the mean, 5^{th} and 95^{th} percentiles of wave steepness, H_{m0}/γ, are also shown in Figure 111. The mean wave steepness at the Humboldt Site is 0.0185 ($\approx$1/54), and the 95th percentile approaches 1/33.

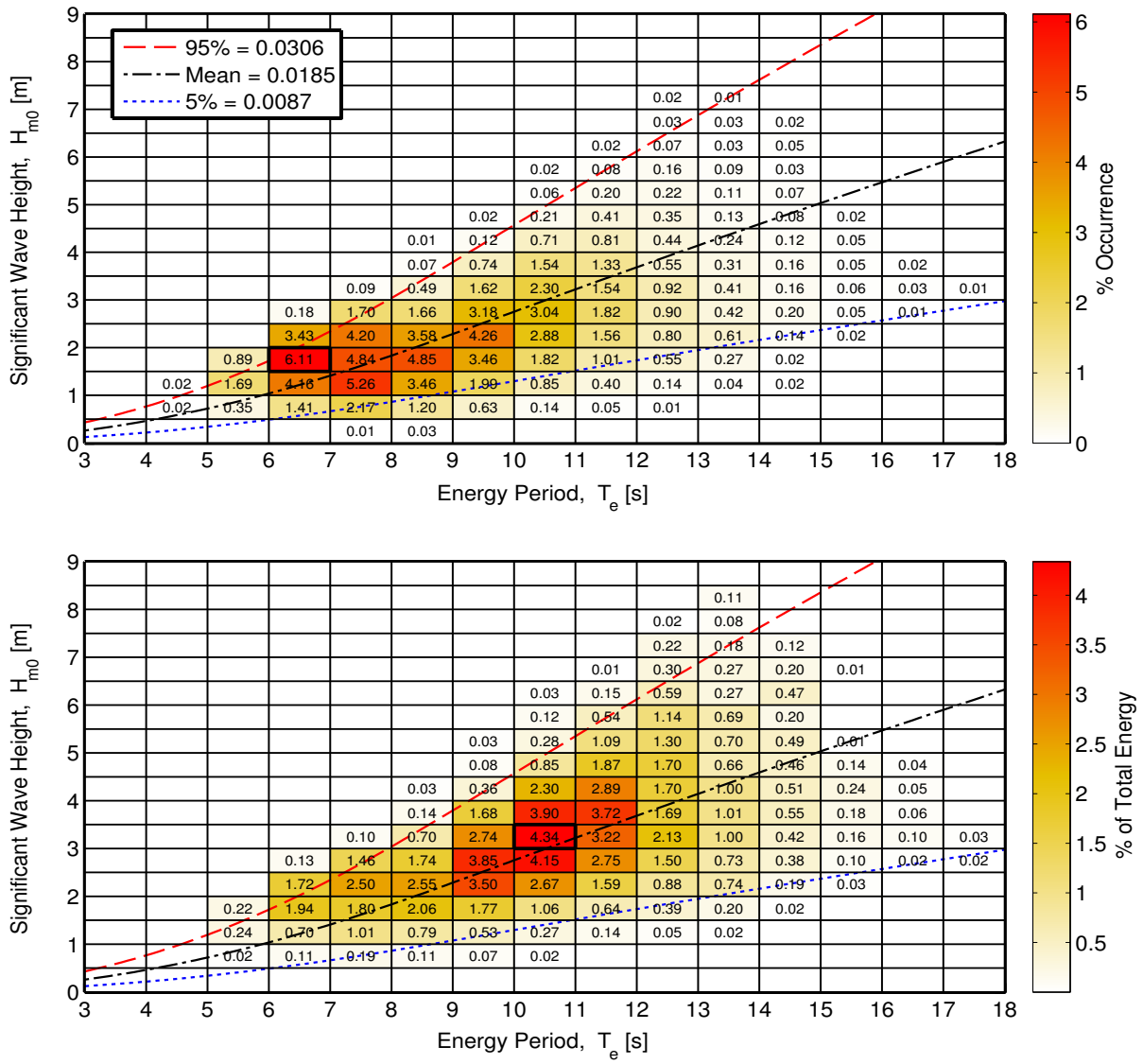

Figure 111: Joint probability distribution of sea states for the Humboldt Site. The top figure is frequency of occurrence and the bottom figure is percentage of total energy, where total energy in an average year is 282,600 kWh/m.

10.4.2. IEC TS Parameters

The monthly means of the six IEC TS parameters, along with the 5^{th} and 95^{th} percentiles, are shown in Figure 112. The values in the figure are summarized in Table 14 in Appendix C.

Monthly means of the omnidirectional wave power, J, significant wave height, H_{m0}, and energy period, T_e, show the greatest seasonal variability compared to the other parameters. Values are largest and vary the most during the winter months. These observations are consistent with the relationship between wave power density, significant wave height and energy period, where wave power density, J, is proportional to the energy period, T_e, and

the square of the significant wave height, H_{m0}.

The direction of maximum directionally resolved wave power (defined as the direction from which waves arrive in degrees clockwise from north), θ_j, is fairly consistent from west/northwest, and varies slightly between seasons. Seasonal variation of the spectral width, ϵ_0, and directionality coefficient (larger values indicate low directional spreading), is much less than the other parameters and barely discernable. Monthly means for ϵ_0 remain nearly constant between 0.3 and 0.35. Similarly, monthly means for d_θ remain nearly constant at ∼0.93.

In summary, the waves at the Humboldt Site, from the perspective of monthly means, have a fairly consistent spectral width, are predominantly from the west/northwest, and exhibit a wave power that has a narrow directional spread.

Wave roses of wave power and significant wave height, presented in Appendix C, Figure 164 and Figure 165, also show the predominant direction of the wave energy at the Humboldt Site, with small shifts to the north and west. Figure 164 shows two dominant direction sectors from west/northwest: 285° and 300°. Along the first direction sector, 285°, the omnidirectional wave power density is at or below 35 kW/m approximately 19% of the time, and greater than 35 kW/m about 15% of the time. Along the second direction sector, 300°, the omnidirectional wave power density is at or below 35 kW/m approximately 27% of the time, but greater than 35 kW/m about 9% of the time.

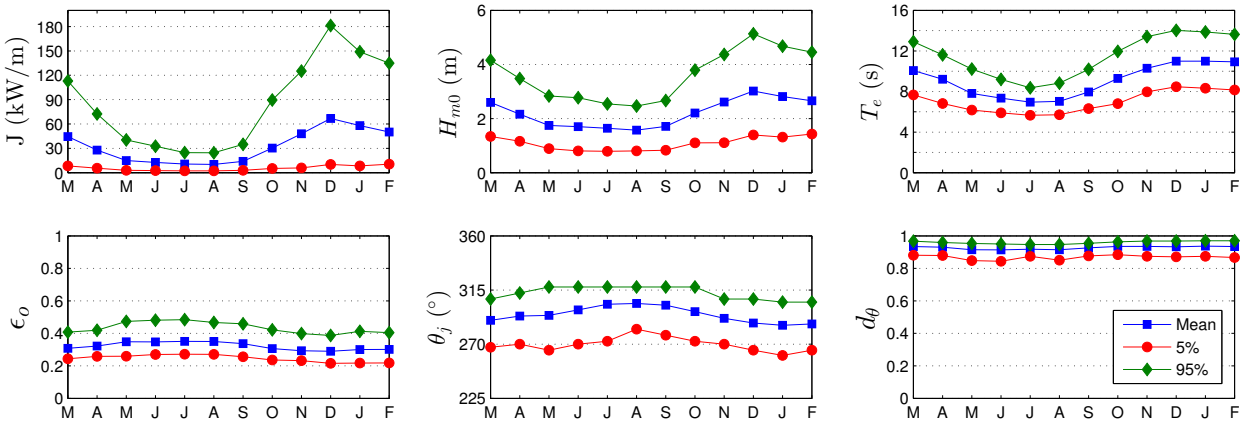

Figure 112: The average, 5th and 95th percentiles of the six parameters at the Humboldt site.

Monthly means, however, smear the significant variability of the six IEC parameters over small time intervals as shown in plots of the parameters at 1-hour intervals in Figure 113 for a representative year. While seasonal patterns described for Figure 112 are still evident, these plots show how sea states can vary abruptly at small time scales with sudden changes, e.g., jumps in the wave power as a result of a storm.

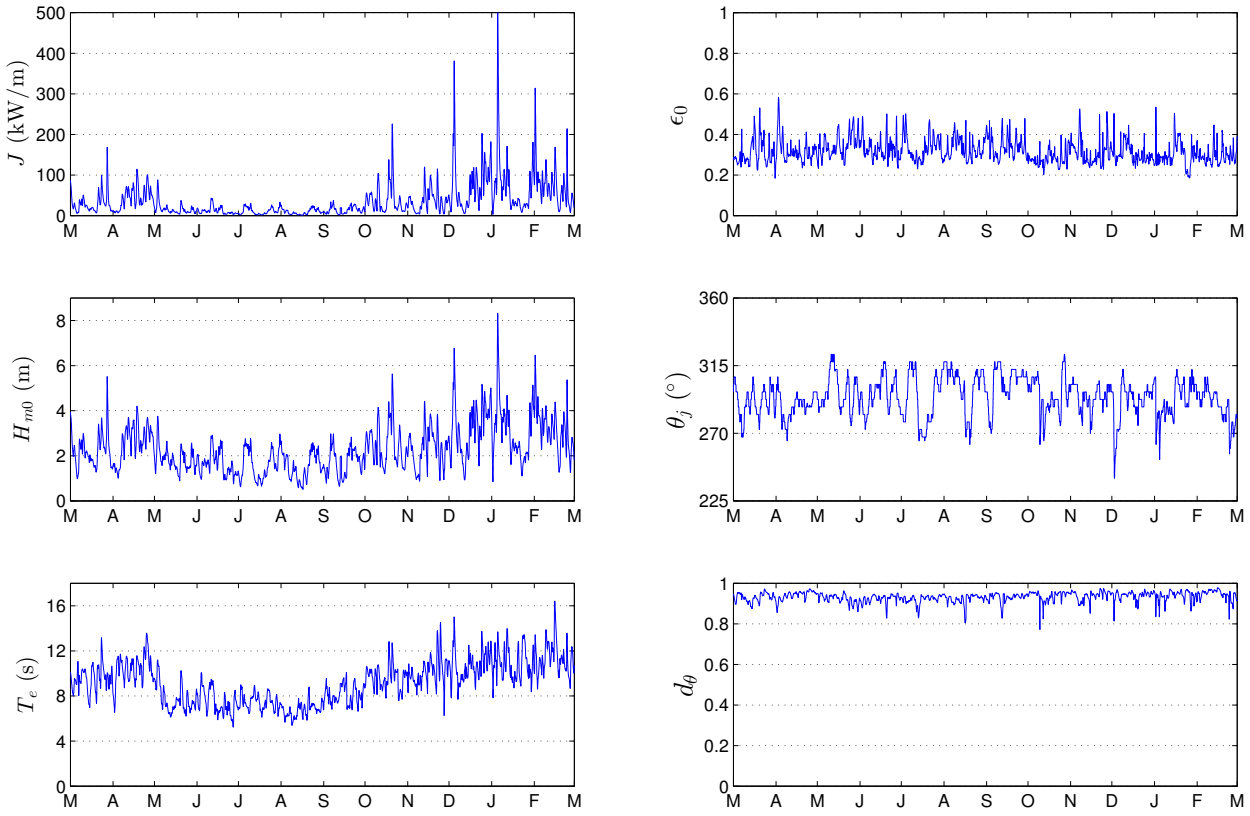

Figure 113: The six parameters of interest over a one-year period, March 2007 – February 2008 at the Humboldt site.

10.4.3. Cumulative Distributions

Annual and seasonal cumulative distributions (a.k.a., cumulative frequency distributions) are shown in Figure 114. Note that spring is defined as March - May, summer as June - August, fall as September - November, and winter as December - February. The cumulative distributions are another way to visualize and describe the frequency of occurrence of individual parameters, such as H_{m0} and T_e. A developer could use cumulative distributions to estimate how often they can access the site to install or perform operations and maintenance based on their specific device, service vessels, and diving operation constraints. For example, if significant wave heights need to be less than or equal to 1 m for installation and recovery, according to Figure 114, this condition occurs about 6% of the time on average within a given year. If significant wave heights need to be less than or equal to 2 m for emergency maintenance, according to Figure 114, this condition occurs about 48% of the time on average within a given year. Cumulative distributions, however, do not account for the duration of a desirable sea state, or weather window, which is needed to plan deployment and servicing of a WEC device at a test site. This limitation is addressed with the construction of weather window plots in the next section.

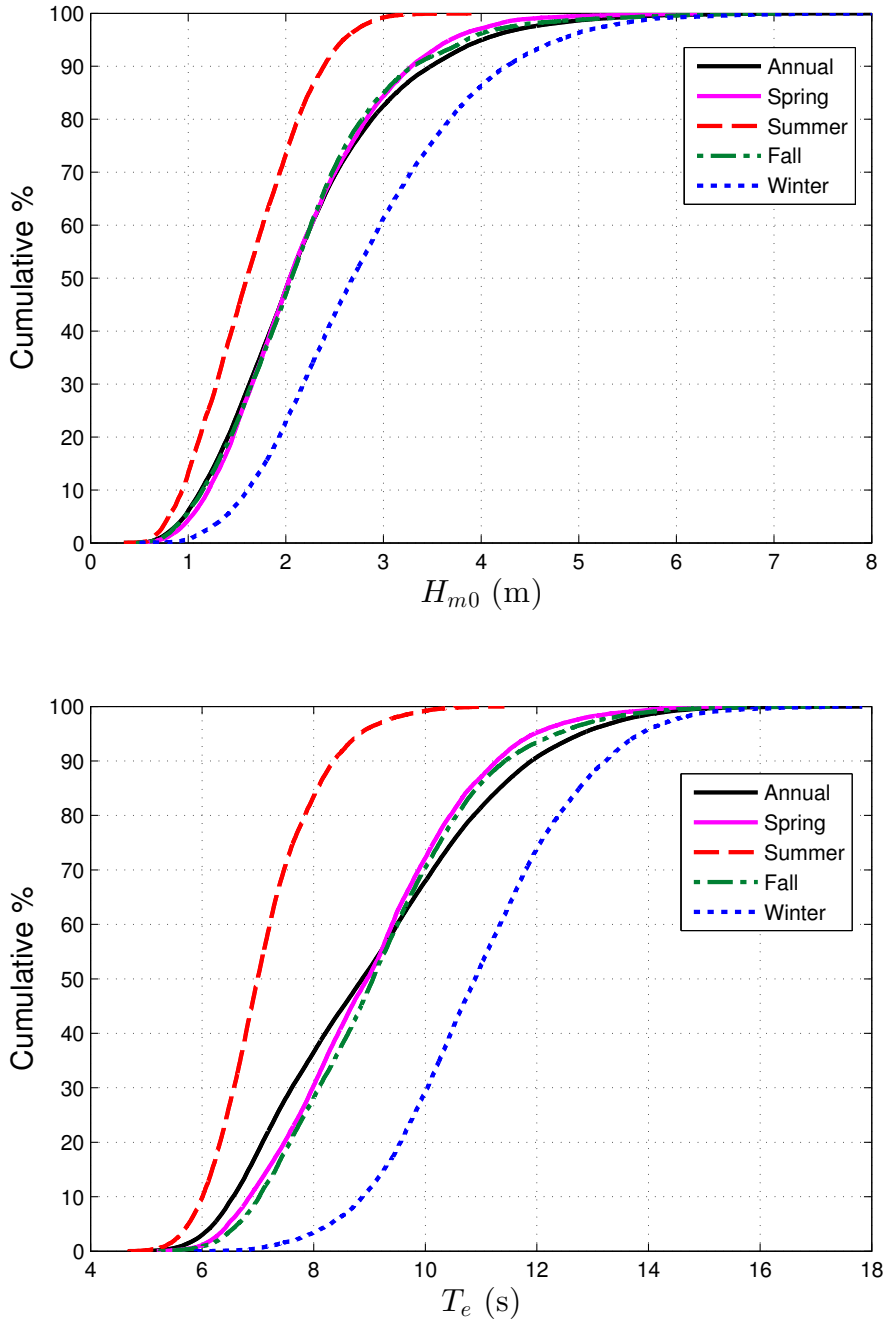

Figure 114: Annual and seasonal cumulative distributions of the significant wave height (top) and energy period (bottom) at the Humboldt site.

10.4.4. Weather Windows

Figure 115 shows the number of weather windows at the Humboldt Site, when significant wave heights are at or below some threshold value for a given duration, for an averaged winter, spring, summer, and fall. In these plots, each occurrence lasts a duration that is some multiple of 6-hours. The minimum weather window is, therefore, 6-hours in duration,

and the maximum is 96-hours (4 days). The significant wave height threshold is the upper bound in each bin and indicates the maximum significant wave height experienced during the weather window. Note that the table is cumulative, so, for example, an occurrence of $H_{m0} \leq 1m$ for at least 54 consecutive hours in the fall is included in the count for 48 consecutive hours as well. In addition, one 12-hour window counts would count as two 6-hour windows. It is clear that there are significantly more occurrences of lower wave heights during the summer than winter, which corresponds to increased opportunities for deployment or operations and maintenance.

Weather window plots provide useful information at test sites when planning schedules for deploying and servicing WEC test devices. For example, if significant wave heights need to be less than or equal to 1 m for at least 12 consecutive hours to service a WEC test device at the Humboldt Site with a given service vessel, there would be, on average, twenty weather windows in the summer, but only one in the winter. When wind speed is also considered, Figure 116 shows the average number of weather windows with the additional restriction of wind speed, $U < 15$ mph. Note that wind data was not available from the hindcast, so data from CFSR was used (see Section 2.3). For shorter durations (6- and 12-hour windows), daylight is necessary. Windows with U <15 mph and only during daylight hours are shown in Figure 117. Daylight was estimated as 5am – 10pm Local Standard Time (LST).

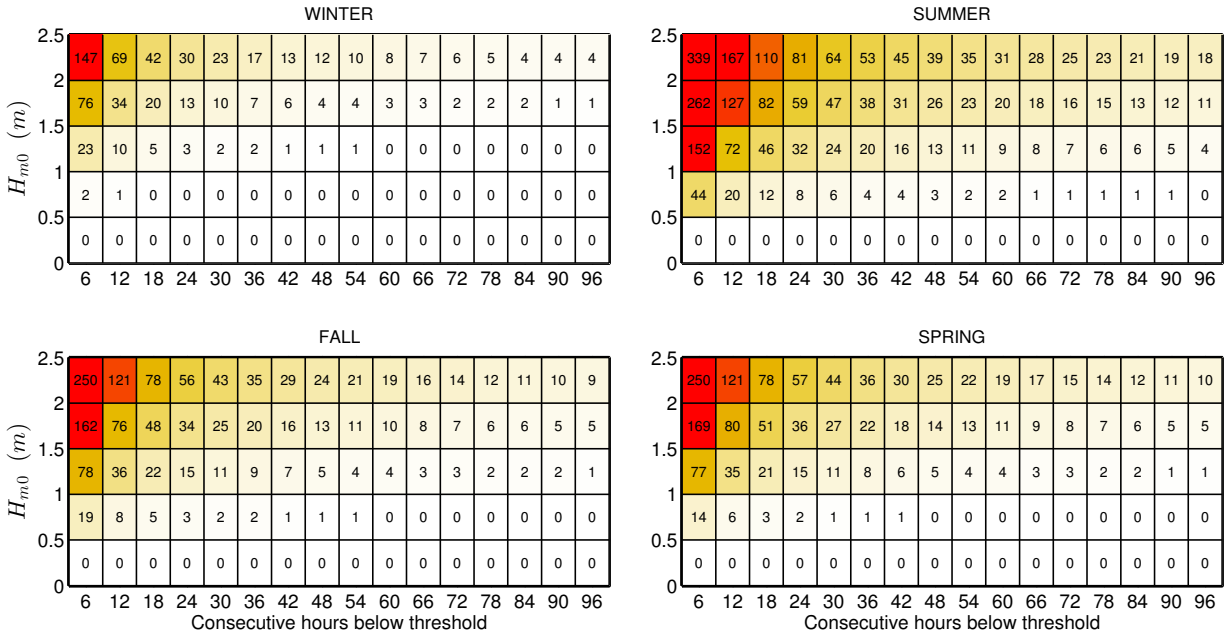

Figure 115: Average cumulative occurrences of wave height thresholds (weather windows) for each season at the Humboldt Site. Winter is defined as December - February, spring as March - May, summer as June - August, and fall as September - November.

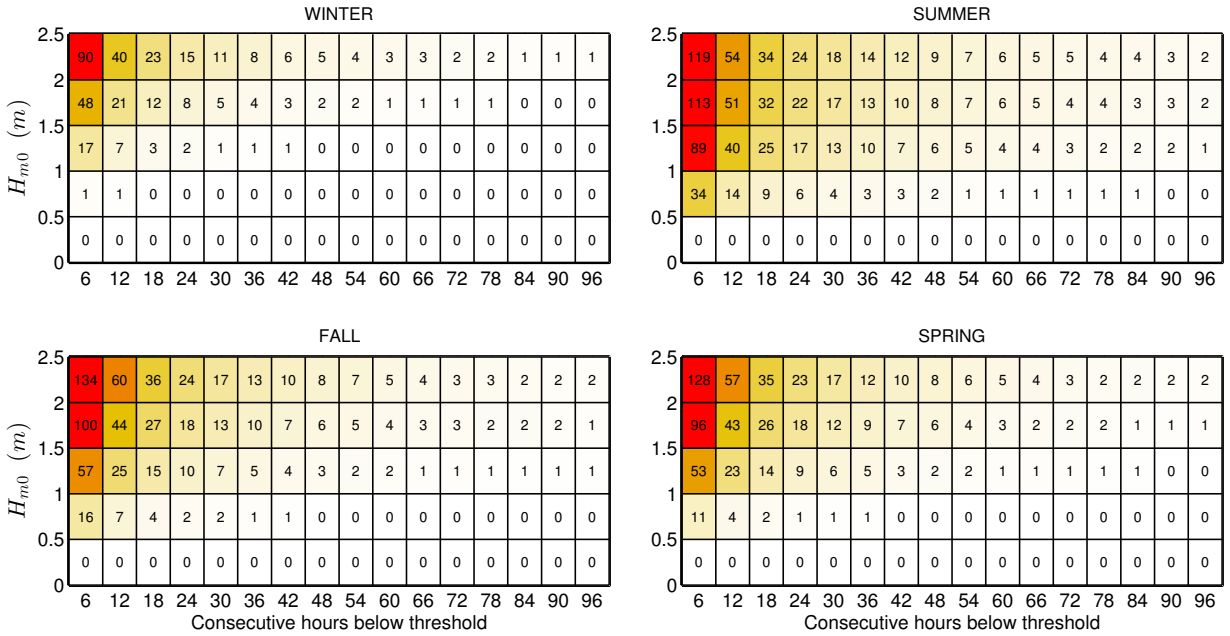

Figure 116: Average cumulative occurrences of wave height thresholds (weather windows) for each season at the Humboldt Site with an additional restriction of $U < 15$ mph.

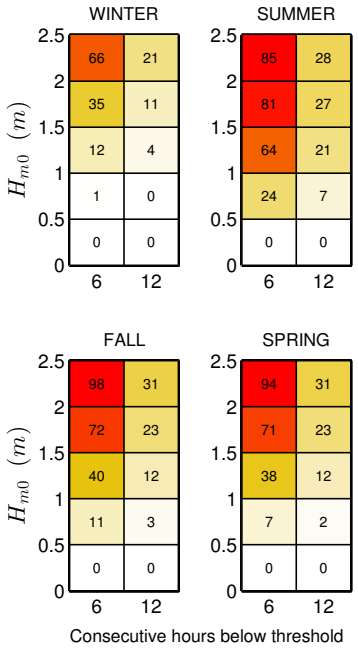

Figure 117: Average cumulative occurrences of wave height thresholds (weather windows) for 6- and 12-hour durations with $U < 15$ mph and only during daylight hours (5am – 10pm LST) at the Humboldt Site.

10.4.5. Extreme Sea States

The modified IFORM was applied using CDIP128 / NDBC46212 to generate the 100-year environmental contour for the Humboldt Site shown in Figure 118. Selected sea states along this contour are listed in Appendix H, Table 44. As stated in Section 1.2, environmental contours are used to determine extreme wave loads on marine structures and design these structures to survive extreme sea states of a given recurrence interval, typically 100-years. For the Humboldt Site, the largest significant wave height estimated to occur every 100-years, is approximately 10.9 m, and has an energy period of about 17.8 s. However, significant wave heights lower than 10.9 m, with energy period less than or greater than 17.8 s, listed in Appendix H, Table 44, could also compromise the survival of the WEC test device under a failure mode scenario in which resonance occurred between the incident wave and WEC device, or its subsystem. For comparison, 50- and 25-year return period contours are also shown in Figure 118. The largest significant wave height on the 50-year contour is 10.4 m with an energy period of about 17.5 s, and on the 25-year contour is 9.9 m and 17.1 s.

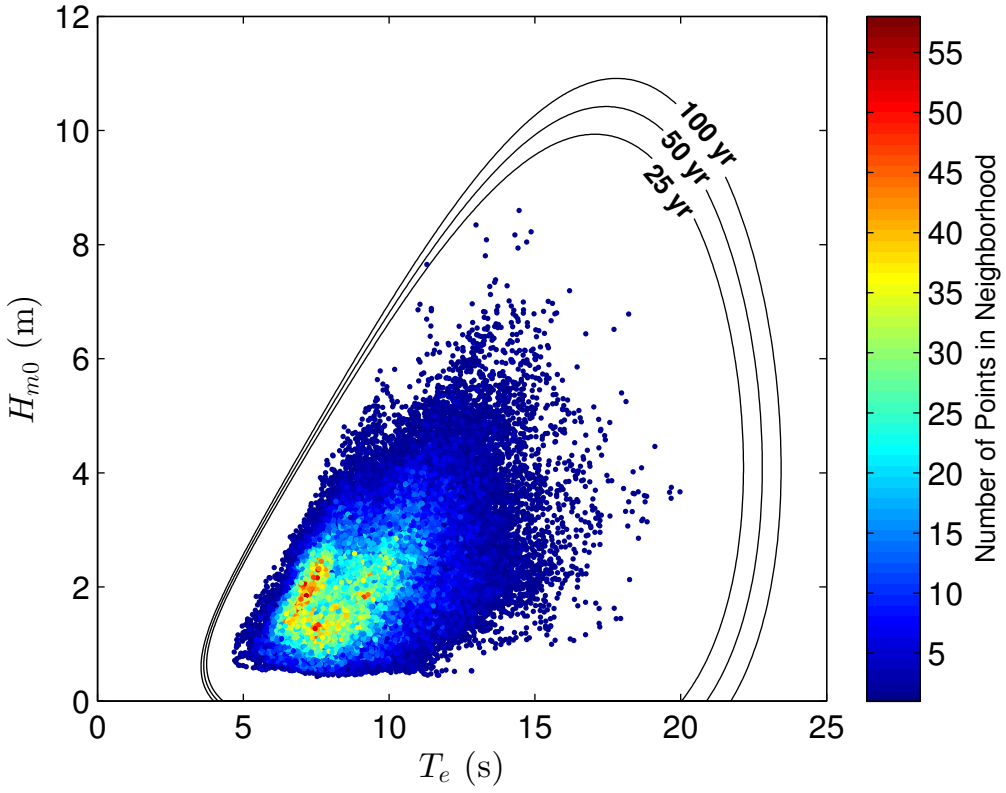

Figure 118: 100-year contour for CDIP128 / NDBC 46212 (2004-2012).

10.4.6. Representative Wave Spectrum

All hourly discrete spectra measured at CDIP128 / NDBC 46212 for the most frequently occurring sea states are shown in Figure 119. The most frequently occurring sea state, which is within the range 1 m $< H_{m0} <$ 1.5 m and 7 s $< T_e <$ 8 s, was selected from a JPD similar to Figure 36 in Section 5.4.1, but based on the CDIP128 / NDBC46212 buoy data. As a result, the JPD, and therefore the most common sea states, generated from buoy data are slightly different from that generated from hindcast data. For example, the most frequently occurring sea state for the JPD generated from hindcast data is a half-meter higher on bounds for H_{m0} (1.5 m $< H_{m0} <$ 2 m) and one second lower for T_e (6 s $< T_e <$ 7 s). Often several sea states will occur at a very similar frequency, and therefore plots of hourly discrete spectra for several other sea states are also provided for comparison. Each of these plots includes the mean spectrum and standard wave spectra, including Bretschneider and JONSWAP, with default constants as described in 2.2.

For the purpose of this study, the mean spectrum is the 'representative' spectrum for each sea state, and the mean spectrum at the most common sea state, shown in Figure 44 (bottom-left plot), is considered the 'representative' spectrum at the site. The hourly spectra vary considerably about this mean spectrum, but this is partly reflective of the bin size chosen for H_{m0} and T_e. Comparisons of the representative spectra in all plots with the Bretschneider and JONSWAP spectra illustrate why modeled spectra with default constants, e.g., the shape

parameter $\gamma = 3.3$ for the JONSWAP spectrum, should be used with caution. Using the constants provided in Section 2.2, the Bretschneider spectra are, at best, fair representations of the mean spectra in Figure 119. If these modeled spectra were to be used at this site, it is recommended that the constants undergo calibration against some mean spectrum, e.g., the representative spectrum constructed here. Using the constants provided in Section 2.2, the Bretschneider spectra are fair representations of the mean spectra in Figure 119, however it does not capture the bimodal nature of the spectra. The mean measured spectra is the best representation of the conditions, however, if these modeled spectra were to be used at this site, it is recommended that the constants undergo calibration against some mean spectrum, e.g., the representative spectrum constructed here. A better alternative may be to explore other methods or spectral forms to describe bimodal spectra (e.g., Mackay 2011) if it is known that the shape is not unimodal.

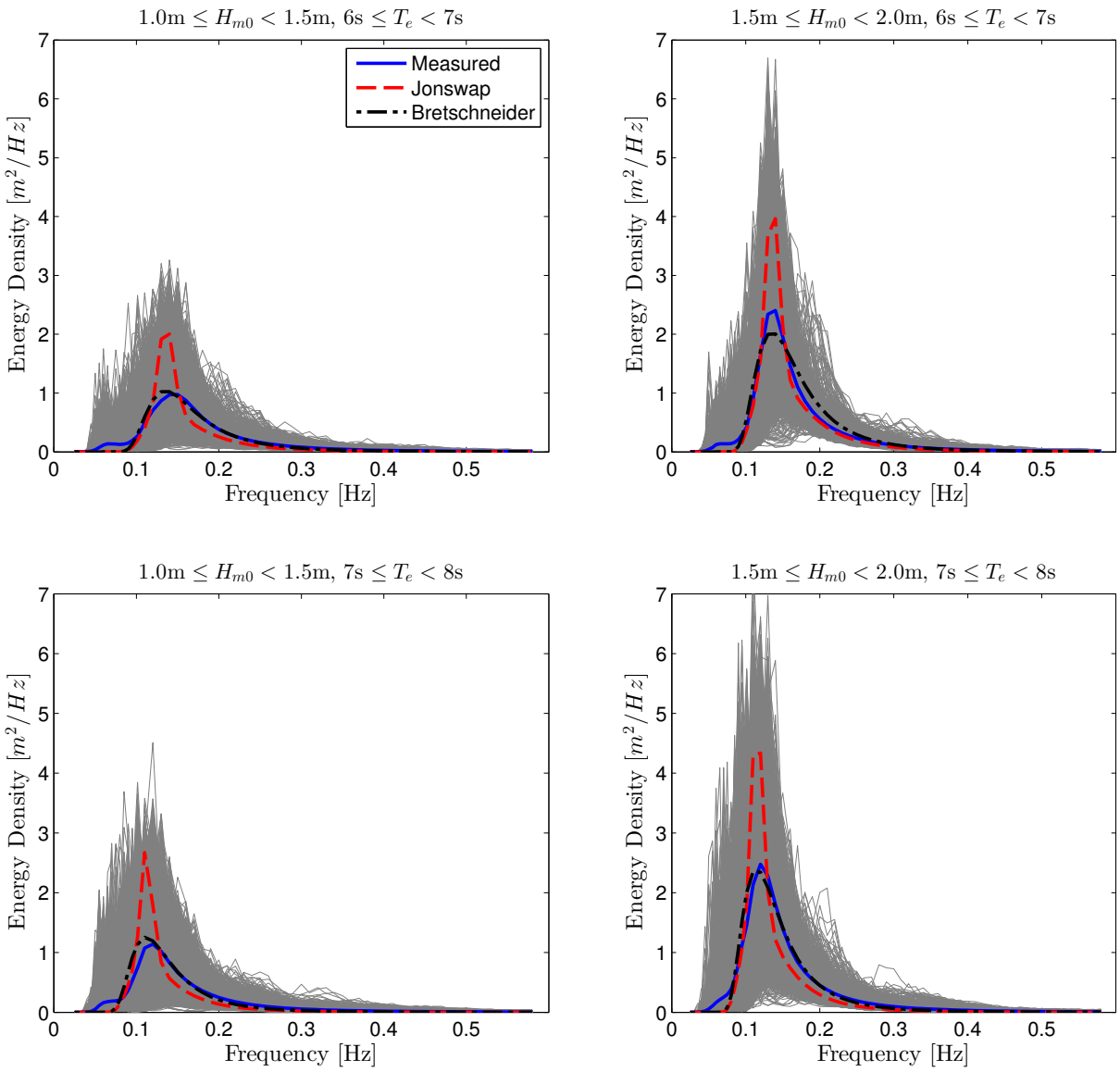

Figure 119: All hourly discrete spectra and the mean spectra measured at CDIP128 / NDBC 46212 within the sea state listed above each plot. The JONSWAP and Bretschneider spectra are represented by red and black dotted lines, respectively.

11. SUMMARY AND CONCLUSIONS

This study provides a comprehensive characterization of eight U.S. WEC test sites. It includes important information on test site infrastructure and services, and catalogues detailed met-ocean data and information derived from numerous data sources. Although there are some differences in the quality of the data sources, e.g., the location of the buoy observations with respect to the test site, and the period of record of the hindcast or buoy observations, the data are processed using uniform and consistent methods. The characterization results, therefore, allow reasonable comparisons between the wave resource characteristics among the different test sites, and selection of test sites that are most suitable for a given device or current testing needs and objectives.

Plots useful for designing WEC test devices include the JPDs, seasonal variation of the six IEC bulk parameters, representative wave spectra, and environmental contours (extreme sea states). They also provide a useful and comprehensive summary of the wave climate and wave energy resource. Cumulative distributions and weather windows can aid in planning WEC deployments and servicing schedules based on the requirements of the service vessel.

The characterization results also allow assessment of the opportunities and risks of testing at each site, how they vary seasonally, and how they can change abruptly within a matter of hours or days. Large waves, associated with both normal and extreme sea states, provide opportunities for testing full scale WEC devices, but they can increase the challenges and risks of testing at the site. These include reduced access to the test device, for deployment or operation and maintenance, and increased risk of damaging or destroying the test device.

NETS is a test site offshore of Newport, OR, where the average annual omnidirectional wave power is 36.8 kW/m. The wave climate at the site varies significantly by season. Calmer seas (lower significant wave heights and energy periods) occur in the summer, while energetic seas occur in the winter, dominated by swells further away in the North Pacific. Larger wave heights occur in the winter months, with a number of events each year exceeding 7 m, and some severe storms producing significant wave heights over 10 m. There are significantly more weather windows that would allow for deployment, and operations and maintenance, in the summer than any other season. Winter would provide opportunities for survival testing for devices at high TRL levels.

WETS is a test site offshore of Oahu, HI, where the average annual omnidirectional wave power is 14.3 kW/m at the 80 m berth. The wave climate varies seasonally, but with less variability than the Pacific Northwest. Calmer seas occur during the summer, produced by year-round trade winds from the northeast, while more energetic seas occur in the winter made up of both wind waves and swell from the North Pacific. Year-round testing has been done at the site because significant wave heights rarely exceed 3 m in the winter. Weather windows are higher in summer, but with less of a difference from winter as other sites, and there are relatively few longer weather windows that might be appropriate for deployment. However, shorter weather windows (opportunities for operations and maintenance),

especially for H_{m0} limits of 1.5 m or more remain high throughout the year.

The Jennette's Pier Wave Energy Test Site is offshore of Nags Head, NC, where the average annual omnidirectional wave power is 6.08 kW/m at 12.6 m depth. The wave climate varies seasonally, but with less variability than the Pacific Northwest. Calmer seas occur during the summer, while more energetic seas occur in the winter. Significant wave heights rarely exceed 3 m, however there are some instances greater than 5 m. Weather windows are high throughout the year due to the lower wave heights, including longer windows that might be appropriate for deployment. There are significantly more weather windows in the summer than winter.

The USACE FRF is offshore of Duck, NC, where the average annual omnidirectional wave power is 3.29 kW/m at 4.8 m depth, although areas in state waters up to depths of approximately 25 m are available for testing. The test site has similar characteristics to the Jennette's Pier Wave Energy Test Site, with calmer seas during the summer, and more energetic seas in the winter. Significant wave heights rarely exceed 3 m at the 4.8 m depth location, and would not typically exceed 5 m at depths available for testing. Similarly to the Jennette's Pier site, weather windows are high throughout the year, including longer windows that might be appropriate for deployment. There are significantly more weather windows in the summer than winter.

The PMEC Lake Washington test site can be considered a proof of concept or 'nursery' site, where the average annual omnidirectional wave power is 0.04 kW/m. The wave climate varies by season, with calm conditions in the summer due to weak northerly winds and more energetic conditions in the winter due to strong southerly winds. The climate is event driven by local wind, and there are periods of very low waves throughout the year. There are no occurrences of significant wave height greater than 1 m, so it is assumed there are ample opportunities for deployment and mainteance in any season, depending on wind restrictions and competing uses of the area in the lake.

SETS is a potential test site located west of NETS, in slightly deeper water depths (58-75 m), where the average annual omnidirectional wave power is 40.7 kW/m. The characteristics are very similar to NETS, however the wave power is greater and there is slightly more directional spreading. Larger wave heights occur in the winter months, with a number of events each year exceeding 8 m. Similarly to NETS, there are significantly more weather windows that would allow for deployment, and operations and maintenance, in the summer than any other season. Winter would provide opportunities for survival testing for devices at high TRL levels.

The CalWave proposed Central Coast WEC Test Site at Vandenberg Air Force Base includes several options for berth locations, although this catalogue focuses on two potential offshore siting alternatives, the 'South', and 'South by Southeast' sites, which are located outside state waters. The average annual omnidirectional wave power is 39.9 kW/m at the South site and 31.4 kW/m at the South by Southeast site. The wave climate at the site varies significantly by season. Calmer seas occur in the summer, while energetic seas occur in the winter, dominated by swells further away in the North Pacific. Typically the site experiences low

directional spread in the waves (nearly unidirectional), however there are occasional swells from the south/southwest that increase the directional spreading. There are significantly more weather windows that would allow for deployment, and operations and maintenance, in the summer than any other season. Depending on restrictions for deployment, finding a suitable weather window may be difficult given that there are, on average, no windows longer than 18 hours for significant wave heights less than 1 m. Winter could provide opportunities for survival testing for devices at high TRL levels.

The Humboldt site is a potential test or commercial deployment site, where the average annual omnidirectional wave power is 32.2 kW/m. Similarly to NETS, the wave climate varies significantly by season with calmer wind waves in the summer and much more energetic seas dominated by swell in the winter. A small percentage of sea states exceed 7 m each winter. The Humboldt Site exhibits the very low directional spreading (nearly unidirectional waves). Similarly to SETS, NETS, and the CalWave Central Coast site, winter storms can be severe at Humboldt, with significant wave heights exceeding 5 m approximately 5% of the time in December.

With the exception of the Lake Washington site, wave direction at the sites generally does not align with the local wind direction because the waves are associated with swells and far-field winds, and they tend to align with the bathymetric contours as they approach shore. However, at most of the sites there is a slight shift towards the wind direction in the summer when swells are less dominant. The local wind data is important for servicing, and is incorporated into the weather windows. It may also be important for determining loads on a low-draft device with a significant above-water profile.

In general, the standard spectra did not match the mean ('representative') measured spectra at the sites very well, and the typical forms of JONSWAP and Bretschneider do not capture bimodal spectra. Therefore these standard spectra should be used with caution, and the mean measured spectra should be considered the best representation of conditions. This should be kept in mind especially for sites that do not exhibit unimodal spectra, and if the measured spectra cannot be used for an analysis, alternative parametric forms should be explored (e.g., Mackay 2011). The wide spread of spectral shapes that occur within a bin of H_{m0} and T_e) should also be considered, and perhaps smaller bin sizes should be used when characterizing the typical spectra.

The monthly mean surface currents at all sites are below 0.4 m/s, well below the IEC TS value of 1.5 m/s for depth-averaged current speed, which is recommended as the threshold beyond which it is important to account for ocean current effects in wave modeling. As surface currents are generally higher than depth-averaged currents, ocean currents at all the sites are not expected to significantly influence the wave dynamics.

REFERENCES

Batten, Belinda. E-mail correspondence to Director of Northwest National Marine Renewable Energy Center, July 24 – September 9, 2014.

Batten, Belinda. Monitoring at North Ocean Test Site, Newport OR. [Powerpoint slides], 2013. Retreived from Tethys: http://tethys.pnnl.gov/sites/default/files/attachments/2013-04-09%201%20Belinda%20Batten.pdf.

Berg, J.C., *Extreme Ocean Wave Conditions for Northern California Wave Energy Conversion Device*, SAND 2011-9304. Sandia National Laboratories, Albuquerque, NM, 2011.

Bitner-Gregersen, E.M, 2001, *Extreme Wave Steepness Estimated from Environmental Contour Plots Contra Traditional Design Practice*, Proceedings of the 20th International Conference on Offshore Mechanics and Arctic Engineering, Rio de Janeiro, Brazil.

Brodtkorb, P.A., Johannesson, P., Lindgren, G., Rychlik, I., Rydén, J. and Sjö, E., 2000, *WAFO - a Matlab toolbox for analysis of random waves and loads.* Proceedings of the 10th International Offshore and Polar Engineering conference, Seattle, Vol III, 343-350 p.

Cahill, B.G., and Lewis, A.W., 2011, *Wave Energy Resource Characterization of the Atlantic Marine Energy Test Site.* Proceedings of the 9th European Wave and Tidal Energy Conference, Southampton, United Kingdom.

Cahill, B.G., and Lewis, A.W., 2013, *Wave energy resource characterization of the Atlantic Marine Energy Test Site*, International Journal of Marine Energy 1, 3-15 p.

Chakrabarti, S.K., 1987, *Hydrodynamics of offshore structures.* WIT Press / Computational Mechanics, UK / Germany.

Coast and Harbor Engineering, 2015, Lake Washington Wave Energy Resource Assessment – Wave Energy Converter (WEC) Test Site, Technical Report.

Coastal Data Information Program, "Station 098-Mokapu Point, HI." Photo taken November 18, 2013. http://cdip.ucsd.edu/?ximg=search&xsearch=098&xsearch_type=Station_ID.

Coastal Data Information Program, "Station 198-Kaneohe Bay, HI." Photo taken November 18, 2013. http://cdip.ucsd.edu/?nav=historic&sub=data&units=metric&tz=UTC&pub=public&stn=198&stream=p1&xitem=stn_gallery3.

Coastal Data Information Program, "Station 192 - Oregon Inlet, NC." Photo taken July 18, 2013. http://cdip.ucsd.edu/?ximg=search&xsearch=192&xsearch_type=Station_ID.

D'Asaro, E. , J. Thomson, A. Shcherbina, R. Harcourt, M. Cronin, M. Hemer, B. Fox-Kemper, Quantifying upper ocean turbulence driven by surface waves, Geophys. Res. Letters, 41 (2014).

Dallman, A.R., Neary, V.S., Stephenson, M., *Investigation of Spatial Variation of Sea States Offshore of Humboldt Bay, CA Using a Hindcast Model,* SAND2014-18207. Sandia National Laboratories, Albuquerque, NM, 2014.

Davey, T., Venugopal, V., Smith, H., Smith, G., Lawrence, J., Luigi, C., Bertotti, L., Prevosto, M., Girard, F., Holmes, B., *EquiMar D2.7 Protocols for wave and tidal resource assessment,* December 2010.

Department of the Navy, *Wave Energy Test Site: Final Environmental Assessment,* Prepared by Alan Suwa, Caroleen Toyama, Jeffrey Fong, Jackie Sanehira, Sean Hanser, Kate Winters, Justin Fujimoto, T.A.F.,Thomas A. Fee, Gail Renard, Corlyn Olson Orr and John Clark, Marine Corps Base Hawaii: January 2014.

De Visser, A., and Vega, L.A., *"Wave Energy Test Site,"* Proceedings of the 7th Annual Global Marine Renewable Energy Conference, April 15-18, 2014.

Det Norske Veritas, 2005, *Guidelines on design and operation of wave energy converters.* Det Norske Veritas, The Carbon Trust, 2005.

Det Norske Veritas, 2014, *Environmental Conditions and Environmental Loads.* Recommended Practice DNV-RP-C205.

Department of Transportation, 2012, *Port of Humboldt Bay* Freight Planning Fact Sheet for Caltrans. http://dot.ca.gov/hq/tpp/offices/ogm/CFMP/Fact_Sheets/Seaports/Humboldt.pdf.

Dooher, B.P., Cheslak, E., Booth, R., Davy, D., Faraglia, A., Caliendo, I. Morimoto, G. and Herman, D. 2011, *PG&E WaveConnect Program Final Report.* DOE/GO/18170-1. Pacific Gas and Electric Company, San Francisco, CA, December 2011. doi: 10.2172/1032845.

Eckert-Gallup, A.C., Sallaberry, C.J., Dallman, A.R., Neary, V.S., *Modified Inverse First Order Reliability Method (I-FORM) for Predicting Extreme Sea State Estimation,* SAND2014-17550. Sandia National Laboratories, Albuquerque, NM, September 2014.

Eckert-Gallup, A.C., Sallaberry, C.J., Dallman, A.R., Neary, V.S., 2015, *Application of principal component analysis (PCA) and improved joint probability distributions to the inverse first-order reliability method (I-FORM) for predicting extreme sea states,* Ocean Engineering, In revision.

Efron, B., Tibshirani, R.J., 1993, *An Introduction to the Bootstrap - Monographs on Statistics and Applied Probability,* Chapman & Hall, New York.

Feld, G., Mork, G., 2004, *A Comparison of Hindcast and Measured Wave Spectra Based on a Directional Spectral Fitting Algorithm,* Proceedings of the 8th International Workshop on Wave Hindcasting & Forecasting, North Shore, Oahu, HI, November 14-19.

Folley, M., Cornett, A., Holmes, B., Lenee-Bluhm, P., Liria, P., 2012, *Standardising resource assessment for wave energy converters,* Proceedings of the 4th Annual International

Conference on Ocean Energy, Dublin.

GarcíaMedina, G., Özkan-Haller, H.T., Ruggiero, P., 2014, *Wave resource assessment in Oregon and southwest Washington, USA*, Renew Energy 64, 203-214 p.

Google Earth, *Duck, NC,* 36°10' N 75°44' W. Data from SIO, NOAA, U.S. Navy, NGA, GEBCO. Image from Landsat. Accessed July 22, 2015.

Google Earth, *Humboldt Bay,* 41°00'07.85" N 124°16'03.18" W. Data from SIO, NOAA, U.S. Navy, NGA, GEBCO, LDEO-Columbia, NSF. Image from Landsat. Accessed July 16, 2014.

Google Earth, *Jennette's Pier, NC,* 35°55' N 75°36' W. Data from SIO, NOAA, U.S. Navy, NGA, GEBCO. Image from Landsat. Accessed July 22, 2015.

Google Earth, *Kaneohe Bay,* 21°27'50.53" N 157°44'19.06"W. Data from USGS. Image from USGS. Accessed July 16, 2014.

Google Earth, *Lake Washington,* 47°37' N 122°16' W. Data from SIO, NOAA, U.S. Navy, NGA, GEBCO, MBARI. Image from Landsat. Accessed July 22, 2015.

Google Earth, *Lompoc, CA,* 34°38' N 120°28' W. Image from Landsat. Accessed July 22, 2015.

Google Earth, *Newport, OR,* 44°38' N 124°3' W. Data from SIO, NOAA, U.S. Navy, NGA, GEBCO, MBARI, LDEO-Columbia, NSF. Image from Landsat. Accessed July 22, 2015.

Hasselmann, K., Barnett, T.P., Bouws, E., Carlson H., Cartwright D.E., Enke, K., Ewing J.A., Gienapp, H., Hasselmann, D.E., Kruseman, P., Meerburg, A., Mller, P., Olbers, D.J., Richter, K., Sell, W., Walden, H., 1973, *Measurements of Win-Wave Growth and Swell Decay During the Joint North sea Wave Project (JONSWAP),* Deutschen Hydro-graphischen Institut, No. 12, Hamburg, Germany.

Hawaii National Marine Renewable Energy Center, "Kaneohe Site." April 25, 2013. Accessed July 14, 2014. http://hinmrec.hnei.hawaii.edu/.

IEC TS 62600-101 Ed. 1.0 Marine energy – Wave, tidal and other water current converters – Part 101: Wave energy resource assessment and characterization.

Johnson, E.S., F. Bonjean, G.S.E. Lagerloef, J.T. Gunn, and G.T. Mitchum, 2007, *Validation and Error Analysis of OSCAR Sea Surface Currents.* Journal of Atmospheric and Oceanic Technology 24, 688701 p. doi: 10.1175/JTECH1971.1.

Jouanne, Annette von, Lettenmaier, Terry, and Sean Moran, *Wave Energy Testing Using the Ocean Sentinel Instrumentation Buoy.* Presented at the 1st Marine Energy Technology Symposium, Washington, DC, April 10-11, 2013. http://www.globalmarinerenewable.com/images/wave%20energy%20testing%20using%20the%20ocean%20sentinel%20instrumentation%20buoy.pdf.

Lenee-Bluhm, P., Paasch, R., Özkan-Haller, H.T., 2011, *Characterizing the wave energy*

resource of the US Pacific Northwest. Renew Energy 36, 2106-2119 p.

Lenee-Bluhm, P., 2010, *The Wave Energy Resource of the US Pacific Northwest,* MS Thesis, Oregon State University, http://ir.library.oregonstate.edu/xmlui/handle/1957/16384.

Li, N. and Cheung, K.F., 2014, *Wave Energy Resource Characterization at the US Navy Wave Energy Test Site and Other Locations in Hawai'i.* Technical Report November 2014. http://hinmrec.hnei.hawaii.edu/.

Li, N., Cheung, K.F., Stopa, J.E., Hisao, F., Chen, Y.-L., Vega, L., Cross, P., 2015, *Thirty-four Years of Hawaii Wave Hindcast from Downscaling of Climate Forecast System Reanalysis.* Ocean Modeling, In review.

Mackay, E., 2011. Modeling and description of omnidirectional wave spectra, In: Proceedings of the 9th Europeam Wave and Tidal Conference, Japan.

Nair, B., Shendure, R., Nachlas, J., Gill, A., Murphree, Z., Campbell, J., Challa, V., Thomson, J., Talbert, J., deKlerk, A., Rusch, C. 2013. Low-Cost Utility-Scale Wave Energy Enabled by Magnetostriction. 1st Marine Energy Technology Symposium, April 2013, Washington, D.C.

National Data Buoy Center, "Station 44014 (LLNR 550) - Virginia Beach 64 NM East of Virginia Beach, VA" http://www.ndbc.noaa.gov/station_page.php?station=44014.

National Data Buoy Center, "Station 44095 - Oregon Inlet, NC - 192" http://www.ndbc.noaa.gov/station_page.php?station=44095.

National Data Buoy Center, "Station 46022 (LLNR 500) - Eel River 17 NM WSW of Eureka, CA" http://www.ndbc.noaa.gov/station_page.php?station=46022.

National Data Buoy Center, "Station 46094 - Buoy NH-10 - West of Newport, OR" http://www.ndbc.noaa.gov/station_page.php?station=46094.

National Data Buoy Center, "Station 46212 - Humboldt Bay South Spit, CA (128)" http://www.ndbc.noaa.gov/station_page.php?station=46212.

National Data Buoy Center, "Station 46218 - Harvest, CA (071)" http://www.ndbc.noaa.gov/station_page.php?station=46218.

National Data Buoy Center, "Station 51202 Mokapu Point, HI (098)" http://www.ndbc.noaa.gov/station_page.php?station=51202.

National Data Buoy Center, "Station 51207 Kaneohe Bay, HI (198)" http://www.ndbc.noaa.gov/station_page.php?station=51207.

National Data Buoy Center, "Station MOKH1 1612480 Mokuoloe, HI" http://www.ndbc.noaa.gov/station_page.php?station=mokh1.

National Data Buoy Center, "Station NWPO3 - Newport, OR" http://www.ndbc.noaa.gov/

station_page.php?station=NWPO3.

National Data Buoy Center, "Station PTGC1 - Point Arguello, CA" http://www.ndbc.noaa.gov/station_page.php?station=PTGC1.

National Oceanic Atmospheric Administration, "OSCAR: Ocean Surface Current Analysis-Real Time." Accessed June 26, 2014. http://www.oscar.noaa.gov/index.html.

NNMREC (Northwest National Marine Renewable Energy Center), Oregon State University. "Northwest National Marine Renewable Energy Center." Accessed July 14th, 2014. http://nnmrec.oregonstate.edu/.

NNMREC (Northwest National Marine Renewable Energy Center), Oregon State University. "Northwest National Marine Renewable Energy Center." Accessed March 3rd, 2015. http://nnmrec.oregonstate.edu/.

NNMREC (Northwest National Marine Renewable Energy Center), Oregon State University. "Northwest National Marine Renewable Energy Center – South Energy Test Site." Accessed March 3rd, 2015. http://nnmrec.oregonstate.edu/facilities/pmec-sets.

O'Connor, M, Holmes, B., *EquiMar D4.3 Test Sites Catalogue,* April 2011.

Oregon State University, "Northwest National Marine Renewable Energy Center." Accessed July 14, 2014. http://nnmrec.oregonstate.edu/pmec-facilities.

Office of Coast Survey, *Chart 19357.* National Ocean and Atmospheric Association, printed March 1, 2013, accessed August 1, 2014. http://www.nauticalcharts.noaa.gov/staff/chartpubs.html

Office of Coast Survey, *Chart 18620.* National Ocean and Atmospheric Association, printed February 1, 2012, accessed August 1, 2014. http://www.nauticalcharts.noaa.gov/staff/chartspubs.html.

Office of Coast Survey, *Chart 18622.* National Ocean and Atmospheric Association, printed June 1, 2010, accessed August 1, 2014. http://www.nauticalcharts.noaa.gov/staff/chartspubs.html.

Office of Coast Survey, *Chart 18561.*, National Ocean and Atmospheric Association, printed December 1, 2011, accessed August 1, 2014. http://www.nauticalcharts.noaa.gov/staff/chartspubs.html.

Port of Newport. "South Beach Marina." Accessed July 28, 2014. http://www.portofnewport.com/recreational-marina/.

Port of Toledo, "Yaquina Boatyard." Accessed July 24, 2014. http://portoftoledo.org/yaquina-boatyard/.

Ruggiero, P., Komar, P.D., Allan, J.C., 2010, *Increasing wave heights and extreme value projections: The wave climate of the U.S. Pacific Northwest.* Coastal Engineering, 57:5,

539-552 p.

State of Hawaii Division of Boating and Ocean Recreation, "Heeia Kea Small Boat Harbor." Accessed July 21, 2014. http://state.hi.us/dlnr/dbor/oahuharbors/heeiahrbr.htm.

Saha, Suranjana, and Coauthors, 2010: *The NCEP Climate Forecast System Reanalysis.* Bull. Amer. Meteor. Soc., 91, 1015-1057 p. doi: 10.1175/2010BAMS3001.1

Saha, Suranjana and Coauthors, 2014: *The NCEP Climate Forecast System Version 2.* J. Climate, 27, 2185-2208 p. doi: http://dx.doi.org/10.1175/JCLI-D-12-00823.1.

Stopa, J.E., Filipot, J.-F., Li, N., Cheung, K.F., Chen, Y.-L., Vega, L., 2013, *Wave energy resources along the Hawaiian Island chain,* Renew Energy 55, 305-321 p.

Thomson, J., Observations of wave breaking dissipation from a SWIFT drifter, J. Atmos. & Ocean. Tech., 29, (2012).

Thomson, J. J.R. Gemmrich, and A.T. Jessup, Energy dissipation and the spectral distribution of whitecaps, Geophys. Res. Let., 36 (2009).

UNC Coastal Studies Institute. E-mail correspondence with Billy Edge, Brian Blanton, and Lindsay Dubbs, 2015.

United States Army Corps of Engineers, "Field Research Facility" (FRF). Accessed March 2015. http://www.frf.usace.army.mil/frf.shtml.

United States Army Corps of Engineers Field Research Facility, "Report for station wvrdr430". Accessed March 2015. http://www.frf.usace.army.mil/realtime.shtml?staid=wvrdr430&dirg=1.

U.S. Census Bureau, *Newport (city) Oregon,* State & County QuickFacts, 2012. Retrieved from http://quickfacts.census.gov/qfd/states/41/4152450.html.

Williams, R.B, Davy, D.M., Sheppard, C., Thomson, J., West, A., Toman, W.I, 2015, *Final Report of the Feasibility Study for the California Wave Energy Test Center (CalWavesm) Final Report.* DOE Contract DE-EE0006517. Cal Poly Corporation, Institute of Advanced Technology and Public Policy, California Polytechnic University, San Luis Obispo, California. July 2015.

Winterstein, S.R., Ude, T.C., Cornell, C.A., Bjerager, P., Haver, S., *Environmental Parameters for Extreme Response: Inverse FORM with Omission Factors,* Proceedings of ICOSSAR-93, Innsbruck, Austria, 1993.

Vega, Luis: University of Hawaii, e-mail correspondence, July 23 – August 29, 2014.

DISTRIBUTION:

1	MS 1124	Ann R. Dallman, 6122
1	MS 1124	Vincent S. Neary, 6122
1	MS 0899	Technical Library, 9536 (electronic copy)

Appendix A: PACIFIC MARINE ENERGY CENTER (PMEC): NORTH ENERGY TEST SITE (NETS)

A.1. IEC TS Parameter Values

Table 9: The average, 5^{th} and 95^{th} percentiles of the six parameters at NETS (see Figure 7).

	$J[kW/m]$			$H_{m0}[m]$			$T_e[s]$		
	5%	**Mean**	**95%**	**5%**	**Mean**	**95%**	**5%**	**Mean**	**95%**
March	9.4	52.2	141.6	1.46	2.86	4.75	7.65	9.92	12.80
April	6.5	36.8	96.3	1.16	2.39	4.03	7.65	9.75	12.04
May	3.6	16.1	42.1	0.87	1.71	2.84	7.01	8.76	10.84
June	3.7	12.2	33.6	0.88	1.52	2.68	6.89	8.84	11.39
July	2.3	9.3	19.0	0.73	1.39	2.05	6.72	8.41	10.46
August	2.8	8.7	20.5	0.83	1.33	2.09	6.60	8.45	10.70
September	4.3	18.1	52.7	0.98	1.74	3.04	7.37	9.31	11.78
October	7.8	38.5	106.5	1.26	2.43	4.19	7.86	9.79	12.28
November	9.1	62.4	162.8	1.35	3.09	5.10	7.75	10.05	12.90
December	8.6	69.3	203.0	1.25	3.13	5.45	8.12	10.66	13.95
January	11.3	66.6	173.5	1.43	3.08	5.06	8.19	10.88	14.13
February	11.1	52.4	141.4	1.43	2.77	4.70	8.24	10.70	13.44

	ϵ_0			$\theta_j[^\circ]$			d_θ		
	5%	**Mean**	**95%**	**5%**	**Mean**	**95%**	**5%**	**Mean**	**95%**
March	0.33	0.43	0.54	242.5	276.0	297.5	0.82	0.91	0.96
April	0.33	0.45	0.55	252.5	280.3	297.5	0.79	0.91	0.96
May	0.32	0.43	0.55	247.5	274.6	302.5	0.80	0.89	0.95
June	0.33	0.45	0.59	242.5	272.1	302.5	0.79	0.88	0.94
July	0.34	0.45	0.56	242.5	278.6	302.5	0.75	0.86	0.93
August	0.33	0.44	0.58	252.5	279.0	302.5	0.78	0.86	0.94
September	0.31	0.43	0.57	247.5	280.6	302.5	0.81	0.89	0.95
October	0.30	0.41	0.52	247.5	281.2	302.5	0.84	0.92	0.96
November	0.29	0.41	0.51	247.5	280.2	302.5	0.83	0.92	0.97
December	0.27	0.41	0.53	237.5	276.5	297.5	0.82	0.92	0.97
January	0.28	0.42	0.53	242.5	275.4	297.5	0.85	0.93	0.97
February	0.27	0.41	0.54	237.5	276.8	302.5	0.82	0.92	0.97

A.2. Wave Roses

The annual wave rose of omnidirectional wave power, J, and direction of maximum directionally resolved wave power, θ_j, is shown in Figure 120, and essentially mirrors that for significant wave height, H_{m0}, and θ_j shown in Figure 121.

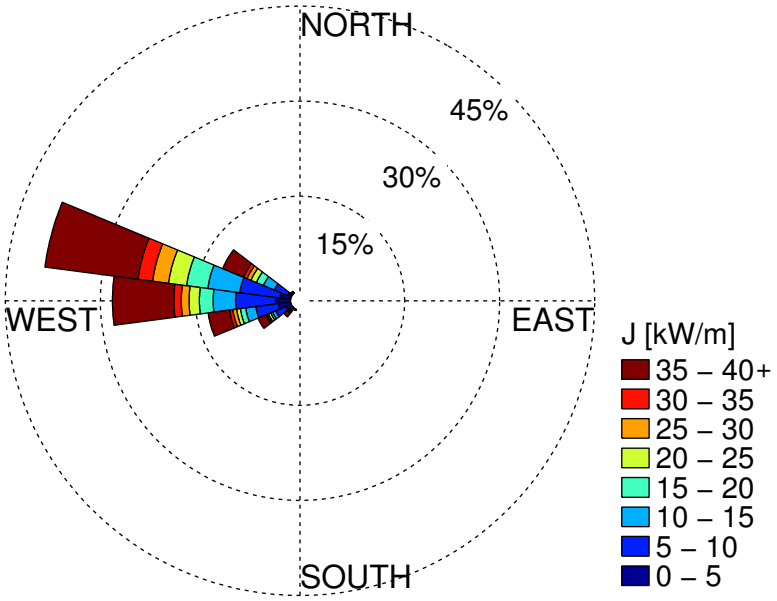

Figure 120: Annual wave rose of omnidirectional wave power and direction of maximally resolved wave power. Values of J greater than 40 kW/m are included in the top bin as shown in the legend.

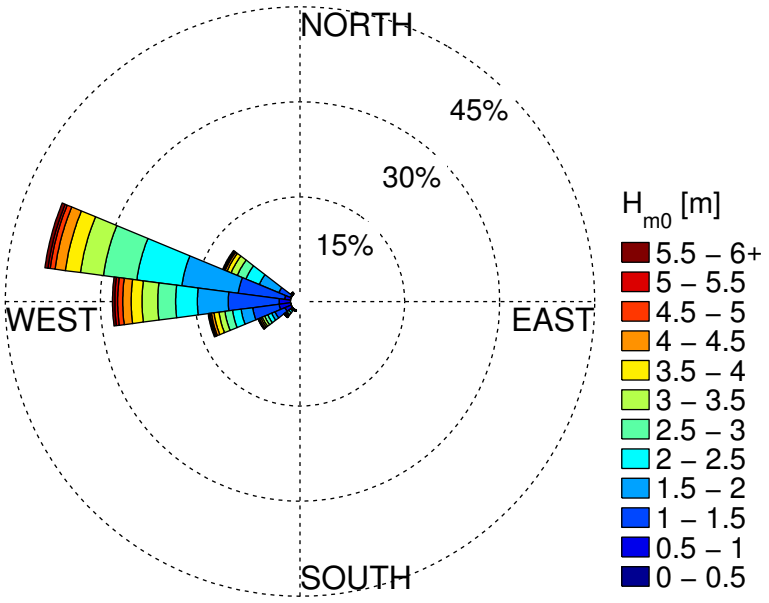

Figure 121: Annual wave rose of significant wave height and direction of maximally resolved wave power. Values of H_{m0} greater than 6 m are included in the top bin as shown in the legend.

A.3. Extreme Sea States

Table 10: Selected values along the 100-year contour for NDBC46050 (see Figure 13).

Significant wave height [m]	Energy period [s]
1	3.80
2	4.58
3	5.32
4	6.00
5	6.64
6	7.25
7	7.83
8	8.39
9	8.95
10	9.50
11	10.07
12	10.65
13	11.27
14	11.94
15	12.71
16	13.66
17	15.14
17.31	16.57
17	18.04
16	19.63
15	20.65
14	21.48
13	22.18
12	22.79
11	23.34
10	23.84
9	24.29
8	24.69
7	25.05
6	25.36
5	25.63
4	25.85
3	26.02
2	26.12
1	26.15

A.4. Wind Data

The wind data for this site (obtained from CFSR), is the mean of magnitude and direction taken at 44.5 N, 124.5 W and 45 N, 124.5 W, which are the nearest data points to NETS. Note that the central location between these two points is approximately 30 km west/northwest of the test site (Figure 1). The average monthly values, along with the 5^{th} and 95^{th} percentiles, of wind are shown in Figure 122. The values are also tabulated in Table 11. The annual and seasonal wind roses are shown in Figure 123.

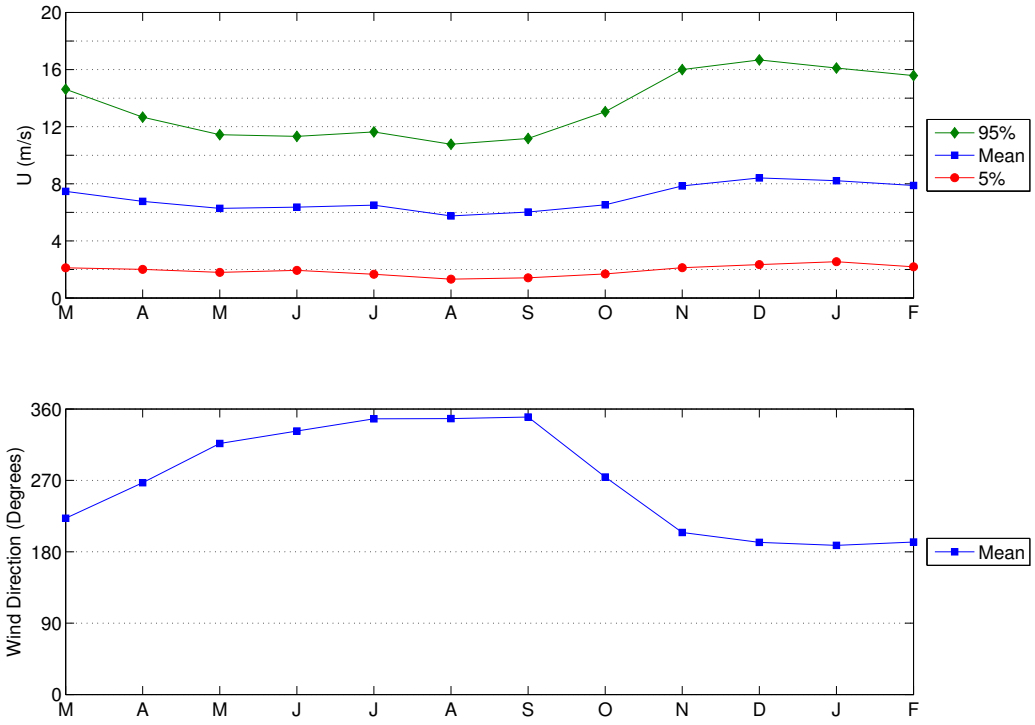

Figure 122: Monthly wind velocity and direction obtained from CSFR data during the period 1/1/1979 to 12/31/2014 at 44.75 N, 124.5 W, located 30 km west/northwest of NETS (Figure 1).

(a)

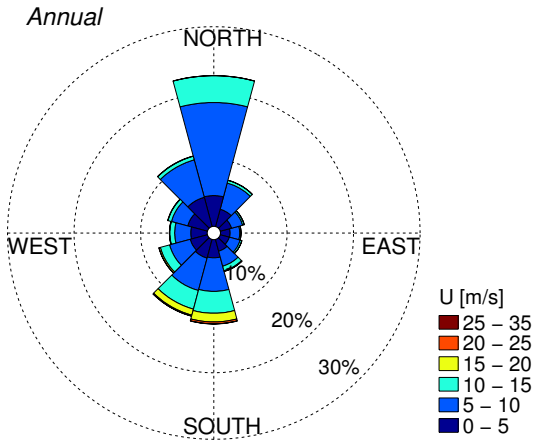

(b)

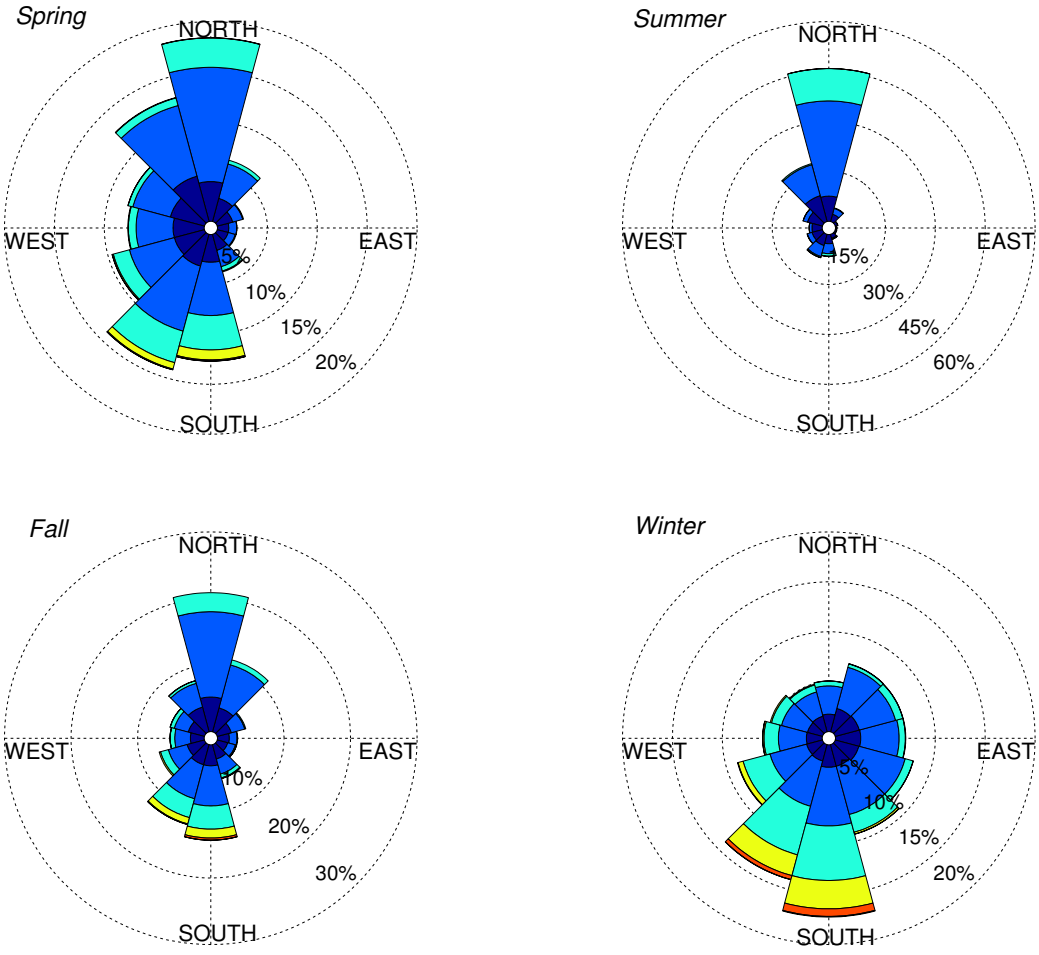

Figure 123: (a) Annual and (b) seasonal wind roses of velocity and direction obtained from CSFR data during the period 1/1/1979 to 12/31/2014. Data taken at 44.75 N, 124.5 W, located approximately 30 km west/northwest of NETS (Figure 1).

Table 11: Monthly wind velocity and direction obtained from CSFR data during the period 1/1/1979 to 12/31/2014 at 44.75 N, 124.5 W, located approximately 30 km west/northwest of NETS.

	$U[m/s]$			$Direction[^\circ]$
	5%	**Mean**	**95%**	**Mean**
March	2.1	7.5	14.6	222
April	2.0	6.8	12.7	267
May	1.8	6.3	11.4	316
June	1.9	6.4	11.3	332
July	1.7	6.5	11.6	348
August	1.3	5.7	10.8	348
September	1.4	6.0	11.2	350
October	1.7	6.5	13.0	274
November	2.1	7.8	16.0	204
December	2.3	8.4	16.7	192
January	2.5	8.2	16.1	188
February	2.2	7.9	15.6	192

A.5. Ocean Surface Current Data

The surface current data (obtained from OSCAR) used for this site is located at 44.5 N, 125.5 W. There is data located closer to the site at 44.5 N, 124.5 W, however the period of record is short (about 2 years). Data from the two years available was compared at both locations. Surface current speeds at 124.5 W are slightly higher in the summer than at 125.5 W, however overall the patterns are similar. Therefore, the data point further out (125.5 W) with the longer period of record (about 20 years) was used for consistency with the other sites. The average monthly values, along with the 5^{th} and 95^{th} percentiles, of current are shown in Figure 124. These data points are listed in Table 12. The annual and seasonal current roses are shown in Figure 125.

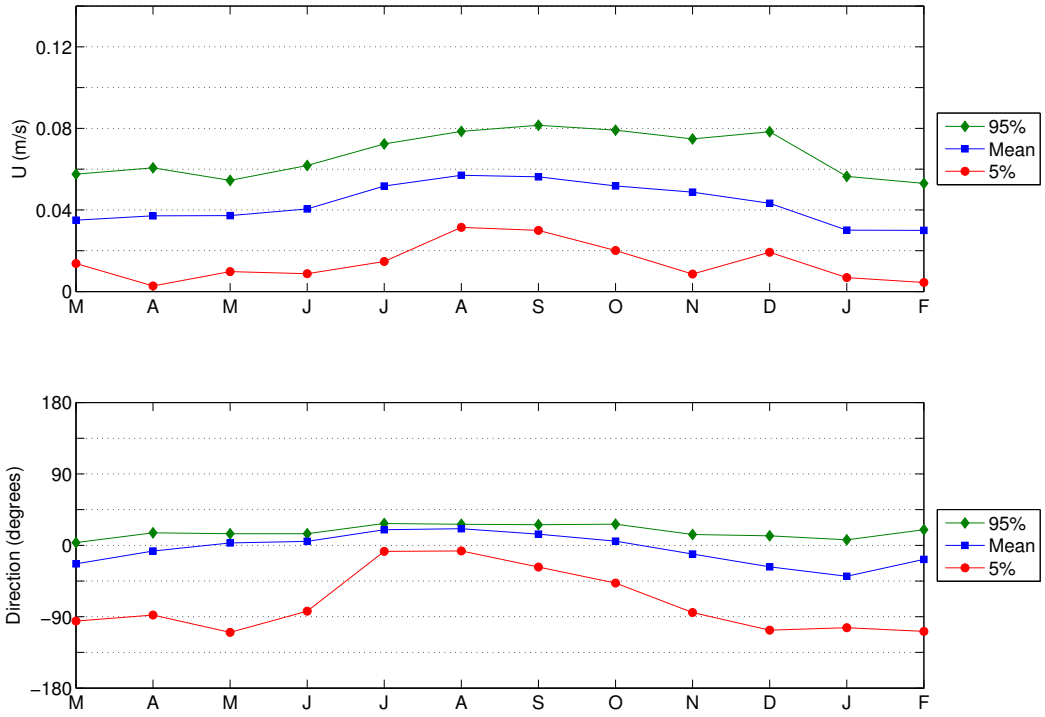

Figure 124: Monthly ocean surface current velocity and direction obtained from OSCAR at 44.5 N, 125.5 W, located approximately 110 km southwest of NETS. Data period 1/1/1993 to 12/30/2014.

(a)

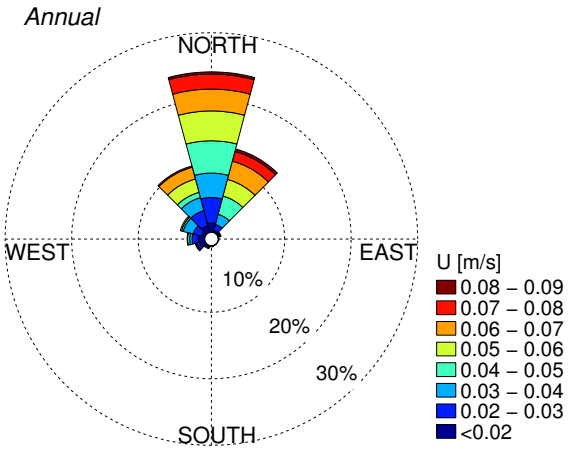

(b)

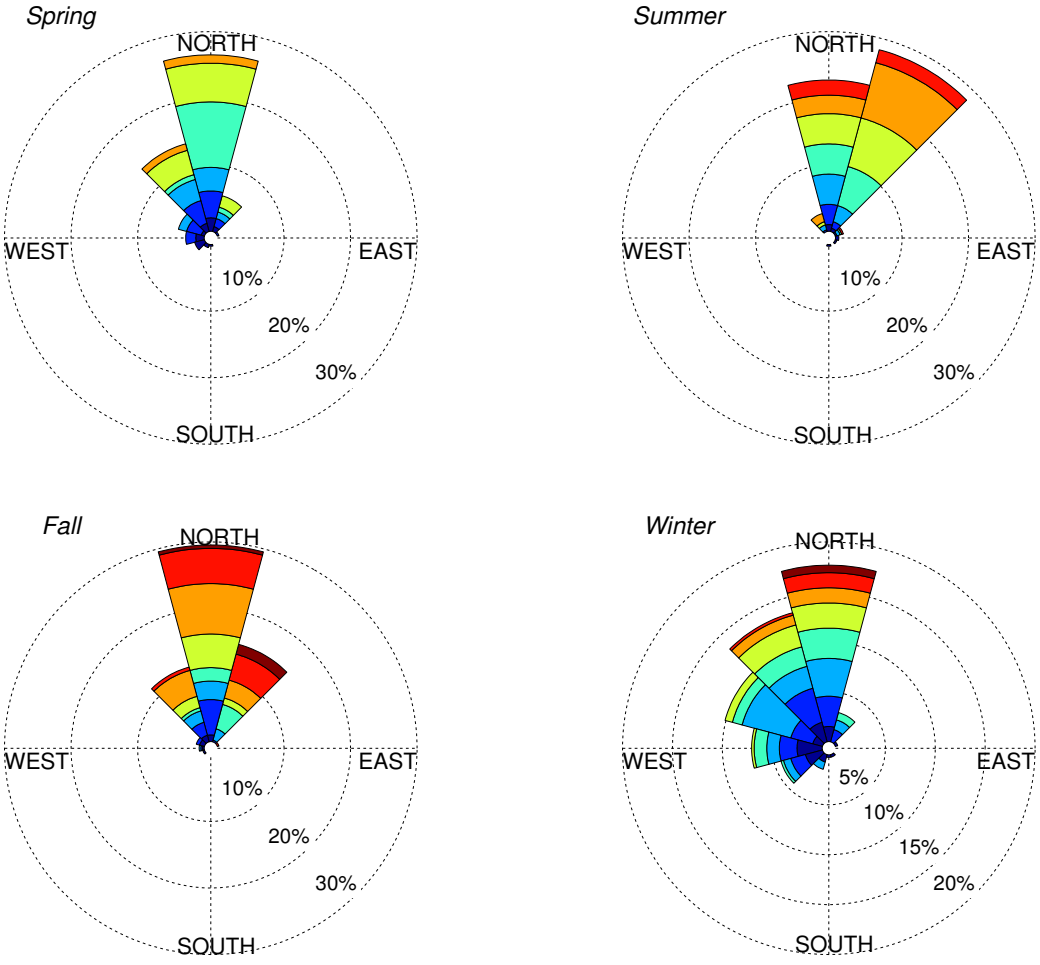

Figure 125: (a) Annual and (b) seasonal current roses of ocean surface current velocity and direction obtained from OSCAR at 44.5 N, 125.5 W. Data period 1/1/1993 to 12/30/2014.

Table 12: Monthly surface current velocity and direction obtained from OSCAR data during the period 1/1/1993 to 12/30/2014 at 44.5 N, 125.5 W.

	$U[m/s]$			$Direction[^\circ]$		
	5%	**Mean**	**95%**	**5%**	**Mean**	**95%**
March	0.014	0.035	0.058	-95	-23	3
April	0.003	0.037	0.061	-88	-7	16
May	0.010	0.037	0.055	-110	3	15
June	0.009	0.040	0.062	-83	5	15
July	0.015	0.052	0.072	-8	20	28
August	0.031	0.057	0.079	-7	21	27
September	0.030	0.056	0.082	-27	14	26
October	0.020	0.052	0.079	-48	5	27
November	0.009	0.049	0.075	-85	-11	14
December	0.019	0.043	0.078	-107	-27	12
January	0.007	0.030	0.056	-104	-39	7
February	0.004	0.030	0.053	-108	-18	20

Appendix B: U.S. NAVY WAVE ENERGY TEST SITE (WETS)

B.1. IEC TS Parameter Values

Table 13: The average, 5^{th} and 95^{th} percentiles of the six parameters at Kaneohe II (see Figure 23).

	$J[kW/m]$			$H_{m0}[m]$			$T_e[s]$		
	5%	**Mean**	**95%**	**5%**	**Mean**	**95%**	**5%**	**Mean**	**95%**
March	4.0	18.1	47.5	0.93	1.85	3.07	6.8	8.7	11.8
April	3.9	14.1	33.1	1.01	1.76	2.68	6.4	7.9	10.5
May	2.5	8.6	18.9	0.82	1.45	2.17	6.1	7.3	9.3
June	2.6	6.9	13.1	0.90	1.41	1.94	5.7	6.6	8.1
July	3.0	7.4	14.2	0.97	1.46	2.00	5.7	6.6	7.6
August	2.4	6.6	13.3	0.87	1.36	1.91	5.6	6.6	8.0
September	2.7	7.3	15.4	0.88	1.33	1.88	6.0	7.4	9.8
October	4.1	11.3	25.9	1.00	1.55	2.27	6.4	8.2	11.1
November	5.1	19.0	50.6	1.09	1.87	2.99	6.9	8.9	12.0
December	5.0	19.7	50.6	1.02	1.87	3.05	7.1	9.5	12.7
January	4.6	18.1	46.3	0.95	1.76	2.90	7.2	9.7	13.0
February	4.6	18.2	46.5	0.98	1.80	2.92	7.0	9.3	12.4

	ϵ_0			$\theta_j[^\circ]$			d_θ		
	5%	**Mean**	**95%**	**5%**	**Mean**	**95%**	**5%**	**Mean**	**95%**
March	0.29	0.38	0.51	-22.5	23.4	67.5	0.66	0.82	0.94
April	0.28	0.37	0.49	-7.5	34.4	67.5	0.67	0.81	0.91
May	0.28	0.37	0.48	-7.5	40.2	67.5	0.68	0.82	0.92
June	0.31	0.37	0.46	22.5	50.9	67.5	0.71	0.84	0.91
July	0.31	0.35	0.43	37.5	53.3	67.5	0.78	0.87	0.91
August	0.30	0.36	0.45	37.5	54.3	67.5	0.74	0.86	0.91
September	0.28	0.38	0.49	-7.5	36.7	67.5	0.71	0.82	0.91
October	0.27	0.38	0.51	-7.5	25.2	52.5	0.69	0.81	0.93
November	0.27	0.38	0.50	-7.5	22.6	67.5	0.68	0.82	0.93
December	0.28	0.38	0.50	-22.5	16.6	67.5	0.67	0.82	0.94
January	0.29	0.38	0.50	-22.5	10.4	67.5	0.67	0.84	0.95
February	0.28	0.38	0.52	-22.5	15.0	67.5	0.66	0.83	0.95

Table 14: The average, 5^{th} and 95^{th} percentiles of the six parameters at WETS (see Figure 24).

	$J[kW/m]$			$H_{m0}[m]$			$T_e[s]$		
	5%	**Mean**	**95%**	**5%**	**Mean**	**95%**	**5%**	**Mean**	**95%**
March	4.4	20.1	52.5	1.00	1.98	3.29	6.81	8.70	11.72
April	4.5	15.9	36.5	1.08	1.89	2.88	6.46	7.93	10.38
May	2.8	9.8	21.1	0.88	1.57	2.35	6.09	7.30	9.33
June	3.1	8.1	15.4	0.97	1.52	2.10	5.75	6.68	8.11
July	3.5	8.6	16.7	1.04	1.57	2.17	5.79	6.63	7.71
August	2.8	7.7	15.6	0.94	1.47	2.08	5.67	6.65	8.10
September	3.1	8.2	17.4	0.94	1.43	2.02	6.01	7.43	9.73
October	4.5	12.4	27.7	1.06	1.65	2.41	6.46	8.22	11.09
November	5.8	20.8	53.9	1.17	2.00	3.17	6.95	8.89	11.92
December	5.6	21.7	54.7	1.09	2.00	3.24	7.19	9.44	12.63
January	5.0	19.7	49.9	1.01	1.86	3.06	7.26	9.73	12.89
February	5.1	19.8	49.7	1.04	1.91	3.08	7.08	9.33	12.39

	ϵ_0			$\theta_j[^\circ]$			d_θ		
	5%	**Mean**	**95%**	**5%**	**Mean**	**95%**	**5%**	**Mean**	**95%**
March	0.28	0.38	0.50	-22.5	28.4	67.5	0.64	0.81	0.94
April	0.27	0.36	0.48	-7.5	39.8	67.5	0.66	0.80	0.91
May	0.28	0.36	0.47	-7.5	45.5	82.5	0.67	0.81	0.92
June	0.30	0.36	0.45	22.5	55.9	67.5	0.70	0.84	0.92
July	0.30	0.35	0.42	37.5	58.2	67.5	0.78	0.87	0.91
August	0.30	0.35	0.44	37.5	59.9	67.5	0.74	0.86	0.92
September	0.28	0.37	0.48	-7.5	41.5	67.5	0.69	0.82	0.91
October	0.27	0.37	0.50	-7.5	29.6	67.5	0.67	0.80	0.93
November	0.26	0.37	0.49	-7.5	27.5	67.5	0.66	0.81	0.93
December	0.27	0.37	0.49	-22.5	21.6	67.5	0.65	0.81	0.94
January	0.28	0.37	0.49	-22.5	14.5	67.5	0.65	0.83	0.95
February	0.27	0.37	0.51	-22.5	19.2	67.5	0.64	0.82	0.95

B.2. Wave Roses

The annual wave rose of omnidirectional wave power, J, and direction of maximum directionally resolved wave power, θ_j, is shown in Figure 126, and essentially mirrors that for significant wave height, H_{m0}, and θ_j shown in Figure 127.

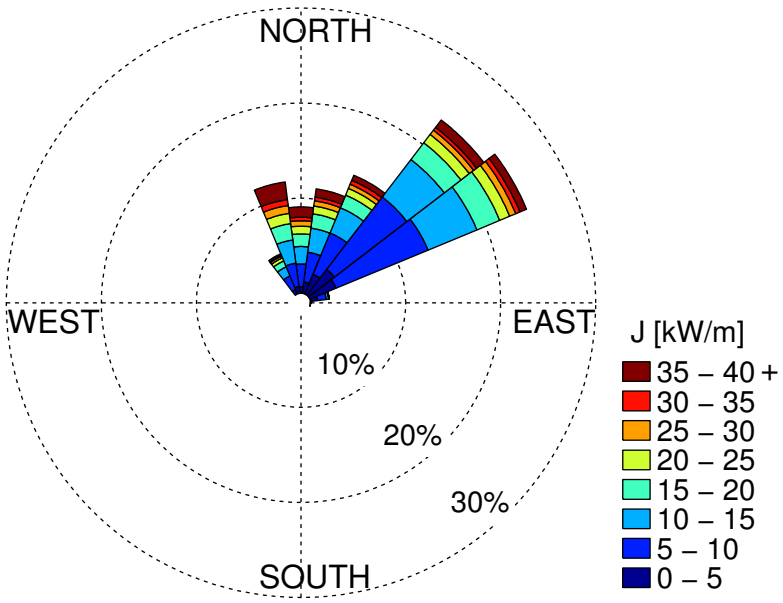

Figure 126: Annual wave rose of omnidirectional wave power and direction of maximum directionally resolved wave power. Values of J greater than 40 kW/m are included in the top bin as shown in the legend. Figure produced by Ning Li (Li and Cheung 2014).

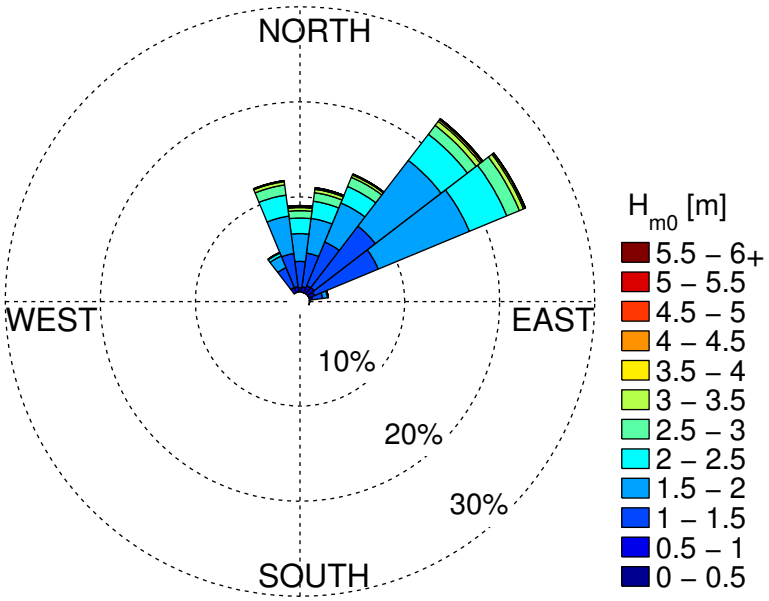

Figure 127: Annual wave rose of significant wave height and direction of maximum directionally resolved wave power. Values of H_{m0} greater than 6 m are included in the top bin as shown in the legend. Figure produced by Ning Li (Li and Cheung 2014).

B.3. Extreme Sea States

Table 15: Selected values along the 100-year contour for CDIP098 (NDBC 51202) (see Figure 30).

Significant wave height [m]	Energy period [s]
1	4.24
2	4.17
3	5.72
4	7.11
5	8.44
6	9.85
7	11.74
7.24	12.98
7	14.05
6	15.18
5	15.72
4	16.05
3	16.24
2	16.31
1	16.25

B.4. Wind Data

The wind data for this site (obtained from CFSR), is taken at 21.5 N, 157.5 W located approximately 25 km east of WETS (Figure 20), which is the nearest data point to the site. The average monthly values, along with the 5^{th} and 95^{th} percentiles, of wind are shown in Figure 128. The values are also tabulated in Table 16. The annual and seasonal wind roses are shown in Figure 129.

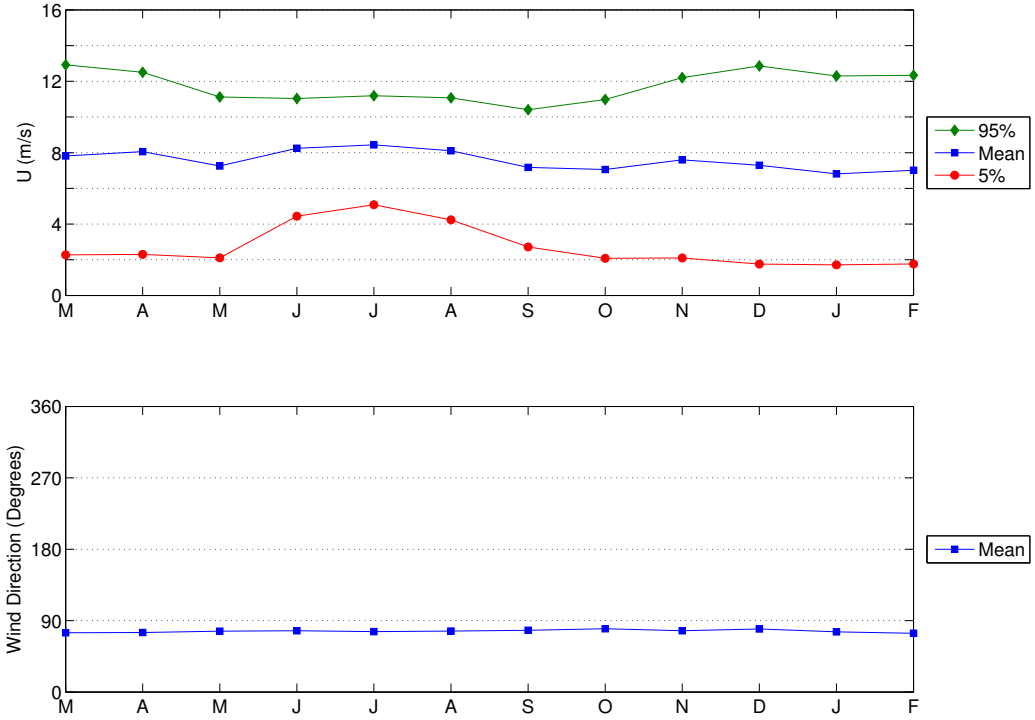

Figure 128: Monthly wind velocity and direction obtained from CSFR data during the period 1/1/1979 to 12/31/2014 at 21.5 N, 157.5 W, located approximately 25 km east of WETS (Figure 20).

(a)

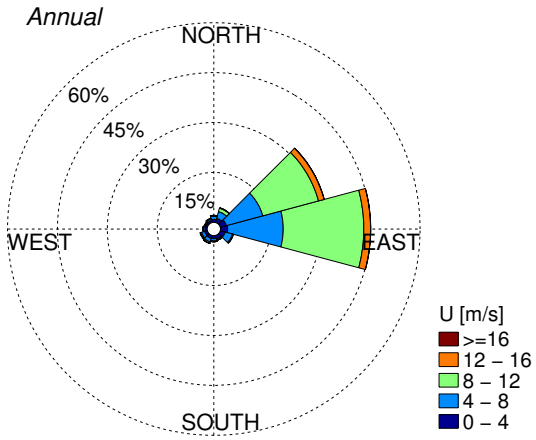

(b)

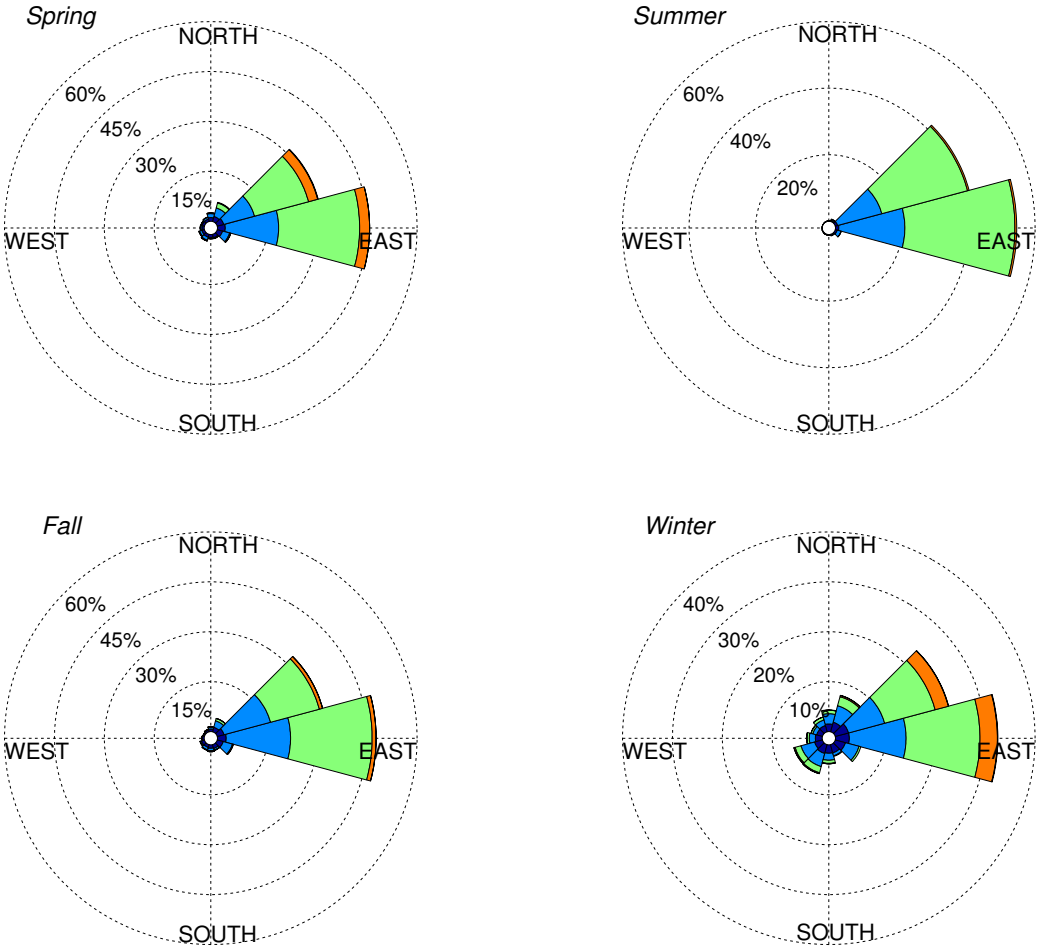

Figure 129: (a) Annual and (b) seasonal wind roses of velocity and direction obtained from CSFR data during the period 1/1/1979 to 12/31/2014. Data taken at 21.5 N, 157.5 W, located approximately 25 km east of WETS (Figure 20).

Table 16: Monthly wind velocity and direction obtained from CSFR data during the period 1/1/1979 to 12/31/2014 at 21.5 N, 157.5 W, located approximately 25 km east of WETS.

	$U[m/s]$			$Direction[^\circ]$
	5%	**Mean**	**95%**	**Mean**
March	2.3	7.8	12.9	75
April	2.3	8.1	12.5	75
May	2.1	7.3	11.1	77
June	4.4	8.2	11.0	77
July	5.1	8.4	11.2	76
August	4.2	8.1	11.1	77
September	2.7	7.2	10.4	78
October	2.1	7.1	11.0	80
November	2.1	7.6	12.2	77
December	1.8	7.3	12.9	79
January	1.7	6.8	12.3	76
February	1.8	7.0	12.3	74

B.5. Ocean Surface Current Data

The surface current data (obtained from OSCAR), is located at 21.5 N, 157.5 W, the closest data point to shore. The average monthly values, along with the 5^{th} and 95^{th} percentiles, of current are shown in Figure 130. These data points are listed in Table 17. The annual and seasonal current roses are shown in Figure 131.

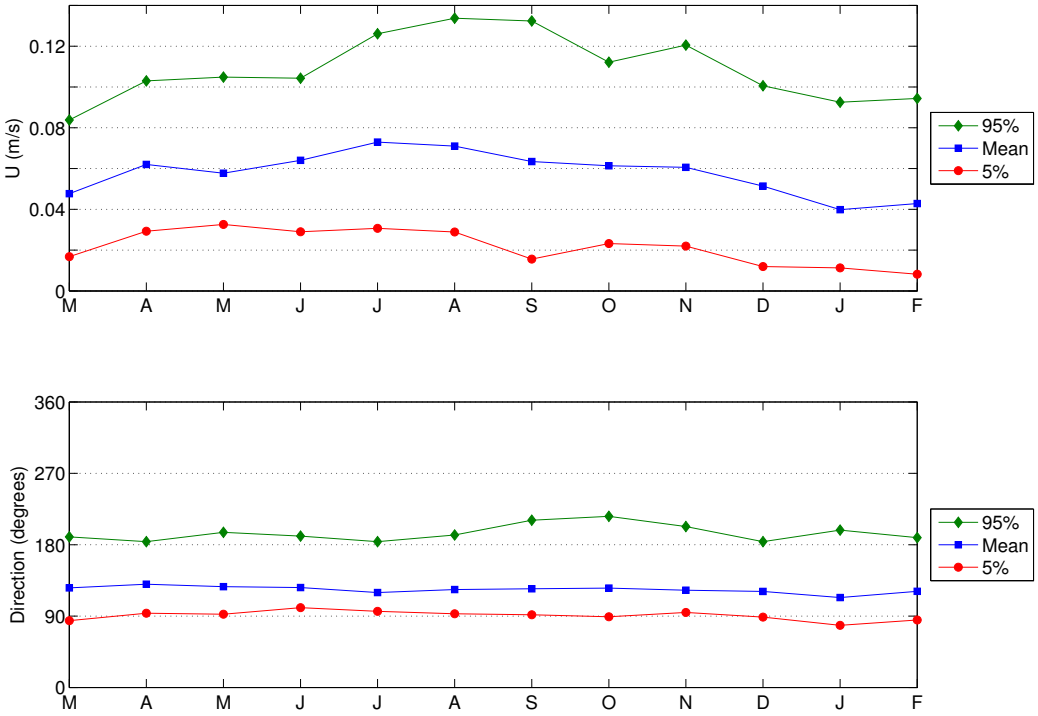

Figure 130: Monthly ocean surface current velocity and direction obtained from OSCAR at 21.5 N, 157.5 W, located approximately 25 km east of WETS. Data period 1/1/1993 to 12/30/2014.

(a)

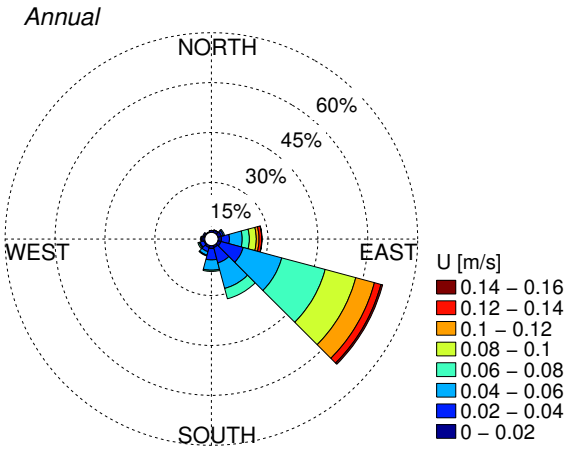

(b)

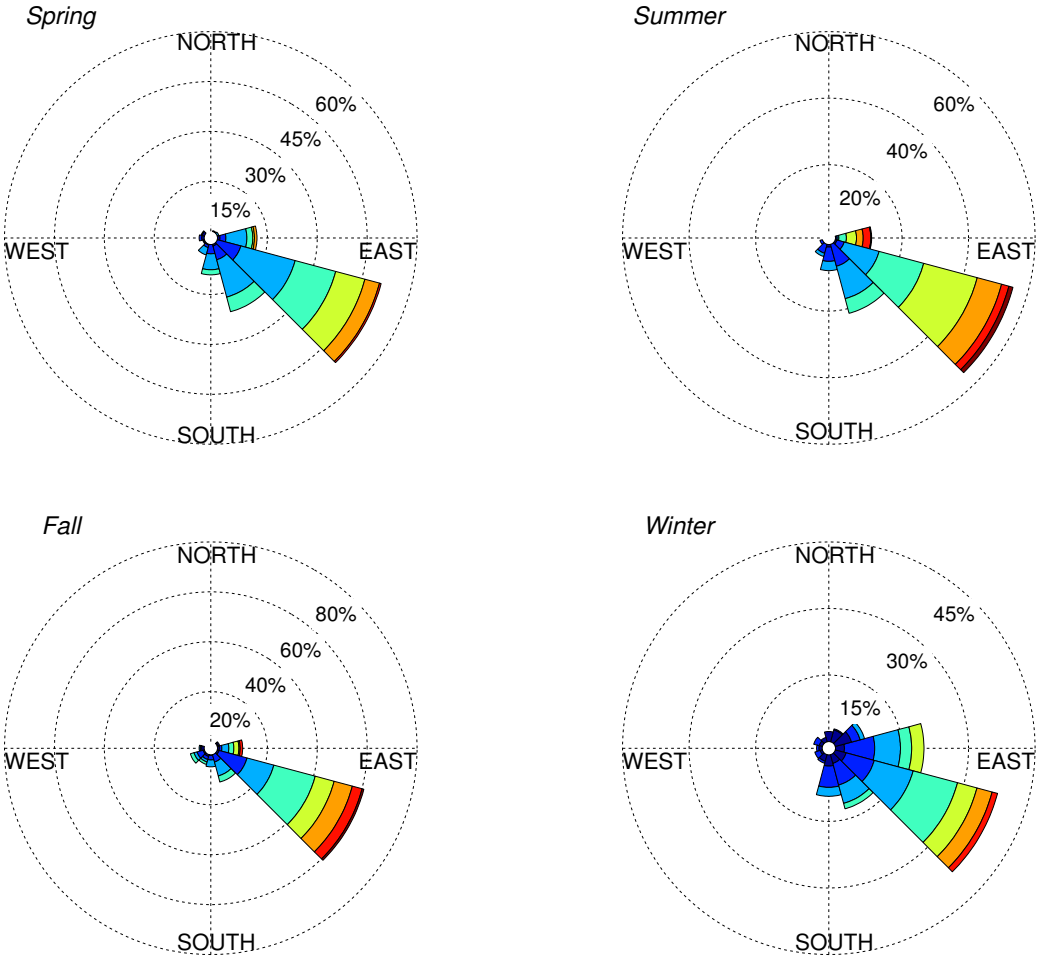

Figure 131: (a) Annual and (b) seasonal current roses of ocean surface current velocity and direction obtained from OSCAR at 21.5 N, 157.5 W, located approximately 25 km east of WETS. Data period 1/1/1993 to 12/30/2014.

Table 17: Monthly surface current velocity and direction obtained from OSCAR data during the period 1/1/1993 to 12/30/2014 at 21.5 N, 157.5 W, located approximately 25 km east of WETS.

	$U[m/s]$			$Direction[^\circ]$		
	5%	**Mean**	**95%**	**5%**	**Mean**	**95%**
March	0.017	0.048	0.084	84	126	190
April	0.029	0.062	0.103	94	130	184
May	0.033	0.058	0.105	92	127	196
June	0.029	0.064	0.104	101	126	191
July	0.031	0.073	0.126	96	120	184
August	0.029	0.071	0.134	93	123	192
September	0.016	0.063	0.132	92	124	211
October	0.023	0.062	0.112	89	125	216
November	0.022	0.061	0.121	95	122	202
December	0.012	0.052	0.099	88	122	183
January	0.011	0.040	0.093	78	113	198
February	0.008	0.043	0.094	85	121	189

Appendix C: JENNETTE'S PIER WAVE ENERGY TEST CENTER

C.1. IEC TS Parameter Values

Table 18: The average, 5^{th} and 95^{th} percentiles of the six parameters at Jennette's Pier (see Figure 37).

	$J[kW/m]$			$H_{m0}[m]$			$T_e[s]$		
	5%	**Mean**	**95%**	**5%**	**Mean**	**95%**	**5%**	**Mean**	**95%**
March	0.80	9.07	31.42	0.50	1.28	2.56	4.74	7.08	10.35
April	0.57	5.83	20.03	0.43	1.04	2.15	4.67	6.74	9.54
May	0.46	4.19	14.25	0.39	0.88	1.88	4.61	6.42	8.68
June	0.39	1.90	5.83	0.36	0.68	1.28	4.51	6.06	7.60
July	0.35	1.41	3.03	0.33	0.59	0.97	4.63	6.06	7.49
August	0.36	3.00	8.54	0.35	0.74	1.48	4.48	6.06	8.35
September	0.56	7.35	28.90	0.43	1.11	2.52	4.58	6.67	10.30
October	0.57	8.06	31.62	0.44	1.19	2.62	4.59	6.61	9.83
November	0.60	8.04	24.05	0.43	1.21	2.34	4.72	6.80	9.84
December	0.69	8.12	28.45	0.47	1.24	2.49	4.73	6.82	9.88
January	0.72	7.74	26.58	0.46	1.24	2.46	4.87	6.85	9.50
February	0.88	8.41	32.16	0.51	1.27	2.63	4.89	6.97	9.84

	ϵ_0			$\theta_j[^\circ]$			d_θ		
	5%	**Mean**	**95%**	**5%**	**Mean**	**95%**	**5%**	**Mean**	**95%**
March	0.24	0.35	0.46	25	73.1	115	0.72	0.87	0.96
April	0.24	0.34	0.46	35	79.1	115	0.70	0.87	0.96
May	0.24	0.33	0.44	45	86.8	115	0.72	0.88	0.96
June	0.24	0.33	0.44	55	96.9	125	0.73	0.89	0.96
July	0.24	0.33	0.44	65	102.7	125	0.74	0.90	0.96
August	0.24	0.33	0.44	55	93.7	115	0.75	0.89	0.96
September	0.24	0.34	0.46	45	81.6	115	0.73	0.88	0.96
October	0.24	0.34	0.45	35	73.2	115	0.72	0.88	0.96
November	0.25	0.35	0.46	25	70.3	115	0.70	0.87	0.96
December	0.25	0.36	0.47	15	65.6	115	0.68	0.86	0.95
January	0.25	0.36	0.47	15	66.6	115	0.68	0.85	0.95
February	0.24	0.35	0.47	25	68.8	115	0.69	0.86	0.96

C.2. Wave Roses

The annual wave rose of omnidirectional wave power, J, and direction of maximum directionally resolved wave power, θ_j, is shown in Figure 132, and essentially mirrors that for significant wave height, H_{m0}, and θ_j shown in Figure 133.

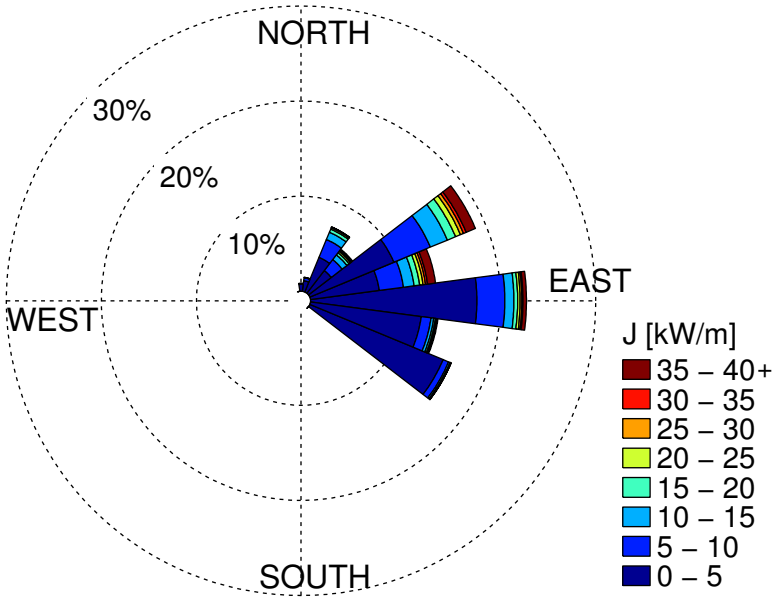

Figure 132: Annual wave rose of omnidirectional wave power and direction of maximally resolved wave power. Values of J greater than 40 kW/m are included in the top bin as shown in the legend.

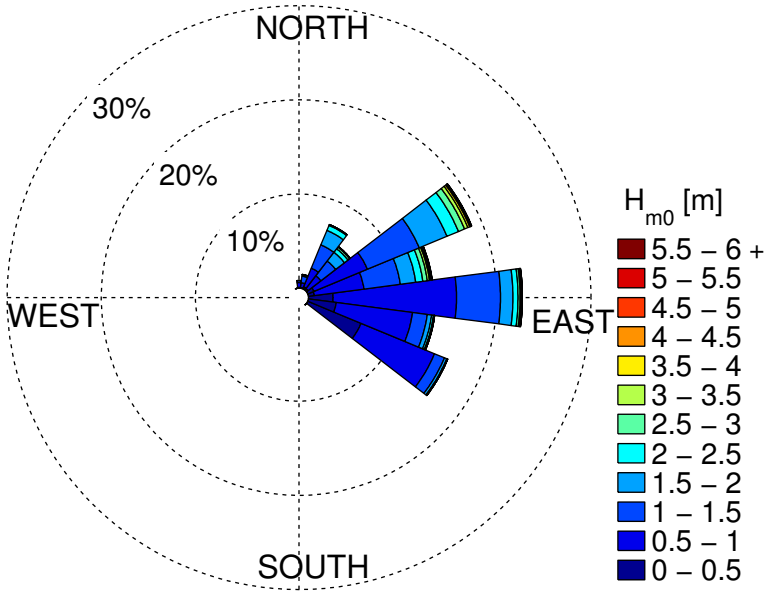

Figure 133: Annual wave rose of significant wave height and direction of maximally resolved wave power. Values of H_{m0} greater than 6 m are included in the top bin as shown in the legend.

C.3. Extreme Sea States

Table 19: Estimates of extreme significant wave height values using the generalized extreme value distribution (see Figure 43).

Return period [years]	Significant wave height [m]
10	6.23
25	6.79
50	7.19
100	7.55

Table 20: Estimates of extreme significant wave height values using the peak over thresholds method (see Figure 44).

Return period [years]	Significant wave height [m]
10	7.34
25	7.81
50	8.14
100	8.46

C.4. Wind Data

The wind data for this site (obtained from CFSR), is taken at 36 N, 75.5 W located approximately 12 km northeast of the site (Figure 35, which is the nearest data point to the site). The average monthly values, along with the 5^{th} and 95^{th} percentiles, of wind are shown in Figure 134. The values are also tabulated in Table 21. The annual and seasonal wind roses are shown in Figure 135.

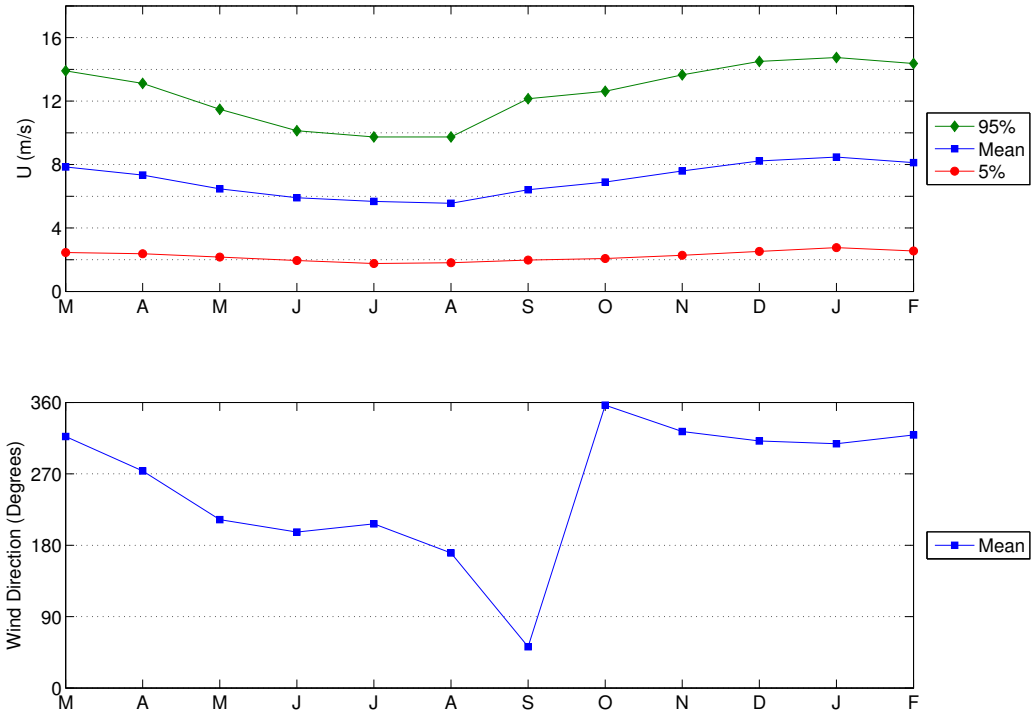

Figure 134: Monthly wind velocity and direction obtained from CSFR data during the period 1/1/1979 to 12/31/2014 at 36 N, 75.5 W, located approximately 12 km northeast of the the Jennette's Pier site (Figure 35).

(a)

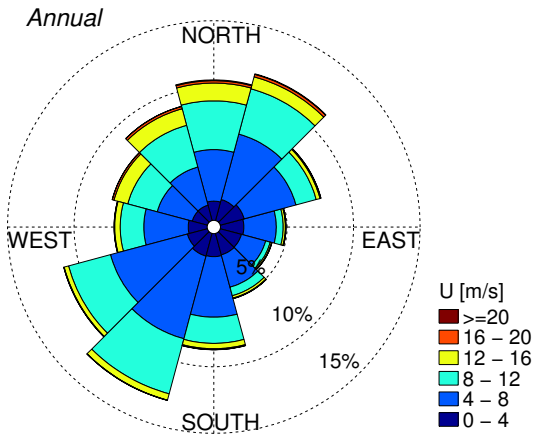

(b)

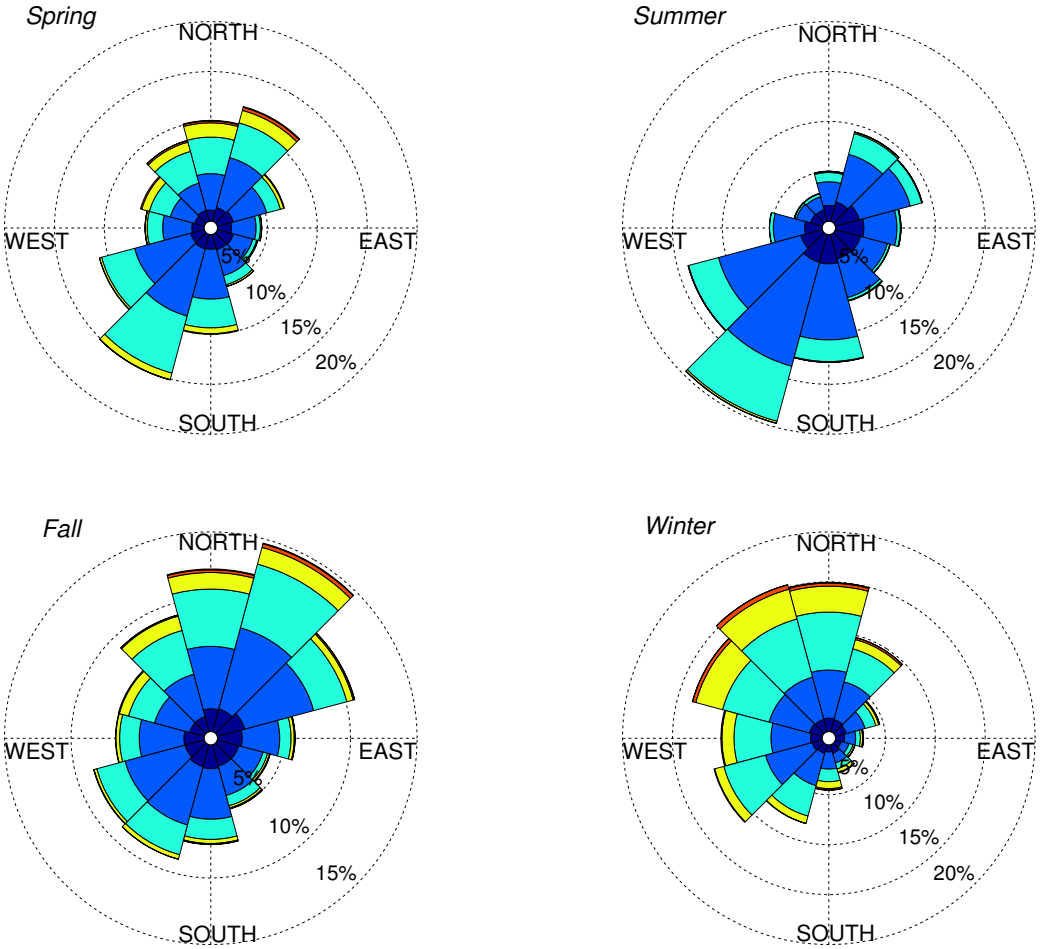

Figure 135: (a)Annual and (b) seasonal wind roses of velocity and direction obtained from CSFR data during the period 1/1/1979 to 12/31/14. Data taken at 36 N, 75.5 W, located approximately 12 km northeast of the the Jennette's Pier site (Figure 35).

Table 21: Monthly wind velocity and direction obtained from CSFR data during the period 1/1/1979 to 12/31/2014 at 36 N, 75.5 W, located approximately 12 km northeast of Jennette's Pier.

	$U[m/s]$			$Direction[^\circ]$
	5%	**Mean**	**95%**	**Mean**
March	2.5	7.8	13.9	317
April	2.4	7.3	13.1	274
May	2.2	6.5	11.5	212
June	1.9	5.9	10.1	197
July	1.8	5.7	9.7	207
August	1.8	5.6	9.7	170
September	2.0	6.4	12.1	52
October	2.1	6.9	12.6	357
November	2.3	7.6	13.7	323
December	2.5	8.2	14.5	311
January	2.8	8.5	14.7	308
February	2.6	8.1	14.4	319

C.5. Ocean Surface Current Data

The surface current data (obtained from OSCAR), is located at 36.5 N, 75.5.5 W, the closest data point to shore. The data point at 35.5 N, 75.5 W, which would be closer to the site, is located west of the Outer Banks. The average monthly values, along with the 5^{th} and 95^{th} percentiles, of current are shown in Figure 136. These data points are listed in Table 22. The annual and seasonal current roses are shown in Figure 137.

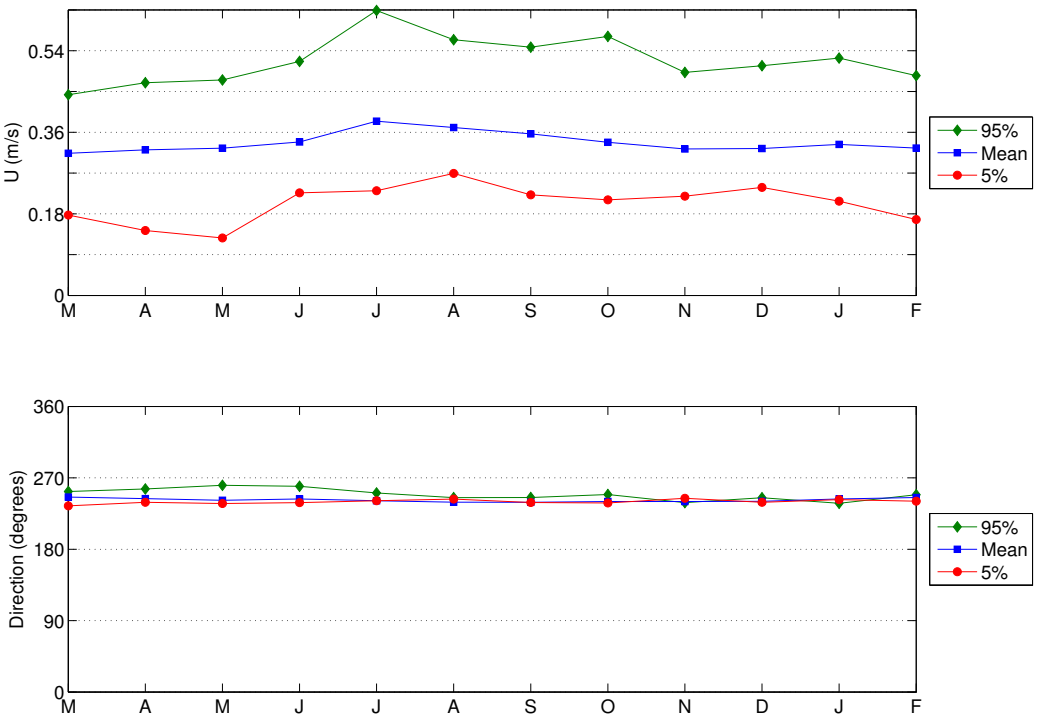

Figure 136: Monthly ocean surface current velocity and direction obtained from OSCAR at 36.5 N, 75.5 W, located approximately 60 km north/northeast of Jennette's Pier. Data period 1/1/1993 to 12/31/2014.

(a)

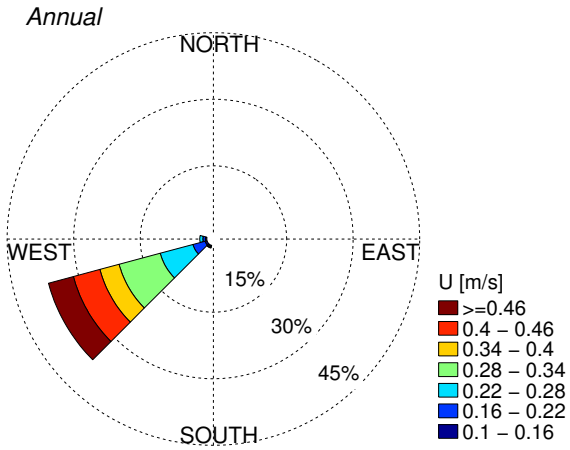

(b)

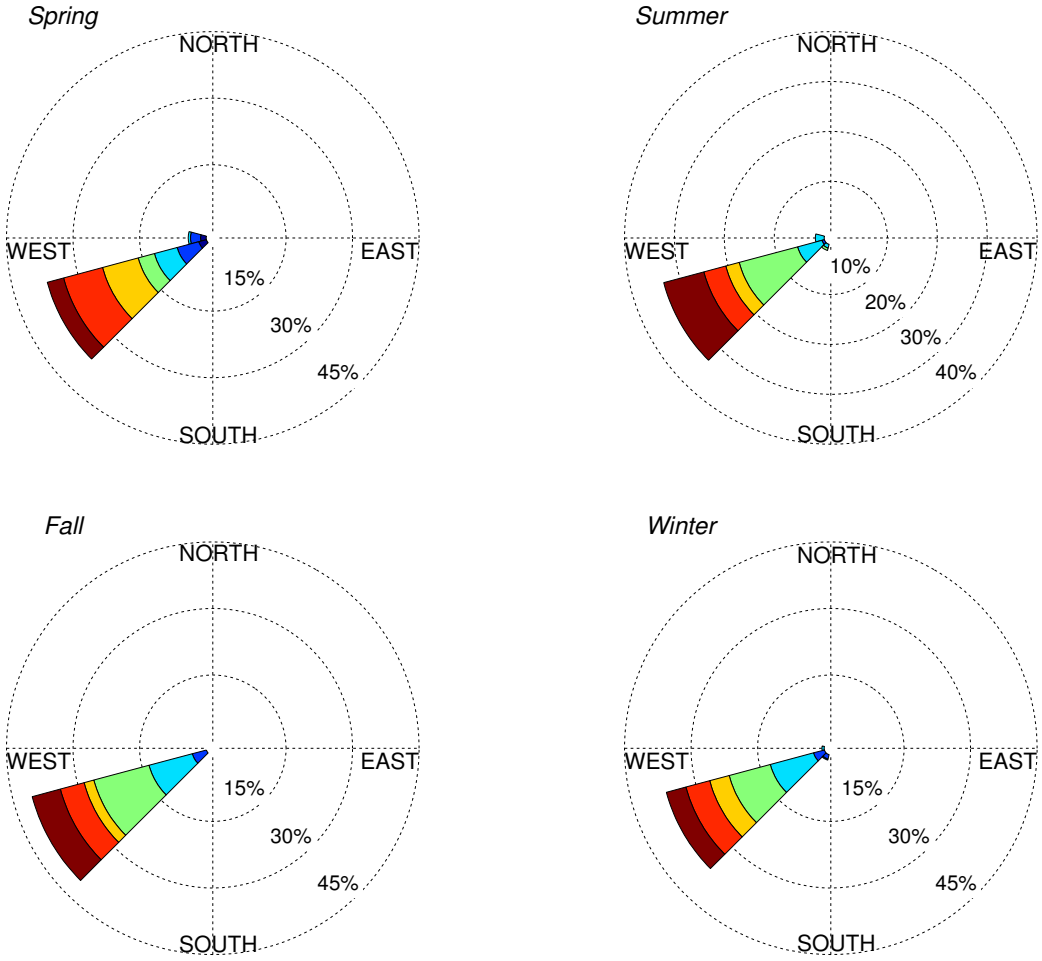

Figure 137: (a) Annual and (b) seasonal current roses of velocity and direction obtained from OSCAR at 36.5 N, 75.5 W, located approximately 60 km north/northeast of Jennette's Pier. Data period 1/1/1993 to 12/31/2014.

Table 22: Monthly surface current velocity and direction obtained from OSCAR data during the period 1/1/1993 to 12/31/2014 at 36.5 N, 75.5 W, located approximately 60 km north/northeast of Jennette's Pier.

	$U[m/s]$			$Direction[^\circ]$		
	5%	**Mean**	**95%**	**5%**	**Mean**	**95%**
March	0.177	0.314	0.443	235	246	253
April	0.143	0.321	0.469	239	244	256
May	0.127	0.325	0.476	238	242	261
June	0.226	0.339	0.516	239	243	259
July	0.231	0.385	0.629	241	241	251
August	0.269	0.370	0.564	243	239	245
September	0.222	0.357	0.548	239	239	245
October	0.211	0.338	0.572	238	240	249
November	0.219	0.323	0.492	244	240	239
December	0.238	0.324	0.507	239	241	245
January	0.208	0.333	0.524	242	243	238
February	0.168	0.325	0.485	241	245	249

Appendix D: U.S. ARMY CORPS OF ENGINEERS (USACE) FIELD RESEARCH FACILITY (FRF)

D.1. IEC TS Parameter Values

Table 23: The average, 5^{th} and 95^{th} percentiles of the six parameters at USACE FRF (see Figure 37).

	$J[kW/m]$			$H_{m0}[m]$			$T_e[s]$		
	5%	**Mean**	**95%**	**5%**	**Mean**	**95%**	**5%**	**Mean**	**95%**
March	0.54	4.54	13.05	0.45	1.07	1.93	4.42	6.86	10.03
April	0.40	3.15	10.53	0.38	0.89	1.76	4.35	6.53	9.10
May	0.32	2.35	8.46	0.34	0.76	1.61	4.40	6.28	8.39
June	0.28	1.30	3.82	0.32	0.61	1.12	4.30	5.95	7.62
July	0.25	1.02	2.23	0.29	0.55	0.87	4.36	5.94	7.62
August	0.26	1.75	5.81	0.31	0.66	1.34	4.26	5.96	8.45
September	0.41	3.89	14.10	0.38	0.95	2.01	4.41	6.64	10.44
October	0.41	4.09	14.01	0.40	1.00	1.99	4.34	6.48	9.66
November	0.42	4.23	12.13	0.41	1.03	1.87	4.43	6.65	9.74
December	0.47	4.29	13.15	0.42	1.05	1.94	4.42	6.65	9.68
January	0.47	4.39	13.21	0.43	1.07	1.95	4.48	6.70	9.36
February	0.62	4.51	14.04	0.47	1.08	1.99	4.54	6.80	9.66

	ϵ_0			$\theta_j[^\circ]$			d_θ		
	5%	**Mean**	**95%**	**5%**	**Mean**	**95%**	**5%**	**Mean**	**95%**
March	0.25	0.37	0.51	35	73.4	105	0.79	0.90	0.97
April	0.25	0.37	0.52	45	78.4	105	0.78	0.90	0.97
May	0.24	0.35	0.49	55	83.5	105	0.79	0.91	0.97
June	0.24	0.36	0.49	65	90.4	115	0.80	0.91	0.96
July	0.24	0.36	0.50	65	94.2	115	0.80	0.91	0.96
August	0.24	0.35	0.48	55	88.0	115	0.80	0.91	0.96
September	0.24	0.35	0.48	55	79.5	105	0.81	0.91	0.97
October	0.25	0.36	0.48	45	73.6	105	0.79	0.91	0.97
November	0.25	0.37	0.51	35	71.7	105	0.77	0.89	0.97
December	0.25	0.38	0.53	35	68.0	105	0.75	0.89	0.96
January	0.25	0.38	0.55	35	68.6	105	0.73	0.88	0.96
February	0.25	0.38	0.53	35	70.0	105	0.76	0.89	0.97

D.2. Wave Roses

The annual wave rose of omnidirectional wave power, J, and direction of maximum directionally resolved wave power, θ_j, is shown in Figure 138, and essentially mirrors that for significant wave height, H_{m0}, and θ_j shown in Figure 139.

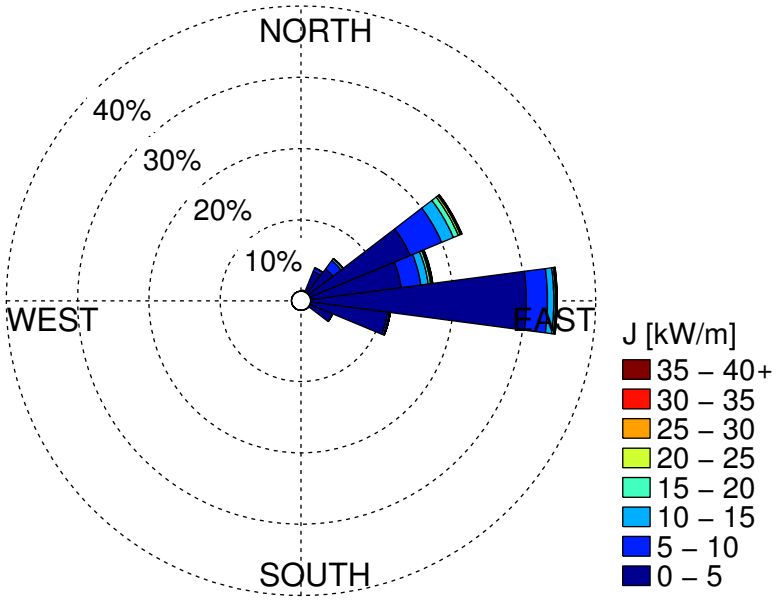

Figure 138: Annual wave rose of omnidirectional wave power and direction of maximally resolved wave power. Values of J greater than 40 kW/m are included in the top bin as shown in the legend.

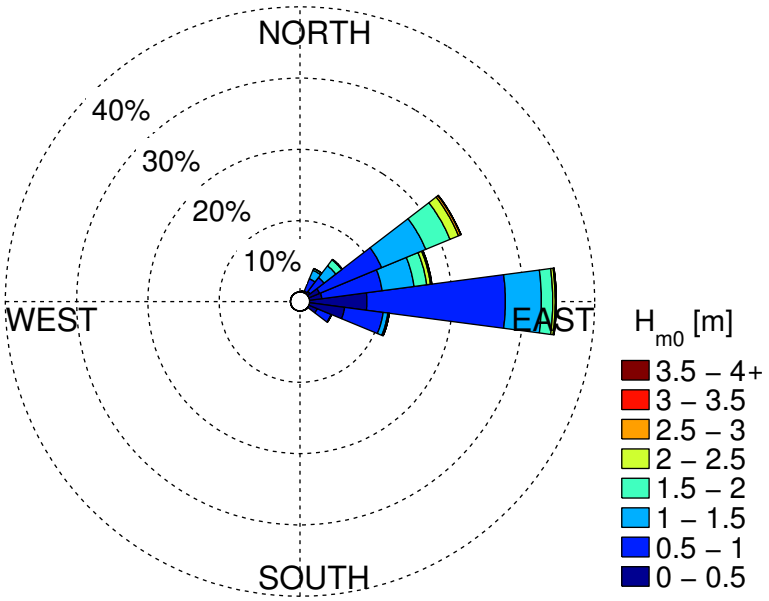

Figure 139: Annual wave rose of significant wave height and direction of maximally resolved wave power. Values of H_{m0} greater than 4 m are included in the top bin as shown in the legend.

D.3. Extreme Sea States

Table 24: Estimates of extreme significant wave height values using the generalized extreme value distribution (see Figure 57).

Return period [years]	Significant wave height [m]
10	6.23
25	6.79
50	7.19
100	7.55

Table 25: Estimates of extreme significant wave height values using the peak over thresholds method (see Figure 58).

Return period [years]	Significant wave height [m]
10	7.34
25	7.81
50	8.14
100	8.46

D.4. Wind Data

The wind data for this site (obtained from CFSR), is taken at 36.25 N, 75.5 W located approximately 23 km northeast of the USACE FRF site (Figure 35), which is the nearest data point to the site. The average monthly values, along with the 5^{th} and 95^{th} percentiles, of wind are shown in Figure 140. The values are also tabulated in Table 26. The annual and seasonal wind roses are shown in Figure 141.

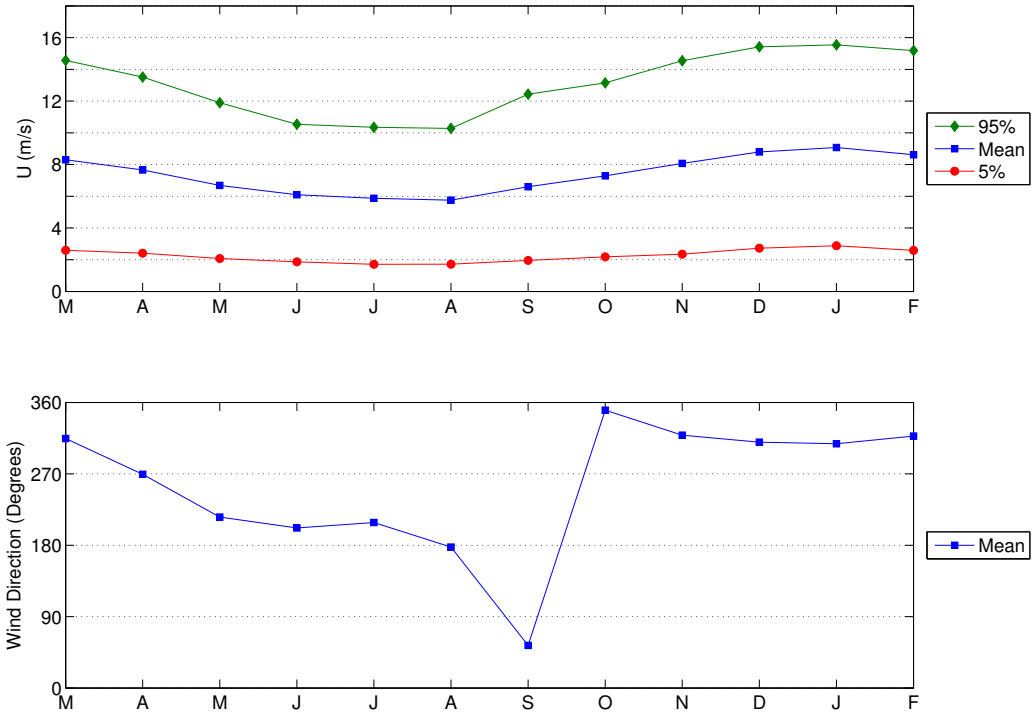

Figure 140: Monthly wind velocity and direction obtained from CSFR data during the period 1/1/1979 to 12/31/2014 at 36.25 N, 75.5 W.

(a)

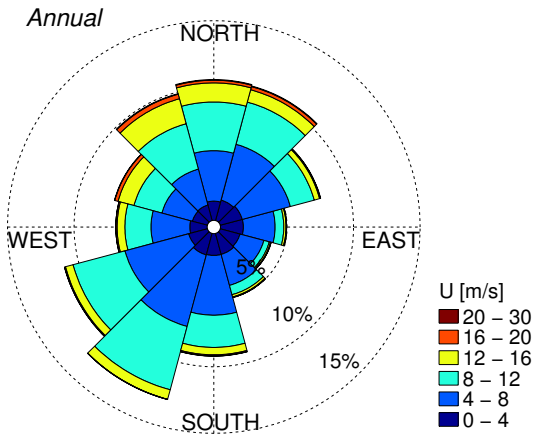

(b)

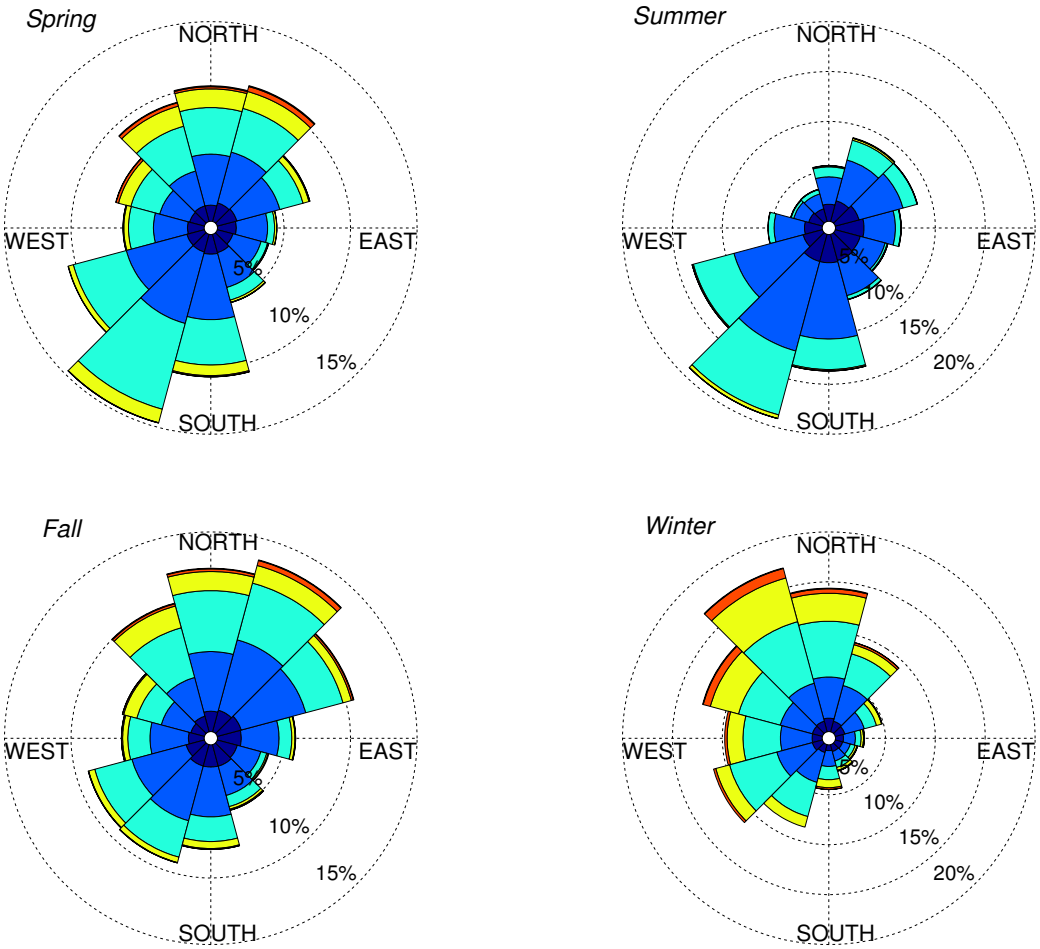

Figure 141: (a) Annual and (b) seasonal wind roses of velocity and direction obtained from CSFR data during the period 1/1/1979 to 12/31/14 at 36.25 N, 75.5 W.

Table 26: Monthly wind velocity and direction obtained from CSFR data during the period 1/1/1979 to 12/31/2014 at 36.25 N, 75.5 W, located approximately 23 km northeast of USACE FRF.

	$U[m/s]$			$Direction[^\circ]$
	5%	**Mean**	**95%**	**Mean**
March	2.6	8.3	14.6	315
April	2.4	7.7	13.5	269
May	2.1	6.7	11.9	215
June	1.9	6.1	10.5	202
July	1.7	5.9	10.4	209
August	1.7	5.8	10.3	178
September	2.0	6.6	12.4	54
October	2.2	7.3	13.1	350
November	2.3	8.1	14.5	319
December	2.7	8.8	15.4	310
January	2.9	9.1	15.5	308
February	2.6	8.6	15.2	318

D.5. Ocean Surface Current Data

The surface current data (obtained from OSCAR), is located at 36.5 N, 75.5 W, the closest data point to shore. The average monthly values, along with the 5^{th} and 95^{th} percentiles, of current are shown in Figure 142. These data points are listed in Table 27. The annual and seasonal current roses are shown in Figure 143.

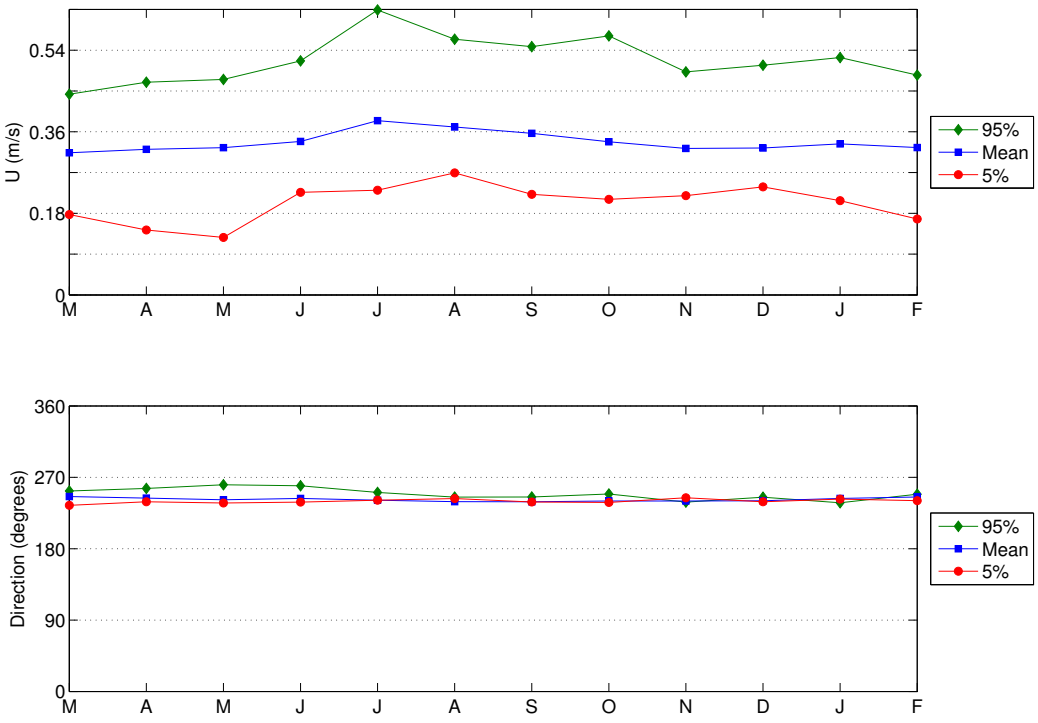

Figure 142: Monthly current velocity and direction obtained from CSFR data during the period 1/1/1993 to 12/31/2014 at 36.5 N, 75.5 W.

(a)

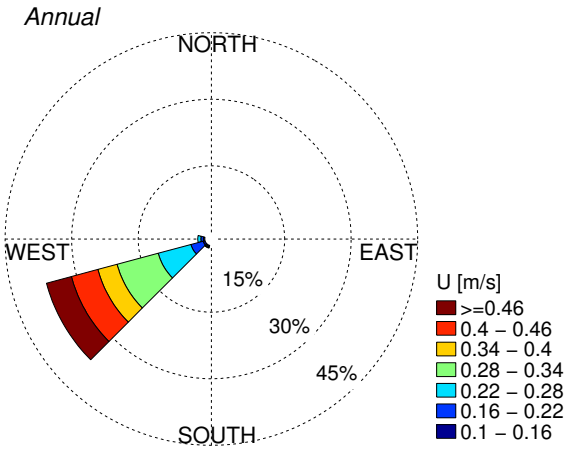

(b)

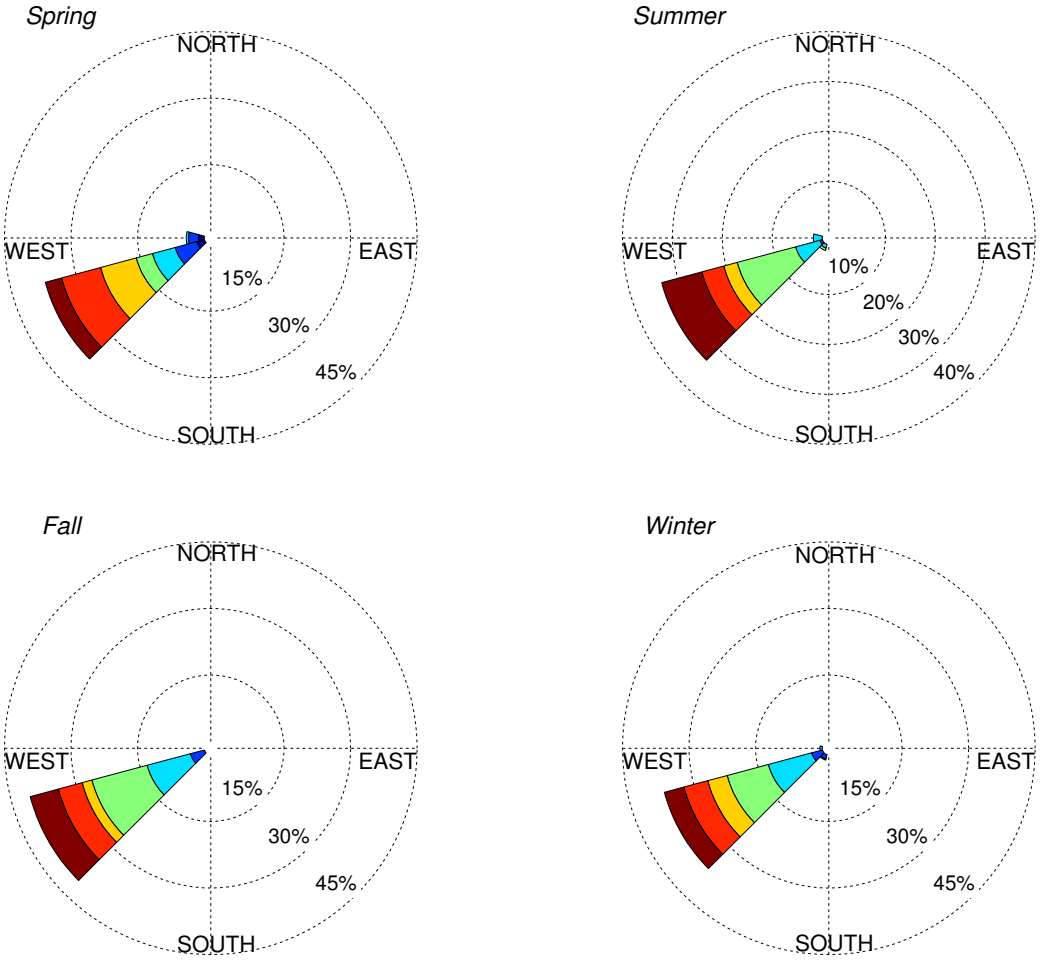

Figure 143: (a)Annual and (b) seasonal current roses of velocity and direction obtained from CSFR data during the period 1/1/1993 to 12/31/14 at 36.5 N, 75.5 W.

Table 27: Monthly surface current velocity and direction obtained from OSCAR data during the period 1/1/1993 to 12/30/2014 at 36.5 N, 75.5 W, located approximately 40 km northeast of the USACE FRF site.

	$U[m/s]$			$Direction[^\circ]$		
	5%	**Mean**	**95%**	**5%**	**Mean**	**95%**
March	0.177	0.314	0.443	235	246	253
April	0.143	0.321	0.469	239	244	256
May	0.127	0.325	0.476	238	242	261
June	0.226	0.339	0.516	239	243	259
July	0.231	0.385	0.629	241	241	251
August	0.269	0.370	0.564	243	239	245
September	0.222	0.357	0.548	239	239	245
October	0.211	0.338	0.572	238	240	249
November	0.219	0.323	0.492	244	240	239
December	0.238	0.324	0.507	239	241	245
January	0.208	0.333	0.524	242	243	238
February	0.168	0.325	0.485	241	245	249

Appendix E: PACIFIC MARINE ENERGY TEST CENTER (PMEC): LAKE WASHINGTON TEST SITE

E.1. IEC TS Parameter Values

Table 28: The average, 5^{th} and 95^{th} percentiles of the six parameters at Lake Washington (see Figure 64).

	$J[kW/m]$			$H_{m0}[m]$			$T_e[s]$		
	5%	**Mean**	**95%**	**5%**	**Mean**	**95%**	**5%**	**Mean**	**95%**
March	0.0026	0.052	0.219	0.071	0.200	0.444	1.06	1.56	2.26
April	0.0025	0.040	0.169	0.070	0.180	0.401	1.05	1.50	2.16
May	0.0024	0.029	0.107	0.069	0.161	0.331	1.05	1.45	2.01
June	0.0024	0.025	0.100	0.069	0.152	0.320	1.04	1.41	1.98
July	0.0023	0.019	0.063	0.068	0.138	0.264	1.03	1.37	1.84
August	0.0023	0.017	0.064	0.068	0.133	0.266	1.03	1.35	1.84
September	0.0023	0.027	0.124	0.067	0.150	0.353	1.02	1.40	2.05
October	0.0023	0.047	0.205	0.067	0.184	0.432	1.02	1.50	2.24
November	0.0026	0.054	0.218	0.070	0.201	0.444	1.05	1.56	2.26
December	0.0024	0.051	0.209	0.069	0.190	0.437	1.03	1.52	2.23
January	0.0024	0.063	0.279	0.069	0.207	0.491	1.04	1.57	2.37
February	0.0023	0.056	0.256	0.068	0.197	0.474	1.02	1.54	2.32

	ϵ_0			$\theta_j[^\circ]$			d_θ		
	5%	**Mean**	**95%**	**5%**	**Mean**	**95%**	**5%**	**Mean**	**95%**
March	0.226	0.241	0.252	75	188.4	325	0.79	0.88	0.95
April	0.226	0.241	0.254	35	191.7	335	0.78	0.88	0.95
May	0.227	0.242	0.255	15	206.5	335	0.77	0.89	0.95
June	0.225	0.242	0.255	25	206.2	345	0.77	0.89	0.95
July	0.223	0.243	0.256	15	260.6	345	0.72	0.88	0.96
August	0.226	0.242	0.255	15	243.6	345	0.73	0.89	0.96
September	0.222	0.241	0.255	15	218.4	345	0.76	0.89	0.96
October	0.223	0.241	0.254	25	190.5	335	0.79	0.89	0.95
November	0.227	0.241	0.254	115	188.0	335	0.83	0.89	0.95
December	0.224	0.240	0.255	75	178.8	335	0.80	0.88	0.95
January	0.226	0.241	0.253	25	187.8	335	0.82	0.89	0.95
February	0.220	0.240	0.254	25	186.3	335	0.77	0.88	0.95

E.2. Wave Roses

The annual wave rose of omnidirectional wave power, J, and direction of maximum directionally resolved wave power, θ_j, is shown in Figure 144, and essentially mirrors that for significant wave height, H_{m0}, and θ_j shown in Figure 145.

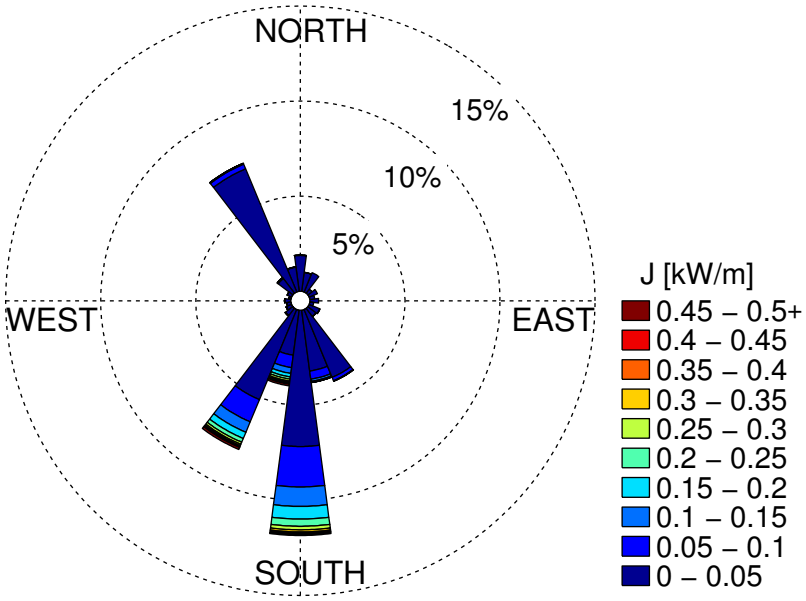

Figure 144: Annual wave rose of omnidirectional wave power and direction of maximally resolved wave power. Values of J greater than 0.5 kW/m are included in the top bin as shown in the legend.

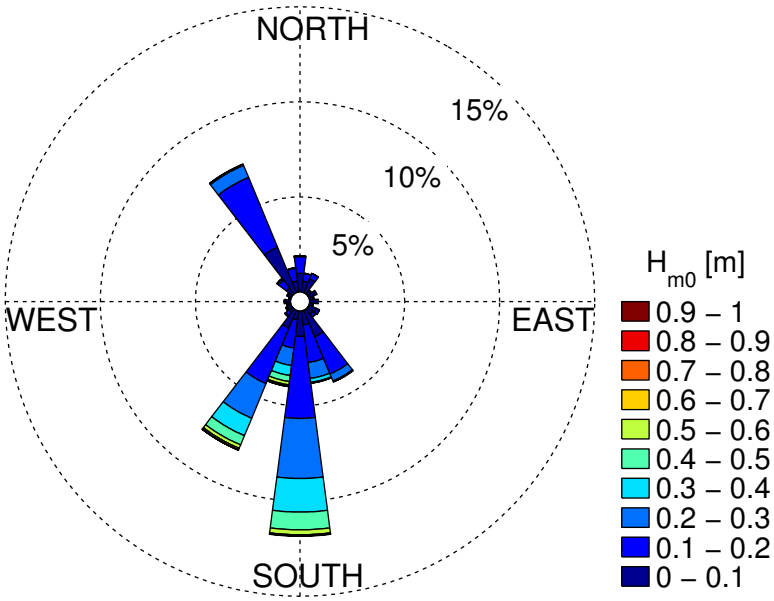

Figure 145: Annual wave rose of significant wave height and direction of maximally resolved wave power. Values of H_{m0} greater than 1 m are included in the top bin as shown in the legend.

E.3. Extreme Sea States

Table 29: Estimates of extreme significant wave height values using the generalized extreme value distribution (see Figure 70).

Return period [years]	Significant wave height [m]
10	0.94
25	1.01
50	1.07
100	1.13

Table 30: Estimates of extreme significant wave height values using the peak over thresholds method (see Figure 71).

Return period [years]	Significant wave height [m]
10	0.93
25	0.98
50	1.01
100	1.04

E.4. Wind Data

The wind data for this site (obtained from the SR 520 bridge weather station), is located approximately 5 km south of the site (Figure 60). The average monthly values, along with the 5^{th} and 95^{th} percentiles, of wind are shown in Figure 146. The values are also tabulated in Table 31. The annual and seasonal wind roses are shown in Figure 147.

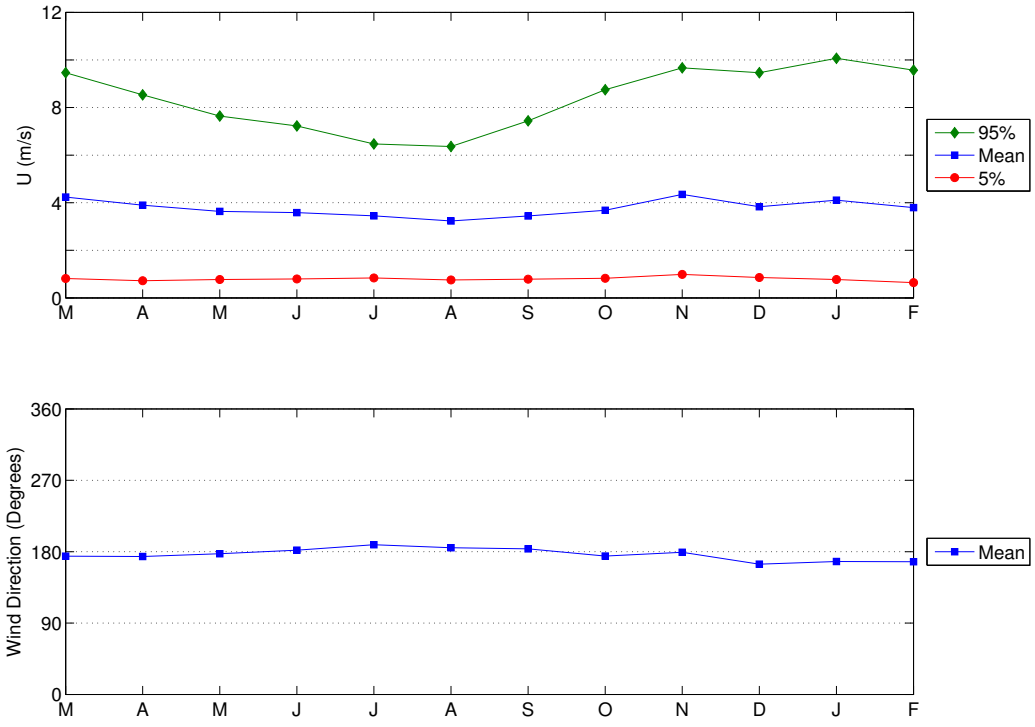

Figure 146: Monthly wind velocity and direction obtained from the SR 520 bridge weather station on Lake Washington during the period 1/1/2005 to 12/31/2014.

(a)

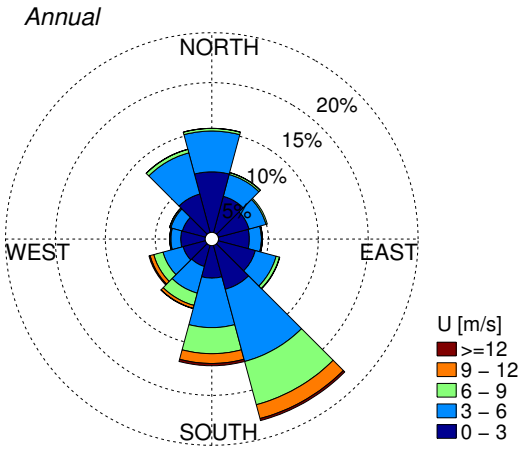

(b)

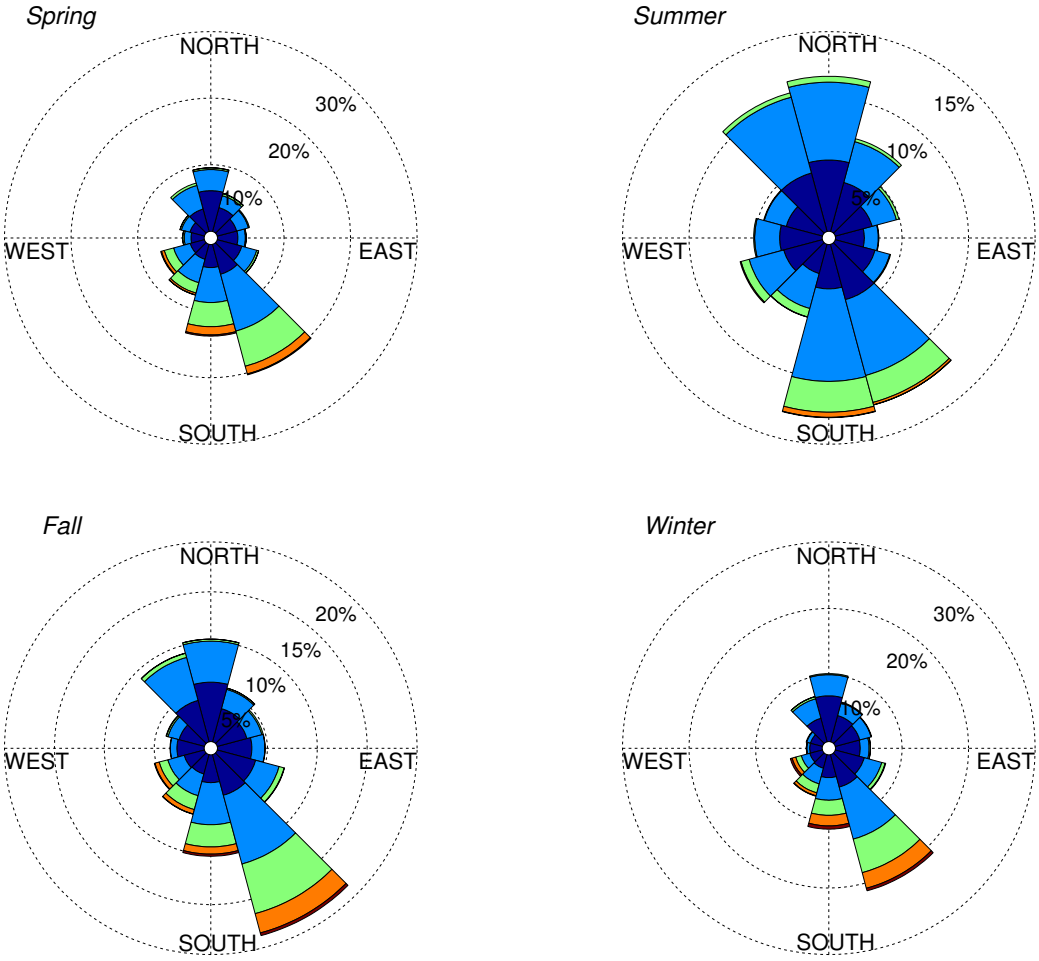

Figure 147: (a) Annual and (b) seasonal wind roses of velocity and direction obtained from the SR 520 bridge weather station during the period 1/1/2005 to 12/31/14.

Table 31: Monthly wind velocity and direction obtained from the SR 520 bridge weather station on Lake Washington during the period 1/1/2005 to 12/31/2014.

	$U[m/s]$			$Direction[^\circ]$
	5%	**Mean**	**95%**	**Mean**
March	0.81	4.2	9.5	174
April	0.72	3.9	8.5	174
May	0.77	3.6	7.6	177
June	0.80	3.6	7.2	182
July	0.84	3.4	6.5	189
August	0.75	3.2	6.4	185
September	0.79	3.4	7.4	184
October	0.83	3.7	8.7	175
November	0.99	4.4	9.7	179
December	0.86	3.8	9.5	164
January	0.77	4.1	10.1	168
February	0.64	3.8	9.6	167

E.5. Ocean Surface Current Data

Neither OSCAR data nor measured surface current data was available at this site. Therefore the surface current data was estimated using the empirical relationship in Madsen (1977), where surface current speeds are approximately 3% of the wind speed measured at 10 m elevation. Note this is a rough estimation of current speeds and should be used with caution. The average monthly values, along with the 5^{th} and 95^{th} percentiles, of current are shown in Figure 148. These data points are listed in Table 32. The annual and seasonal current roses are shown in Figure 149, which exactly mirror the wind roses because the direction is assumed to be the same.

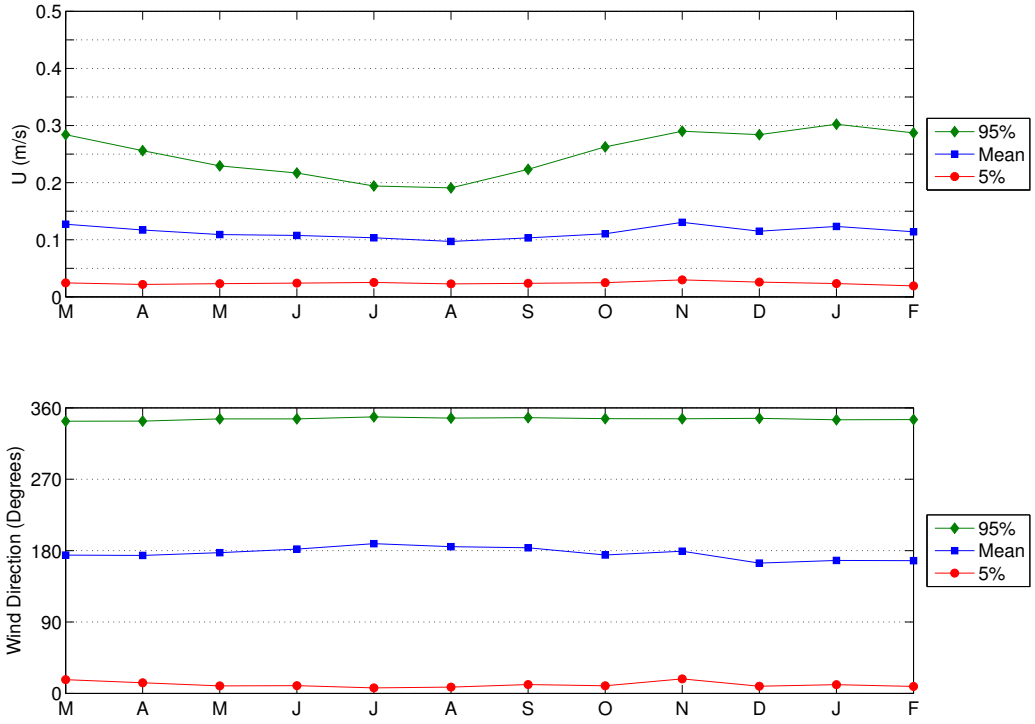

Figure 148: Monthly current velocity and direction estimated using the SR 520 bridge wind data on Lake Washington during the period 1/1/2005 to 12/31/2014.

(a)

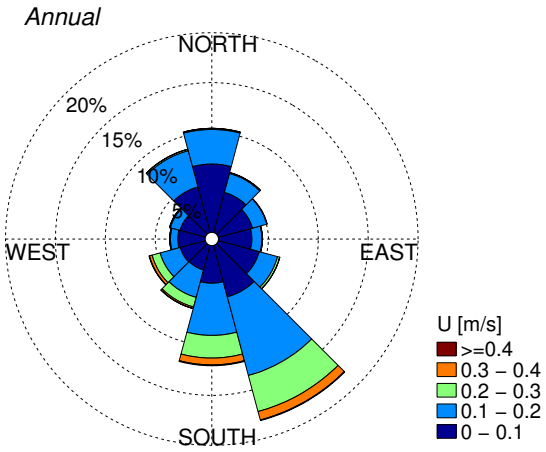

(b)

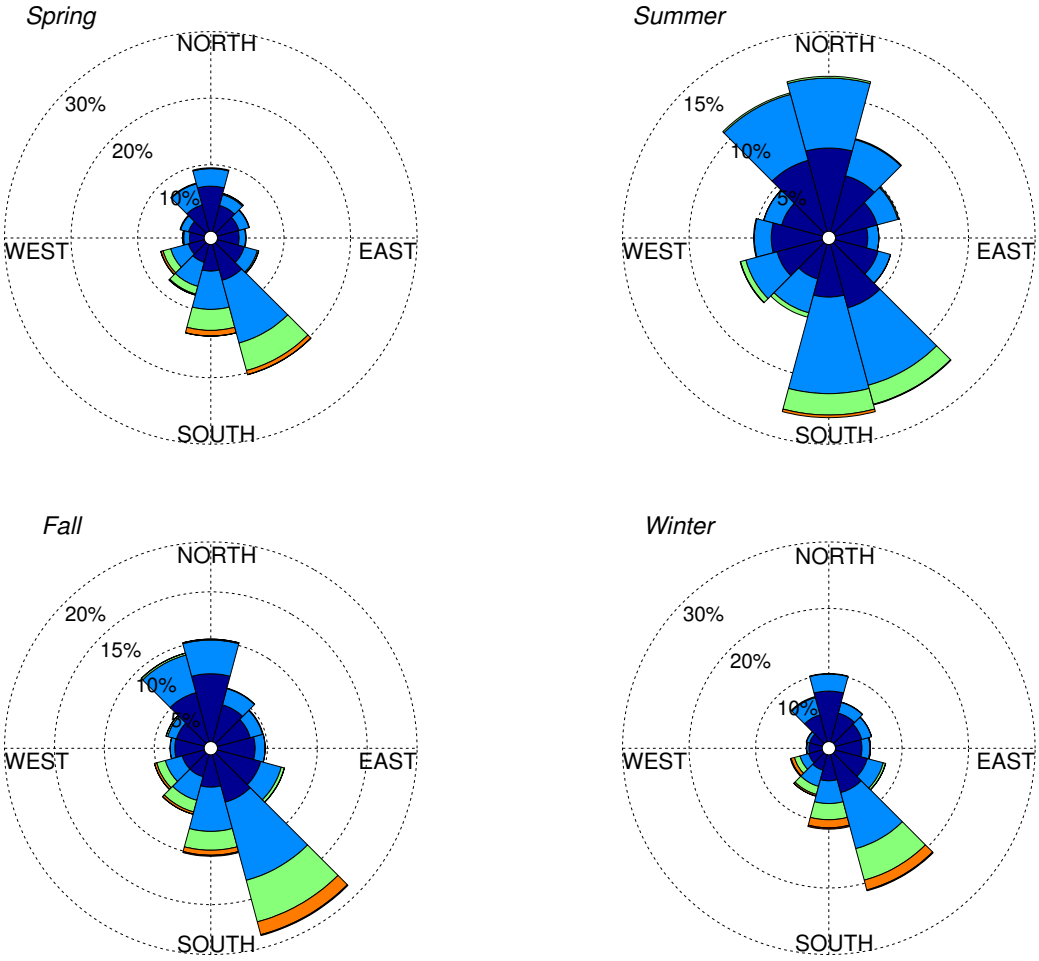

Figure 149: (a) Annual and (b) seasonal current roses of velocity and direction estimated using the SR 520 bridge wind data during the period 1/1/2005 to 12/31/14.

Table 32: Monthly surface current velocity and direction estimes using the SR 520 bridge wind data during the period 1/1/2005 to 12/31/14.

	$U[m/s]$			$Direction[^\circ]$		
	5%	**Mean**	**95%**	**5%**	**Mean**	**95%**
March	0.024	0.127	0.284	17	174	343
April	0.022	0.117	0.256	13	174	343
May	0.023	0.109	0.229	9	177	346
June	0.024	0.108	0.217	10	182	346
July	0.025	0.103	0.194	7	189	349
August	0.023	0.097	0.191	8	185	347
September	0.024	0.103	0.223	11	184	348
October	0.025	0.110	0.262	10	175	346
November	0.030	0.131	0.290	18	179	346
December	0.026	0.115	0.284	9	164	347
January	0.023	0.123	0.302	11	168	345
February	0.019	0.114	0.287	9	167	345

Appendix F: PACIFIC MARINE ENERGY TEST CENTER (PMEC): SOUTH ENERGY TEST SITE (SETS)

F.1. IEC TS Parameter Values

Table 33: The average, 5^{th} and 95^{th} percentiles of the six parameters at SETS (see Figure 78).

	$J[kW/m]$			$H_{m0}[m]$			$T_e[s]$		
	5%	**Mean**	**95%**	**5%**	**Mean**	**95%**	**5%**	**Mean**	**95%**
March	10.4	59.0	165.9	1.54	3.05	5.14	7.73	10.03	12.81
April	6.8	40.7	107.9	1.22	2.53	4.26	7.72	9.83	12.06
May	3.8	17.8	47.0	0.92	1.81	3.04	7.07	8.83	10.90
June	4.0	13.1	36.8	0.92	1.59	2.81	6.97	8.87	11.34
July	2.5	9.8	19.7	0.76	1.44	2.11	6.80	8.48	10.52
August	3.0	9.2	21.3	0.85	1.38	2.15	6.67	8.50	10.66
September	4.7	19.7	59.3	1.02	1.82	3.24	7.44	9.37	11.78
October	8.3	42.2	120.9	1.33	2.56	4.53	7.94	9.86	12.31
November	10.7	69.7	185.1	1.44	3.27	5.42	7.83	10.12	12.88
December	9.6	78.2	231.0	1.33	3.34	5.83	8.23	10.76	13.96
January	12.6	77.1	204.4	1.52	3.31	5.51	8.36	11.00	14.10
February	12.5	59.6	159.4	1.53	2.96	5.00	8.34	10.81	13.48

	ϵ_0			$\theta_j[^\circ]$			d_θ		
	5%	**Mean**	**95%**	**5%**	**Mean**	**95%**	**5%**	**Mean**	**95%**
March	0.23	0.30	0.40	242.5	274.9	297.5	0.81	0.91	0.96
April	0.24	0.32	0.47	252.5	279.0	297.5	0.76	0.90	0.96
May	0.25	0.35	0.48	242.5	273.2	302.5	0.76	0.88	0.95
June	0.27	0.38	0.51	237.5	269.6	302.5	0.74	0.85	0.93
July	0.29	0.40	0.53	242.5	276.5	307.5	0.70	0.82	0.92
August	0.27	0.40	0.53	247.5	276.6	307.5	0.72	0.82	0.92
September	0.24	0.35	0.49	242.5	278.9	302.5	0.76	0.87	0.94
October	0.22	0.29	0.41	247.5	280.1	302.5	0.82	0.90	0.95
November	0.22	0.29	0.36	242.5	279.5	302.5	0.82	0.91	0.96
December	0.19	0.28	0.36	237.5	276.4	302.5	0.82	0.91	0.96
January	0.20	0.29	0.38	247.5	274.0	297.5	0.85	0.92	0.97
February	0.19	0.28	0.38	237.5	275.3	302.5	0.82	0.92	0.97

F.2. Wave Roses

The annual wave rose of omnidirectional wave power, J, and direction of maximum directionally resolved wave power, θ_j, is shown in Figure 150, and essentially mirrors that for significant wave height, H_{m0}, and θ_j shown in Figure 151.

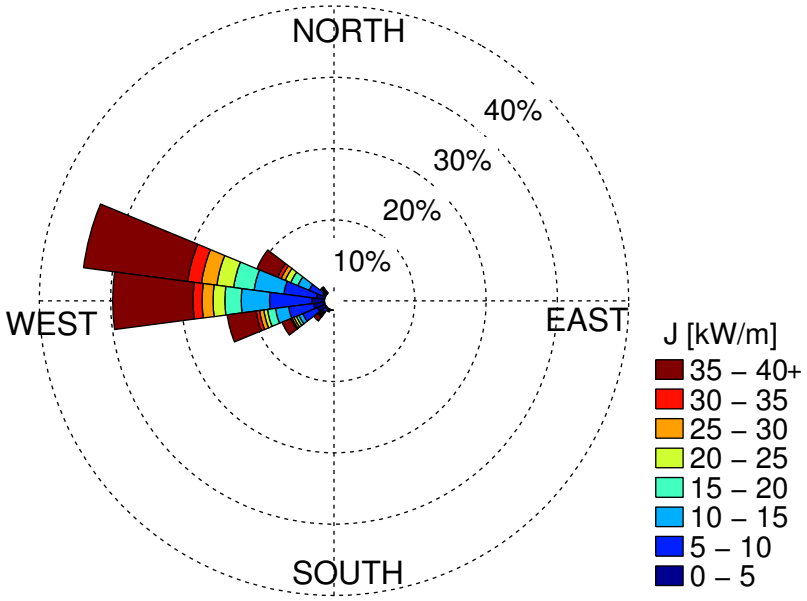

Figure 150: Annual wave rose of omnidirectional wave power and direction of maximally resolved wave power. Values of J greater than 40 kW/m are included in the top bin as shown in the legend.

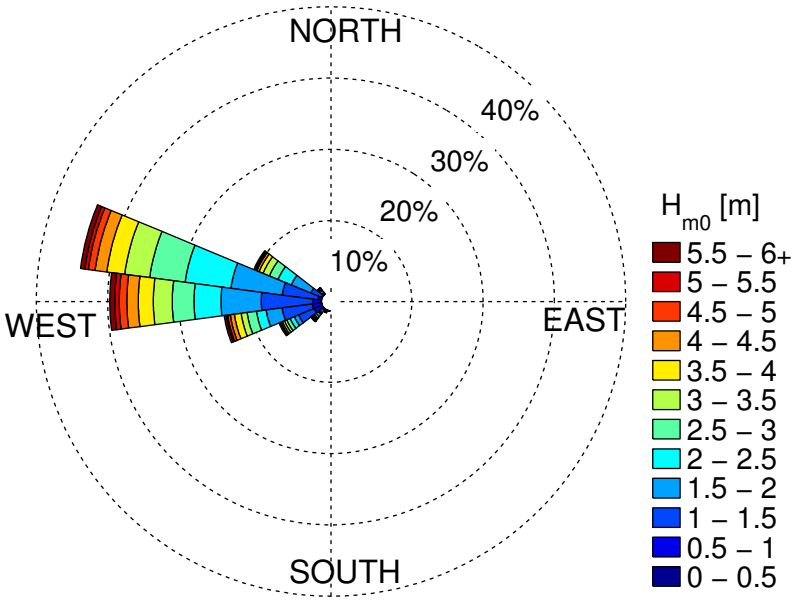

Figure 151: Annual wave rose of significant wave height and direction of maximally resolved wave power. Values of H_{m0} greater than 6 m are included in the top bin as shown in the legend.

F.3. Extreme Sea States

Table 34: Selected values along the 100-year contour for NDBC46050 (see Figure 84).

Significant wave height [m]	Energy period [s]
1	3.80
2	4.58
3	5.32
4	6.00
5	6.64
6	7.25
7	7.83
8	8.39
9	8.95
10	9.50
11	10.07
12	10.65
13	11.27
14	11.94
15	12.71
16	13.66
17	15.14
17.31	16.57
17	18.04
16	19.63
15	20.65
14	21.48
13	22.18
12	22.79
11	23.34
10	23.84
9	24.29
8	24.69
7	25.05
6	25.36
5	25.63
4	25.85
3	26.02
2	26.12
1	26.15

F.4. Wind Data

The wind data for this site (obtained from CFSR), is taken at 44.5 N, 124.5 W located approximately 23 km west/southwest of SETS (Figure 76), which is the nearest data point to the site. The average monthly values, along with the 5^{th} and 95^{th} percentiles, of wind are shown in Figure 152. The values are also tabulated in Table 35. The annual and seasonal wind roses are shown in Figure 153.

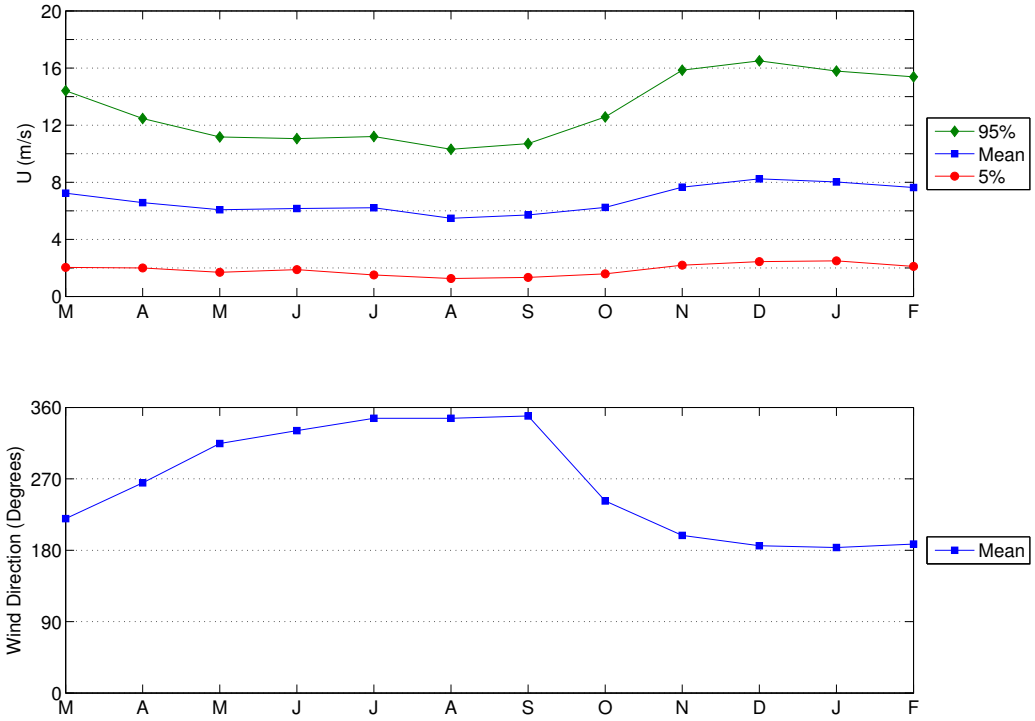

Figure 152: Monthly wind velocity and direction obtained from CSFR data during the period 1/1/1979 to 12/31/2014 at 44.5 N, 124.5 W, located 23 km west/southwest of SETS (Figure 76).

(a)

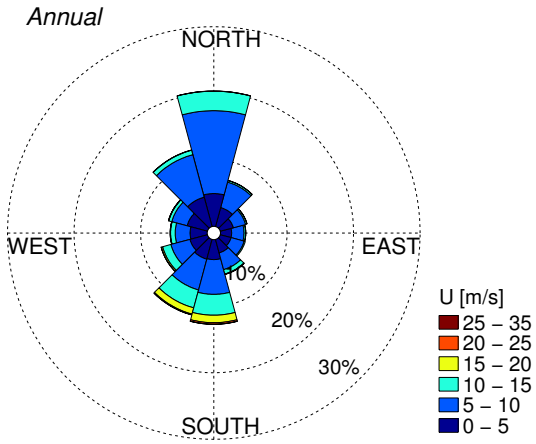

(b)

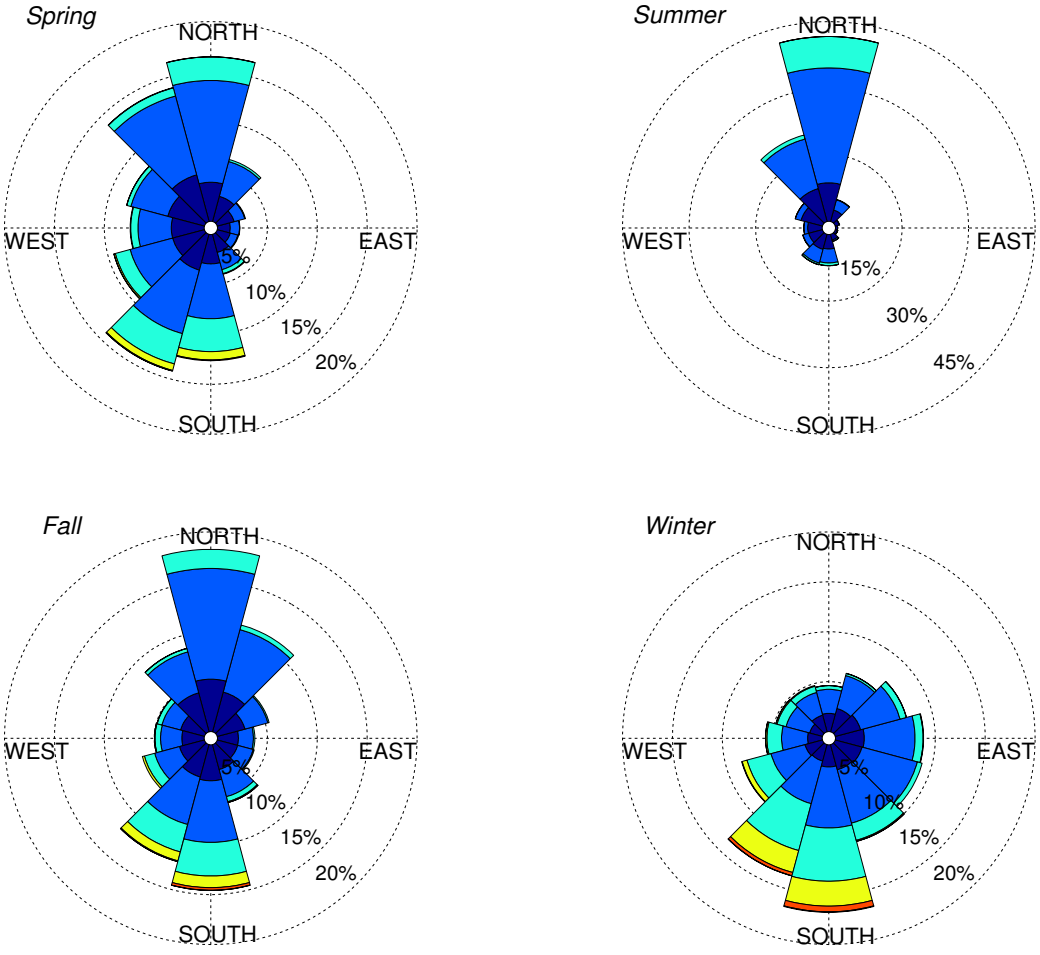

Figure 153: (a) Annual and (b) seasonal wind roses of velocity and direction obtained from CSFR data during the period 1/1/1979 to 12/31/2014.

Table 35: Monthly wind velocity and direction obtained from CSFR data during the period 1/1/1979 to 12/31/2014 at 44.5 N, 124.5 W, located approximately 23 km west/southwest of SETS.

	$U[m/s]$			$Direction[^\circ]$
	5%	**Mean**	**95%**	**Mean**
March	2.0	7.2	14.4	220
April	2.0	6.6	12.5	265
May	1.7	6.1	11.2	314
June	1.9	6.2	11.1	331
July	1.5	6.2	11.2	346
August	1.3	5.5	10.3	346
September	1.3	5.7	10.7	349
October	1.6	6.2	12.6	242
November	2.2	7.7	15.9	199
December	2.4	8.2	16.5	186
January	2.5	8.0	15.8	183
February	2.1	7.6	15.4	188

F.5. Ocean Surface Current Data

The surface current data (obtained from OSCAR) used for this site is located at 44.5 N, 125.5 W. There is data located closer to the site at 44.5 N, 124.5 W, however the period of record is short (about 2 years). Data from the two years available was compared at both locations. Surface current speeds at 124.5 W are slightly higher in the summer than at 125.5 W, however overall the patterns are similar. Therefore, the data point further out (125.5 W) with the longer period of record (about 20 years) was used for consistency with the other sites. The average monthly values, along with the 5^{th} and 95^{th} percentiles, of current are shown in Figure 154. These data points are listed in Table 36. The annual and seasonal current roses are shown in Figure 155.

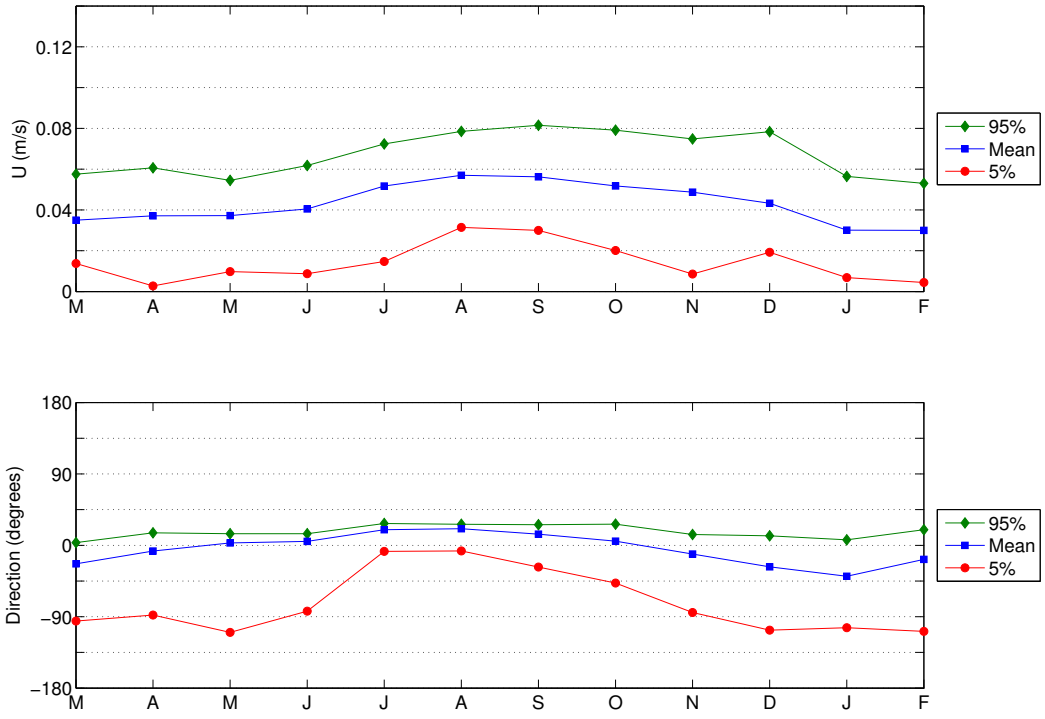

Figure 154: Monthly ocean surface current velocity and direction obtained from OSCAR at 44.5 N, 125.5 W. Data period 1/1/1993 to 12/30/2014.

(a)

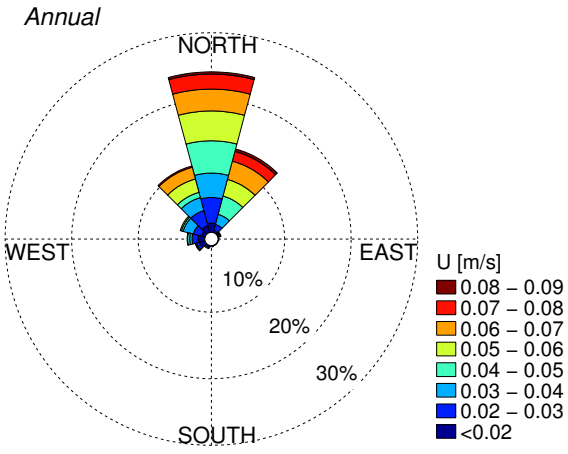

(b)

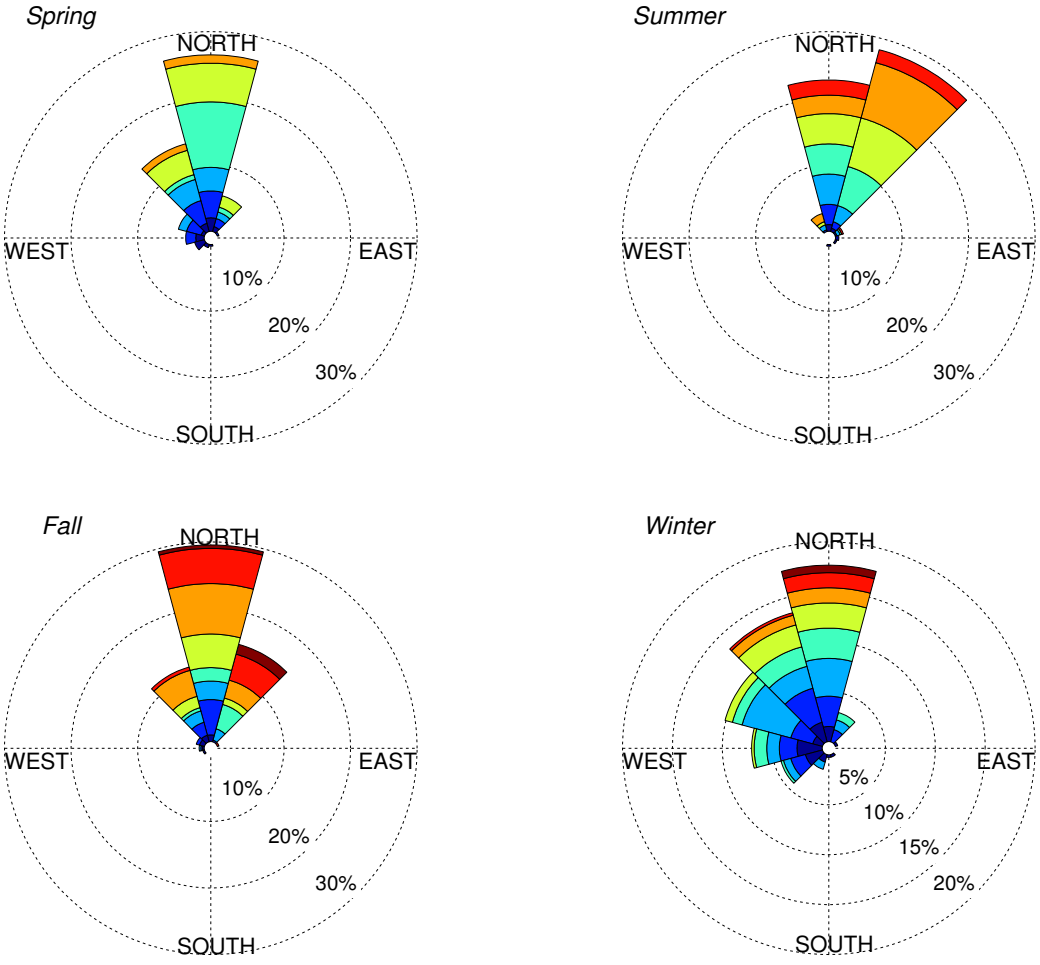

Figure 155: (a) Annual and (b) seasonal current roses of ocean surface current velocity and direction obtained from OSCAR at 44.5 N, 125.5 W. Data period 1/1/1993 to 12/30/2014.

Table 36: Monthly surface current velocity and direction obtained from OSCAR data during the period 1/1/1993 to 12/30/2014 at 44.5 N, 125.5 W.

	$U[m/s]$			$Direction[^\circ]$		
	5%	**Mean**	**95%**	**5%**	**Mean**	**95%**
March	0.014	0.035	0.058	-95	-23	3
April	0.003	0.037	0.061	-88	-7	16
May	0.010	0.037	0.055	-110	3	15
June	0.009	0.040	0.062	-83	5	15
July	0.015	0.052	0.072	-8	20	28
August	0.031	0.057	0.079	-7	21	27
September	0.030	0.056	0.082	-27	14	26
October	0.020	0.052	0.079	-48	5	27
November	0.009	0.049	0.075	-85	-11	14
December	0.019	0.043	0.078	-107	-27	12
January	0.007	0.030	0.056	-104	-39	7
February	0.004	0.030	0.053	-108	-18	20

Appendix G: CALWAVE PROPOSED CENTRAL COAST WEC TEST SITE AT VANDENBERG AIR FORCE BASE (VAFB)

G.1. IEC TS Parameter Values

Table 37: The average, 5^{th} and 95^{th} percentiles of the six parameters at the South Vandenberg site (see Figure 92).

	$J[kW/m]$			$H_{m0}[m]$			$T_e[s]$		
	5%	**Mean**	**95%**	**5%**	**Mean**	**95%**	**5%**	**Mean**	**95%**
March	9.5	55.0	143.9	1.33	2.75	4.43	9.19	11.98	15.54
April	9.2	38.3	91.3	1.39	2.50	3.89	7.35	10.75	14.24
May	6.2	27.3	62.1	1.18	2.19	3.35	6.13	10.17	15.63
June	6.9	24.9	54.2	1.18	2.21	3.29	6.18	9.47	14.87
July	5.3	16.0	32.0	1.07	1.82	2.60	5.76	9.13	14.79
August	3.4	16.6	33.6	0.95	1.81	2.57	5.76	9.48	14.92
September	5.2	20.0	45.8	1.08	1.84	2.83	5.98	10.36	14.82
October	7.1	31.0	81.7	1.20	2.20	3.63	7.96	10.88	14.72
November	10.7	46.1	128.1	1.42	2.56	4.26	8.73	11.58	14.70
December	11.9	65.8	166.7	1.43	2.94	4.68	9.59	12.29	15.68
January	12.4	67.9	173.1	1.56	2.95	4.84	9.13	12.47	15.99
February	15.4	74.6	202.2	1.61	3.09	5.19	9.62	12.53	15.97

	ϵ_0			$\theta_j[^\circ]$			d_θ		
	5%	**Mean**	**95%**	**5%**	**Mean**	**95%**	**5%**	**Mean**	**95%**
March	0.23	0.24	0.25	275.0	291.4	307.5	0.98	0.98	0.99
April	0.23	0.23	0.24	207.5	290.2	312.5	0.98	0.98	0.99
May	0.23	0.23	0.24	192.5	272.6	312.5	0.98	0.98	0.99
June	0.23	0.23	0.24	192.5	284.0	312.5	0.98	0.98	0.99
July	0.23	0.24	0.25	192.5	279.5	317.5	0.98	0.98	0.99
August	0.23	0.24	0.24	187.5	272.6	312.5	0.98	0.98	0.99
September	0.23	0.24	0.25	192.5	272.1	312.5	0.97	0.98	0.99
October	0.23	0.23	0.24	202.5	289.6	312.5	0.98	0.98	0.99
November	0.23	0.24	0.25	277.5	295.2	312.5	0.98	0.98	0.99
December	0.23	0.24	0.25	277.5	293.5	312.5	0.98	0.98	0.99
January	0.23	0.24	0.24	272.5	288.6	307.5	0.98	0.98	0.99
February	0.23	0.24	0.24	272.5	288.2	307.5	0.98	0.98	0.99

Table 38: The average, 5^{th} and 95^{th} percentiles of the six parameters at the South by Southeast Vandenberg site (see Figure 93).

	$J[kW/m]$			$H_{m0}[m]$			$T_e[s]$		
	5%	**Mean**	**95%**	**5%**	**Mean**	**95%**	**5%**	**Mean**	**95%**
March	7.9	42.4	105.8	1.22	2.44	3.94	8.96	11.70	15.21
April	8.0	30.0	68.3	1.26	2.24	3.42	7.21	10.50	13.99
May	4.9	22.6	50.6	1.07	2.01	3.03	6.11	10.02	15.51
June	5.9	20.5	42.9	1.10	2.02	2.96	6.12	9.31	14.81
July	4.2	13.6	28.1	0.99	1.68	2.39	5.74	9.01	14.69
August	2.3	13.9	28.4	0.81	1.66	2.35	5.73	9.32	14.79
September	3.6	16.3	36.8	0.87	1.67	2.50	5.97	10.22	14.72
October	5.8	23.6	58.4	1.08	1.94	3.07	7.74	10.64	14.56
November	8.2	34.2	91.3	1.26	2.23	3.69	8.50	11.27	14.37
December	9.4	49.2	125.8	1.30	2.56	4.14	9.32	11.98	15.35
January	10.3	54.8	140.8	1.41	2.66	4.42	8.89	12.22	15.78
February	12.5	59.0	165.2	1.45	2.75	4.60	9.36	12.26	15.72

	ϵ_0			$\theta_j[^\circ]$			d_θ		
	5%	**Mean**	**95%**	**5%**	**Mean**	**95%**	**5%**	**Mean**	**95%**
March	0.23	0.25	0.27	272.5	286.7	303.8	0.98	0.98	0.99
April	0.23	0.25	0.26	202.5	286.5	305.0	0.98	0.98	0.99
May	0.23	0.24	0.26	192.5	270.5	310.0	0.98	0.98	0.99
June	0.23	0.24	0.25	195.0	281.4	310.0	0.98	0.98	0.99
July	0.23	0.24	0.27	195.0	277.1	312.5	0.97	0.98	0.99
August	0.23	0.24	0.26	190.0	271.6	310.0	0.98	0.98	0.99
September	0.23	0.25	0.27	192.5	269.4	310.0	0.97	0.98	0.99
October	0.23	0.25	0.27	202.5	285.0	310.0	0.98	0.98	0.99
November	0.24	0.25	0.27	273.8	290.2	305.0	0.98	0.98	0.99
December	0.24	0.25	0.27	275.0	288.3	305.0	0.98	0.98	0.99
January	0.23	0.25	0.27	270.0	284.1	300.0	0.98	0.98	0.99
February	0.23	0.25	0.27	270.0	283.6	300.0	0.98	0.98	0.99

G.2. Wave Roses

The annual wave rose of omnidirectional wave power, J, and direction of maximum directionally resolved wave power, θ_j, is shown in Figures 156 and 157, and essentially mirrors that for significant wave height, H_{m0}, and θ_j shown in Figures 158 and 159 for the South and SSE sites.

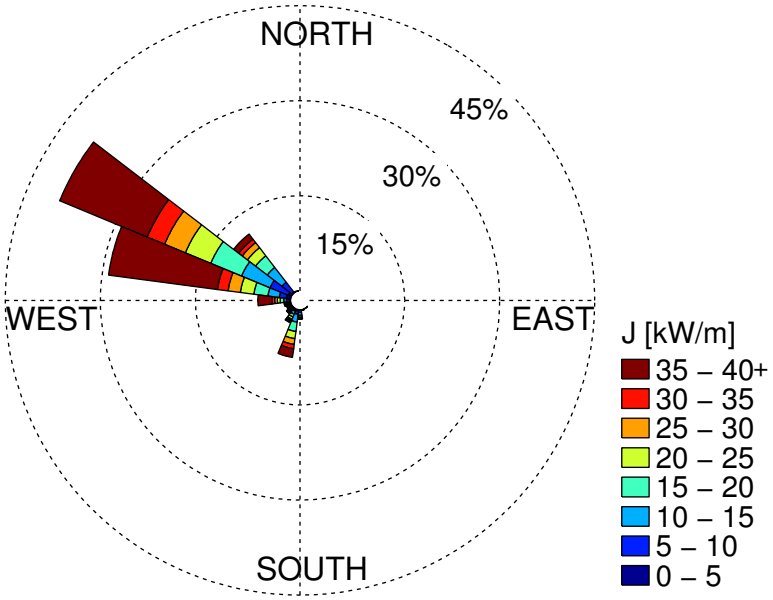

Figure 156: Annual wave rose of omnidirectional wave power and direction of maximally resolved wave power at the South location. Values of J greater than 40 kW/m are included in the top bin as shown in the legend.

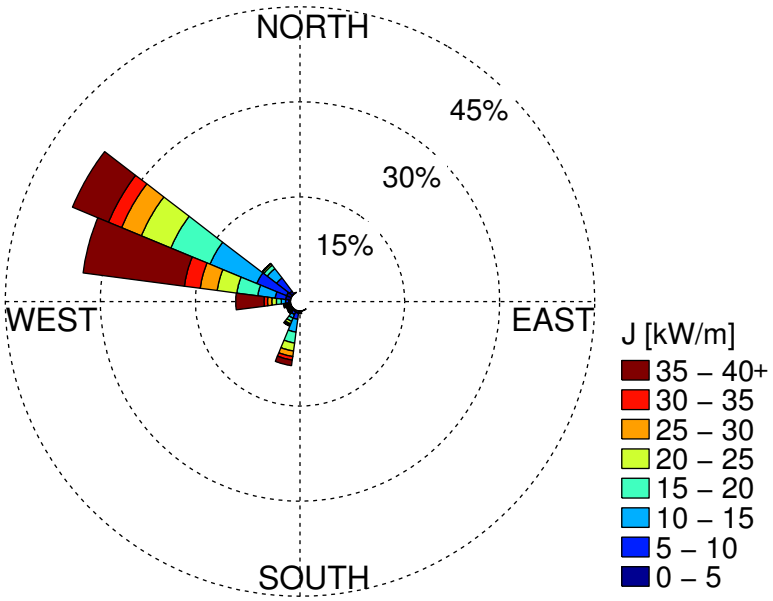

Figure 157: Annual wave rose of omnidirectional wave power and direction of maximally resolved wave power at the SSE location. Values of J greater than 40 kW/m are included in the top bin as shown in the legend.

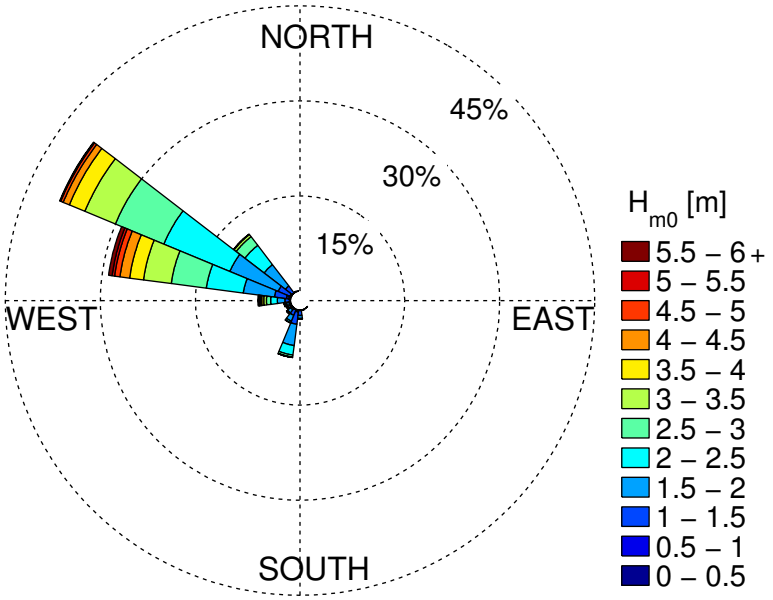

Figure 158: Annual wave rose of significant wave height and direction of maximally resolved wave power at the South location. Values of H_{m0} greater than 6 m are included in the top bin as shown in the legend.

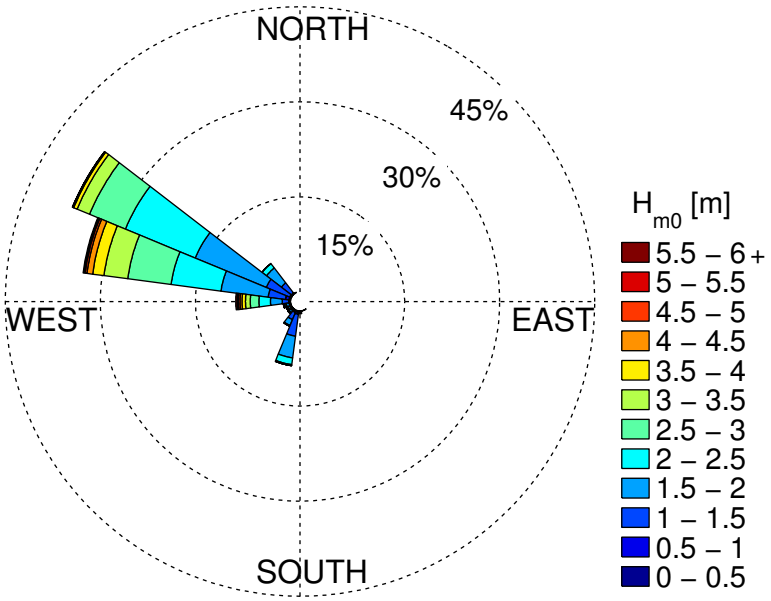

Figure 159: Annual wave rose of significant wave height and direction of maximally resolved wave power at the SSE location. Values of H_{m0} greater than 6 m are included in the top bin as shown in the legend.

G.3. Extreme Sea States

Table 39: Estimates of extreme significant wave height values using the generalized extreme value distribution (see Figure 104).

Return period [years]	Significant wave height [m]
10	8.17
25	8.90
50	9.44
100	9.98

Table 40: Estimates of extreme significant wave height values using the peak over thresholds method (see Figure 105).

Return period [years]	Significant wave height [m]
10	8.62
25	9.05
50	9.35
100	9.63

G.4. Wind Data

The wind data for this site (obtained from CFSR), is taken at 34.5 N, 121 W located approximately 30 km west of the site (Figure 89), which is the nearest data point to the site. The average monthly values, along with the 5^{th} and 95^{th} percentiles, of wind are shown in Figure 160. The values are also tabulated in Table 41. The annual and seasonal wind roses are shown in Figure 161.

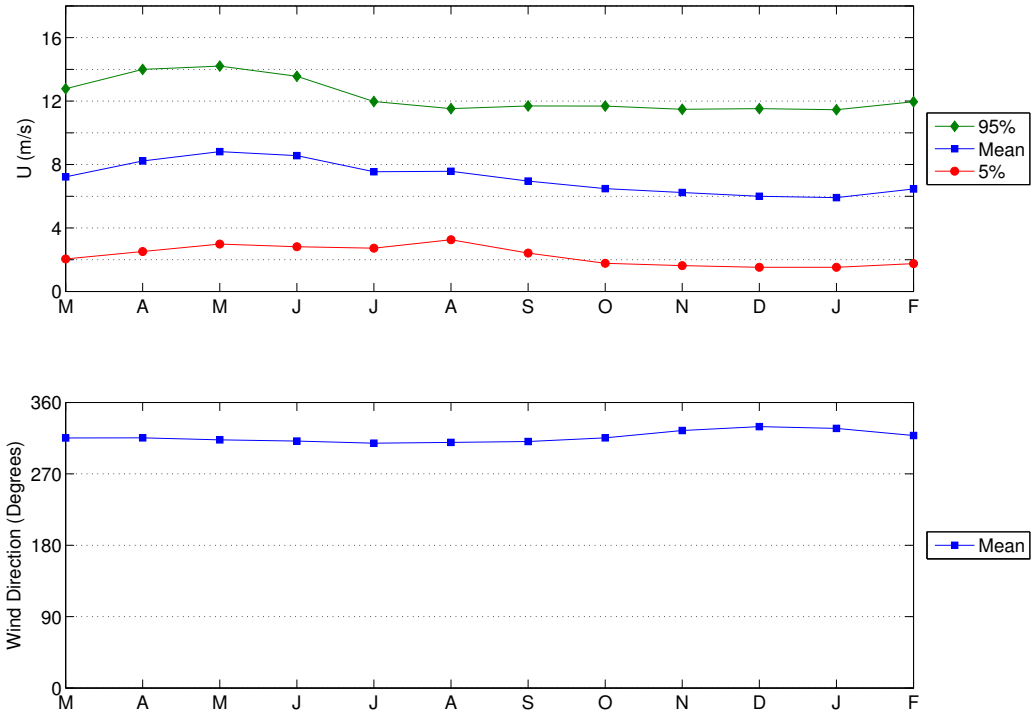

Figure 160: Monthly wind velocity and direction obtained from CSFR data during the period 1/1/1979 to 12/31/2014 at 34.5 N, 121 W, located approximately 30 km west of the test site.

(a)

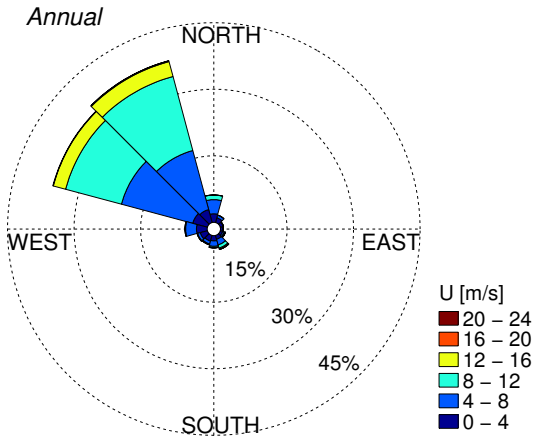

(b)

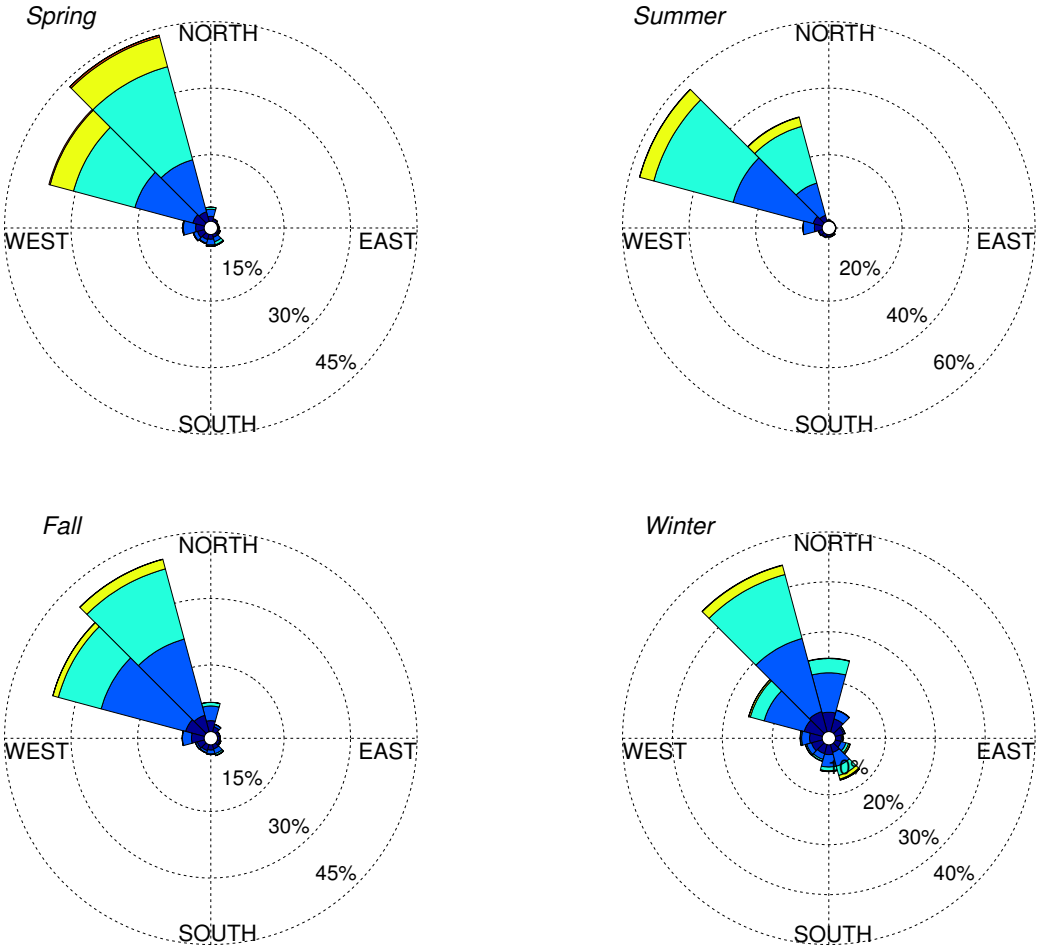

Figure 161: (a)Annual and (b) seasonal wind roses of velocity and direction obtained from CSFR data during the period 1/1/1979 to 12/31/14. Data taken at 34.5 N, 121 W, located approximately 30 km west of the test site.

Table 41: Monthly wind velocity and direction obtained from CSFR data during the period 1/1/1979 to 12/31/2014 at 34.5 N, 121 W, located approximately 30 km west of the Vandenberg AFB site.

	$U[m/s]$			$Direction[^\circ]$
	5%	**Mean**	**95%**	**Mean**
March	2.05	7.2	12.8	315
April	2.51	8.2	14.0	315
May	2.99	8.8	14.2	313
June	2.82	8.6	13.6	311
July	2.73	7.5	12.0	309
August	3.26	7.6	11.5	310
September	2.42	7.0	11.7	311
October	1.77	6.5	11.7	315
November	1.63	6.2	11.5	325
December	1.52	6.0	11.5	330
January	1.52	5.9	11.5	327
February	1.76	6.5	12.0	318

G.5. Ocean Surface Current Data

The surface current data (obtained from OSCAR), is located at 34.5 N, 121.5 W, the closest data point. The average monthly values, along with the 5^{th} and 95^{th} percentiles, of current are shown in Figure 162. These data points are listed in Table 42. The annual and seasonal current roses are shown in Figure 163.

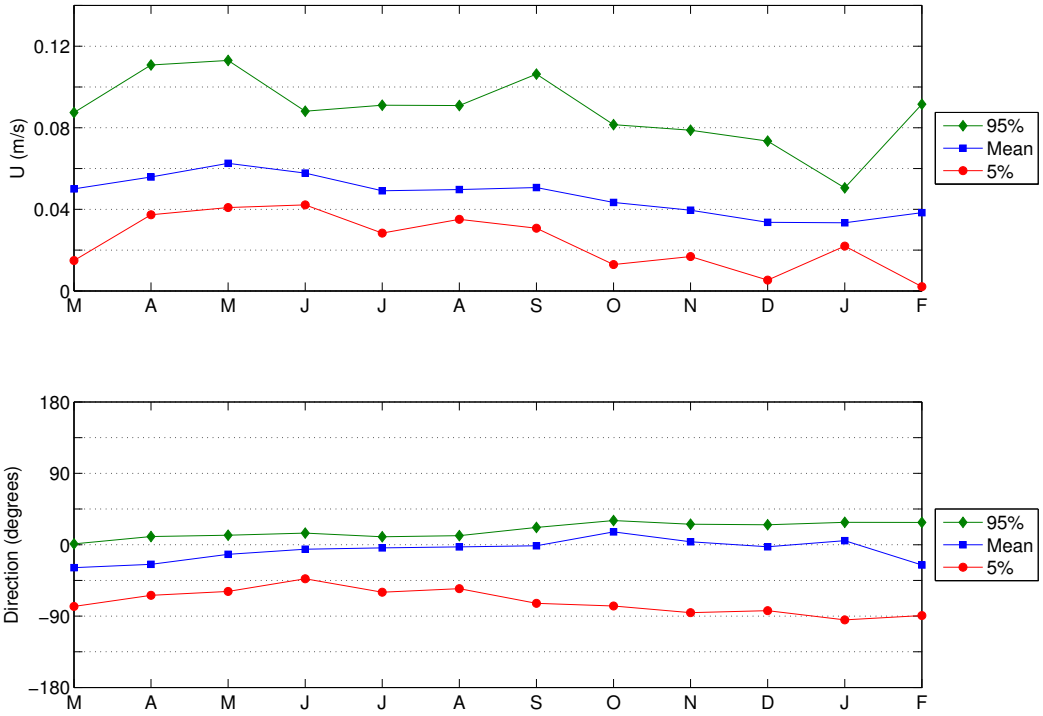

Figure 162: Monthly current velocity and direction obtained from CSFR data during the period 1/1/1993 to 12/31/2014 at 34.5 N, 121.5 W.

(a)

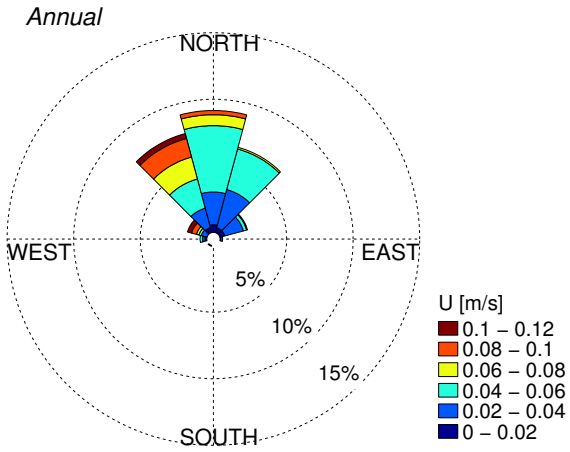

(b)

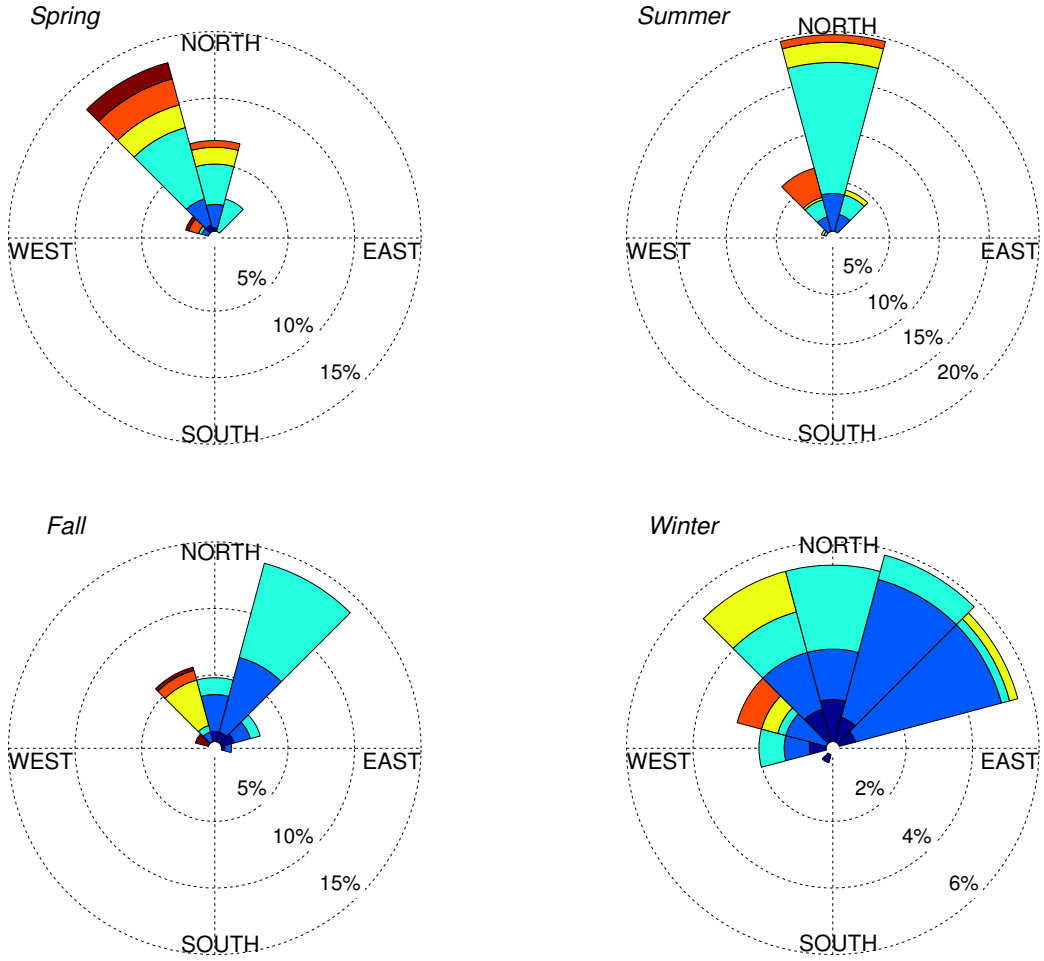

Figure 163: (a)Annual and (b) seasonal current roses of velocity and direction obtained from CSFR data during the period 1/1/1993 to 12/31/14. Data taken at 34.5 N, 121.5 W.

Table 42: Monthly surface current velocity and direction obtained from OSCAR data during the period 1/1/1993 to 12/31/2014 at 34.5 N, 121.5 W, located approximately 75 km from the site.

	$U[m/s]$			$Direction[^\circ]$		
	5%	**Mean**	**95%**	**5%**	**Mean**	**95%**
March	0.015	0.050	0.087	-78	-29	1
April	0.037	0.056	0.111	-64	-25	10
May	0.041	0.063	0.113	-59	-12	12
June	0.042	0.058	0.088	-43	-6	15
July	0.028	0.049	0.091	-60	-4	10
August	0.035	0.050	0.091	-55	-3	11
September	0.031	0.051	0.106	-74	-1	22
October	0.013	0.043	0.082	-77	16	30
November	0.017	0.040	0.079	-86	4	26
December	0.005	0.034	0.073	-83	-3	25
January	0.022	0.033	0.051	-95	5	28
February	0.002	0.038	0.092	-89	-26	28

Appendix H: HUMBOLDT BAY, CALIFORNIA: POTENTIAL WEC TEST SITE

H.1. IEC TS Parameter Values

Table 43: The average, 5^{th} and 95^{th} percentiles of the six parameters at Humboldt (see Figure 112).

	$J[kW/m]$			$H_{m0}[m]$			$T_e[s]$		
	5%	**Mean**	**95%**	**5%**	**Mean**	**95%**	**5%**	**Mean**	**95%**
March	8.3	44.5	113.0	1.34	2.60	4.16	7.66	10.07	12.91
April	5.6	27.7	72.4	1.16	2.16	3.48	6.81	9.21	11.61
May	2.9	14.9	40.4	0.89	1.74	2.84	6.18	7.81	10.21
June	2.6	12.7	32.6	0.81	1.70	2.77	5.89	7.35	9.19
July	2.3	10.7	24.7	0.79	1.64	2.54	5.66	6.95	8.36
August	2.3	10.1	24.6	0.80	1.57	2.46	5.72	7.03	8.83
September	2.9	14.0	34.9	0.83	1.71	2.67	6.32	7.95	10.19
October	5.2	30.3	89.6	1.10	2.20	3.79	6.81	9.28	11.95
November	5.9	47.9	125.2	1.11	2.61	4.37	7.96	10.28	13.41
December	10.1	66.8	181.2	1.39	3.02	5.13	8.47	11.00	14.03
January	8.3	58.0	148.9	1.31	2.82	4.67	8.33	10.99	13.87
February	10.4	50.1	134.9	1.43	2.66	4.45	8.15	10.93	13.63

	ϵ_0			$\theta_j[^\circ]$			d_θ		
	5%	**Mean**	**95%**	**5%**	**Mean**	**95%**	**5%**	**Mean**	**95%**
March	0.24	0.31	0.41	267.5	289.8	307.5	0.88	0.93	0.97
April	0.26	0.32	0.42	270.0	293.4	312.5	0.88	0.93	0.96
May	0.26	0.35	0.47	265.0	293.9	317.5	0.85	0.91	0.95
June	0.27	0.35	0.48	270.0	298.5	317.5	0.84	0.91	0.95
July	0.27	0.35	0.48	272.5	303.2	317.5	0.87	0.92	0.95
August	0.27	0.35	0.47	282.5	303.9	317.5	0.85	0.91	0.95
September	0.26	0.34	0.46	277.5	302.4	317.5	0.88	0.93	0.95
October	0.24	0.31	0.42	272.5	297.0	317.5	0.88	0.93	0.96
November	0.23	0.29	0.40	270.0	291.5	307.5	0.87	0.93	0.97
December	0.22	0.29	0.39	265.0	287.6	307.5	0.87	0.93	0.97
January	0.22	0.30	0.41	260.6	285.7	305.0	0.87	0.94	0.97
February	0.22	0.30	0.40	265.0	286.9	305.0	0.87	0.93	0.97

H.2. Wave Roses

The annual wave rose of omnidirectional wave power, J, and direction of maximum directionally resolved wave power, θ_j, is shown in Figure 164, and essentially mirrors that for significant wave height, H_{m0}, and θ_j shown in Figure 165.

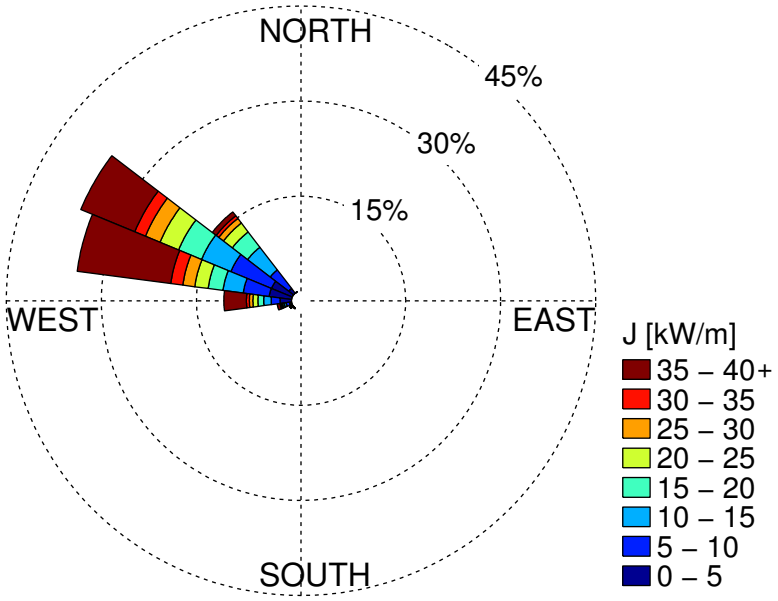

Figure 164: Annual wave rose of omnidirectional wave power and direction of maximum directionally resolved wave power. Values of J greater than 40 kW/m are included in the top bin as shown in the legend.

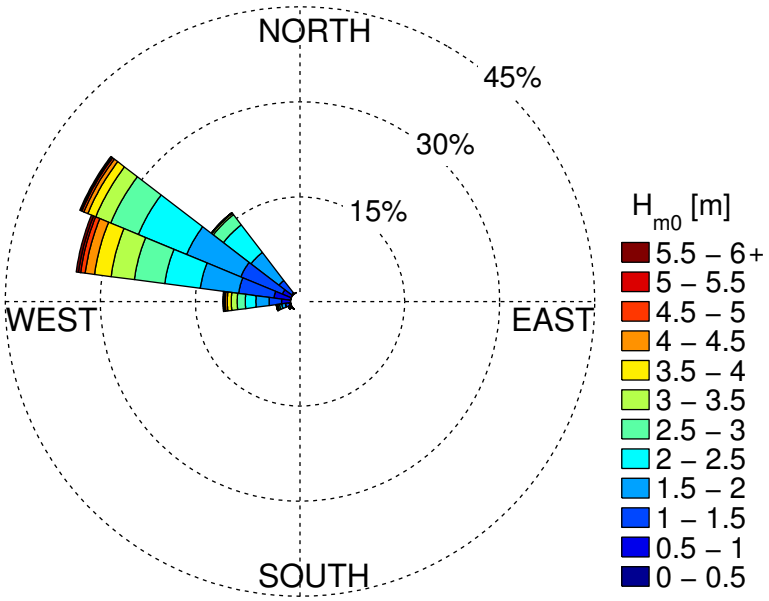

Figure 165: Annual wave rose of significant wave height and direction of maximum directionally resolved wave power. Values of H_{m0} greater than 6 m are included in the top bin as shown in the legend.

H.3. Extreme Sea States

Table 44: Selected values along the 100-year contour for CDIP128 (NDBC 46212) (see Figure 118).

Significant wave height [m]	Energy period [s]
1	3.66
2	4.43
3	5.46
4	6.56
5	7.69
6	8.84
7	10.04
8	11.31
9	12.71
10	14.43
10.91	17.78
10	20.63
9	21.70
8	22.39
7	22.87
6	23.19
5	23.38
4	23.44
3	23.35
2	23.09
1	22.60

H.4. Wind Data

The wind data for this site (obtained from CFSR), is the mean of magnitude and direction taken at 40.5 N, 124.5 W and 41 N, 124.5 W. Note that the central location between these two points is approximately 25 km southwest of the test site (Figure 110). The average monthly values, along with the 5^{th} and 95^{th} percentiles, of wind are shown in Figure 166. The values are also tabulated in Table 45. The annual and seasonal wind roses are shown in Figure 167. In the summer, the predominant direction of winds and waves correlate well. In the winter, the waves are dominated by distant swells, and the local winds have little effect.

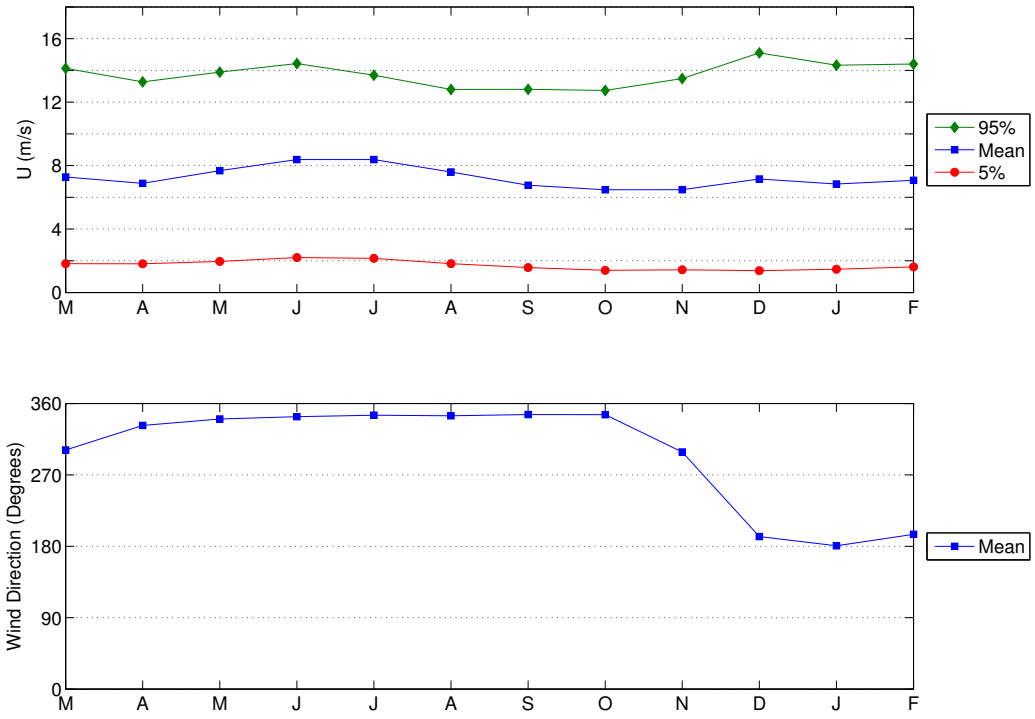

Figure 166: Monthly wind velocity and direction obtained from CSFR data during the period 1/1/1979 to 12/31/2014 at 40.75 N, 124.5 W, located approximately 25 km southwest of the test site (Figure 110).

(a)

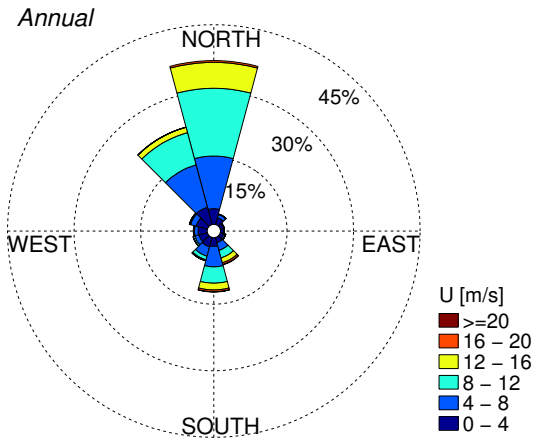

(b)

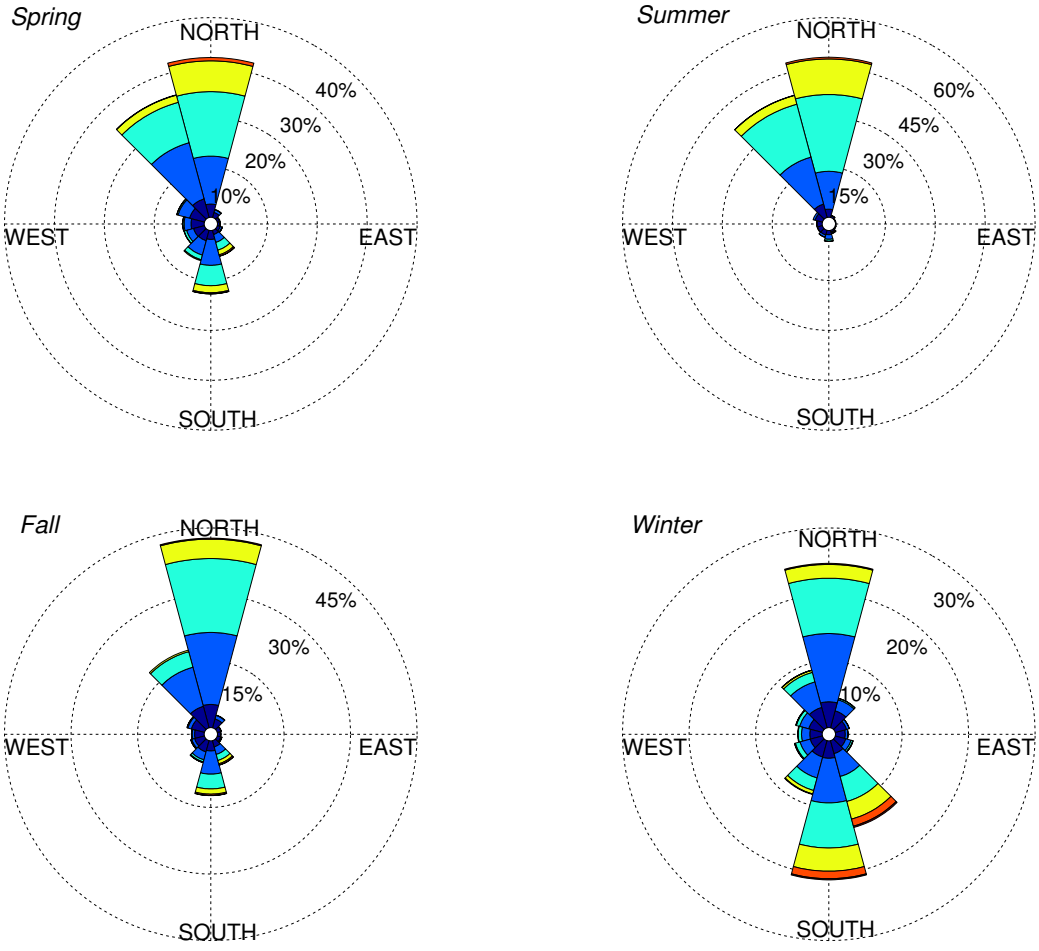

Figure 167: (a)Annual and (b) seasonal wind roses of velocity and direction obtained from CSFR data during the period 1/1/1979 to 12/31/14. Data taken at 40.75 N, 124.5 W, located approximately 25 km southwest of the test site.

Table 45: Monthly wind velocity and direction obtained from CSFR data during the period 1/1/1979 to 12/31/2014 at 40.75 N, 124.5 W, located approximately 25 km southwest of the Humboldt site.

	$U[m/s]$			$Direction[^\circ]$
	5%	**Mean**	**95%**	**Mean**
March	1.8	7.3	14.1	301
April	1.8	6.9	13.3	332
May	2.0	7.7	13.9	340
June	2.2	8.4	14.4	343
July	2.2	8.4	13.7	345
August	1.8	7.6	12.8	345
September	1.6	6.8	12.8	346
October	1.4	6.5	12.7	346
November	1.4	6.5	13.5	299
December	1.4	7.2	15.1	192
January	1.5	6.8	14.3	181
February	1.6	7.1	14.4	195

H.5. Ocean Surface Current Data

The current data (obtained from OSCAR), is located at 40.5 N, 125.5 W, the closest data point. The average monthly values, along with the 5^{th} and 95^{th} percentiles, of current are shown in Figure 168. These data points are listed in Table 46. The annual and seasonal current roses are shown in Figure 169.

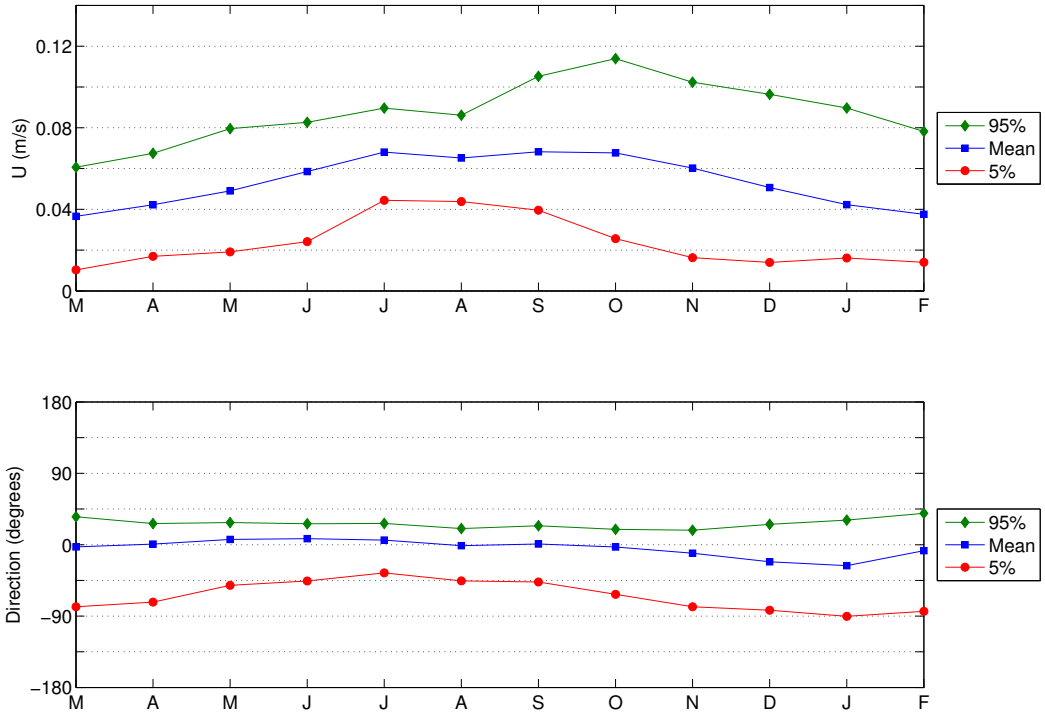

Figure 168: Monthly ocean surface current velocity and direction obtained from OSCAR at 40.5 N, 125.5 W, located approximately 110 km southwest of the Humboldt Site. Data period 1/1/1993 to 12/30/2014.

(a)

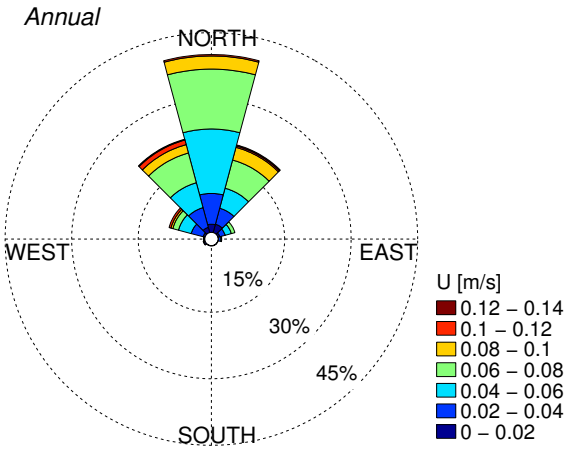

(b)

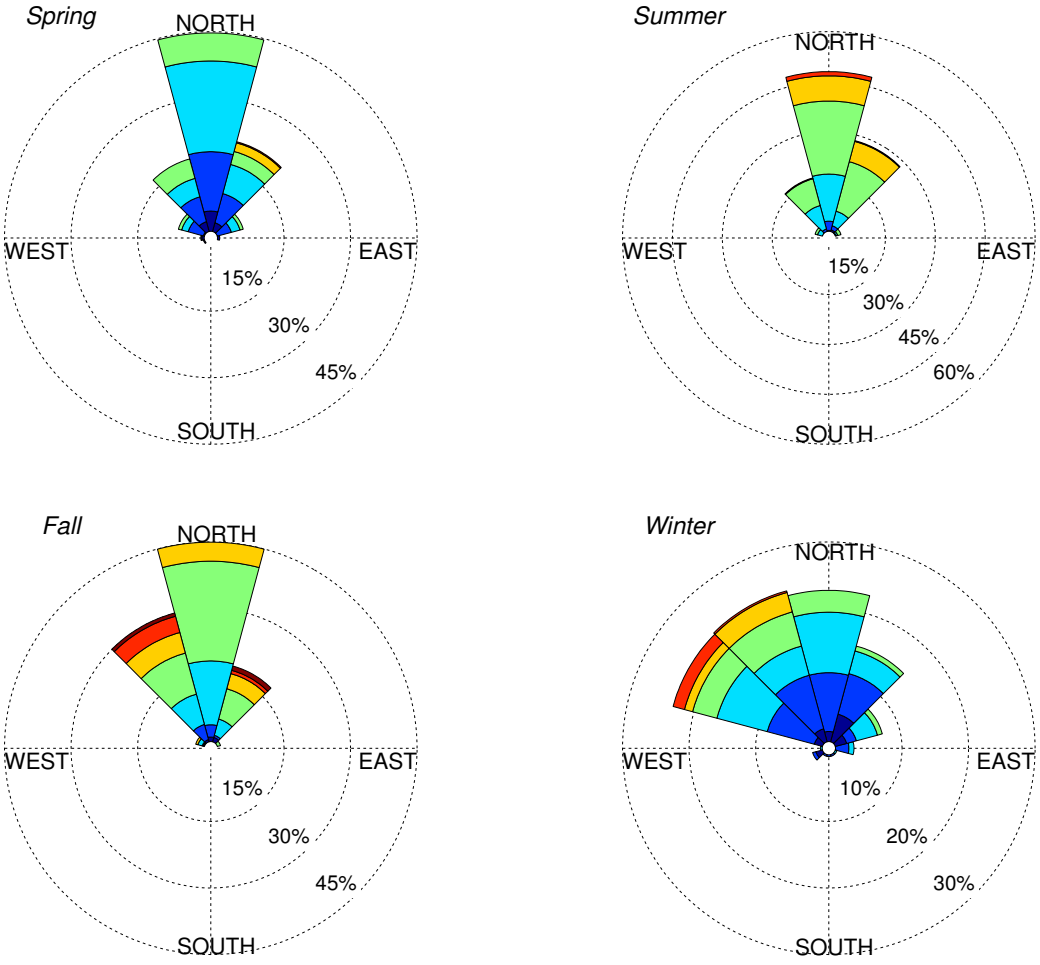

Figure 169: (a)Annual and (b) seasonal current roses of ocean surface current velocity and direction obtained from OSCAR at 40.5 N, 125.5 W, located approximately 110 km southwest of the Humboldt Site. Data period 1/1/1993 to 12/30/2014.

Table 46: Monthly surface current velocity and direction obtained from OSCAR data during the period 1/1/1993 to 12/30/2014 at 40.5 N, 125.5 W, located approximately 110 km from Humboldt test site.

	$U[m/s]$			$Direction[^\circ]$		
	5%	**Mean**	**95%**	**5%**	**Mean**	**95%**
March	0.010	0.037	0.061	-78	-3	35
April	0.017	0.042	0.067	-72	1	27
May	0.019	0.049	0.080	-51	7	28
June	0.024	0.059	0.083	-46	8	26
July	0.044	0.068	0.090	-36	6	27
August	0.044	0.065	0.086	-46	-1	20
September	0.040	0.068	0.105	-47	1	24
October	0.026	0.068	0.114	-62	-3	19
November	0.017	0.061	0.101	-78	-11	18
December	0.014	0.051	0.093	-82	-20	25
January	0.016	0.042	0.090	-90	-26	31
February	0.014	0.038	0.078	-84	-7	40


Sandia National Laboratories